2017

A Study on the Electrochemical Dissolution of Ilmenite, Zircon and Lead Sulphate

Zakaria, Md. Golam

University of Rajshahi

A Study on the Electrochemical Dissolution of Ilmenite, Zircon and Lead Sulphate

A Dissertation
Submitted to the Department of Applied Chemistry and Chemical Engineering, University of Rajshahi, Bangladesh in Partial Fulfillment of the Requirements for the Degree of Doctor of Philosophy

By

Md. Golam Zakaria
Roll No.: 11907, Registration No.: 2066
Session: 2011-2012

Under the Supervision of

Professor Dr. Ranjit Kumar Biswas
&
Professor Dr. M. Rostom Ali
Metallurgy and Electrochemistry Research Laboratory
Department of Applied Chemistry and Chemical Engineering
Faculty of Engineering
University of Rajshahi
Bangladesh

June 2017

DECLARATION

I do hereby declare that the entire research work submitted as the thesis entitled "**A Study on the Electrochemical Dissolution of Ilmenite, Zircon and Lead Sulphate**" under the supervision of **Dr. Ranjit Kumar Biswas and Dr. M. Rostom Ali**, Professors of Applied Chemistry and Chemical Engineering, towards the fulfillment for the degree of Doctor of Philosophy in the Department of Applied Chemistry and Chemical Engineering, University of Rajshahi is based on the results of my own investigation and has not ever been submitted before in any form for any other degree at any place (except publication).

(Md. Golam Zakaria)
Ph.D. Fellow
Roll No: 11907, Registration No: 2066
Session: 2011-2012
Metallurgy and Electrochemistry Research Laboratory
Department of Applied Chemistry and Chemical Engineering
Faculty of Engineering
University of Rajshahi, Rajshahi, Bangladesh

CERTIFICATE OF RESEARCH

This is to certify that the Ph. D. thesis entitled "**A Study on the Electrochemical Dissolution of Ilmenite, Zircon and Lead Sulphate**" submitted by **Md. Golam Zakaria**, Roll No.: 11907, Registration No.:2066, Session: 2011-2012, Department of Applied Chemistry and Chemical Engineering, University of Rajshahi, Rajshahi, Bangladesh has been completed under our supervision. This is a bonafide record of the research carried out by the candidate.

To the best of our knowledge, this thesis has not been submitted for the award of any degree elsewhere.

Prof. Dr. M. Rostom Ali
Co-Supervisor
Department of Applied Chemistry and Chemical Engineering
Faculty of Engineering
University of Rajshahi
Rajshahi, Bangladesh.

Prof. Dr. Ranjit Kumar Biswas
Principal Supervisor
Department of Applied Chemistry and Chemical Engineering
Faculty of Engineering
University of Rajshahi
Rajshahi, Bangladesh.

Dedicated

To

My Parents

ACKNOWLEDGEMENT

The research work presented in this dissertation was investigated in the metallurgy and Electrochemistry Research Laboratory, Department of Applied Chemistry and Chemical Engineering, University of Rajshahi, Rajshahi, Bangladesh. Regarding the outcome of this thesis, I express my deepest gratitude, sincere appreciation indebtedness to supervisor **Dr. Ranjit Kumar Biswas and** co-supervisor **Dr. M. Rostom Ali**, Professors of the Department of Applied Chemistry and Chemical Engineering, University of Rajshahi, for their valuable suggestion, generous help with the experimental work, constructive criticism, encouragement and keen interest throughout the research work. I am so much grateful to Professor Dr. Dil Afroz Begum (Chairman) and all honorable teachers.

I cordially thank to Professor Atshushi Nishikata, Department of Chemistry and Ceramics Science, Tokyo Institute of Technology, Tokyo-152, Japan, for his kind assistance and cooperation in conducting XRD data of the raw samples.

I am also grateful to the all staffs of this Department. I am also grateful to Siddhartha Sankar Saha, Assistant professor, Department of Chemistry, Rajshahi University of Engineering and Technology, Rajshahi-6204, Bangladesh and Md. Moynul Islam, Lecturer, Dept. of Chemistry BAUET, Qadirabad Cantonment, Natore and Fellow of Electrochemistry Research Laboratory for their help during my research work.

I am also grateful to Iftekhar Md. Noor and Md. Muorshedul Alam (Senior Instrument Engineers, Research & Operation) of Central Science Laboratory, Rajshahi University for their kind co-operation to use pellet making machine and AAS in their laboratories.

I convey my deepest gratitude to the higher officials of the Ministry of Education and the training section of the Directorate of Secondary and Higher Education, Bangladesh, Dhaka for allowing me to conduct the research. I must gratefully thank to the Ministry of National Science and Technology for giving me their Ph. D. fellowship.

I am so grateful to my spouse Most. Nazneen Akhtar Banu who inspired and helped me to completed this Ph. D. research work. I am very much kind and grateful to my son Zarif and my daughter Arisha who sacrificed their love during the research period for a long time absence of residence. I am greatly indebted to my father, mother, sister, brother and all my friends.

The Author

ABSTRACT

Ilmenite and zircon used in the investigation were collected in a single lot from Bangladesh Atomic Energy Commission's Pilot Plant for separation of heavy minerals from beach sands at Cox's Bazar. The lead sulphate was collected on dismantling of locally available waste lead-acid batteries. The ilmenite, zircon and lead sulphate were characterized by XRD and EDAX analyses. The electrochemical dissolution technique was used to investigate on the dissolutions of ilmenite, zircon and lead sulphate in sulfuric acid solutions, sodium hydroxide solutions and nitric acid solutions, respectively, at various conditions.

Cyclic voltammetry was used as a reliable source to determine the dissolution potentials of ilmenite, zircon and lead sulphate. It was seen from the cyclic voltammetric studies that the dissolution of ilmenite was very difficult without the addition of graphite powder in ilmenite. The effects of ilmenite-graphite ratio, acid concentration and temperature on cyclic voltammograms were investigated to understand the dissolution process of ilmenite. The investigated results showed that the dissolution rate of ilmenite ($FeTiO_3$) was low at low applied reduction potentials (<-0.40 V) and temperatures (<60° C). However, the dissolution rate was increased at more negative applied reduction potentials and higher temperatures. The dissolution rate was also increased on increasing acid concentration up to 1 mol dm^{-3}; and at more acid concentration and higher reduction potential, it was decreased due to the starting of H_2 gas evolution which eventually decreased the active surface area of pellet by adsorption. The activation energy (E_a) was estimated as 50±10 kJ mol^{-1} in the higher temperature region (htr) and ~15±5 kJ mol^{-1} in the lower temperature region (ltr). The value of activation energy suggested the process to be diffusion controlled at ltr and chemically controlled at htr.

The dissolution of zircon fraction could not be obtained in NaOH solution without the addition of graphite in zircon fraction due to low conductivity of zircon fraction.

The effects of zircon-graphite ratio, acid concentration and temperature on cyclic voltammograms were investigated to understand the dissolution process of zircon. The dissolution rate of zircon ($ZrSiO_4$) was low at low applied reduction potentials (<-0.30 V) and temperatures (<75° C). At more negative potentials and higher temperatures, the dissolution rate of zircon was increased through increasing rate of the reduction of Zr^{4+}. The dissolution rate was also increased on increasing alkali concentration up to 3 mol dm^{-3}; and at higher alkali concentration and higher reduction potentials, it was decreased due to the starting of H_2 gas evolution which eventually decreased the active surface area of zircon pellet by adsorption. The values of E_a in the higher (~ 85° C), intermediate (~70° C) and lower (~30° C) temperature regions are 23±1 kJ mol^{-1}, 45±10 kJ mol^{-1} and 20±5 kJ mol^{-1}, respectively. The values of $E_{a,}$ at low temperature region suggested that the process was diffusion controlled; and with the rise of temperature, the diffusion layer/film was anyhow destroyed to convert the process to be chemical controlling at ~70° C. Low value of activation energy at higher temperature was an indicative to two parallel reactions.

The dissolution of storage battery waste product ($PbSO_4$) could not be obtained in HNO_3 solution without the addition of graphite in battery waste due to low conductivity of battery waste product ($PbSO_4$). The dissolution rate of lead from storage battery waste product ($PbSO_4$) was low at applied reduction potentials up to -0.52 V and temperatures below 60° C. At higher temperatures, the dissolution rate of lead from battery waste product ($PbSO_4$) was increased through increasing rate of the reduction of PbO_2 and $PbSO_4$. The dissolution rate of lead was also increased on increasing HNO_3 acid concentration up to 1 mol dm^{-3}; and at more higher HNO_3 concentration (>1.0 mol dm^{-3}), the slow increasing rate of the dissolution of lead from storage battery waste was observed due to the starting of H_2 gas evolution resulting in the decrease of the active surface area of storage battery waste pellet by adsorption. The values of E_a in the higher (>60° C)) and lower temperature regions (<60° C) were estimated to be 45±5 kJ mol^{-1} and 2±1 kJ mol^{-1}, respectively. The values of E_a suggested the existence of a diffusion film at lower temperature which was believed to be destroyed at higher temperature. At lower temperature region, the process was diffusion controlled and with the rise of temperature, the process became chemically controlling.

LIST OF ABBREVIATIONS

The following acronyms and abbreviations are used throughout this thesis:

$C/C_{(gr)}$	Graphitic carbon
° C	Degree celcius
θ	Degree
ρ	Density
η	Viscosity
ΔH	Enthalpy change in reaction
μm	Micro-meter
ΔS	Entropy change in reaction
A	Surface area
AAS	Atomic Absorption Spectrophotometer
AZST	Acid zirconium sulphate tetrahydrate
b.p.	Boiling point
BAEC	Bangladesh Atomic Energy Commission
C_1	First reduction wave
C_2	Second reduction wave
CV	Cyclic voltammetry
D	Diffusion coefficient
E_a	Activation energy
EDAX	X-ray energy dispersive spectroscopic analyses
E_p	Peak potential
GPE	Graphite paste electrode
htr	Higher temperature region
i_p	Peak current density
IPS	Instant Power Supply
ltr	Lower temperature region
m.p.	Melting point

mol dm^{-3}	Mole per cubic decimeter
n	Number of electron
P_{a1}	First oxidation peak
P_{a2}	Second oxidation peak
ppm	parts per million
rpm	Rotation per minute
SEM	Scanning electron microscope
sp. gr.	Specific gravity
TBP	Tributyl phosphate
TGA	Thermogravimetric analysis
v	Scan rate
XRD	X-ray diffraction

CONTENTS

LIST OF TABLES

LIST OF FIGURES

CHAPTER 1
INTRODUCTION

1.1 Ilmenite Ore and its Occurrences

1.2 Ilmenite in Beach Sand

1.3 Zircon and its Occurrences

1.4 Zircon and Ilmenite in Bangladesh

1.5 Sources of Lead Sulphate

1.6 Conventional Methods for Ilmenite Processing

1.7 Conventional Methods for Processing of Zircon

1.8 Conventional Methods for Processing of $PbSO_4$

1.9 Role and Position of Titanium Dioxide

1.10 Role and Position of Zircon/Zirconia

1.11 Role and Position of Lead Sulphate

1.12 Electrometallurgical Methods

1.13 Electrochemical Techniques

1.14 Electrochemical Dissolution of Ores

1.15 Graphite Paste Electrode (GPE)

1.16 Thesis Outline

1 INTRODUCTION

1.1 Ilmenite Ore and its Occurrences

Ilmenite is the most commonly available ore for titanium (the ninth most common abundant element in the earth's crust). It is the titanium-iron oxide mineral with the idealized formula $TiFeO_3$. It is magnetic next to magnetite, black or steel-gray solid. From the commercial perspective, ilmenite is the most important ore of titanium[1]. Ilmenite crystallizes in the trigonal system. The ilmenite crystal structure consists of an ordered derivative of the corundum structure; in corundum all cations are identical but in ilmenite Fe^{2+} and Ti^{4+} ions occupy alternating layers perpendicular to the trigonal c axis as shown in Fig. 1.1. Another ore mineral of titanium is rutile (one of the three crystalline forms of titanium dioxide TiO_2) which is widely used for titanium extraction.

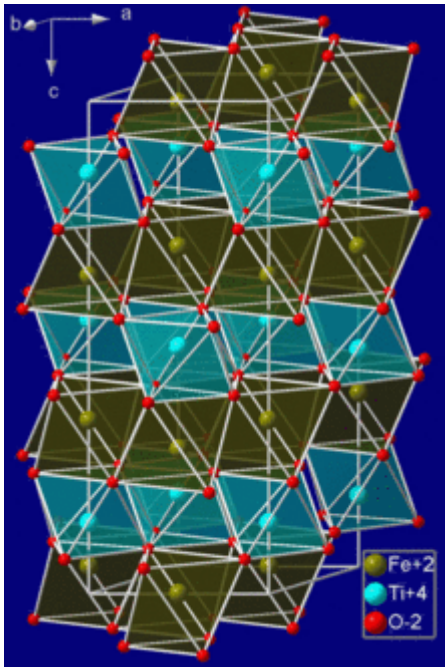

Figure 1.1 Model crystal structure of ilmenite

A number of countries all over the world including Bangladesh have ilmenite deposit. Rockey deposits of massive ilmenite containing about 18% titanium dioxide have been found in Virginia[2-5] and North Carolina State of the USA[6]. However, this form of ilmenite is not so common in the earth. The Ilmen Mountain (from which the mineral is named) of the USSR[7] have a remarkable reserve of ilmenite containing about 14% titanium dioxide, 54% iron and 0.60% vanadium pentoxide.

The ilmenite-magnetite deposit is rather more common than the massive ilmenite deposit in the world. Ilmenite-magnetite deposits containing 7-23% titanium dioxide are found to occur in the Adirondack Mountain of New York State.[8] On the other hand; the Sandford Hill in Essex country[9] contains ilmenite-magnetide deposit having 18% titanium dioxide. Moreover, the Lake and Cook Counties of Minnesota[10] have deposits containing 3-20% titanium dioxide. Huge deposits of ilmenite-magnetite are also available in South Africa[11], Mozambique[12], Belgium, Congo and Madagascar. These deposits contain an average of about 11% titanium dioxide. In Quebec Province of Canada[13], mixed deposits of ilmenite-magnetite and ilmenite-hematite have been found. In Europe, Norway[14] has the richest deposit (42% titanium dioxide) at her south-western part. The important Asian deposits are in the Arabian Desert[15], India[16], Korea, Manchuria and Indo-China.

Rutile, the other ore for titanium, is found abundantly in Algeria, Brazil[17], Cameroon[18], Greenland (East)[19], Madagascar[20], Quebec[21], South Norway and USSR (Kyzylkum)[22]. The rutile content of these deposits varies within 5-20%.

1.2 Ilmenite in Beach Sand

Almost all black sands of sea beaches on the earth have mineral values. Some streams of black sands also possess this character. Due to their high stability, ores of titanium are left behind in the weathered rocks and in the course of time due to erosion and other natural phenomena are accumulated in the black sand of streams and beaches. The mineralogical composition of the beach sand is related with the composition of the weathered rocks nearby. The heavy mineral contents of these sands are within 3-50% (such as ilmenite, zircon, monazite etc.).

The black beach sands of the Australian coast (Naracoopa, New South Wales to Queensland)[23], Argentina, Brazil (South–eastern coast)[24], Egypt[25], Guatemala, Italy, India (South-western coast), Japan[26], Malaysia, Mexico, New Zealand[27], Portugal, Srilanka[28], Senegal[29], USA (Florida[30], Arkansas[31], California), West Africa[32], Yugoslavia etc. have mineralogical values for a number of valuable metals like titanium, zirconium, thorium and lanthanides. So, it is clear that beach sands are sources of many valuable metals. The beach sands can be effectively fractionated into different portions by various comminution and concentration process.

The ilmentie fraction obtained from beach sands generally contains oxides of Ti (IV) and oxides of Fe (II and III) in variable proportions depending on the place of occurrence. Besides these oxides other metallic oxides are also found to occur. Table 1.1 shows the percentage of different metallic oxides and silica in the ilmenite fractions obtained from different coastal areas of the world.

Table 1.1 Composition of ilmenite fraction of the beach sands obtained from different coastal areas of the world[33]

Origin	Percentage of						
	TiO_2	FeO	Fe_2O_3	MnO	V_2O_5	Cr_2O_3	SiO_2
BRAZIL	~55.10	~17.15	~23.40	~0.50	~0.13	~0.30	1.40
CANADA : Ivry	37.50	~30.30	~20.00	~0.04	~0.36	~0.15	~2.00
INDIA: Travarncore	~57.05	~18.55	~19.10	~0.45	~0.16	~0.10	~1.23
MALAYSIA	~52.85	~36.90	~4.76	~3.56	~0.04	~0.02	~0.75
NORWAY	~41.06	~34.17	~15.06	~0.31	~0.36	~0.06	~2.46
PORTUGAL	52.20	42.10	-	5.00	-	-	0.27
SENEGAL	~55.36	~10.75	29.25	0.76	0.27	~0.27	~1.10
USA:							
California	48.20	39.10	10.40	0.10	0.05	0.03	1.40
Florida	52.00	-	-	-	-	-	-
Georgia	34.40	11.30	7.80	1.89	-	-	43.10
New York	44.30	36.70	4.40	0.35	0.24	0.001	3.20
Roseland	51.40	37.90	1.60	0.70	0.07	-	4.60
Virginia Piney River	~44.53	~36.76	~14.26	~0.31	~0.17	~0.14	~1.60
USSR	44.00	31.40	16.90	0.72	-	0.05	1.84

1.3 Zircon and its Occurrences

Zircon is the most commonly available ore for zirconium (the eighteenth most abundant element and the ninth most abundant metal in the earth's crust). The name zircon derives from the Arabic word Zargon, meaning vermillion or perhaps from the persian zargun, meaning golden colored. These words are corrupted into "Jargoon", a term applied to light-colored zircons. Yellow zircon is called hyacinth, from a word of

East Indian origin. In the middle Ages, all yellow stones of East Indian origin were called hyacinth but today this term is restricted to the yellow zircons.

The natural color of zircon varies between colorless, yellow, golden, red, brown and green. Colorless specimens that show gem quality are used as a popular substitute for diamond, these specimens are also known as "Matura Diamond".

Zircon is available in abundant quantities in concentrated form and is the most important raw material for producing metallic zirconium, its alloys and its compounds[34-38]. It is found as an accessory mineral in silica rich igneseous rocks such as granite, pegmatite and nepheline syenite[34-36] and also in metamorphic and sedimentary rocks. Because of its high specific gravity of 4.6-4.8, zircon is found concentrated with other heavy mineral e.g. rutile, limonite, monazite, leucoxene and garnet etc. in river and beach sands with titanium and iron as the main constituents[37-39]. Zircon is commonly produced as a byproduct in the mining and processing of heavy mineral sands such as rutile and ilmenite[37]. Consequently there is no mine totally devoted to zircon[37].

Zircon is a common accessory mineral and found worldwide. Noted occurrences include in the Ural Mountains, Trentino (Monte Somma), Vesuvius (Italy), Arendal (Norway), Sri Lanka, India, Thailand, Ratanakiri (Combodia), Kimberly mines (Republic of South Africa) Madagascar, Renfrew Country (Ontario, Canada) and Grenville (Quebec, Canada). In the United States, zircon is available in Litchfield, Maine, Chesterfield, Massachusetts, Oragone and St. Lawrence Country (in Essex), New York, Henderson Country (in North Carolina), Pikes Peak district (Colorado) and Liano country (Texas).

The chemical name of zircon is zirconium silicate and its formula is $ZrSiO_4$. The crystal structure of zircon is tetragonal with high co-ordinated bisdisphenoids, ZrO_8 and low coordinated SiO_4[40, 41] as shown in Fig.1.2. Drawbacks to zircon processing is that it contains many impurity metals, especially radioactive impurities like U and Th[42, 43], which cannot be removed by acid leaching. Impurities are included in zircon lattice. The structure of zircon creates a safe habitate for the impurities.

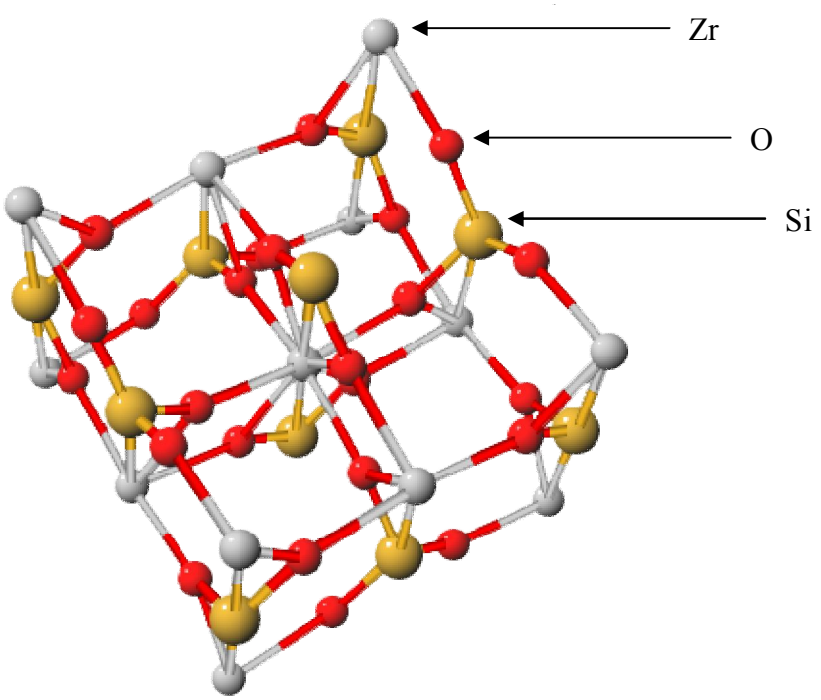

Figure 1.2 Model crystal structure of zircon.

Large crystals of zircon are seldom abundant. Their average size e.g. in granite rocks is about 200-300 μm but it can also grow up to sizes of several centimeters, especially in pigments. The world production zirconium minerals (zircon) in varies countries are given in Table 1.2.

Table 1.2 Zirconium mineral concentrates: world production (metric tons) by country [1, 2].

Country[3]	2001[4]	2002[4]	2003[e]	2004[e]	2005[e]
Australia	393000	412000	462000	441000	445000
Brazil[e.5]	20553	20000	29900	34855	35000
China[e]	15000	15000	15000	17000	17000
India[e]	19000	19000	20000	20000	2000
Indonesia[e]	250	250	250	200	200
Malaysia	3768	5293	3456	6886	3500
Russia[e.6]	6500	6500	6500	6500	6500
South Africa[e.7]	245000	274000	300000	302000	305000
Ukraine[e]	33600	34300	35000	35000	35000
United States	W	W	W	W	W
Vietnam[e]	8000	11000	13000	14000	14000
Total[8]	745000	797000	885000	877000	881000

[e] Estimated; [1]Revised; W: Withheld to avoid disclosing company proprietary; not included in total.

[1] World totals and estimated data are rounded to no more than three significant digits; may not add to totals shown.

[2] Includes data available through May 9, 2006

[3] Small amounts of zirconium concentrates were produced in various countries; however, information is not sufficient to estimate output.

[4] Reported figure

[5] Includes production of baddeleyite-caldasite

[6] Production of baddeleyite concentrate averaging 98% ZrO_2.

[7] Includes production of byproduct zircon from titanium sands mining and until 2002, 15000 to 20000 metric tons per year of baddeleyite from Palabora Mining Co. Ltd

[8] Does not include US data which are withheld to avoid disclosing company proprietary data.

It is seen from the table that Australia produces the highest amount of zirconium mineral concentrates and South Africa is the second and then Ukraine and Brazil. The total world production of zirconium mineral concentrates in 2005 was 881000 metric tons (excluding USA), which was all most similar to that in 2003 and 2004. Therefore, it can be said that the total world production is nearly constant for the last few years. Australia and South Africa produce about 85% of the world production excluding USA. In South Africa zircon is mainly collected from Richard's bay and Namakwa. The chemical analyses of zircon typical from three sources are provided in table 1.3

Table 1.3 Typical zircon chemical analysis* (concentration in mass percent)

Composition	Richard's bay zircon	Namakwa zircon	SARM13	Utah zircon
$ZrO_2 + HfO_2$	66.2	66.2	63.31	68.45
SiO_2 (total)	32.6	32.46	32.56	-
Fe_2O_3	0.05	0.05	0.187	<0.1
TiO_2	0.11	0.11	0.295	0.03
Al_2O_3	1.2	0.24	0.61	0.07
Cr_2O_3	<0.01	<0.01	-	<0.01
CaO	<0.05	0.05	0.14	0.02
P_2O_5	0.11	0.11	-	-
V_2O_5	0.01	0.01	-	-
MgO	-	-	440 ppm	<0.01
U	-	235 ppm	328 ppm	-
Th	-	165 ppm	300 ppm	-
U+Th	-	400 ppm	628 ppm	< 150 ppm

- Samples do not contain Na_2O and Y_2O_3.

The loss of the periodic crystal structure of a mineral due to the result of accumulation of radiation damage over time is termed as metamictization. Metamictization occurs in zircon as a result of the radioactive decay of U and Th incorporated during crystal growth, as well as from decay of their daughter products. The α-recoil nuclei directly amorphize the structure, whereas point defects created by α-particles, together with the tangent stress from adjacent amorphous regions, induce swelling of crystal structure. The terms 'amorphization', 'radiation damage', 'weathering', 'α-decay event damage of zircon are used for metamictazations of zircon. There are many studies on the metamictazation of zircon[44-51]. Due to different parts of the world, the chemical behaviour is expected to be at least little varied with zircon from different part of the world.

1.3.1 Baddeleyite

Baddeleyite is the naturally occurring monoclinic form of zirconia (ZrO_2) and is used as the second important source of zirconium. It always contains a small amount of hafnium oxide together with the impurities[40, 52]. It is found in Phalaborwa (South Africa) and Kola Peninsula (Russia).

1.4 Zircon and Ilmenite in Bangladesh

The longest sea beach in the world, (which belongs to Bangladesh (South-Eastern Coastal area)), is saturated with a huge reserve of heavy minerals like ilmenite, zircon, magnetite, rutile and garnet etc. The coastal belt covering the beach ranging from Sitakundu to Teknaf (about 250 km long) possesses such deposits. Recent investigations show that not only the coastal area but also some islands on the off share like Maheshkhali, Matarbari, Kutubdia and Nizhum Dwip[53] are rich in a large reserve of above heavy minerals as shown in Fig 1.3.

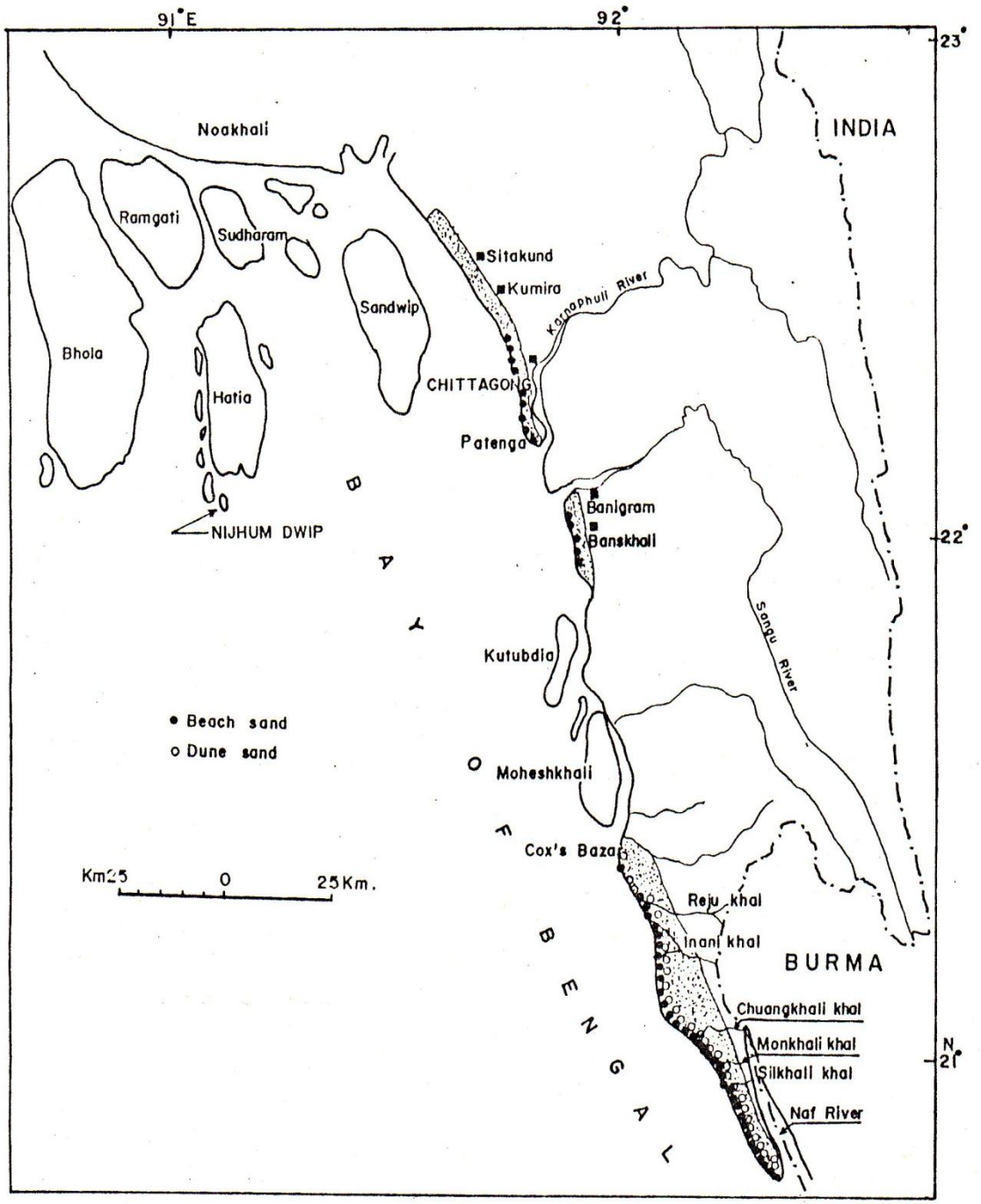

Figure 1.3 South-eastern coastal region and ilands of Bangladesh.

The total amount of heavy mineral contents in the raw sands varies from about 5 to 50%. Table 1.4 shows the percentage of some valuable minerals in the beach sands of different localities in Bangladesh. These coastal sands have been found to contain more than 10% heavy minerals which are in turn contains about 27% ilmenite[54].

Table 1.4 Percentage of some valuable minerals in the beach sands of different localities in Bangladesh

Locality	Percentage of							
	Ilmenite	Magnetite	Rutile	Zircon	Garnet	Monazite	Others*	Rest**
Badormokam[55]	3.80	1.50	0.10	0.37	-	0.001	11.77	82.46
Banskhali[56]	18.51	-	0.67	0.76	5.80	-	25.26	49.00
Cox's Bazar[57]	2.60	0.60	0.10	0.28	1.60	-	-	94.82
Maheskhali back dune[55]	2.64	0.024	-	0.68	2.08	-	-	94.57
Maheshkhali fore dune[55]	7.10	0.50	2.70	0.75	-	-	24.59	64.36
Nizhum Dwip[57]	5.20	1.12	0.33	2.32	3.75	0.16	11.50	75.62
Potengha[56]	15.00	-	0.90	2.66	3.50	-	20.96	56.98
Tekhaf-Inani beach[56]	0.30	-	0.02	0.07	0.20	-	2.22	97.19
Teknaf-Inani dune[56]	0.70	-	0.05	0.16	0.70	-	4.43	93.96

* Others include leucoxene, kyanite, epidote, amphiboles, biotite, apatite etc.

** The rest being the light fraction which contains mainly quartz (~90%), feldspar (~7%), mica (~0.5%) etc[58].

It is seen from the table that the beach sand of Banskhali and Potenga contains 16.75% ilmenite. Nizhum Dwip and Potenga contain 2.5% zircon. In Moheshkhali and Banshkhali the zircon percentage is ~0.7%.

The Beach sand exploitation centre of Bangladesh Atomic Energy Commission (BAEC) at Cox's Bazar, Chittagong has been succeeded in fractionating the raw beach sands of different localities into two fractions viz, (1) the light fraction (sp.gr.<2.9) and (2) the heavy fraction (sp. gr.> 2.9). Table 1.5 shows the average light mineral composition of different sediments types from Cox's Bazar coastal zone of the Bay of Bengal.

Table 1.5 Average percentage of light mineral composition (by volume) of different sediment types from Cox's Bazar coastal zone of the Bay of Bengal[59]

Sediment type	Quartz	Feldspar	Mica	Rock fragment	Glauconite
Beach sand	90.00	7.00	0.40	2.40	-
Dune sand	88.50	8.90	1.00	1.60	-
Storm ridge sand	99.40	0.50	-	-	-
Sand stone	83.20	11.20	2.50	3.10	0.05

Table 1.6: shows the percentage of heavy minerals identified and counted in different sediment types from Cox's Bazar coastal zone of the Bay of Bengal.

Table 1.6 Percentage of heavy minerals in different sediment types from Cox's Bazar Coastal zone of the Bay of Bengal[60]

Mineral	Sediment types (%)			
	Beach Sand	**Dune Sand**	**Storm Ridge sand**	**Sand stone**
Apatite [$3Ca_3(PO_4)_2.CaF_2$]	1.10	-	-	-
Epidote [$HCa_2(Al.Fe)_3Si_3O_{16}$]	11.20	9.80	0.30	4.60
Garnet ($A_3^{2+}B_2^{3+}Si_3O_{12}$)	16.90	22.10	2.70	13.20
Ilmenite ($TiFeO_3$)	17.50	19.50	25.00	7.30
Monazite ($Th.Ln\ PO_4$)	-	-	2.90	-
Leucoxene [(Ca or Na)(Ti, Al, Fe or Nb) (O.OH or F)SO_4]	0.30	-	-	-
Magnetite (Fe_3O_4)	3.50	7.75	64.50	-
Rutile (TiO_2)	0.70	-	-	-
Pyroxene	3.50	-	-	1.90
Sphene, ($CaTiSiO_5$)	2.20	-	-	1.00
Zircon ($ZrSiO_4$)	2.50	3.14	4.80	2.20

Besides these, other heavy mineral such as amphiboles [$M_x(SiO_3)_y$; M= Ca, Mg, Fe and alkali metals], kyanite [$Al_2O_3.SiO_2$], mica [$X_2Y_{4-6}Z_8O_{20}(OH.F)_4$; where X= K, Na or Ca; Y= Al, Mg or Fe; Z= Si or Al], amphiboles [XY_2Z_5(Si, Al, Ti)$_8O_{22}(OH.F)_2$; X= Na^+, K^+; Y= Na^+, Ca^{2+}, Fe^{2+}, Li^+, Mn^{2+}, Al^{3+}, Mg^{2+}, Z = Fe^{3+}, Mn^{3+}, Cr^{3+}, Al^{3+}, Ti^{4+}, Fe^{2+}, Li^+, Mn^{2+}.] staurolite [$Fe_2Mg_2Al_9O_6(SiO_4)_4(O.OH)$], sillimanite ($Al_2SiO_5$), zoisite ($Ca_2Al_3Si_3O_{12}(OH)$], biotite $K(Mg,Fe)_3.AlSi_3O_{10}(F.OH)_2$] etc. of variable amounts are also present in different sediment types.

The ilmenite fraction obtained by proper fractionating the raw beach sand of Bangladesh has been analysed to get its composition. Analysis has been performed at home and in Australia. However, the analysis results give different composition of ilmenite fraction.

Table 1.7 shows the composition of Bangladesh beach sands analysed in Australia[61] and at home[62].

Table 1.7 Composition of ilmenite of Bangladesh beach sands

Constituent	% composition analysed in	
	Australia	**Home**
TiO_2	38.50	29.46
Fe_2O_3	25.62	47.48
FeO	29.75	15.00
SiO_2	1.20	2.56
P_2O_5	0.03	-
MnO	1.30	0.43
Cr_2O_3	1.08	0.114
MgO	-	0.47
Al_2O_3	-	0.41
ThO_2	-	0.046
ZrO_2	-	15.78

It is clear however that in the second analyses, zirconia fraction has not been separated from the ilmenite fraction. Although the analyses are not identical, it is certain that the ilmenite fraction obtained from the beach sands of Bangladesh contains a good proportion of recoverable titanium with considerable proportion of chromium and manganese, which cause a bad coloring effect on the product, TiO_2 when conventional sulphate process being used for the processing of ilmenite obtained from our sea-shores. So, it goes without saying that the beach sands of Bangladesh have a great potential for ilmenite if a method can be developed. For its proper utilization a process other than conventional sulphate process needs to be developed.

1.5 Sources of Lead Sulphate

The lead-acid batteries represent about 60% of batteries sold in the entire world[63-65]. Lead is a material very easy to recycle and, provided that adequate procedures are implemented, the final product (secondary lead) is indistinguishable from the primary lead produced from ores. About 50% of the lead consumed worldwide is derived from recycled and reused materials[66].

The recovery of metals from metal scrap has the advantage that it is easier and for less energy dependent than the production of primary lead from ores. The production of

recycled lead requires 35-40% of the energy necessary to produce lead from ores. In addition, the recovery of lead decreases the lead dispersion in the environment and preserves the mineral reserves for the future. It is estimated that at least 85% of lead-acid batteries are recycled[66, 67].

A large number of lead accumulators are used in vehicles and IPS (Instant Power Supply) units in Bangladesh. Lead in storage battery is ultimately converted to lead sulphate on repeated charging and short-circuiting within a few months/years by the following reaction:

$$Pb + PbO_2 + 2H_2SO_4 \underset{\text{discharging}}{\overset{\text{charging}}{\rightleftharpoons}} 2PbSO_4 + 2H_2O$$

When charging-short circuiting is stopped, it is treated as a damaged material. It is reported that almost one hundred thousand lead storage batteries are required annually in Bangladesh[68], and the demand is steadily increasing. These are obtained either by direct import or assembled here by importing necessary components from abroad. Perhaps same numbers of batteries are gone out of order each year.

It is well known that there is no lead source in Bangladesh. So, all the lead containing materials are imported from abroad. In our country lead compounds are imported worth about one core (Taka) each year[69]. If a proper technology could be developed for the recycling of lead from used batteries a heavy dependence of lead compounds on external sources can be eliminated and at the same time, the pollution hazard of waste lead sulphate obtained from the condemned batteries can be controlled especially in the city environment. The dissolution of $PbSO_4$ is a chemical problem. It can be dissolved in expensive ethanolamines and the leached solution can be easily treated to obtain Pb-oxide which in turn may be reduced to metallic lead. So the waste lead accumulator ($PbSO_4$) has a great potential for lead if a method can be developed.

1.6 Conventional Methods for Ilmenite Processing

As pointed out earlier, the beach sand is a potential source of many metals, particularly of titanium and zircon, and beach sand can be effectively fractionated into different parts (one part being rich in a particular mineral) by various combination of concentration processes like float sink using a heavy liquid medium (e.g. bromoform,

sp. gr. 2.85), magnetic separation and electrostatic separation. The ilmenite fraction often obtained from the beach sands contains mainly titanium dioxide, ferrous oxide and ferric oxide in variable proportions depending on the place of occurrence. Besides the above oxides, ilmenite may contain some silicon dioxide, manganous oxide, zirconium oxide, chromium oxide, cobalt oxide, magnesium oxide etc.

There are two viable techniques for the processing of ilmenite in the production of titanium dioxide from ilmenite, namely-

i) The conventional sulphate process

ii) The conventional chloride process.

Sulphate process is the most commonly practiced method for titanium dioxide production. Prior to 1959, this was the only method for the production of pigment grade titanium dioxide. However, now-a-days another competitive method known chloride method has been developed by DuPont Company of the USA. The titanium dioxide obtained by chloride process has superior qualities and is potentially a lower cost process than the sulphate process.

For the production of titanium dioxide by either of the processes, the names of the leading companies are American Cyanamid, DuPont, Kerr McGee, Glidden Co., National lead and New Jersey Zinc company of the USA; British Titan products of the Great Britain and Laporte Industries of the Australia. In India, two units are also manufacturing titanium dioxide by making use of ilmenite. They are Travancore Titanium Product Ltd. and Dhrangadhra Chemical Works Ltd.

Western Australia holds over 70% of the world production capacity of synthetic rutile[70], which is used as a feed stock for the manufacture of pigment grade TiO_2 via the chlorination route[71]. The present world production of titanium dioxide is more than two million tons per annum.

The sulphate and chloride methods demand separate raw materials. For sulphate process, the material is ilmenite but not rutile as it is not attacked appreciably by sulphuric acid of any concentration; whereas, the chloride process prefers natural rutile or a mixture of rutile and ilmenite or beneficiated ilmenite to avoid excessive chlorine

requirement and waste handling. Certain other restrictions should be noted here. Ilmenite with high chromium content cannot be used in the sulphate process, because of the deterioration of the color of the product by the presence of chromium compounds. On the other hand magnesium, manganese and other alkaline earth metals in the starting material may cause operational difficulties in the chloride process. For either process, however, less sulphuric acid or chlorine is required and less by-products or waste products are formed with increasing percentages of titanium dioxide in the feed material.

Now-a-days, the feed material for the sulphate process has been significantly upgrated (w.r.t. titanium dioxide content) by the slag process. The uses of slag reduce both the quantities of sulphuric acid required and the waste produced. It is an electrothermal process which produces slag containing about 70% titanium dioxide. The slag is however easily attacked by sulphuric acid because of the fact that titanium exists as a mixed magnesium-iron titanate and not rutile.

For the manufacture of titanium dioxide the world supply of raw materials are at present: USA ilmenite 21.50%, Australian ilmenite 16.50%, Norwegion ilmenite 15%, other ilmenite 9.50%, Australian rutile 9.50%, synthetic rutile 1.50%, other rutile 1.50% and slag 25%. It is evident that the world supply of ilmenite is more prominent than that of rutile.

Table 1.8 Ilmente deposits which are being worked today in the world

Country	**Reserves of titanium bearing are (million ton)**	**Titanium dioxide content of deposit (%)**	**Titanium dioxide content of mineral after treatment (%)**
Canada	200-220	35	37
USA-New-York	100	17	43
Virginia	5	8	44
Florida	180	0.5-3	63
Norway	250	17	43
Finland	50	13.5	44
India	100	20-40	59
South-Africa	20	5	49
Australia	15	30	50-60

Since the natural rutile reserve is very small, the feed material of the chlorination method is synthetic rutile. Rutile can be synthesized from ilmenite by the following schemes.

SCHEME-I

$2FeTiO_3 + \frac{1}{2} O_2 = Fe_2TiO_5 + TiO_2$ (Oxidation)

$2Fe_2TiO_5 + C = 4FeO + 2TiO_2 + CO_2$ (Reduction)

$FeO + 2HCl = H_2O + FeCl_2$ (Partial leaching)

$2\ FeCl_2 + 2H_2O + \frac{1}{2} O_2 = Fe_2O_3 + 4HCl$ (Regeneration of leaching agent)

SCHEMS – II

$FeTiO_3 + Cl_2 + \frac{1}{2} C = FeCl_2 + TiO_2 + \frac{1}{2} CO_2$ (Reductive Chlorination).

$4\ FeCl_2 + 6\ CO_2 = 4Cl_2 + 2Fe_2O_3 + 6\ CO$ (Regeneration of chlorine).

In both scheme, products containing more than 92% titanium dioxide are produced.

1.6.1 The sulphate process

The typical analyses of three sources of raw materials commonly used for the sulphate process are given in Table 1.9

Table 1.9 Composition of ilmentite used for sulphate process

Constituent	Norwegian ilmenite (%)	Australian ilmenite (%)	Candian slag (%)
TiO_2	44	54.20	60.1
Ti_2O_3	-	-	8.30
Fe	-	-	0.20
FeO	34.60	23.30	12.60
Fe_2O_3	11.80	17.30	-
Cr_2O_3	0.08	0.04	0.02
V_2O_5	0.02	0.01	0.50
SiO_2	5.00	1.00	4.60
Al_2O_3	0.70	0.70	4.00
P_2O_5	0.04	0.08	0.03
MgO	3.70	0.20	5.00
MnO	0.30	2.00	0.20

Apart from the various impurity levels, the efficiency of extraction by sulphuric acid tends to be increased by an increase in the FeO to Fe_2O_3 ratio.

In this process, ground ilmenite or slag is digested with concentrated sulphuric acid (>95%, 60% excess for the stoichiometric requirement) at an elevated temperature; the resultant titanium and iron compounds are leached with water or dilute acid and the ferric ion is reduced to ferrous ion by the addition of scrap iron to crystallize out ferrous sulphate after clarification and cooling. After centrifugal separation of $FeSO_4.7H_2O$ crystals, the mother liquor is treated with steam for hydrolysis of titanyl sulphate. Some seed crystals are however added before hydrolysis. The hydrated titanium dioxide is precipitated. The precipitates are filtered, washed and calcined to produce TiO_2.

The overall efficiency of the process is over 80%. The sulphuric acid requirement is about 4-5 tons per ton titanium dioxide produced.

The waste and by-products from a plant producing 50,000 tons of pigment per annum by sulphate process may be as high as 140000 ton $FeSO_4.7\ H_2O$, 75000 ton strong acid (calculated on 100% purity), 40000 ton weak acid (calculated on 100% purity) and 83000 ton $FeSO_4$ (soluble, calculated as $FeSO_4.7H_2O$). The quantities of waste products are however strictly related to the type of raw material used. Theoretically, it is possible to recover the sulphur value, from $FeSO_4.7H_2O$ or from the waste acid or alternatively convert them into saleable products. Unfortunately, neither of these processes is economic.

The degree of difficulty and cost involved in recovering sulphur values are due to the following-

a) The strong acid rejected from the process is between 10-20% strength. For re-use it must be concentrated to 96% strength. Since vast quantities of water have to be evaporated, this process is highly energy intensive.

b) During the evaporation step, metallic salts precipitated in the form of slurries are difficult to separate from the liquid. Certain salts remain in solution even at high acid strength, and recycling of such salts leads to deterioration of color of the pigment.

c) High temperature roasting of the various salts is also energy intensive, and both this step and the acid evaporation lead to high quality gaseous emission of water vapor containing residual sulphur dioxide.

d) Process economics have been plagued with significant variations of fresh sulphur prices. Since 1973, energy costs have quadrupled. The ratio energy cost/sulphur value has fluctuated widely and recently in a worsening direction. The situation is further complicated because in the production of sulphuric acid from sulphur a very significant quantity of energy is released which can be easily utilized in the associated titanium dioxide plant.

Many paper studies have been made on alternative processes. Mention will be made here only of the limited numbers which have achieved some commercial application by 1976.

a) Neutralization with limestone/lime and dumping of neutralized products- this require large scale availability of limestone and disposal areas for the neutralized solids. It is operated by one small company.

b) Neutralization with limestone to produce saleable gypsum-this requires availability of limestone and suitable market. It is operated on a small scale in the USA and Japan.

c) Neutralization with metallic iron in the production of beneficiated ilmenite. This is operated by one Japanese company, but leads to higher discharge of iron salts.

d) Limited quantities of $FeSO_4.\ 7H_2O$ are used for water treatment, or can be converted into soil conditioners.

e) Production of iron oxide pigments from $FeSO_4.\ 7H_2O$ this is operated in Germany.

f) Neutralization with other alkali to produce saleable by-products (ammonium sulphate, sodium sulphate). This requires close proximity to markets, because of relatively low values of these chemicals. It is operated by one Japanese company.

1.6.2 The chloride process

This process essentially consists of theproduction of $TiCl_4$ from the raw material, purification of $TiCl_4$ produced, and subsequent oxidation by oxygen enriched air to TiO_2.

Preparation of $TiCl_4$ is carried out by chlorination of the raw material in a reducing atmosphere at about 950° C:

$$2TiO_2 + 3C + 4Cl_2 = 2TiCl_4 + CO_2 + 2CO$$

The Combustion of $TiCl_4$ in oxygen enriched air starts at 1000° C and once initiated the temperature rises sharply to ~ 1500° C.

$$TiCl_4+O_2+N_2 = TiO_2+2Cl_2+N_2$$

During reductive chlorination, other oxides present including FeO and Fe_2O_3 are also converted to respective metal chlorides. Although many methods claim the economic recovery of Cl_2 from $FeCl_2$, there is no plant in operation at the present time which uses ilmenite directly as raw materials. The chlorination reaction is usually carried out in a fluid bed reactor and the out coming gas consists of the vapour of titanium and the other impurity metal chlorides, graphite monoxide and graphite dioxide (unchanged chlorine gas is seldom mixed with exit gas). The vapour is condensed and the most impurities are removed as dry solids. Excepting VCl_5 all metal impurity chlorides can effectively be removed from $TiCl_4$ by fractional distillation. For separation of VCl_5, H_2S gas should be passed into the crude $TiCl_4$ solution to reduce vanadium to its lower valency state.

1.7 Conventional Methods for Processing of Zircon

The processing of zircon is a difficult task for its chemical inertness. A large number of works are available in journals as well as patents on various routes to process zircon for zirconia (ZrO_2). The works on this line have been started since the discovery of zirconium by Klaproth in 1789. With few examples of very old works, the works those have been reported within the last 50 years will be summarized below under process, headings.

1.7.1 Chlorination process

On pelletization of milled zircon with coke, it is directly chlorinated by chlorine gas in a fluidized bed reactor at 800-1200° C to produce $ZrCl_4$ and $SiCl_4$ (van Arkle deboer method)[72-77] as represented by following reaction:

$$ZrSiO_4 + C + 4Cl_2 \xrightarrow{\sim 1000\,^\circ C} ZrCl_4 + SiCl_4 + 4CO$$

The reaction is endothermic[72-76]. Zirconium tetrachloride is distilled and collected in a condenser at almost 150-200° C [71-73] and silicon tetrachloride at ~10-20° C in a secondary condenser. The condensed $ZrCl_4$ containing impurites like $AlCl_3$, $TiCl_4$, $FeCl_3$ and $SiCl_4$ can be heated to 900° C to form ZrO_2 (impure) [42, 43]. Otherwise, it is hydrolysed to $ZrOCl_2.8H_2O$, which on addition of NaOH solution produces $ZrO_2.nH_2O$ as precipitate. This precipitate can be dried at 85° C followed by calcination to get ZrO_2[42, 43, 72]. As an alternative, $ZrOCl_2.8H_2O$ can be crystallized at 20-65° C which can be filtered, dried (85° C) and calcined to ZrO_2[72].

1.7.2 Fusion Process

Zircon can be fused with NaOH or Na_2CO_3 in 1:4 or 1:2 ratio respectively, at ~ 700° C (1000° C for Na_2CO_3) to produce sodium zirconate and sodium silicate [42, 72, 73, 74, 78-81] according to the following reactions:

$$ZrSiO_4 + 4NaOH \rightarrow Na_2ZrO_3 + Na_2SiO_3 + 2H_2O\uparrow$$

$$ZrSiO_4 + 2Na_2CO_3 \rightarrow Na_2ZrO_3 + Na_2SiO_3 + 2CO_2\uparrow$$

The fused product is treated with water. Sodium silicate is dissolved, whereas, sodium zirconate is hydrolyzed to soluble NaOH and insoluble hydrous zirconia [72-74]. Hydrous zirconia is separated by filtration. Numerous ways exist on how to treat the hydrous zirconia to produce zirconia of different purities.

The hydrous zirconia can be simply fired to zirconia. Otherwise it is dissolved in HCl to form $ZrOCl_2$ solution which on crystallization produces $ZrOCl_2.8H_2O$ crystals. This may be dried and calcined to produce zirconia. But the high purity zirconia can be produced by the de wet process [82-85]. In this process, zirconyl chloride solution is treated with H_2SO_4 and crystallized to get the crystal of acid zirconium sulphate

tettahydrate (AZST) free from impurities. The AZST crystals are washed, dried and calcined at 1000° C to very pure zirconia[85].

1.7.3 Carbidizing process

Carbidizing of zircon by C, CaC_2, CaO+C, petroleum coke etc. have been studied by several workers[86-93]. Using any of these reagents, particularly coke, zircon is converted into carbide in an open top electric arc furnace at ~2500° C. Insufficient reagents is used so that SiO is not reoxidized and vaporized[74].

Except the techniques mentioned above, the following fusion of zircon by very early workers has been reported.

i. $KOH/K_2CO_3 + KOH$ [94, 95]

ii. $K_2CO_3 + K_3BF_6$ [96]

iii. $Na_2CO_3 + S/NaOH + Na_2CO_3$ [97]

iv. Alkali metal hydroxide/alkali earth graphiteite + $NaCl/CaCl_2$ [98]

v. $KHSO_4$ [99, 100]

vi. KHF_2 [101] etc.

1.8 Conventional Methods for Processing of $PbSO_4$

As pointed out earlier, the lead accumulator is used in motor vehicles in Bangladesh. On using Pb and PbO_2 are gradually converted into $PbSO_4$. There are some techniques for processing of $PbSO_4$, generated by waste lead accumulators. The techniques are as follows:

1.8.1 Reduction process[102]

The lead sulphate is reduced by sulphide of lead sulphide (PbS, galena) to metallic lead. The molten lead is drawn off and further purified:

$$PbSO_4 + PbS = 2Pb + 2SO_2$$

1.8.2 Qualitative lead extraction by EDTA[103]

Lead sulphate is highly soluble in EDTA saturated solution, by the formation of Pb-EDTA complex:

$PbSO_4 + EDTA \rightarrow Pb - EDTA + SO_4^{2-}$

The Pb-EDTA complex is colorless. The addition of cations (like Fe^{3+}) with EDTA complex formation constants higher than or near to the EDTA-Pb complex aims the displacement of lead from its EDTA complex, allowing its reprecipitation in the form of PbI_2[104]. This latter is a yellow salt of easy visual identification. From the cations evaluated, the only that caused the displacement of the lead from its complex with EDTA.

$Pb\text{-}EDTA\ (aq) + I^-\ (aq) + M^{3+} \rightarrow EDTA\text{-}M\ (aq) + PbI_2$

The tests were carried out in a qualitative way confirming the lead extraction by the formation of a yellow precipitate of lead Iodide.

1.8.3 Selective reduction of $PbSO_4$[105]

Selective reduction of $PbSO_4$ to PbS with graphite and flotation treatment of synthetic galena by the following reactions:

$PbSO_4 + 4C \leftrightharpoons PbS + 4\ CO\ (g)$

$PbSO_4 + 2C \leftrightharpoons PbS + 2\ CO_2\ (g)$

$PbSO_4 + 4\ CO\ (g) \leftrightharpoons PbS + 4\ CO_2\ (g)$

$PbSO_4 \leftrightharpoons \frac{1}{2} PbO.PbSO_4 + \frac{1}{2} S0_3\ (g)$

$PbSO_4 + \frac{1}{2} C \leftrightharpoons \frac{1}{2} PbO.PbSO_4 + \frac{1}{2}\ SO_2\ (g) + \frac{1}{2} CO\ (g)$

$PbSO_4 + \frac{1}{2} CO\ (g) \leftrightharpoons \frac{1}{2}\ PbO.PbSO_4 + \frac{1}{2} SO_2\ (g) + \frac{1}{2}\ CO_2\ (g)$

$PbSO_4 + \frac{1}{2} CO\ (g) \leftrightharpoons \frac{1}{2} PbO.PbSO_4 + \frac{1}{2} SO_2\ (g) + \frac{1}{2} CO_2\ (g)$

$PbSO_4 + CO\ (g) \leftrightharpoons PbO + SO_2\ (g) + CO_2\ (g)$

$PbSO_4 + \frac{1}{3} Pb \leftrightharpoons \frac{4}{3} PbO + \frac{4}{3} SO_2$

$PbO + CO\ (g) \leftrightharpoons Pb + CO_2\ (g)$

In this process the highest lead recovery could reach up to 75.32%.

1.9 Role and Position of Titanium Dioxide

The product titanium dioxide is widely used in paint, plastic, paper, textile and rubber industries. On the paint industry, it is by far the most effective white pigment in terms of covering power (refractive index, 2.5-2.9). Paint industries utilize about 62% in Europe and 51% in the USA of their total production of TiO_2. The plastic, paper, textile and rubber industries utilize about 13%, 8%, 5%, 3% respectively, in Europe and 23%, 10%, 3% (ceramics instead of textile), 3% respectively, in the USA. In these areas no substitute products represent serious threats to titanium dioxide's established position.

Nevertheless, a further break through is needed for the development of other methods for the manufacture of titanium dioxide from ores which do not meet the specification requirement for the sulphate or chloride process. For examples, our beach sand deposits cannot be used effectively by the sulphate process for high chromium content. Moreover both conventional process are energy intensive and criticized by waste disposal problems.

1.10 Role and Position of Zircon/Zirconia

Zircon is used as the main source of zirconium and zirconium chemicals. Zriconia (ZrO_2) is used as the second important source of zirconium.

The most important use of zirconium is in nuclear reactors for cladding fuel rods, for alloying with uranium and for reactor core structures because of its unique combination of properties. It has good strength at elevated temperatures, resists corrosion from the rapidly circulating coolants, does not form highly radioactive isotopes and withstands mechanical damage from neutron bombardment. The other applications are:

- The ground flour of zircon is commonly used in refractory paint for coating the outer surface of moulds.
- In steel production, zircon sands are used to produce ladle brick, coating mortars and as ladle nozzle fill.
- It can be used to make refractory bricks and blocks that are widely used in like kilns, glass melting furnaces and in hearths for containing molten metals due to its resistance to melt in high temperatures.

- It is used to produce zirconia and zirconia alumina abrasive materials and to clear turbines in electrical generating plant.
- A micronized zircon has replaced more expensive tin as an opacifier in ceramic glazes and vitreous enamels due to its high refractive index (1.85).
- Zircon is also used in TV face plate glass.

1.11 Role and Position of Lead Sulphate

Lead seens to be the least glamorous of the metals of anitiquity. Because of its softness and lack of lusture, it found little application in weaponry or jewelry. Nevertheless, lead possessed other unique properties that were to make it one of the most useful industrial metals in Greek and Roman times. Because of its corrosion resistance and formability, it was extensively used in plumbing, building and ship construction, as well as for stationary. Its density and malleability made it attractive as plumbers and sinkers for fishing nets and lines. Its low melting point, further reduced by the addition of tin, ensured its use as solder in remote antiquity. The addition of lead to bronzes makes them easier to cast and result in what Pliny in Natural History called "statue metal". Because of its atomic configuration, large amounts of lead could be added to silicate glasses where it functioned as an opacifier or a colorant. Several compounds of lead are brilliantly colored and were valued as pigments since Paloelithic times[106].

The cumulative worldwide production of lead from the earliest times to the Fall of Roman Empire has been estimated to be about 39 million tons (above). The utilization of lead reached such an impressive level during Roman times that lead is often referred to as a “Roman metal”.The pervasive use of lead by Rome presumably led to considerable contamination of food and drink and the theory has been advanced by Gilfillan (1965)[107] that the decline of Roman civilization was orchestrated by endemic lead poisoning of the ruling class[105].

The most important use of lead is in storage batteries secondary cells. Only two of them the lead acid cell and the nickel-iron alkali cell, have been developed, and the former by reason of its higher voltage, compactness and cheapness is most commonly used. White lead is our most popular pigment because of its law cost, permanence, covering power and extreme whiteness. In cable covering, roofing it is used because of its great resistance to corrosion by the atmosphere, sulfur compounds, and underground

waters. As such it is also used in paper industry, sulfuric acid manufacture and as anodes in electrolysis. Lead is also used as type metal, red lead and litherage. Hand lead (1 to 4 percent antimony) has almost double strength of the pure metal and is much harder.

Being “self-lubricating” the metal is universally used for bearing in machinery while the some property confers free cutting properties on brasses and bronzes when present in small amounts. Recently this property has been taken advantage of in developing free cutting steel. For the high density, lead can be turned to advantage in ammunition, for small caliber projectiles, in naval vessels as balast, as counter weights in anti-aircraft artillery and in airplane rudders and airlines. Minor uses are for shot, antivibration pads for machinery, for expansion bolts, rope sockets, calking material, tank lining, protection from x-rays, heat treating baths and industrial flouring.

1.12 Electrometallurgical Methods

The name electrometallurgy is derived from the fact that the process/method utilizes electrical energy at some stages in the production of metal from its ore.

In some cases, for example, in the production of reactive metals such as alkali and alkaline earth metals, aluminium, chromium etc. pyrometallurgy is ineffective. This is due to necessity of high temperature and of powerful and expensive reducing agents to produce metals from their highly stable oxides salts. Moreover, they are expected to form metal carbides when graphite is used as reducing agent at high temperature. Again hydrometallurgical methods are not practical in these cases. This method finds successful applications in the production of these metals.

The process demands ore minerals (raw materials) of high purity. This is to avoid unsatisfactory operation and formation of low grade metal, which need further refining. Sources of the impurities are the mineral associates, fuels, fluxes, atmosphere and materials of the plant construction of the cell linings and from the electrode materials. So the electrode materials of the cell are chosen very carefully. The usual fire-refining methods are not suitable for the reactive metals. Sometimes the minerals are needed to convert to another more suitable form by chemical means. Although impurities usually modify the properties of the deposited metal to some extent but in a number of cases they are harmful. Some impurities (the precious metals) however, become an essential

constituent. Generally, it is necessary to remove the impurities within permissible limits. The electrode constituent materials are thoroughly purified before electrolysis. Minerals possessing reasonable melting point and conductivity are electrolyzed on their own, but often mixtures of salts are used. It is a necessary factor to maintain the density of the bath sufficiently greater or less than that of the molten metal. Once a bath is melted, it is usually kept hot enough by the heating effect of the electrolyzing current. The additions to the bath affect the decomposition of the metallic mineral on heating. Metal produced by electrometallurgy is of high purity and need no further treatment apart from melting and casting into ingots.

1.12.1 Different terms used in electrolysis

Electrometallurgy usually implies the electrolytic processes, so, the terminology of electrolysis are the terminology for electrometallurgy. Some important terms used in electrolysis are given below:

Decomposition Potential (Reversible): It is the difference of the (equilibrium) electrode potentials under the conditions of concentration, pressure and temperature obtaining, neglecting the resistance of the electrolyte and provided there is no polarization.

Dissolution Potential: Dissolution potential of a metal is the potential at which dissolution of the metal commences. So when a metal is made an anode and an external potential is applied, it will begin to dissolve as soon as it's potential (external) exceeds the reversible value by an infinitesimal amount. In other words, the dissolution potential of a metal when made an anode should be equal to its reversible (oxidation) potential.

Discharge or Deposition Potential: The discharge or deposition potential of a metal is the reverse of the dissolution (oxidation) potential. It is the potential at which metal deposition commences at the cathode.

All these potentials depend on the nature and concentration of the solution (electrolyte), activity of the ions in the solution (electrolyte) with respect to which the metal is reversible, nature of the electrode, temperature of the bath and current density.

These also depend on the solution pressure of the metal i.e. for cathodic deposition of a metal with high solution pressure requires more potentials than the practical values. This is due to the various simultaneous electrode reactions. In a working electrolytic cell the rate of cell reaction depends on the applied potentials i.e. greater the potential faster the reaction. If an electrolyte or electrode containing a number of different ionic species or metals is electrolysed and if there is no disturbing factors each ionic discharge or dissolution will occur as the appropriate potential is reached. The cathodic process where reduction takes place will proceed in the order of decreasing reduction potential or in the order of increasing oxidation potential. Similarly the anodic process will occur in the reverse order.

Over potentials: In metallurgical electrolysis, metal is liberated at the cathode and a gas at the anode. Due to the evolution of gases polarization occurs, causing higher potential requirement than theoretical value of potential of decomposition. The difference is known as the over potential for the concerned electrode. When hydrogen gas is liberated at the cathode, over potential caused by the evolution of this gas is called the hydrogen over potential and the over potential caused by the evolution of oxygen at the anode is called the oxygen over potential. However, the polarization depends on the nature of the electrodes.

The over potential depends on the nature of the electrodes, pH of the electrolyte, temperature and current density. It is generally influenced by the roughness as well as the purity of the electrode and decreased with the roughness of the electrode. With the increase of temperature the over potential is reduced and the change is approximately 2 mV per degree. The effect of pH of the electrolyte on hydrogen over potential is dependent both on the mechanism of the electrode process and on the distribution of ions immediately adjacent to the cathode surface, Addition of a neutral salt though does not change the pH of the solution but changes the hydrogen over potential.

Provided the conditions are such that the hydrogen is not removed by reaction with oxygen or other oxidizing agent, or by diffusion away from the cathode, the over potential increases with increasing current density. Hydrogen over potential also depends on the time of current passing through the cathode surface.

In an electrolytic process there may also arise another types of over potential as ohmic or resistance over potential and activation over potential. Ohmic over potential again depends on several factors, chief of which is the cell current and varies directly with it. It also depends on the nature and concentration of the electrolyte, stirring of electrolyte and electrode-electrode distance.

During electrolysis metal ions goes into solution at the anode and others are precipitated on the cathode. Due to slowness of diffusion, the concentration of metal ion is increased at the anodic vicinity and decreased on the cathodic vicinity. This concentration difference results in a concentration potential acting against the applied potential and is known as concentration over potential. However, this can be removed by agitating the electrolyte.

Efficiencies: Due to various losses, in practice larger amounts of electricity are required than the theoretical amounts. Efficiency of an electrolytic process is the actual amounts of metal ion to be precipitated or dissolved, divided by the theoretical amounts precipitated or dissolved and multiplied by 100. The current efficiency is the theoretical amount of electricity required divided by the actual amount used, and multiplied by 100. In an electrolytic process another kind of efficiency is considered namely, energy efficiency. The energy efficiency of an electrolytic process is the amount of electrical energy consumed in the production of unit quantity of the final recovered products. A common technical unit for energy efficiency is kWh/lb. or kWh/kg.

Current Density (C. D.): It is defined as the current per unit area of an electrode; it is generally expressed as amp. (A) or milliamp. (mA) per square cm. or per square dm.

Electrolyte: It is the conducting solution or fluid.

Electrolysis: The process of decomposition of compounds, either in the state of fusion or of solution, when electric current is passed through it, is termed as electrolysis.

Electrode: The metal plates or graphite/graphite poles by which current is conveyed to or out of an electrolyte is called the electrode.

Anode: Electrode through which current enters the electrolyte, and is connected to the positive pole of the current source.

Cathode: Electrode through which current leaves the electrolyte, and is connected to the negative pole of the current source.

Anolyte: The part of the electrolyte in the immediate vicinity of the anode is termed as anolyte.

Catholyte: It is the electrolyte in the immediate vicinity of the cathodic part of the electrolyte.

Anodic, Cathodic Reactions: The processes that take place at the electrodes (anode, cathode).

Overall Cell Reaction: It is the net chemical change that takes place in the system as a result of the electrode process.

Faraday: The amount of electricity (measured in Coulomb, the unit of electricity) carried by 1 g eq of any ion, gaseous or in solution, having unit charge is called Faraday. It is expressed by F. If z is the valence of an atom or radical, then the corresponding ion contains z g eq and hence must carry a charge of zF coulombs. Its numerical value is 96500 Coulombs.

According to Faraday's law, the quantity of the elements liberated at either the anode or cathode or going into the solution is proportional to the quantity of electricity that passes through the solution. Again a given quantity of electricity causes the amounts of elements liberated to be in the ratios of their respective chemical equivalents. In aqueous electrolytes, hydrogen with the metal ions is liberated at the cathode. The efficiency of the process is usually less than 100%.

There are many causes of apparent deviations from Faraday's laws i.e. of current efficiency below 100%. They are as follows:

a) Recombination of primary electrode products. If precautions are taken to prevent contact of the incoming electrode products this may be overcome.

b) Instability of primary electrode products.

c) Physical or chemical interaction between the electrodes/electrolytes and the electrode products. The electrode products can attack the electrode so as to shorten the electrode life. The electrode products may also react with the electrolyte causing contamination of the final product.

d) Unproductive simultaneous electrode reactions. These commonly arise from the deposition or dissolution of some extraneous substance present as an impurity or even as a necessary component of the electrolyte.

e) Generation of heat. The amount of heat produced in an electrolytic cell is directly proportional to the resistance of the current path and to the square of the current. Thus, the current efficiency is raised by an increase in conductivity of the electrolyte and by a decrease in current.

The electrolysis operation is accomplished by passing a direct current or a rectified alternating current through the cell. The source of electromotive force may be a storage battery.

1.13 Electrochemical Techniques

The electrochemical techniques under four main headings are discussed below:

1.13.1 Precipitation of metals from aqueous leach liquors by electrolysis using insoluble anodes

The technique embodies the preparation of an electrolyte enriched in metal ions and deposition of the metal from the electrolyte using suitable insoluble electrodes. Depending on the mode of electrolyte preparation and metal deposition the technique includes electrowinning, electroplating, electroforming and electrotyping, and metal powder production. In all these cases the purity of the electrolyte plays an important and vital role in the maintenance of a high current efficiency and physical nature of the deposit. Among the impurities, those at high concentration and with similar potentials under the existing conditions are likely to be going into the solution or be co-deposited. However electrolyte with high desired metal ion concentration produces sound deposits at high current density and reduces the tendency for co-deposition of impurities dissolved in electrolyte. Again, increasing amount of free acid in the electrolyte increases the conductivity of the electrolyte but at the same time evolution of hydrogen also increased, which decreases the efficiency of the cell.

In electrowinning technique the electrolyte is obtained by leaching of the ore mineral by hydrometallurgical treatment of the concerned ore mineral. Leaching is done after calcinations and/or roasting of the ore mineral, thus aqueous leach liquor of the metal is obtained. Generally, leaching is conducted in acid solution. Leach liquor after proper purification is electrolysed using insoluble electrodes. Metal is liberated at the cathode, which is then stripped to get pure metal. The spent electrolyte is pumped from the cell for adjustment of leaching agent concentration and is afterwards recirculated over fresh ore. The electrolyte, newly enriched in metal ions, passes again through the cell for the deposition of more metals. This cyclic process is often arranged for continuous large- scale operation.

There is another metal deposition technique in which metals are deposited on a basis metal but without winning is practised. The technique is called the electroplating and is used both for decoration and for protection of the basis metal from corrosion. The important part of the technique is to secure adherent and coherent coating on the basis metal with simultaneous continuity and uniformity. To achieve continuous and uniform deposition, it is necessary for the basis metal to be ductile, free from grease and corrosion products, and the deposits have to be fine grained and relatively pure. The grain of the deposit is controlled by attention to such variables as electrolytic composition, current density and temperature. Some electrolytes are corrosive towards the basis metal until there is a formation of a complete film of the deposited metal; as a result, poor adhesion with progressive contamination of the electrolyte is evident.

Simultaneous deposition of two different types of metals also is a common practice; this is attained by maintaining the potential of the electrode at a suitable value, common to that of different metal decomposition. Using metal deposition technique manufacturing of metal articles such as thin sheets, tubes, dies and variety of machine parts, and building up worn and damaged metal articles are also practised, the techniques are termed as electroforming and electrotyping.

In the production of metal powders this technique is very successful. Poor adhesion and cohesion of the electrodeposited metals are maintained on the cathode so that it can fall away into the electrolyte; this is done by increasing the cathodic current density.

1.13.2 Electrolytic extraction of metals from a fused-salt bath using insoluble anodes

Minerals are directly used in this method. Minerals in fused state are used to get the metal. The conductivity of a fused electrolyte is usually noticeably greater than the same material in aqueous solution at room temperature. The salts should have higher decomposition potential than the metal source or the metal may have a melting point below that of the salt, so that the metal can exist in molten state. Generally, a mineral is mixed with other compounds to bring down the melting point. The mixture of the molten mineral in other molten salt is then electrolysed using two insoluble electrodes. Minerals of chloride compounds are electrolysed using a graphite anode and an iron or steel cathode. The metal thus obtained is in molten state and according to the relative densities of the metal and salt floats on the surface of the melt or sink to the bottom of the cell. When the mineral in oxide form is electrolysed, oxygen is liberated at the anode, which consumes the anode. The product metal should have little adhesion to the cathode. Compounds are so chosen that compound itself will not be electrolysed in preference to or in addition to the main electrolytic process. For a poorly designed cell there is every possibility for the electrodes of being short-circuited by the floating or sinking molten metal layer. In order to overcome the difficulty, the liberated metal itself is made into the cathodes, which exist at the bottom of the cell and at a distance from the anode. Anodic effect characterized by marked increase in voltage and reduction in current, and formation of a metal fog decreases the efficiency of the process.

1.13.3 Extraction of extra pure metals from its crude form using soluble anodes in aqueous electrolytes

In some cases metals of extra purity are demanded. Pyrometallurgical or hydrometallurgical methods are unable to produce such metal purity. In these eases extra pure metals are produced by electrolysis. This is also known as electrorefining of metals. In this technique crude metals are made into the anode and a thin sheet of the same metal of high purity is used as the cathode. Solution of a salt of the same metal and acid containing identical anion is used as electrolyte. The electrodes are generally arranged vertically in parallel or multiple although bipolar electrodes in series are often used. The anodes have to be removed before they are completely dissolved. Usually, a coherent cathodic deposition is obtained in this technique. The more noble constituents

of the crude metal are left as an insoluble residue or slime at the anode. For successful operation, impurities in the crude metal are not to be anodically dissolved forming sludge, but if the necessity for dissolving arises, plating out on the cathode is not allowed. Relatively low decomposition potential is required in this technique. This is due to the fact that anodic and cathodic reactions are same but in opposite direction, and equal ionic strength and temperature in the anolyte and catholyte. In practice the cell voltage is usually less than one volt, although, several refining processes operate at less than half a volt across the cell.

1.13.4 Electrolytic refining with a fused salt bath, metal treated being in the form of a soluble anode

This type of technique has comparatively few applications. It is useful specially, for reactive metals. An example is the process used for making high purity aluminium.

1.14 Electrochemical Dissolution of Ores

In ore/mineral processing, electrochemical dissolution or electrochemical leaching technique for metal extraction has not yet been developed and reported works in this regard are not numerous. It is due to the fact that, most of the oxide minerals[108] and many sulphide minerals are either insulator (e.g. sphalente[109(a)], antimonate[109(b)], bournonite[109(c)], cinnabar[109(d)], orpiment[109(e)], proustite[109(f)], etc) or poor conductor (e.g. molybdenite[109(g)], pyrite[109(h)], enargite[109(i)], etc. However, some conducting minerals (sulphide minerals) are also available, as for example, pyrrhotite[109(j)], millerite[109(k)], pentlandite [109(l)], bornite[109(m)], arsenopyrite[109(n)] etc.

High conductivity of mineral makes it suitable to use as a conventional electrode and this can be used as a massive electrode in electrochemical investigation. Now-a-days for electrochemical investigation of non-conducting or semi-conducting mineral graphite paste electrode and graphite-paste electro active electrode is commonly practiced.

1.15 Graphite Paste Electrode (GPE)

Use of non-conducting or semi conducting ore mineral, as a conventional electrode is not practical. However, minerals can be made conducting by milling them with graphite or graphite powder and can be used for the electrochemical purpose.

Electrode thus made is called graphite paste electrode (GPE). Graphite paste electrode was first introduced by Adams in 1958[110] for organic polarography. Since then the GPE has mainly been used for analytical purpose for organic[111-113] as well as inorganic compounds[114-118]. The graphite paste electrode consists of the sample mineral, finely dispersed graphite or graphite and a binder. The binder can be conducting[119, 120] or non-conducting[121]. The electrochemical behavior of a GPE with conducting binder is quite different from a GPE with non-conducting binder. A GPE with conducting binder can be regarded as an inert electrode in the same sense as glassy graphite and platinum electrode. Therefore GPE is an alternative to various electrochemical purposes where conventional electrode method is not practical. Due to high polarization range and low residual current a graphite paste electrode possesses high sensitivity. This constitutes an advantage in comparison to other inert electrode, such platinum, which can be oxidized at anodic potentials and also has lower overpotential for the oxygen and hydrogen evolution reactions. The low residual current is due to the small double layer capacitance at the electrode-electrolyte interface. The hydrophobic binder used in GPE lowers the double layer capacitance. The capacitance of GPE, and consequently the residual current, decrease with the incoming density of the binder (the length of its molecular chain) used in the paste[122]. However, this is accompanied by a decrease on the role of the charge transfer processes taking place at the interface[123].

1.15.1 Graphite paste electroactive electrode

In mineral processing non-conducting and semi conducting minerals can be made highly conducting by mixing with graphite or graphite and the same time with pulverized metal powder and make it suitable to use as conventional electrode. A graphite paste electrode with electroactive materials introduced in to the electrode is termed as a graphite paste electroactive electrode (GPEE). In GPEE also conducting[124] or non conducting binder can be used. A GPEE may be used as a conventional electrode. Graphite paste electro active electrode with organic binder is highly hydrophobic, which lowers the rate of the reaction taking place at the electrode interface[125, 126] and penetration of the eletrolyte in to the electrode is unlikely. Thus the electrochemical reactions take place solely at the interface and the dissolution of the electro active material more or less stops after depletion of the outer layer of the paste[127]. In the case of a GPEE with conducting binder the electrochemical reactions

may take place at the electrode surface as well as inside the electrode bulk material and the electrochemical response originates mainly from the dissolved species.[128] Species with more noble potentials than graphite introduced into the paste may thus undergo redox reaction with the graphite pasticles, for example Fe^{3+} [129].

The investigated ore, ilmenite is also a non-conductor. So, its traditional electrochemical investigation could not be performed using it as massive electrode. The present study has been taken in order to investigate the electrochemical dissolution of ilmenite by making it conducting with graphite (from waste dry cell battery).

1.16 Thesis Outline

The beach sand of the south eastern part of Bangladesh contains huge amount of ilmenite together with zircon. The Pilot Plant of BAEC at Cox's Bazar has fractionated these minerals. Ilmenite can be used as source of pigment grade TiO_2 or Ti- bearing alloys for aero-space industry. On the other hand, zircon is also a valuable mineral and can be used as a source of zirconia (ZrO_2) which has diversified applications. The processing of ilmenite and zircon faces difficulty due to their chemical inertness. Once they are solublized, the methods are available to get TiO_2 and ZrO_2 from the leach solution. Likewise, a huge number of lead accumulators are used in motor vehicles of Bangladesh. Waste lead-accumulators create environmental pollution. In these waste accumulators, lead exists as sulphate. The dissolution of $PbSO_4$ is another chemical problem. It can be dissolved in expensive ethanolamines and the leached solution can be easily treated to obtain Pb-oxide which in turn may be easily reduced to metallic lead.

The main purposes of this study are electrochemical dissolution of ilmenite, zircon and lead waste (lead sulphate) in acid or alkali solutions.

The dissertation consists six parts, which are summarized as follows:

Chapter 1: Introduction

The general discussion and conventional methods for processing of ilmenite, zircon and lead sulphate and electrometallurgical methods are described.

Chapter 2: Literature Review

Literatures reviewed are described in this chapter.

Chapter 3: Objective of the present investigation

The main objectives are described in this chapter.

Chapter 4: Materials and Methods

The sources of chemicals, preparations of different solutions, and basic principles of cyclic voltammetry, spectrophotometry & Atomic Absorption of spectrophotometry are described in this chapter.

Chapter 5: Result and Discussion

The X-ray diffraction patterns of ilmenite, zircon and lead waste (lead sulphate); the effects on cyclic voltammograms on ilmenite, zircon and lead waste pellet in electrolysed solution under various conditions (ratios, temperature, time, volts) and the dissolution rates are described in this chapter.

Chapter 6: Summary

The summaries are described in this chapter.

The references are inserted at the end of the thesis in six chapters.

CHAPTER 2
LITERATURE REVIEW

2.1 The Literature Review on Ilmenite Processing

2.2 The Literature Review on Zircon Processing

2.3 The Literature Review on Lead Sulphate Processing

2 Literature Review

Before going to the objectives and experimental details of the work, this chapter summarizes the important reports of our interests, so far, appeared either as journal paper or as patent. The chapter is divided into three parts, viz.

1. The literature review on ilmenite processing.
2. The literature review on zircon and processing
3. The literature review on lead sulphate processing.

2.1 The Literature Review on Ilmenite Processing

The part of the review focuses on the fractionation of ilmenite containing raw materials, direct leaching of ilmenite, treatment of leached liquor, electrowinning and electrochemical dissolutions of metals from ilmenite using either as a massive electrode or a graphite paste electrode.

Ilmenite usually occurs in beach sand and in some desert sands, and also as titaniferrous magnetite deposits. In most cases [130-142, 53-57], the fractionation involves (i) grinding, (ii) dense media (float-sink) separation, (iii) froath flotation, (iv) high and low intensity magnetic separation, (v) high voltage electrostatic separation and (vi) tabling and wilflery table. From beach sands, fractions like ilmenite, zircon, monazite, magnetite etc. are separated.

2.1.1 Leaching of ilmenite by sulphuric acid solution

There are substantial numbers of published works related to direct leaching of ilmenite in sulphuric acid solution followed by processing for obtaining TiO_2. Some of them are noted in the following paragraphs.

Many patents are available[143-152] describing the leaching of nontreated ilmenite with sulphuric acid of different strength to get either partial or complete dissolution of ilmenite for pigment grade TiO_2. For production of pigment grade titanium dioxide, dissolution of ilmenite in sulphuric acid was investigated by Yoshio *et al.*[153]. The leached solution was hydrolysed and rehydrolysed to get controlled particle size of TiO_2 with color index 1.50. Both the dissolution and hydrolysis process were carried out at the boiling point.

Leaching of ilmenite in sulphuric acid and subsequent production of titanium dioxide was reported by Brain and Joseph[154]. Ilmenite was heated in 43% sulphuric acid at 108° C with powdered iron. On cooling of the solution at ≤110° C, the unreacted residue was separated. Crystallization of the hydrated ferrous sulphate ($FeSO_4.7H_2O$) was carried out by cooling the mixture at 10-20° C and under reduced pressure. Hydrolysis of the resultant solution produced titanium hydroxide, which was then calcined to produce TiO_2. Waldman *et al.*[155] discussed a process for producing a stable titanyl sulphate solution from a titaniferrous material by treatment with 25-60% sulphuric acid solution at 140° C.

B.R. Davis[156] reported the extraction of titanium dioxide from ilmenite of <0.149 mm. The leaching was carried out with 25-60% sulphuric acid at 140° C in a cylindrical reaction vessel equipped with an agitator. Recycling of the unreacted ore, reduction of Fe^{3+} to Fe^{2+} and Ti^{4+} to Ti^{3+}, and controlled hydrolysis of titanium sulphate were used for the production of TiO_2. Sulphuric acid leaching of titanium iron containing raw material to recover titanium dioxide was presented by Motov *et al.*[157]. The raw material was heated with 250-300 g dm^{-3} sulphuric acid solutions at 40-70° C at 1:3-5 solid-liquid ratios for 1-20 h hydrolyzing the resulting solution in the presence of TiO_2 seed crystals and calcining the resulting precipitate gave TiO_2. Lailach *et al.*[158] reported the leaching of ilmenite in sulphuric acid. Titanyl sulphate was obtained by the decomposition of raw materials with sulphuric acid. The spend acid was concentrated to 60-70% and without filtering recycled to the raw materials decomposition stage. With due separation of unreacted solids and ferrous sulphate, the resulting solution was hydrolyzed and then calcined to produce titianium dioxide.

Leaching behaviour of ilmenite in sulphuric acid was investigated by Han *et al.*[159] In the investigation, effect of acid concentration, temperature, particle size and string speed were included. Maximum dissolution was obtained at the sulphuric acid concentration of ≤14 mol dm^{-3} and above this a decrease was observed. The maximum recovery at 14 mol dm^{-3} was explained partially by the H^+ concentration peaks at about this concentration. The reaction products titanyl sulphate and ferrous sulphate covered the surface of ilmenite when high concentration of sulphuric acid was used but dissolved in water and was removed from the surface when dilute sulphuric acid involved. Sugawara *et al.*[160] investigated a process for sulphuric acid digestion of ilmente of relatively large particle size. Digestion was conducted in a non-isothermal batch reactor.

Thermal and reaction characteristics were studied. The digestion process was characterized by fracturing of the particles due to growth of iron sulphate crystals in the ore. By processing small particles in a 70 volume % sulphuric acid solution at 120-160° C sequential changes were observed in the extent of titanium and iron recovery.

Preparation of high purity TiO_2 by sulphuric acid leaching was investigated by Daisuke *et al.*[161] The process included hydrolysis of the resulting solution, precipitation of titanium tetrahydroxide and calcinations of the hydroxide. Titanyl sulphate was obtained by leaching ilmenite in sulphuric acid. During precipitation, prior to hydrolysis, sulphuric acid concentration was controlled for keeping impurity viz. niobium dissolved in the aqueous solution. Leaching of ilmenite in concentrated sulphuric acid was also investigated by Bachman[162], Katim[163] and Farup[164]. Dissolution of titanium dioxide was obtained but not of iron probably due to the fact that iron become passive in contract with the concentrated acid. Continuous leaching of ilmenite in sulphuric acid for a long time was also reported. Davis and Rahm[165] improved the leaching of ilmenite in sulphuric acid. Ilmenite containing powdered iron was leached with 25-80% sulphuric acid in five stages. Continuous digestion process for 10.5 h in each stage at 104°, 80°, 76° and 72° C was carried out for 64%, 79%, 88% and 92% conversion of TiO_2. The titanyl sulphate solution obtained by digestion was usually separated from unreacted solid particles, ferrous sulphate was separated, and the resultant solution was hydrolyzed and calcined to get the product.

High temperature leaching of ilmenite in sulphuric acid was reported by Belyakoua *et al.*[166]. Ilmenite was digested with concentrated sulphuric acid (88%) at 200° C for 3 h and then leached with water to form titanyl sulphate, which was separated from sulphate. The product was then hydrolyzed and calcined to get TiO_2.

Works on the recovery of titanium values from titanium bearing slag were also reposted[167-168]. In these works, slags were reacted with highly concentrated sulphuric acid (>95%) at higher temperatures to obtained $TiO.SO_4$ solutions.

Orderinde *et al.*[169] reported the kinetic of ilmenite dissolution in sulphuric acid. Rates of Ti(IV) and Fe(III) dissolutions could be explained by shrinking core model. The activation energies were 64.02 kJ mol^{-1} and 60.76 kJ mol^{-1} for Ti(IV) and Fe(III) dissolutions, respectively.

Works on mechanical activation prior to leaching were also reported. A.I. Vorobeichik[170, 171] investigated the effect of mechanical activation (size reduction) on the reactivity and solubility of ilmenite, rutile and natural titanates respectively, in sulphuric acid. Activation was carried out by grinding in a planetary centrifugal mill. This increased the reactivity and solubility and was due to increased surface area, distortion of and defect formation in crystal lattice. Pryikkina *et al.*[172] studied the mechanical activation for increasing the reactivity of ilmenite concentrate in sulphuric acid. The increase of the mechanical activation time (by using different types of disintegrators) from zero to ninety minutes increased the reactivity of the concentrates from 71.9 to 93.40%. Based on X-ray diffraction data, the effect of the mechanical activation was attributed to the decrease of the ore particle size and change of the mineral structure.

2.1.2 Modifications in sulphuric acid leaching ilmenite by post treatment of the resultant solution to produce TiO_2 were reported.

For the manufacture of TiO_2, ilmenite was decomposed in sulphuethyric acid by Kuprina *et al.*[173]. The resulting cake was leached and the mother liquor was treated with various flocculants. 0.25% solution of polyethylene glycol with a molecular weight of 600 gave the maximum result. Purification of hydrated titanium dioxide was investigated by Pockekovskii *et al.*[174]. Purification was done by heating the solution with powdered metallic reducing agent. Dissolution of ilmenite along with slag was reported by Riek *et al.*[175]. Ilmenite slag mixture was treated with oleum and subsequently with recycled sulphuric acid followed by the addition of water, while the heat of dilution was used for heating the reaction mixture. The reaction solution was hydrolyzed to precipitate and the precipitate was calcined to produce TiO_2, 94.60% yield obtained. Preparation of TiO_2 using a reducing agent was investigated by Rahm and Cole[176, 177]. Ilmenite in the presence of powdered iron as reducing agent was heated with 42.90% sulphuric acid at $\leq 140^\circ$ C for a long time. The insoluble solids were separated to get titanyl sulphate, which was then hydrolyzed and calcined to produce TiO_2.

Decomposition of ilmenite with concentrated sulphuric acid was investigated by Knotopchik *et al.*[178]. Decomposition was carried out by the addition of concentrated sulphuric acid with subsequent introduction of water and mixing with compressed air.

Titanyl sulphate thus obtained was hydrolyzed and calcined to produce TiO_2. Decomposition of ilmenite was reported by Samoilova *et al.*[179]. Ilmenite was decomposed with concentrated sulphuric acid while the reactants were mixed with air. The degree of extraction was increased by decomposing in the presence of a solution of sulphuric acid (0.30-1.00%) and Fe(II), Fe(III) or their mixture. Andreeva *et al.*[180] reported the treatment of titanyl sulphate obtained by leaching of ilmenite in sulphuric acid. Titanyl sulphate was treated with ammonium sulphate, aqueous ammonia and ammonium graphiteate to produce precipitate of graphiteated hydrated titanium dioxide. The precipitate was then separated and heat treated to produce TiO_2. Production of TiO_2 by sulphuric acid leaching of ilmenite with subsequent separation of solid impurities from the resultant titanyl sulphate by filtration was reported by Dobrovl Skilie *et al.*[181]. Prior to filtration, hydroxyethylated alkyl phenols were added to the solution. Garken *et al.*[182] reported auto-thermal decompositon of ilmenite in concentrated sulphuric acid (80-88%) containing $FeSO_4.Al_2(SO_4)_3$ and/or $MgSO_4$ with subsequent formation of a cake. Dissolution of the cake in water formed titanyl sulphate solution, which was separated from $FeSO_4$. Hydrolyzed and calcined to produce TiO_2. Edgar Klein[183] reported the preparation of TiO_2 by precipitating hydrated titanium dioxide from titanyl sulphate solution adding sodium hydroxide. Titanyl sulphate was obtained from decompositon of ilmenite in sulphuric acid. Leaching of ilmenite in sulphuric acid to produce TiO_2 was studied by Roehrborn[184]. Ilmenite powder of particle size <60 μm was treated in ~10% sulphuric acid at 180° C and high pressure to give a concentration, which was then reduced with coal after optional oxidation stage. The reduced mass was then leached with the acid filtrate from the first leaching at above temperature and pressure. Fe(II) salt separated and resultant solution hydrolyzed and calcined to give TiO_2. Discontinous dissolution of ilmentite in sulphuric acid was studied by Lailach *et al.*[185] to produce TiO_2. During the reaction, steam or an air-steam mixture was blown to the mixture. The resultant solution was separated from $FeSO_4.7H_2O$, hydrolyzed and calcined to give TiO_2. The spent acid was evaporated and recycled with oleum. Denecker *et al.*[186] studied the manufacture of TiO_2 from ilmenite by sulphuric acid leaching. The leach liquor was extracted with an organophosphorous compound. The overall titanium extraction was 99.20%.

Koverda *et al.*[187] studied a process for the manufacture of TiO_2 by leaching ilmenite in sulphuric acid. The resulting solution was treated with a metallic reducing agent (aluminium), which was treated with a mercurous nitrate solution. The leached liquor was separated from solid particles, hydrolyzed and calcined to produce TiO_2. Gruzdev *et al.*[188] reported a process for the manufacture of TiO_2 by decomposition of ilmenite in sulphuric acid, hydrolysis of the resulting solution and calcination of the titanium hydroxide. Modification of the resulting TiO_2 was done with an inorgonic compound containing aluminum, filtration of the slurry, reslurrying and drying of the cake and crushing of the final product. Yokota and Naka[189] investigated the preparation of TiO_2 from titanium hydroxide, precipitated from titanyl sulphate solution and obtained by sulphuric acid leaching of ilmenite. Titanium hydroxide was obtained from titanyl sulphate by using urea as precipitant. TiO_2 with high whiteness was produced by Stremilova *et al.*[190] from titanium containing raw materials. It was prepared by decomposition of titanium containing row materials in sulphuric acid. The solution was hydrolyzed; titanium hydroxide precipitate was washed and was bleached with sulphuric acid solution containing ground titanium hydroxide having 0.4-4% hydrogen. The precipitate was washed, dried and calcined. Stremilova *et al.*[191] produced TiO_2 by sulphation of ilmenite. The sulphation product was leached, activated titanium was added to the solution, reduced Fe^{3+}, the solution was hydrolyzed and finally the precipitate was separated, dried and calcined. The titanium activation was done by hydrogen at 150-250° C for 0.5-2 h.

2.1.3 Works on leaching of pre and post treated ilmenite in sulphuric acid are summarized below

Leaching of ilmenite in 10% sulphuric acid at high temperature (160° C) and pressure (200 psi) was carried out by Hans[192] and Backman[193]. Treatment of ilmenite in a solution of lignosulphuric acid for selective dissolution of Fe(III) from ilmenite was reported by Ahonen[194] and thus environmental problem due to TiO_2 containing Fe(III) was solved. Leaching of ilmenite in dilute sulphuric acid at 120-122° C in an autoclave after mechanochemical treatment was reported by Eberhand Gock[195]. Thus Fe, Cr, Mn, V etc. were completely removed from ilmenite, leaving crystals of Ti and insoluble silicates. Koryukova *et al.*[196] studied the structure and properties of the hydrated titanium oxide obtained on leaching of ilmenite in sulfuric acid. Thermal analysis, X-ray

diffracion, IR spectroscopy, proton resonance and chemical analysis were studied. Sabanove *et al.*[197]studied the effect of conditions for the thermal hydrolysis of Ti and sorption properties of the resulting product which was prepared from the leaching of ilmenite in sulphuric acid.

Leaching of ilmenite in sulphuric acid mixed with others was also reported. Leaching of ilmenite with a mixture of sulphuric acid and sodium chloride by Farbenind[198], and with a mixture of sulphuric acid and potassium sulphate solution at 350°C by Tung *et al.*[199] were reported. Manufacture of rutile from ilmenite in sulphuric acid and regeneration of sulphuric acid from the waste solution were investigated by Nayar[200]. Removal of P from P containing ilmenite with dilute sulphuric acid at 30° C was reported by Maksimova*et al.*[201]. A study on the leaching of ilmenite in sulphuric acid for V and Cr removal was done by Achim[202]. Heribet *et al.*[203] investigated the concentrated titanyl sulphate solution obtained from leaching of ilmenite cake for subsequent formation of titanium dioxide. The cake was prepared by continuous treatment of ilmenite with concentrated sulphuric acid. This was then dissolved in titanium slag leaching solutions. The final titanyl sulphate solution did not tend to hydrolyze prematurely and was used for the hydrolytic precipitation of TiO_2 without preliminary thickening. Pashuta and Kuznetsov[204] investigated the preparation of titanium dioxide by leaching of a melt obtained by sulphatization of titanium containing raw materials. Leaching was conducted in the presence of polyacrylamide. The leach liquor was reduced by hydroxyethylated alcohol and the solid slurry was removed by setling. This was then hydrolyzed and calcined to get TiO_2.

2.1.4 Leaching of ilmenite by hydrochloric acid solution

There are substantial number of published works related to either only direct leaching of ilmenite in hydrochloric acid or pre-leaching and leaching in hydrochloric acid by processing for obtaining TiO_2. Some of them are noted in the following paragraphs.

Works [205-209] on the direct leaching of non-pretreated ilmenite with hydrochloric acid of different concentration to achieve either partial dissolution or complete dissolution with an aim to prepare pigment grade titanium dioxide were reported. Besides these works, leaching of phosphorus containing ilmenite in hydrochloric acid

for the production of pigment grade titanium dioxide was investigated by Judd[210]. Leaching was done at solid to liquid ratio of with 0.025 kg dm^{-3} aqueous hydrochloric acid for 15 min. The product was then separated and dired to give ilmenite containing 0.06% phosphorous pentoxide. The ilmenite was then treated with 33% w/w hydrochloric acid at 88° C for 4 h ferrous chloride was precipitated and separated. The leach liquor was hydrolyzed by boiling using seed crystals and the resulting titanium hydrate was calcined at 800° C to give TiO_2 containing 30 ppm Fe and 0.12% P_2O_5 vs. 90 ppm and 0.60% for TiO_2 prepared from the same ilmenite without the dilute HCl preleaching and $FeCl_2$ precipitation steps. Removal of Cr, V, Nb and/ or Zr from ilmenite wastes by leaching in hydrochloric acid was investigated by Meer *et al.*[211]. Orderinde *et al.*[169] reported the kinetics of ilmenite dissolution in hydrochloric acid. The effect of temperature (30-60° C), time (1-6 h) and hydrochloric acid concentration (2.3-6.0 mol dm^{-3}) on titanium and iron dissolution were investigated.

Partial equilibrium model and kinetics and solution chemistry in the leaching of ilmenite in hydrochloric acid was investigated by Orth and Liddell[212]. The kinetics and mechanism of ilmenite leaching by hydrochloric acid were studied to develop a partial equilibrium model describing the dissolution rate of titanium and iron and the ion composition charge of the liquid phase during leaching. The leaching rate of Fe_2O_3 and Fe_3O_4 from ilmenite was high in the initial stage and the titanium concentration increased with increasing leaching time.

J. Burastero[213] reported that chromium could be removed from chromium containing ilmenite by prior oxidation and reduction of ilmenite. The product was then leached with hydrochloric acid and leach liquor was then hydrolyzed to produce TiO_2. Sinha[214] investigated the formation of rutile from ilmenite by removing iorn. Ilmenite was oxidized at 900° C and then reduced in fludized bed at 800-900° C. The product was then leached with dilute hydrochloric acid. On hydrolyzing the solution TiO_2 was precipitated. Burastero[215] studied the precipitation of rutile from ilmenite by pre-oxidation of ilmenite at 1000° C for 30 min, pre-reduction with charcoal at 950° C for one hour and subsequent leaching with 20% hydrochloric acid. The resultant solution might be hydrolyzed to produce TiO_2. Tolley[216] patented a work on the leaching of pre-roasted ilmenite at 600-900° C with hydrochloric acid solution at 80-110° C.

Jakkiwar *et al.*[217] studied the segregation roasting of ilmenite fraction obtained from titanomagnetite. The fraction was heated at 1010° C with 15.40% charcoal and 10% calcium chloride for 12 min. The roasted mass was then leached with 50% hydrochloric acid for 10 min at 50° C, leaching yielded a concentrate containing 56.80% TiO_2. Tolley[218] investigated the recovery of titanium from ilmenite. Ilmenite (-100 mesh) was roasted for 1 h at 750° C under a flow of graphite monoxide (320 dm^3 min^{-1}) and hydrogen (320 dm^3 min^{-1}). The cooled mass was then leached with concentrated hydrochloric acid at 85-100° C for 1 h. The leach liquor was cooled to -5° C and purged with hydrochloric acid. After 30 min the precipitated ferrous chloride was removed to give liquor containing titanium trichloride which was then precipitated out. The crystals were dried in air and heated at 400° C under graphite monoxide, roasted for 1 h at 750° C under chlorine and cooled under chlorine to give a residue containing Ti 71%, iron 0.10% and vanadium 0.05%.

Tolley[219] improved a process for the production of high purity TiO_2. It was prepared by reducing ilmenite at 600-1000° C with hydrogen or a mixture of hydrogen and graphite monoxide. The roasted mass was leached with hydrochloric acid; filtered off the gangue and cooled the filtrate was cooled to crystallize out ferrous chloride. The liquor was stirred at 70-100° C with ferric oxide, and the TiO_2 was filtered and leached with hydrochloric acid. Treatment was repeated with a 2.50-50 fold excess of ferric oxide. Ferrous chloride was decomposed thermally to get reusable ferric oxide and hydrochloric acid. TiO_2 thus obtained was 99.80%. The production of synthetic rutile from ilmenite was investigated by Borowice[220]. Ilmenite was reduced at 950° C for 1 h then oxidized at 750° C for 1 h. The mass was then leached with hydrochloric acid. The yield of TiO_2 and leaching degree of iron were studied as a function of acid concentration, temperature, leaching time, solid/liquid phase ratio and stirring rate.

Preparation and quality examination of synthetic rutile from ilmenite were reported by Zaharescu *et al.*[221]. Ilmenite was reductive roasted and leached with hydrochloric acid. When the Fe^{3+} was reduced to Fe^{2+} most of the iron was removed by leaching with refluxed hydrochloric acid, when Fe^{3+} was reduced completely to elemental iron, the removal of iron was more complete than Fe^{2+}. Oxidation of ilmenite and subsequent leaching with hydrochloric acid was reported by Ismail *et al.*[222]. Ilmenite was oxidized with air at 900-1000° C. The product was mixed with sawdust in a closed container and

heated at 1100° C when ferric oxide was reduced to iron. The mass was then leached with hydrochloric acid was recovered and reused. Levin *et al.*[223] investigated the leaching of ilmenite with vibration. Ilmenite was leached with 20% hydrochloric acid at 102-104° C in a experimental laboratory reactor with vibration. The recovery was 94.60% titanium into the rutile and 89.60% iron into solution. Subsequent magnetic separation resulted in a purified rutile containing 95.00% TiO_2 and 0.79% Fe. Sulphidization of titaniferrous ore to produce TiO_2 was studied by Lee *et al.*[224]. The materials (-150 mesh) were sulphidized with sulphur dioxide and graphite at 800° C for 1 h. Flow rate of sulphur dioxide was 100 dm^3 min^{-1}, weight ratio of graphite to ore was 0.70. The synthetic rutile was prepared by leaching the sulphidized product with hydrochloric acid which on subsequent hydroxylation and calcination yielded 82.15% TiO_2.

The production of TiO_2 from ilmenite by sulphidization and leaching process has been investigated by Kurihara *et al.*[225]. Ilmenite was sulphidized with hydrogen sulphide mixed with nitrogen and graphite monoxide at 800-900° C. The mass was then leached with dilute hydrochloric acid. In 3 h, 95% iron in ilmenite was sulphidized. Leaching with 60% excessive hydrochloric acid at 80-102° C for 1 h 95% iron was removed and leached residue containing 95% TiO_2 was obtained. Limitation in gaseous reduction and oxidation of ilmenite was investigated by Patterson and Cameron[226]. At 945° C, 2 h reduction of ilmenite in hydrogen produced a product, which on leaching with 18% hydrochloric acid at 45° C for 2 h resulted in the removal of 92-96% iron. The decrease of the removal of iorn was obtained when the ore was reduced at >945° C after air oxidation.

Yoshikoshi and Nakahara[227] have prepared synthetic rutile from ilmenite. It was prepared by oxidation of the ore at 1000° C for 1 hour, reduction with coke oven gas at 800° C and leaching at 100-105° C with hydrochloric acid containing ferrous chloride. The leached solution was filtered. The filtrate was washed, dried and fired at 900° C to give the product. The coke oven gas was reformed over a nickel catalyst at 200-350° C. Buckman[228] prepared TiO_2 from beneficiated ilmenite. A mixture of ilmenite, sulphur, barium sulphate and coke was heated in a Blast Furnace. The melt was dissolved in strong hydrochloric acid to get TiO_2, which was done by proper, hydrolyses and calcination of the product. Production of TiO_2 by sintering ilmenite with coke was

reported by Garica *et al.*[229]. The sintered ore on smelting in a blast furnace produced TiO_2.

Hussen *et al.*[230] reported that iron removal from ilmenite by hydrochloric acid at 50-90° C was the lowest after pre oxidation, 35% from powdered ilmenite and 95% from pre-reduced ilmenite (by hydrogen at 700° C). High temperature leaching of ilmenite in hydrochloric acid (20 wt %), after giving pre oxidation and pre-reduction treatment was reported by Yoshikoshi *et al.*[231]. Hard *et al.*[232] informed the preparation of Ti metal from ilmenite by fluorination method. Ilmenite was mixed with Na_2F_6Si and graphite forming briquettes, calcined at 750° C for 6 h, and cooled and leached with 5% hydrochloric acid at 96° C for 2 h Na_2TiF_6 thus formed was crystallized and separated, then mixed with Al and Zn and heated at 620° C for 1 h and cooled to form Ti-Zn alloy. Zn was distilled at 910° C in Ar leaving Ti. Manufacture of TiO_2 from ilmenite by chloride process was investigated by Narita *et al.*[233]. Selective extraction of Ti(IV) and Fe(III) from hydrochloric acid leach liquor of ilmenite by tributyl phosphate (TBP) in benzene was reported. Fe(III) was extracted into the TBP phase, selectively from 3-6 mol dm^{-3} hydrochloric acid solution. Ti(IV) in the residual aqueous phase was extracted as $TiCl_4.3TBP$ as a concentration range of chloride ion is greater than 7 mol dm^{-3}.

The recovery process of high purity TiO_2 has been reported by Taijro[234]. Titanium containing raw materials on dissolving in aqueous hydrochloric acid was extracted with a C_{4-10} ether, alcohol, and ketone or with a C_{4-8} alkyl phosphate to remove iron, after adjusting initial <8 mol dm^{-3} free hydrochloric acid. The titanium was stripped into aqueous 3-7 or 3-4 mol dm^{-3} hydrochloric acid and hydrolyzed. The precipitate was filtered, washed and calcined to produce TiO_2. Production of TiO_2 from ilmenite was reported by Baldwin *et al.*[235]. Ilmenite was premixed with excess concentrated sulphuric acid heated at 600-1100° C in the presence of C, H or hydrographites, then leached with dilute hydrochloric acid in a autoclave at 120-150° C and at 10-14 psig. The feasibility of hydrochlorination of ilmenite for production of rutile and iron powder was investigated by Smith *et al.*[236]. Ilmenite was treated with hydrochloric acid hydrogen mixture of molar ratio 1:1 and iron was removed as ferrous chloride which was then reduced with hydrogen.

Turker *et al*.[237] studied the dissolution of ilmenite in hydrogen chloride method and hydrogen chloride-ethanol systems at room temperature. Better results for the dissolution of iron from ilmenite were obtained for hydrogen-chloride acid methanol and hydrogen chloride-ethanol system compared with hydrogen-chloride water system. Wang *et al*.[238] studied the production of TiO_2 from ilmenite by hydrochloric acid leaching. Ilmenite was leached with hydrochloric acid to remove ferrous oxide and ferric oxide, the resulting yellowish TiO_2 was treated with hydrogen chloride, chlorine or a mixture of hydrogen and chlorine at high temperature to obtain crude titania. By controlling the reaction time and temperature, TiO_2 of different grades were obtained. Leaching of reductive roasted ilmenite in hydrchloric acid was investigated by Tolley and Laughlin[239]. The soluble titanium halide was extracted with bis (2-ethyl hexyl) phosphate (298-07-7) in kerosine (10-50 volume %) by shaking for 10 min. The organic solution was stripped with sulphuric acid containing hydrogen peroxide solution thus obtained was hydrolyzed to precipitate TiO_2.

Liddell[240] reported a model for the recovery of titanium from mixtures of ilmenite and hematite by hydrochloric acid leaching. The model includes (1) redox reaction converting Ti(IV) to Ti(III) and Fe(II) to Fe(III), (2) formation of chloro complexes, (3) hydrolysis and (4) dissociation in water.

P. Farup[241] dissolved iron from ilmenite by heating it with three times of its weight 20% hydrochloric acid at 70-80° C for 12 h and then titanium dioxide residue was converted into soluble form by digestion with concentrated sulphuric acid to form titanyl sulphate, which was then hydrolyzed, precipitated and calcined to produced TiO_2.

2.1.5 Metallo-thermic reduction of ilmenite

Few workers investigated on the metallo-thermic reduction of ilmenite. Behra and Mohanty[242] reduced an ilmenite with aluminum-silicon mixture in the presence of potassium chloride, magnesium oxide, barium peroxide, fluorspar and lime to yield ferrotitanium alloy. Maximum titanium recovery of 59.24% and alloy yield of 84.34% was achieved with 12.5% silicon in addition of potassium chlorate. Sumitomo Metal Ind. Ltd., Japan [243, 244] prepared ferro-titanate by Thermit reaction of ilmenite and powdered

aluminum and calcium. Ilmenite (137 kg), powdered aluminium (8 kg) and calcium (80 kg) were mixed and ignited with barium peroxide to yield metal (60.8kg, 38.90 titanium of 61.26% yield), 50.50 iron, 3% aluminum and 2.50% silicon and 162 kg slag.

2.1.6 Roasting of ilmenite in presence of alkali metal compounds

Roasting of ilmenite in presence of alkali metal compounds has been investigated by several workers. Pellereau *et al.*[245] reported a combined fusion and reduction of ilmenite. Ilmenite was fused with sodium graphiteate and reduced with anthracite dust at 800° C. The resultant mass was water leached and graphiteated to separate sodium graphiteate. This was again leached with dilute sulphuric acid to remove iron. The residue thus obtained with concentrated sulphuric acid to produce titanyl sulphate solution, which was then hydrolyzed, separated from solids and calcined to prduce TiO_2.

Blaskeawicz and Borewice[246] investigated the fusion of ilmenite with sodium graphiteate and sodium sulphite. Itmenite was fused with a mixture of sodium graphiteate and sodium sulphite at below 1100° C. Titanium dioxide and iron oxide were magnetically separated from the non magnetic gangue and partially leached with dilute sulphuric acid to give ~90% TiO_2.

Allan and Anthony[247] investigated the recovery of titanium dioxide from ilmenite by high temperature borate fusion. Ilmenite was fused with $Li_2O.6B_2O_3$ at 1273 K, on boiling with water of the crushed solidified melts water insoluble residue was obtained. Extraction with hot 18 g mol dm^{-3} sulphuric acid of the residue yielded a product containing 86% TiO_2 and only a trace of iron.

2.1.7 Works published after 1990 to date

Zhang *et al.*[248] have published a literature review of titanium metallurgical process. Laxmi *et al.*[249] have reported with the recovery of ilmenite mineral from red sediments of badlands topography and suggested flow sheet with material balance. The results of these investigations reveal that the red sediment samples contain 33.20% total heavy mineral, in which ilmenite mineral concentrate is 28.71% (by weight). The ilmenite concentrate recovered from red sediment sample by physical beneficiation process, which included scrubbing, deliming, gravity concentration, magnetic and electrostatic separation contains 99.41% grade with 97.30% recovery. The ilmenite

mineral concentrate recovered from red sediments is also suitable for industrial applications. The characterization studies on ilmenite reveal that the TiO_2 percentage is marginally increasing from 46.69% to 47.86% with increasing magnetic intensity from 0.46 to 1.55 T.

Baba *et al.*[250] have investigated the characterization and H_2SO_4 leaching behavior of a Nigerian ilmenite ore following mechanical activation and alkali roasting. The effects of NaOH/ore ratio, H_2SO_4 concentration, leaching and roasting temperature on the Ti recovery from the milled ore have been examined. The results show that mechanical activation significantly enhances the dissolution of ilmenite ore. Under the leaching conditions of 90^o C, 60% (v/v) H_2SO_4 and 4 h, about 72% Ti extraction is obtained from a milled ore roasted at 850° C with 60% NaOH. X-ray diffraction (XRD) phase analysis of the roasted mass, water treated residue and leach residue supports the reaction mechanism and experimental results.

Mozammel and Mohammadzadeh[251] have performed to model and optimized the response of Iranian ilmenite to pre-oxidation and leaching parameters using fractional factorial design. The Ti and Fe leaching percentages are considered as leaching response with respect to leaching parameters as the particle size, temperature, time, hydrochloric acid molarity, solid to liquid ratio and stirring speed. In order to detect the effect of pre-oxidation on leaching process half of the samples are oxidized at 900° C for 120 min. Then experiments have been performed at the designed condition and consequently Ti and Fe leaching percentages are measured using an atomic absorption spectroscopy. Finally the most significant factors affected on Fe and Ti leaching percentages and optimum conditions are obtained using analysis of variance. It is concluded that the use of statistical method is useful not only for optimizing and modeling the leaching parameters but also for understanding the detrimental effect of pre-oxidation on Fe and Ti extraction.

Jia *et al.*[252] have reported the beneficiation of titania (TiO_2) by sulfuric acid (H_2SO_4) pressure leaching of Panzhihua ilmenite. The reaction temperature, H_2SO_4 concentration, and concentration of ferrous ions (Fe^{2+}) had significant effects on the enrichment of TiO_2. With increasing reaction temperatures, the dissolution of iron from

ilmenite is enhanced, while the titanium loss is reduced. Increasing concentration of Fe^{2+} has an adverse effect on the beneficiation of TiO_2. In contrast, the dissolution of iron from ilmenite is accelerated by increasing concentrations of H_2SO_4, up to 40 wt % H_2SO_4. SEM analyses of the leach residues under different leaching conditions indicate that severe agglomeration occurs among the primary hydrolysate particles at high concentrations of H_2SO_4 or with the addition of ferrous sulfate ($FeSO_4$). Furthermore, a compact layer is formed on the surface of unreacted ilmenite particles, thus retarding the ilmenite leaching. The agglomeration might have resulted from the adsorption of H_2SO_4 on the primary particle surfaces, as revealed by energy-dispersive X-ray spectroscopy (EDX) and thermogravimetric analysis (TGA). The optimal conditions for the beneficiation process are as follows: H_2SO_4 concentration 40 wt %, acid/ore mass ratio 2:1, reaction temperature 150° C, and reaction time 3 h. Thus, a Ti-rich material with a TiO_2 content of ~85 wt % is obtained. Moreover, the results demonstrate the technical feasibility of upgrading Panzhihua ilmenite in 40 wt % sulfuric acid obtained by concentrating the diluted acid waste discharged from the sulfate TiO_2 process.

Gireesh *et al.*[253] have reported the reduction of iron content of ilmenite by leaching the ore with hydrochloric acid. The enriched TiO_2 mineral thus obtained is called synthetic rutile (SR) or beneficiated ilmenite (BI). The quality of the synthetic rutile (in terms of TiO_2 content) mainly depends on the condition of leaching process. The study envisages the effect of acid concentration, temperature, and agitation speed on the leaching of the ore. The kinetics of the leaching reaction follows the first order at normal and stimulated leaching conditions. The highest rate constant value of $5.18\times10^{-3}min^{-1}$ is observed for leaching the ilmenite with 30% hydrochloric acid under 700 rpm and at 70° C. The enthalpy change in the reaction (ΔH) is calculated as 24.157 kJ mol^{-1}, and the entropy change in the reaction (ΔS) is calculated as 26.25 kJ mol^{-1}. The positive value of ΔH indicates the endothermic nature of reaction. The value of ΔG at different temperature is found to be negative indicating the feasibility of the process and the spontaneous nature of the reaction. The addition of gypsum enhances the leaching process. The rate constant is increased with the increase in the gypsum concentration in leaching process. The rate constant is increased to 6.15×10^{-3} min^{-1} by introducing 100 mg of gypsum in the leaching process carried out with 30% hydrochloric acid at 70° C and 500 rpm.

Wu *et al*. [254] have developed a simple and efficient process to synthesize high-value TiO_2 nanowires from natural ilmenite, combining acid and alkali leaching together. Valuable Fe and Ti are selectively divided from ilmenite by hydrochloric acid leaching, and then the obtained hydrolyzed titania residue with mainly precipitated hydrated TiO_2 is leached by sodium hydroxide and hydrogen peroxide. Ti and Si are monitored by ICP and EDS during the process. The effects of NaOH to hydrolyzed titania residue (Na^+/Ti^{4+}) molar ratio, H_2O_2 to-hydrolyzed titania residue (O_2^{2-}/Ti^{4+}) molar ratio, leaching temperature and leaching time on leaching of hydrolyzed titania residue have been investigated. Results indicate that the recovery of Ti is 96.39% and dissolution of Si is 67.9% under the optimal conditions: Na^+/Ti^{4+} molar ratio of 8/1, O_2^{2-}/Ti^{4+} molar ratio of 6/1, leaching temperature of 30° C and leaching time of 30 min. and then simple boiling divides the Ti and Si very efficiently resulting in high-purity of synthetic TiO_2 containing 0.47% of SiO_2. Meanwhile, the high-value TiO_2 exhibits echinus-like structure with aggregations of nanowires and well-crystallized anatase phase at 400° C.

Akhgar *et al*.[255] have investigated the preparation of titania compounds by double-reductive hydrochloric acid leaching of ilmenite concentrate. A rod-shaped nanostructure titania compound has been obtained via centrifugation of leach liquors as a by-product. The liquors of leaching experiments are subjected to zetasizer test. The suspended particles in leach liquors are investigated using SEM and TEM analysis. The results reveal that the rod-shaped particles are smaller than 100 nm in width. The XRD analysis verifies the formation of rutile and pseudorutile phases as main phases. The XRF analysis demonstrates that the TiO_2 content of ilmenite is increased from 33% in ilmenite concentrate to about 80% in the product containing some constituents such as Fe_2O_3, SiO_2 and Al_2O_3.

Tao *et al*.[256] have reported a new combination method consisting of ball milling, carbothermic reduction and hydrochloric acid leaching for the preparation of nanosized synthetic rutile from natural ilmenite. The ball milling is employed to grind ilmenite into small particles. The carbothermic reduction is carried out to yield a high titanium slag, which can be easily purified by subsequent leaching procedure. Factors affecting the hydrochloric acid process, namely the leaching time, temperature and acid concentration have been studied. After leaching and calcining the milled and annealed

mixture of $FeTiO_3$/C under the optimal conditions, the TiO_2 nanoparticles with size of 10-200 nm and purity >98.00% are obtained.

Janssen and Putnis [257] have investigated the oxidation of ilmenite from Tellnes (Tellnes ilmenite is an important feedstock for the production of high-grade titanium pigment), Norway, at 700° C in air and compared the leaching ability of pre-heated and non-heated Tellnes ilmenite in 20% HCl solution at 160° C. Through the heat treatment, ilmenite ($FeTiO_3$) is oxidized to hematite (Fe_2O_3) and rutile (TiO_2) via a solid-state reaction mechanism. The leaching experiments revealed that after the pre-heating step the iron dissolution in the leaching process is limited due to the lower solubility of ferric iron in the hydrochloric acid. Furthermore, in both experiments the impurity phases such feldspar and orthopyroxene are less soluble in the hydrochloric acid and pollute the replacement product rutile because Si released from the impurity phases is incorporated in the rutile. The leaching reaction mechanism is interpreted as a pseudomorphic, interface-coupled dissolution–reprecipitation process, through which the external form of the parent ilmenite as well as its crystallographic orientation is inherited by rutile.

Xiong *et al.*[258] have developed a new process of "mechanical activation–hydrochloric acid leaching–concentrated sulfuric acid decomposition–water leaching–separation of Fe^{3+} with EDTA during hydrolysis" to prepare high-purity TiO_2 from Panzhihua ilmenite. The hydrolyzed titania residue prepared from mechanically activated Panzhihua ilmenite has been leached by hydrochloric acid, decomposed by concentrated sulfuric acid and subsequently dissolved in water yielding titanium sulfate solution. In order to improve the purity of the precursor during the hydrolysis of TiO^{2+}, EDTA is used as an additive to restrain the hydrolysis of Fe^{3+}. The effects of sulfuric acid concentration, acid-to-titania residue mass ratio in the process of acid digestion and the significant effects of water leaching time, leaching temperature and liquid-to-solid mass ratios on the recovery of Ti from the residue have been reported. The recovery of Ti is above 98% under optimal conditions. Well-crystallized anatase TiO_2 and rutile TiO_2 could be obtained through calcining at different temperatures and no impurity can be detected by EDS in titanium dioxide. The results demonstrate that the process is inexpensive, environment friendly and promising in preparing high-purity TiO_2 from ilmenite with a high content of gangues like in Panzhihua ilmenite.

Zhang *et al.*[259] have reported on the effects of oxidation–reduction treatment and mechanical activation on the hydrochloric acid leaching performance of Panxi ilmenite concentration from Sichuan province of China. The results show that both of oxidation–reduction treatment and mechanical activation do not only significantly accelerate the extraction of Fe, Ca and Mg from Panxi ilmenite concentration, but also apparently put forward the initial hydrolysis time of titanium ion in hydrochloric acid solution. In addition, oxidation–reduction treatment can obviously decrease the Ti extraction in hydrochloric acid solution. The formation of pseudobrookite by oxidizing at 900° C is more favorable to upgrade Panxi ilmenite concentration to synthetic rutile. A process of "oxidation–reduction–mechanical activation–hydrochloric acid leaching" has been proposed, and this process has successfully prepared the synthetic rutile which meets the requirements of chlorination process. In this process, the Panxi ilmenite concentration is first oxidized at 900° C in the presence of oxygen for 15 min then reduced at 750° C by hydrogen for 30 min. After cooling to room temperature in a nitrogen atmosphere, the oxidized–reduced ilmenite concentration obtained is milled in a planetary ball mill for 2 h under nitrogen atmosphere immediately. After the milling, the oxidized–reduced–mechanically activated ilmenite concentration proceeds to a leaching at ambient pressure using 20 wt.% hydrochloric acid for 10 h. Finally, the leached product is subjected to filtration, wash and calcination to produce a synthetic rutile containing 90.50 wt. % TiO_2 and 1.37 wt.% total iron as well as combined CaO and MgO of 1.00 wt.%. The results demonstrate that the process of "oxidation–reduction–mechanical activation–hydrochloric acid leaching" can excellently upgrade high Panxi ilmenite containing high amount of gangue material synthetic rutile which meets the requirements of chlorination process.

Sasikumar *et al.*[260] have discussed about the effect of the change in phase constitution, particle size distribution, surface area, crystallite size, strain and lattice parameters introduced by mechanical activation of the altered beach sand ilmenite from Manavalakurichi region, India on the dissolution kinetics of leaching by HCl and H_2SO_4. The altered ilmenite shows different physico-chemical characteristics and is found to be more resistant to acid leaching than the less altered ilmenite from the Chatrapur beach sands, India investigated earlier. The dissolution behavior is also different in H_2SO_4 and HCl. For sulfuric acid leaching, the dissolutions of Fe and Ti are

increased monotonically with time of milling and show a continuous increase with time of leaching, whereas hydrolysis of titanium occurs in HCl medium, especially for the activated samples at lower acid concentration, lower solid to liquid ratio and higher temperature leading to lower solution recoveries. The dissolution kinetics in both H_2SO_4 and HCl prior to hydrolysis conforms initially to the reaction rate control model and for higher leaching times to the shrinking core model where diffusion through the product layer is rate controlling. It is postulated that the anatase formed by hydrolysis in milled samples impedes the further progress of leaching. The activation energies for the dissolutions of Fe and Ti decreased with time of milling and are marginally lower in HCl than in H_2SO_4. An attempt has also been made to correlate the decrease in activation energy to the increase in the energy input to the material through high-energy milling. The relative contribution of the increase in surface area and structural disorder on the enhancement of the dissolution rates has been evaluated.

El-Hazek *et al*.[261] have reported the leaching characteristics of TiO_2 from ilmenite by hydrochloric acid. This can be considered as an alternative to selective iron dissolution and insolubilization of TiO_2 in the form of synthetic rutile. The relevant criteria for TiO_2 leaching in hydrochloric acid are studied, including the acid concentration and solid/liquid ratio which control the acid/ilmenite molar ratio – as well as the effect of reduction. The data reveals that the optimum conditions involve working with 12 mol dm^{-3} acid with a solid/liquid ratio of 1/20 at 80° C for 2.5 h, using ore ground to ~200 mesh size. Under similar reducing conditions using 0.1 kg metallic iron powder/kg ilmenite, there is a marked decrease in the optimum solid/liquid ratio to 1/8 and in the leaching time to 1.5 h.

Li *et al*.[262] have discussed about the dissolution of mechanically activated Panzhihua ilmenite in 5–20% sulphuric acid solutions. With high milling intensity the milling atmosphere significantly affects the dissolution with milling under vacuum almost double the dissolution of ilmenite milled in air. This is due to formation of a lot of acid-resistant pseudorutile and lowering level of the lattice strains, especially in the *c*-axis direction of the ilmenite unit cell, upon milling in air. Under the experimental conditions applied, titanium and iron are dissolved at a nearly stoichiometric ratio. Hydrolysis of the dissolved titanium, however, is also in progress simultaneously. The

sulphuric acid concentration and reaction temperature remarkably influences the hydrolysis rate, thus affecting the microstructure of the hydrolysate. In 5 wt. % and 10 wt. % acid solutions, the hydrolyzed product is poorly compacted and dissolution could continue. In contrast, the product in 20 wt. % acid exhibits a compact structure and is strongly adherent preventing further dissolution of the un-reacted ilmenite. In both cases the hydrolysis product appears to be rutile TiO_2. The experimental results show that significant hydrolysis is inevitable when the acid concentration is ≤20 wt. %. Therefore, preparation of synthetic rutile from mechanically activated ilmenite is a better alternative to direct production of pigment grade TiO_2. The method can directly and fully reuse the spent acid discharged in the sulphate process.

Zhang and Nicol [263] have reported on the kinetics of the dissolution of titanium and iron from an ilmenite sample in moderately strong sulfuric acid solutions in the absence and presence of reducing agents such as titanium(III) ions and sulfur dioxide. The effects of particle size, temperature, solid/liquid ratio, sulfuric acid concentration and titanium(III) concentration on the kinetics of dissolution have been investigated. The results have shown that both particle size and acid concentration have relatively minor effects on the rate of dissolution of titanium while temperature has a significant effect under the studied conditions. The batch leach kinetics of ilmenite in acid solutions appears to fit a shrinking particle model, while in the presence of a decreasing titanium(III) concentration, the rate of dissolution of titanium can be fitted to a shrinking core model. Mathematical expressions for the batch leaching of the ilmenite have been established. The results suggest that the rate of dissolution of ilmenite in acid solutions is controlled by a slow chemical reaction on the surface of the mineral, while in the presence of a reducing agent such as titanous ions; the dissolution rate of ilmenite is significantly enhanced. The use of SO_2 as a reductant increases the dissolution of titanium only in the presence of ferrous ions. The role of Ti(III) ions and SO_2 during leaching is assumed to involve reduction of the iron(III) component in the mineral by a redox reaction on the surface.

Zhang *et al.*[264] have investigated the effects of mechanical activation on the hydrochloric acid leaching performance of Panxi ilmenite from Sichuan province of China. The inactivated and mechanically activated ilmenites are characterized using X-ray diffraction (XRD), particle size analysis, and Scanning Electron Microscope (SEM)

techniques to determine the structural changes of Panxi ilmenite during the mechanical activation process. The results show that mechanical activation elevates the calcium, magnesium and iron extraction of Panxi ilmenite irreversibly which mostly attributes to the lattice disorder of Panxi ilmenite. All the results show that a great amount of magnesium in Panxi ilmenite uniformly substitutes for iron in the structure of ilmenite, while minority magnesium exists in gangue minerals, and calcium more likely exists in gangue minerals. The sites of magnesium, calcium and iron in ilmenite will not be redistributed during the treatment of mechanical activation.

Zhang and Nicol[265] have used an electrochemical technique to investigate the reduction and dissolution of two different ilmenite samples in 450 g dm^{-3} sulphuric acid solutions at elevated temperatures. The results have shown that the dissolution rate of ilmenite ($FeTiO_3$) is low at low potentials. Above about 0.3 V the dissolution of ilmenite and the reduction of hematite (if present in the ilmenite sample) are the main reactions. At more negative potentials the dissolution of ilmenite increases simultaneously with reduction of ilmenite to trivalent titanium. These observations are consistent with those predicted from thermodynamic data. Hematite has a higher dissolution rate under reductive conditions than ilmenite. Studies of effect of temperature on the dissolution of ilmenite at low potentials such as 0 V have shown that in the temperature range of 65-95° C, the activation energy in about 50 kJ mol^{-1} and this together with the high ratio of the charge passed to metals dissolved suggests that the rate of the non-reductive dissolution reaction is not significant under these conditions.

Jaya Kumari *et al.*[266] have been reported a new process for the production of synthetic rutile, aeration rusting is the major step where metallic iron is converted to iron oxide in the presence of catalysts such as NH_4Cl and air. An electrochemical investigation to understand the anodic dissolution of reduced ilmenite (RI) has been carried out using a reduced ilmente graphite paste (GP) electrode at 30° C. Intermediate products with different iron contents were formed during the rusting reaction. Synthetic rutile with negligible iron content was used for the investigation. The mechanism and the influence of TiO_2 matrix were studied.

White *et al.*[267] reported that the natural samples of magnetite and ilmenite were experimentally weathered in pH 1-7 anoxic solutions of temperature of 2-65° C.

Reaction of magnetite is described as Fe_3O_4 (magnetite) $+2H^+ \rightarrow Fe_2O_3 + Fe^{2+} + H_2O$. Dynamic polarization experiments using magnetite electrodes confirmed that this reaction is controlled by two electrochemical half cells, $3Fe_3O_4$ (magnetite) $\rightarrow 4Fe_2O_3 + Fe^{2+} + 2e$ and $Fe_3O_4 + 8H^+ + 2e^- \rightarrow 3Fe^{2+} + 4H_2O$, which result in solid state Fe^{3+}reduction, formation of an oxidized layer and release of Fe(II) to solution. XPS data revealed that iron is present in the ferric state in the surfaces of reacted magnetite and ilmenite and that the Ti/Fe ratio increased with reaction pH for ilmenite. Short term (<36 h) release rates of Fe(II) were linear with time. Between pH 1 and 7, rates varied between 0.3 and 13×10^{-14} mol cm^{-2} S^{-1} for magnetite and 0.05 and 12.3×10^{-14} mol cm^{-2} S^{-1} for ilmenite. These rates are two orders of magnitude slower than electrochemical rates determined by Tafel and polarization resistance measurements. Discrepancies are due to both differences in geometric and BET surface area estimates and in the oxidation state of the mineral surface. In long term closed-system experiments (<120 d), Fe(III) release slowed with time due to the passivation of the surface by increasing thickness of oxide surface layers. A shrinking core model, coupling surface reaction and diffusion transport, predicted that at the neutral pH, the mean residence time for sand-size grains of magnetite and ilmenite will exceed 10^7 y. This agrees with long term stability of these oxides in the geologic time period.

Sunil Jayasekera and co-workers *et al.*[268] reported that the anodic dissolution of iron and cathodic reduction of oxygen were studied in ammonium chloride solutions over the temperature range 30-150° C and a total pressure up to 780 KP_a using the rotating disk electrode technique. Corrosion current densities determined by Evan's diagram and linear polarization method showed that the corrosion rate increases with increasing temperatures and oxygen partial pressures. The industrial importance of this reaction is in the production of synthetic rutile via the Becher process which involves the high temperature reduction of ilmenite followed by the forced corrosion of metallic iron from the reduced ilmenite matrix. Results obtained from a series of pressure leaching trials showed that, by carrying out this reaction of above ambient oxygen partial pressures and at elevated temperatures, the corrosion rate can be significantly increased above that achieved in the conventional aeration process.

2.1.8 Works on ilmenite processing carried out in the Metallurgical Research Laboratory of the Department of Applied Chemistry and Chemical Technology/ Engineering, Rajshahi University

Biswas and Mondal[269] worked on the dissolution of titanium and iron from ilmenite sand (<130 μm particles) in various inorganic acids to indicate that only hydrofluoric acid was effective. Leaching in hydrofluoric acid was investigated as regards to contact time, acid concentration, solid to liquid phase ratio, number of leaching stages and temperature. About 81% titanium was dissolved within 5 h by 6.4 mol dm^{-3} hydrofluoric acid at boiling point, while only 26% iron was dissolved. Multi-stage leaching was not so advantageous, but the extent of leaching increased greatly with temperature. The optimum solid to liquid phase ratio was found to be 1/20 kg dm^{-3}.

Biswas *et al.*[270] recovered pigment grade titanium dioxide (99.90% (wt.) TiO_2 and 0.004% (wt.) Fe) from the hydrofluoric acid leach solution of ilmenite using the following steps: (1) precipitating out of the Ti and Fe compounds from fluoride leach solution using sodium hydroxide solution; (2) oxidizing Fe(II) to Fe(III) using HNO_3 acid; (3) dissolving the solid mass in 7.5 mol dm^{-3} HCl; (4) extracting most of the Fe(III) by a two-stage methylisobutylketone (MIBK) extraction; (5) adjusting the pH of the aqueous phase to zero in order to extract titanium with di-2-ethylhexylphosphoric acid (D2EHPA) and leave siliceous materials in the aqueous phase; (6) stripping the organic phase with 0.50 mol dm^{-3} Na_2CO_3 solution to get a quantitative precipitation of metatitanic acid; and (7) filtration of the aqueous suspension of metatitanic acid, oven-drying and finally ignition at 1000^{o} C. The overall recovery yield of TiO_2 from the leach solution was greater than 92.50% (wt.). The MIBK, HCl and D2EHPA could be recovered and recycled.

The ilmenite fraction of beach sand of Bangladesh has been reported to be processed through salt (NaCl, $NaNO_3$ and Na_2SO_4)–water vapor roasting, followed by hydrochloric acid leaching by Biswas *et al.*[271]. The optimum conditions for roasting are: 800° C (885° C for Na_2SO_4); 90 min (75 min for NaCl); ilmenite to salt (wt.) ratio 1.70 for $NaNO_3$, 2.00 for Na_2SO_4 and 0.67 for NaCl; N_2 flow rate 84 cm^3 min^{-1}; and water vapor pressure 0.042 bar. For the optimum leaching for ore, with a solid to liquid phase ratio (S/L) of 0.02 kg dm^{-3}, a HCl concentration of 6 mol dm^{-3} (2 mol dm^{-3} for Na_2SO_4), a temperature of ~110° C, and a pulp agitation speed of ~350 min^{-1} are required. Under the

above conditions, 72.50 %, 44.50% and 86.50% titanium and 96.00%, 55.90% and 71.0% iron are dissolved from ilmenite for NaCl, Na_2SO_4 and $NaNO_3$ systems, respectively.

Biswas *et al.*[272] have reported leaching of ilmenite with 6 mol dm^{-3} hydrochloric and/or 3 mol dm^{-3} sulphuric acid after being roasted at (700±15)° C; with LPG flow rate of 230 cm^3 min^{-1} for 75 min at a particle size of 63-125 μm.The maximum weight percentages of metals dissolved from the roasted mass are ~85 % titanium and 82.10% iron with 6 g eq dm^{-3} hydrochloric acid, whereas it is 52.3% titanium and 60.80% iron with 6 mol dm^{-3} sulphuric acid system. The optimum leaching with hydrochloric acid solution requires a higher acid concentration than 6 mol dm^{-3}, 110° C temperature, solid to liquid phase ratio (S/L) of 0.02 kg dm^{-3} and a pulp agitation speed of 350 rpm for 5 h. Identical concentration of sulphuric acid always gives poorer dissolution. Comparison of the X-ray powder diffraction patterns (XRD) of ilmenite and the roasted mass suggests certain chemical/physical changes occurring during treatment.

Prior to the leaching of ilmenite with 6 mol dm^{-3} hydrochloric acid and 3 mol dm^{-3} sulphuric acid, it has been heated with reformed product of the liquefied petroleum gas-water vapour mixture produced in presence of nickel catalyst by Biswas *et al.*[273]. The optimum roasting condition with LPG-H_2O vapor reformed products are (700±15)° C temperature, 110 cm^3 min^{-1} LPG flow rate, 0.041 atm. water vapor pressure and 40 min time. XRD shows the changes but the composition of roasted mass cannot be identified. Hydrochloride acid gives better leaching results than sulphuric acid of identical concentration. About 93% titanium and 95% iron are dissolved on leaching in 6 mol dm^{-3} hydrochloric acid at its boiling point, S/L ratio of 0.02 kg dm^{-3} and 350 rpm for 4h. Under similar condition, only 46% titanium and 64% iron are dissolved in sulphuric acid. From hydrochloric acid leach solution, titanium has been recovered easily as a pigment grade titanium dioxide (0.005% Fe, OAY=87.9%, RY=94.5%).

Biswas *et al.*[274] have processed heavy fraction of the beach sand containing ilmenite through Na_2CO_3-H_2O vapor roasting followed by hydrochloric acid leaching, liquid-liquid extraction, precipitation etc. to obtain white pigment grade TiO_2 and black

iron oxide. The optimum condition for the roasting is temperature 850^{o} C, time 45 min, ilmenite to Na_2CO_3 weight ratio 1.50, N_2 flow rate 420 cm^3 min^{-1}, and water vapor pressure 0.042 bar, whereas for leaching, hydrochloric acid concentration is 6 mol dm^{-3}, temperature 110^{o} C, solid to liquid ratio (S/L) 0.02 kg dm^{-3} and the pulp agitation speed 350 rpm. Under the above condition 96.50% titanium and 74% iron are dissolved from ilmenite. White pigment grade TiO_2 (over all yield 91%) can be isolated from this leach solution by a modified method.

Kinetics of leaching of sodium graphite -water vapor roasted mass with hydrochloric acid solution have been investigated as functions of hydrochloric acid concentration, temperature and phase mixing rate by Biswas *et al*.[275]. It is appeared that the kinetics of leaching is complicated by the co-existence of more than one chemical reaction occurring simultaneously during leaching. The rate constants for the leaching constituents have been evaluated and the mechanism of leaching has been proposed. From the temperature dependence studies, the activation energies have been calculated.

Habib *et al*.[276] have reported the effect of adding ethanol and phenol in leachant hydrochloric acid on dissolution of ilmenite. The kinetics of the dissolution processes have also reported. Addition of little amount of ethanol or phenol in hydrochloric acid enhances the extent of dissolution of ilmenite. The leaching with 6 mol dm^{-3} HCl + 0.50 mol dm^{-3} C_2H_5OH at 110° C and solid to liquid ratio (S/L) of 0.02 g dm^{-3} dissolves as much as 88% Ti and ~94% Fe compared to dissolutions of 74% Ti and 81.50% Fe in 6 mol dm^{-3} HCl alone. Under similar condition, 6 mol dm^{-3} HCl + 0.10 mol dm^{-3} C_6H_5OH dissolves as much as 81% Ti and 85% Fe. Decrease in leaching temperature and HCl concentration and increase in S/L ratio result in decrease in the extent of dissolution percentages. The kinetics of dissolution have been investigated by measuring rates of dissolution on HCl concentration, phenol or ethanol concentration, temperature and phase agitation speed. From temperature dependences of rate, the values of activation energy have been evaluated. The kinetic data could be fitted to the shrinking core model of dissolution.

Biswas and Chakraborty[277] prepared an amorphous compound having composition of $TiOHPO_4.11H_2O$ by the addition of H_3PO_4 solution to the iron free titanium(IV) solution made from ilmenite. The product showed ion-exchange property towards alkali

(Na^{+}) and alkaline earth (Ba^{2+}) metal ions to a limited extent. The product cannot be crystallized by the conventional method. The crystalline tetravalent metal phosphates, particularly those of Zr^{4+} and Ti^{4+} having α- and γ-layered structures have become an interesting group of compounds for their ion-exchange, intercalation, ion-conduction and catalytic properties. Starting materials ($ZrOCl_2$ and $TiCl_4$) are rather expensive and the yields are usually very low. So an attempt has been undertaken to prepare insoluble titanium(IV) phosphate (amorphous or crystalline) starting from a cheap source, viz., ilmenite which is abundantly available in the sea-shore of Bangladesh.

2.2 The Literature Review on Zircon Processing

As pointed out in the Introduction section that the processing of zircon is a difficult task for its inertness, a large number of works are available in journals, as well as, patents on various routes to process zircon for zirconia (ZrO_2). The work on this line have been started since the discovery of zirconium by Klaproth in 1789 with few examples of very old works, the works those have been done within the last 50 years will be summarized under different process headings.

(a) Thermal dissociation

When zircon is heated with graphite in a plasma arc furnace[278-285] at about 1750° C, it is dissociated to zircon and silica. When temperature is raised to 2000° C, silica is reduced by graphite to volatile SiO which at 2400° C oxidized again to SiO_2. Thus zirconia is left in the furnace heated at 2000° C.

Otherwise, the decomposed mixture of ZrO_2 and SiO_2 is leached with H_2SO_4 to dissolve ZrO_2 as $Zr(SO_4)_2$ or $ZrOSO_4$ which on filtration, crystallization and heating to 900° C can produce ZrO_2.

(b) Fluorosilicate fusion

At 700° C, zircon can be fused with sodium or potassium hexafluorosilicate (K_2SiF_6) to produce potassium hexaflurozirconate[285-287]. This reaction can be carried out in a rotary furnace at temperatures between 650-700° C[288]. The fusion reaction is:

$$ZrSiO_4 + K_2SiF_6 \xrightarrow{700^\circ C} K_2ZrF_6 + 2\ SiO_2$$

The fused product is milled and leached in 1% HCl solution at 85° C for two hours. After filtration, the filtrate is allowed to crystallize out K_2ZrF_6. A 3% solution of

the crystal is prepared to which ammonium hydroxide solution is added. As a result the precipitate of $ZrO_2.nH_2O$ appears according to the following reaction:

$$K_2ZrF_6 + 4NH_4OH \rightarrow ZrO.nH_2O + 2KF + 4NH_4F$$

The precipitate of $ZrO_2.nH_2O$ can be dried and calcined to get ZrO_2.

(c) High stoichiometric caustic soda (NaOH) fusion

By taking zircon to sodium hydroxide mole ratio of 1:6, the following reaction is reported [278, 285, 289, 290] to occur at 600° C:

$$ZrSiO_4 + 6NaOH \xrightarrow{600^\circ C} Na_2ZrO_3 + Na_4SiO_4 + 3H_2O\uparrow$$

When the moler ratio of Na_2CO_3 to zircon is adjusted at 3:1 then the following reaction takes place at 1000° C.

$$ZrSiO_4 + 3Na_2CO_3 \xrightarrow{1000^\circ C} Na_2ZrO_3 + Na_4SiO_4 + 3CO_2\uparrow$$

The fused product is crushed and slurried in water. Silicate is dissolved and separated from zirconate. Sodium zirconate is virtually hydrolyzed by water to sodium hydroxide and a complex hydrated oxide of zirconium. Sodium hydroxide solution is separated. The solid can be treated in various ways to get zirconia.

2.2.1 Mechanical activation of zircon

All the workers mentioned above use the high temperature conditions. But it is possible to dissolve zircon within 110° C by leaching with concentrated acid solutions following the mechanical activations or milling or fritting of zircon with basic oxides and alkali and alkaline earth metal hydroxides for long time (~15 d) at room temperature as well as elevated temperatures. Some workers on this line are summarized below:

The study on fritting reaction of zircon with sodium hydroxide was investigated thoroughly using DTA and XRD techniques by Choi and Cross in 1964[291]. Similar study relating to prepare pure zirconium compounds from zircon has been carried out by Choi[292]. In this report it is stated that during milling operation different phases are formed depending on milling time and NaOH to zircon ratio.

Abdel-Rehim[293] has reported a study on extracting zirconium from Egyptian zircon by it simultaneous ball milling and pressure alkaline leaching. Experiments have been carried out in stainless steel ball-mills of cylindrical shape under different conditions of temperature, pressure and time. The ball-mills are heated and mechanically rotated in electric furnace by means of roll mechanism. After operations, the mass is filtered and the filtrate is treated with $Ca(OH)_2$ to regenerate NaOH and to precipitate silicate as calcium salt. The study has indicated that the complete recovery of zirconium from zircon (99.70%) is possible by simultaneous ball-milling and alkaline pressure leaching at 250° C for 3 h, using 50% excess of NaOH.

The hydrometallergical processing of zircon separated from Egyptian black sands has been attained by leaching with NaOH of mechanically pretreated zircon concentrate at relatively high temperature (260° C)[294]. The effects of temperature, sodium hydroxide concentration, grinding (milling) time, grain size and leaching time as well as kinetics of the leaching process have been investigated. It is stated that a short leaching time of 90 min at 260° C lead to removal of over 85% of zirconium after 5 h's of grinding in an attraitor using 1:2 ratio of NaOH to zircon concentrate (particle size of 12~μm). The overall leaching reaction is chemically rate controlled.

The mechanochemical processing of mineral zircon ($ZrSiO_4$) has been investigated by Puclin *et al.*[295], with a view to exchanging the zirconium for other metals, leading to an easily extracted zirconia (ZrO_2) phase. Room temperature – ball milling of ziron with calcium and magnesium in dry conditions and with calcium hydroxide and sodium hydroxide in wet conditions has been examined. XRD, SEM and DTA are employed in analysis of as milled and annealed powder. The effects of milling time and subsequent heat treatment on structure and morphology are reported. The results indicate that mechanochemical processing significantly increases the reactivity of zircon towards reducing metals. No immediate exchange reaction is found for as-milled powders, but after annealing at 1000° C all samples showed partial or complete decompositions of $ZrSiO_4$ resulting in multiphase systems. In these systems, the major crystalline products are identified as ZrO_2 or $CaZrO_3$.

A commercial grade of zircon ($ZrSiO_4$) concentrate has been reported to be[296] mechanically milled with MgO for up to 100 h in a laboratory scale mill. The resultant powders are subjected to thermal processing, chemical leaching and X-ray diffraction (XRD). There is no direct evidence of reaction during the milling step, with no new phases evident from XRD. Leaching of the powder has showed that a reaction has occurred and increased solubility with milling time is attributed to the formation of a nanostructured Mg-Zr-Si oxide, which dissolves congruently. Heating of powders results in a number of thermal events, including the formation/crystallization of ZrO_2 and Mg_2SiO_4. Thermal treatment of the milled powders allows selective chemical leaching of the magnesium and silicon, leaving powder containing ~90% ZrO_2.

Alkaline earth metal oxides have been mechanically milled by Welham[297], with zircon for up to 200 h with the aim of forming zirconia or zirconates, either within the mill or during subsequent annealing at up to 1200° C. At a 1:1 molar ratio, all samples react during milling, forming ziconia and a metal silicate. Increased fractions of metal oxides result in reaction of the zircon to zirconates and metal silicates, except for magnesium, which formed zirconia and magnesium silicate. The zirconia formed is of the metastable tetragonal form, which revertedto the low-temperature monoclinic form after heating to 1200° C. The powders milled for 200 h are leached for 6 h at 25° C in 18% HCl; their solubility is very high, ranging from 88 to 92% for the lower oxide ratio (except for magnesium) and >95% for all powders of the higher oxide ratio; the only remaining phase after leaching is found to be zircon. Milling zircon in the absence of metal oxide shows a solubility of 9% confirming that reaction occurs during milling.

Arno Kaiser *et al.*[298] have reported the thermal dissociation of $ZrSiO_4$ within 1673±10° C. $ZrSiO_4$ decomposes by a solid state reaction releasing SiO_2 in form of discrete metastable intermediate phases with super stoichiometric Si- Content. The eutectic temperature in the ZrO_2-SiO_2 system was set to 1687±10° C.

2.2.2 In the following few paragraphs, the chemistry of zirconium and zirconia have been summarized

Larsen[299] have reported that there are several complete compilations of the literature concerning zirconium and hafnium that take the reader up to about 1960. Since then several reviews of more limited scope have been published, one on the

structural aspects of zirconium chemistry, and others on the separation of zirconium and hafnium, aqueous chemistry and ion exchange properties of zirconium compounds. In general the data in the present review are drawn from publications since 1960, although references to earlier work are included where necessary to complete the picture. The discovery that the thermal neutral cross section capture of zirconium containing the natural 2% hafnium contest was largely due to the very high thermal-neutral cross-section of the hafnium stimulated the present interest in the chemical and physical properties of these elements. The use of hafnium-free zirconium alloys for cladding nuclear fuels and the use of hafnium for control rods in nuclear reactors account for the fact that much of the recent literature deals with the reduction, purity, working properties, and alloy formation of these elements.

Nawrocki *et al.*[300] have been reported the purpose of this review is to shed some light on the complex properties of zirconia's surface chemistry in order to better understand its behaviour under chromatographic conditions. We emphasize the great differences between the much better known chemistry of silica surface and the chemistry of zirconia's surface. The review describes both physical and chemical properties of zirconium dioxide for a chromatographic point of view. The chemistry of monoclinic zirconia surface is developed from its underlying crystalline structure. The paper describes the dependence of the specific surface area, pore volume, porosity and mechanical strength on thermal treatment. Methods of synthesis of chromatographically useful zirconia are out lined. The review also covers the adsorption properties of zirconica at both gas-solid and liquid-solid interfaces. Adsorption of water, graphite dioxide, graphite monoxide, and ammonia are described and the controversies concerning the surface concentration of adsorption site are presented. The complex chemistry of a zirconia surface is pointed out and the importance of ligand exchange reactions is emphasized. In contrast to a silica surface, ligand exchange plays an important role in liquid chromatographic applications of zirconia. Strong, hard lewis acid sites, present on a zirconia surface, can interact with hard Lewis bases and these interactions, sometimes troublesome, can be successfully exploited even for protein separations. Zirconia's surface can be modified in many ways: dynamically by addition of competing Lewis bases to the mobile phase or permanently, by covering its surface with polymers or by depositing graphite. The review also shows that the main difficulty

in achieving a wider variety of applications is probably our lack of knowledge and poor understanding of zirconia's surface chemistry.

2.2.3 In the following paragraph, the kinetics of dissolution of zircon ($ZrSiO_4$) has been summarized

Mwakio P. Tole[301] has reported that the dissolution of amorphous zircon obeys first order kinetics and over long periods of time, the dissolution is decreased due to precipitation of new phase from solution. The dissolution reaction has activation energy of 12.8 kcal mol^{-1}. Crystalline zircon has low solubility in aqueous solution and methods capable of detecting Zr and Si in solution at concentrations of the order of 0.001 ppb are needed for successfull evaluation of the kinetics of dissolution of crystal dissolution-precipitation creep of K-feldspar in mid-crustal granite mylonites.

Minghua Mao *et al.*[302] have reported the electrokinetic and surface charge behaviours of a very pure natural zircon sample and a commercial grade zircon as functions of pH and KNO_3 concentration. The isoelectric point (IEP) and point of zero charge (PZC) of the natural zircon are determined to fall at a pH of 5.7±0.1 and 5.9±0.1, respectively. For the commercial grade zircon, the IEP and PZC values are 5.5±0.1 and 6.1±0.1, respectively. A triple layer site binding model has been used to describe the electrical properties of the zircon-water interface. The surface charge and the zero potential have been simultaneously calculated using this model and are in good agreement with the experimental data. The best fit-parameters pertaining to this model have been extracted by using both graphical extrapolation and computational methods. Infrared and X-ray photoelectron spectroscopy both indicated that kaolinite was present as an impurity in the commercial grade zircon.

2.2.4 Electrochemistry of vanadium doped $ZrSiO_4$

Site selective electro catalytic effect on nitrite oxidation has been reported by Antonio Domenecha *et al.*[303]. The electrochemistry of vanadium-doped zircon (V_xZrSiO_4, $0<x<0.10$) has been studied using abrasive conditioned paraffin impregnated graphite electrodes. It is compared with that of $ZrSiO_4$, ZrO_2 and vanadium-doped tetragonal and monoclinic zirconias. In contact with acetic/acetate and HCl+NaCl electrolytes, zirconium materials are reduced to Zr(III) at potentials near to -0.5 versus AgCl/Ag and to Zr metal at potentials more negative than -1.2 V, via proton-

assisted reductive processes, influenced by the complexing action of chloride ions. Vanadium-centered oxidation processes appear at potentials from +0.2 to +0.7 V enabling for a distinction between different coordinative arrangements. $ZrSiO_4$ exerts a significant electrocatalytic effect on nitrite oxidation in acetic/acetate buffers, slightly enhanced in the presence of increasing vanadium loadings. Electrocatalytic data are indicative that only V centres substituting Zr are catalytically active, whereas V substituting Si is catalytically silent.

2.2.5 Electrochemical characterization of praseodymium/doped zircon

Catalytic effect on the electrochemical reduction of molecular oxygen in polar organic solvents has been reported by Antonio Domencha *et al.*[304]. The voltammetry of microparticles and scanning electrochemical microscopy methodologies are applied to characterize praseodymium centers in praseodymia-doped ziron ($Pr_xZr_{(1-y)}Si_{(1-z)}O_4$; $y+z=x$; $0.02< x<0.10$) specimens prepared via sol-gel synthetic routes. In contact with aqueous electrolytes, two overlapping Pr-centered cathodic processes, attributable to the Pr(IV) to Pr(III) reduction of Pr centers in different sites are obtained. In water-containing, air-saturated acetone and DMSO solutions as solvent, $Pr_xZr_{(1-y)}Si_{(1-z)}O_4$ materials produce a significant catalytic effect on the electrochemical reduction of peroxide radical anion electro-chemically generated. These electrochemical factures denote that most of the Pr centers are originally in its 4+ oxidation state in the parent $Pr_xZr_{(1-y)}Si_{(1-z)}O_4$ specimens. The variation of the catalytic performance of such specimens with potential scan rate, water concentration and Pr loading suggest that Pr is not uniformly distributed within the zircon grains, being concentrated in the outer region of such grains.

2.2.6 In the following few paragraphs, the various types dissolution have been summarized

The step-wise dissolution of zircons has been reported by Jean-Louis Paquettea *et al.*[305]. A geochronological study using the step-wise dissolution technique and in situ ion microproble analysis is applied to late Archean metamict zirons of granitoids from north eastern Madagascar basement. Both techniques provide concordant U-Pb ages. Additionally, the ion microprobe study provided in situ measurements on the Pb isotopic composition of the metamict domains. Finally Pb-Pb evaporation ages were found to be slightly but systematically younger than the dating obtained by the two

other methods. Based on these data, granites from the Antongil belt were emplaced during at least three episodes separated by periods of magnetic inactivity of about 10 Ma at 2513, 2523 and 2532 Ma, respectively. These results are consistent with previous whole-rock Rb-Sr and U-Pb zircon dating from this part of Madagascar. The occurrence of this late Archean basement in northeastern Madagascar can be related to southern Indian where large volumes of contemporaneous granitoids were emplaced.

Dissolution-reprecipitation of igneous zircon in mid-ocean ridge gabbro, Atlantis Bank, Southwest Indian Ridge have been reported by Joshuea J. Schwartza[306] *et al.* zircons recovered from oceanic gabbro exposed on Atlantis Bank, Southwest India Ridge, typically display oscillatory and sector zoning consistent with igneous crystallization from magic magmas. In one rock (of twenty Investigated), weak-oscillatory zonation patterns are overprinted by secondary textural features characterized by mottled, convoluted and wavy internal zomation patterns that are frequently associated with secondary micron-to submicron scale micro-porosity. These zircons are hosted in a felsic vein that intruded on oxide gabbro, both of which are cross-cut by monomineralic amphibole and quartz-rich veinlets. Zircons with weak-oscillatory-zonation patterns record a weighted average 206Pb/238 U age of 12.76±0.20 Ma (mswd=1.5), and have high trace element concentrations [e.g., ∑REEs(~0.4-2.2 wt. %), Y(~0.6-2.8 wt %),] P(~0.4-0.9 wt %), and Th/U (0.1-0.5). These zircons are anomalously old (≥ 1Myr) relative to the magnetic age for this portion of oceanic crust (11.75 Ma). In contrast, zircons with nonigneious, secondary textures have a younger weighted-average 206pb/238U age of 12.00±0.16 Ma (mswd=1.7) and have lower trace element concentrations [e.g., ∑Rees (~0.2-0.8 wt %), Y(~0.3-1.0 wt %), P(~0.1-0.3 wt %)] and slightly lower (Th/U (0.1-0.3). The weighted average age of these zircons is similar to the magnetic anomaly age, and other 206 Pb/238U ages of nearly rocks. We do not observe a correlation between crystallographic misorientation, internal texture, or trace element chemistry. We suggest that the decrease in trace element concentrations associated with the development of non-igneous alteration textures is attributed to the purging of non-essential structural constituent cations from the zircon crystal lattice at amphibolite, facies conditions. The mechanism of alteration/re-equilibration was likely an interface-coupled dissolution-representation processes that affected pre-existing, anomalously old zircons during shallow-level magmatic construction of Atlantis Bank at ~12.0 Ma.

Dissolution of $ZrSiO_4$ after mechanical milling with Al_2O_3 has been investigated by puclin *et al.*[307]. They have reported a mixture of alumina (Al_2O_3) and Zircon ($ZrSiO_4$) was subjected to mechanical milling. The presence of alumina was found to greatly enhance the disordering of zircon. Acid leaching of the milled oxide mixtures resulted in complete dissolution of the zirconium, along with a proportion of alumina and only traces of silica. Zirconium leaching was not possible with zircon milled alone.

2.2.7 In the following few paragraphs, production of nuclear grade zirconium have been summarized

A review on production of nuclear grade zirconium has been published by L. Xua, *et al.*[308]. Zirconium is an ideal material for nuclear reactors due to its low absorption cross-section for thermal neutrons; whereas the typically contained hafnium with strong neutron absorption is very harmful for zirconium as a fuel cladding material. This paper provides an overview of the processes for nuclear grade zirconium production with emphasis on the methods of Zr-Hf separation. The separation processes are roughly classified into hydro- and pyro-metallurgical. Zr-Hf separation methods are discussed based on the following reaction features: redox characteristics, volatility, electrochemical properties and molten salt metal equilibrium. In the present paper, the available Zr-Hf separation technologies are compared.

Nuclear-grade zirconium prepared by combining combustion synthesis with molten-salt electrorefining technique has been investigated by Hui Lia *et al.*[309].

Zirconium has a low absorption cross-section for neutrons, which makes it an ideal material for use in nuclear reactor applications. However, hafnium typically contained in zirconium causes it to be far less useful for nuclear reactor materials because of its high neutron absorbing properties. In this study a novel effective method has been developed for the production of hafnium free zirconium. The process includes two main stages: magnesio-thermic reduction of $ZrSiO_4$ under a combustion mode, to produce zirconium silicide (ZrSi), and recovery of hafnium free zirconium by molten salt electrorefining. It was found that, depending on the electrorefining procedure, it is possible to produce zirconium powder with low hafnium content: 70 ppm determined by ICP-AES analysis.

2.2.8 Works done in the Metallurgical Research Laboratory of the Department of Applied Chemistry and Chemical Technology/ Engineering, Rajshahi University

Biswas and Hayat[310] have reported the extraction for Zr(IV) from aqueous acidic $SO_4^{=}$-Ac^- medium with bis- (2-ethyl hexyl) phosphoric acid (HDEHP or H_2A_2) in benzene has been investigated as functions of contact time, aqueous phase Zr(IV), SO_4^{2-}, Ac^- and H^+ concentrations, organic phase HDEHP concentration, temperature and the nature of the diluents. The equilibration time is less than 7 min. The pH, HDEHP and SO_4^{2-} dependences of 1, 1, and -1 respectively on the extraction radio suggest the extraction by the following reaction: $[ZrO(OH)SO_4]^- + H_2A_2 \leftrightharpoons ZrOA_2 + H_2O + H^+ + SO_4^{2-}$. Acetate ion has no effect. Temperature dependence data gives apparent ΔH value of 43.47 kJ mol^{-1}. The log K_{ex} value has been evaluated to be 1.389. The structure of the isolated solid complex has been suggested from its molecular weight, P to Zr atom ratio, magnetic moment, infrared spectra and loading test.

Biswas and Habib[311]has reported the extraction of Zr(IV) from aqueous sulphate medium by di-o-tolyl phosphoric acid (HDTP, HA) in graphite tetrachloride containing 20% hexanol as de-emulsifier as function of contact time, aqueous phase metal ion, sulphate and hydrogen ion concentrations, organic phase HDTP concentration and temperature. The extraction occurs very fast; about 2 minutes are required for equilibration. The acidity and HDTP dependences of Zr(IV) are dependent on the experimental parameters and concentration ranges. It is due to the change in the chemical species of Zr(IV) in aqueous solution with change in acidity of the aqueous solution and also due to the different degrees of solvation. The mechanism of extraction at various conditions has been postulated. The extraction of Zr(IV) decreases remarkably with increasing sulphate ion concentration in aqueous phase. The temperature dependence data give ΔH value of -8.40 kJ mol^{-1}, indicates the extraction process to be exothermic. The zirconium(IV) to monomeric HDTP ratio in high loaded complex is about 2:3 and loading capacity is 21.06 g Zr(IV)/100 g of the extractant.

Biswas and Hayat[312] have reported that the apparent equilibrium of extraction of zironium(IV) from chloride media by D2EHPA in kerosine is found to depend on ageing of the aqueous phase. When the aqueous phase, just after preparation is used in the extraction study, reproducible results are not obtained. With increasing ageing time,

the apparent distribution ratio (*D*) is increased for a particular set of experimental parameters. The system has been thoroughly investigated for 1- and 30- d ageing. In both cases, the apparent equilibration time is 15 min. *D* is decreased with increasing Zr(IV) concentration in the aqueous phase but the nature depends on ageing. In both cases of ageing, logD Vs. -log[HCl] plots are peculiar in nature. For 1-day ageing, the slope is ~-1 above 3 mol dm^{-3} HCl and also below 0.3 mol dm^{-3} HCl, and is zero within 0.3-3.0 mol dm^{-3} HCl. In contrast, for 30-d aged system, the slope is ~ -2 above 2 mol dm^{-3} HCl, ~-1 below 0.5 mol dm^{-3} HCl, and zero between 0.5 and 2.0 mol dm^{-3} HCl. The extractant dependencies are 2 and 4 for 1- and 30-d aged systems respectively. Chloride ion has a larger effect on *D* for the 1-d aged system, but no effect on *D* for the 30-d aged system. From the temperature dependence data, ΔH values have been determined. The possible extraction equilibrium reactions have been suggested and supported by the loading tests, as well as, by the molecular weight, Zr/P ratio, Zr/Cl ratio and infrared spectral data of the extracted species.

Biswas and Hayat[313] have also reported the kinetics of the extraction of zironium (IV) from chloride media by D2EHPA in kerosine have been investigated by the single drop technique for 1-d ageing of the aqueous phase. The flux equation have been derived for three aqueous acidities of 0.10, 1.00 and 5.00 mol dm^{-3} HCl, respectively, as: J (kmol m^{-2} s^{-1})= $10^{-5.37}$ $(1+0.00036\ [Zr(IV)^{-1})^{-1}\ [H^+]\ [H_2A_2]_{(0)}\ (1+0.69\ [Cl^-])$, J (kmol m^{-2} s^{-1})=$10^{-5.77}$ $(1+0.0056\ [Zr(IV)^{-1})^{-1}\ [H_2A_2]_{(0)}\ [Cl^-])$ and J (kmol m^{-2} s^{-1})=$10^{-6.62}$ $(1+0.0056\ [Zr\ (IV)^{-1})^{-1}\ [H+]\ [H_2A_2]_{(0)}\ [C^{l-}])$. The value of E_a (kJ mol^{-1}), $\Delta H^{\pm}$ (kJ mol^{-1}) and $\Delta S^{\pm}$ for each of the above conditions have been estimated to be 8.60, 7.70 and -425; 19.20, 16.80 and -369; and 26.40, 23.40 and -330, respectively, in the higher temperature region (htr) of investigation; and 89.60, 76.60 and -192; 69.50, 71.90 and -187; and 59.90, 60.10 and -205, respectively, in the lower temperature region (ltr). On the basis of these rate data, the mechanisms of extraction in different conditions have been suggested.

Biswas *et al.*[314] have reported the kinetics of the extraction of zironium (IV) by D2EHPA investigated by the Lewis cell technique for 1-day ageing of the aqueous phase and compared with those obtained from the single drop technique. The mass

transfer flux equations for Zr(IV) have been derived for three aqueous acidities of 0.10, 1 and 5 mol dm^{-3} HCl, respectively, as; J (kmol m^{-2} s^{-1} = $10^{-5.53\pm0.04}$ (1+0.0038 $[Zr(IV)^{-1}]^{-1}$ $[H^+]$ $[H_2A_2]_{(0)}$ (1+0.70 $[Cl^-]$), J (kmol m^{-2} s^{-1})=$10^{-5.80\pm0.02}$(1+0.004 $[Zr(IV)]^{-1}$ $(H_2A_2)_{(0)}$ $[Cl^-]$) and J (kmol m^{-2} s^{-1}=$10^{-6.58\pm0.03}$ (1+0.0038 $[Zr(IV)]^{-1})^{-1}$ [H+] $[H_2A_2]_{(0)}$ $[Cl^-]$).The values of E_a (kJ mol^{-1}) in kinetic and diffusion regimes are 92 & 14.7 and 84 & 15 for 1 and 5 mol dm^{-3} HCl systems, respectively. For 0.10 mol dm^{-3} HCl system, E_a value cannot be measured for kinetic regime but its value is 15 kJ mol^{-1} of diffusion regime. At intermediate controlled regime (Zr(IV) ≈ 3 mmol dm^{-3}), E_a value varies from 11, 12 and 15 kJ mol^{-1} to 42, 105 and 108 kJ mol^{-1}, respectively, for 0.10, 1 and 5 mol dm^{-3} HCl systems on varying the temperature from 318 K to 288 K. On the basis of these data, mechanisms of extraction in different conditions have been suggested.

Biswas and Hayat **[315]** have reported the kinetics of solvent extraction of Zr(IV) from acidic chloride solution by D2EHPA investigated by the single drop technique after 30-d ageing of the aqueous phase. The flux equation at 303 K have been derived for three aqueous acidities of 010, 1.00 and 5.00 mol dm^{-3} HCl, respectively, as: *J* (kmol m^{-2} s^{-1}) = $10^{-4.57}$ $(1+0.0036\ [Zr(IV)]^{-1})^{-1}$ $[H^+]$ $[H_2A_2]_{(0)}$. The values of the activation energy (E_a) depend on the Zr(IV) concentration and temperature regions. The values of E_a, $\Delta H^{\pm}$, $\Delta S^{\pm}$ have been determined under various conditions. The flux equation and the value of E_a indicate that the extraction process are chemically controlled at lower temperature and Zr(IV) concentration regions. The reacting Zr(IV) species that satisfy the rate data are either $[Zr_8(OH)_{20}(H_2O)_{24}\ Cl_{13}]^-$ or $[Z_4(OH)_{8/9}\ (H_2O)_{16}\ Cl_{9/8}]^-$ in 0.10 mol dm^{-3} HCl; $[Zr_4(OH)\ (H_2O)_{16}\ Cl_8]$ or $Zr(OH)\ Cl_3$ in I mol dm^{-3} HCl and $[Zr(H_2O)_4\ Cl_4]^{2-}$ in 5 mol dm^{-3} HCl. On the other hand, at higher temperature and Zr(IV) concentration regions, extraction processes are diffusion controlled, where the rates of diffusion of $H_3A_2^+$ are slower than the rates of diffusion of $[Zr_8(OH)_{20}(H_2O)_{24}\ Cl_{13}]^-$, $[Zr_4(OH)_8\ (H_2O)_{16}\ Cl_8]$ and $[Zr(H_2O)_4\ Cl_4]^{-2}$ in 0.10, 1 and 5 mol dm^{-3} HCl media, respectively.

Biswas *et al.***[316]** reported the synthesis of a number of useful zirconium compounds, such as hydrated zirconium chloride, zirconium sulfate, zirconium dioxide, γ-zirconium ammonium phosphate, γ-zirconium phosphate, γ-zirconium phosphate

phosphite, and γ -zirconium phosphate hypophosphite from Bangladeshi zircon following the NaOH-fusion, acid (HCl and H_2SO_4)-leaching, precipitation, calcination/pyrolysis, condensation polymerization, ion exchange and the tap tactic reaction methods. The products have been characterized by chemical and thermogravimetric analyses in all cases, together with the XRD patterns and sodium exchange capacities in some cases.

Biswas *et al.*[317] have reported that the dry ground bangladeshi zircon (44-53 μm) is found completely inert in 6 mol dm^{-3} HCl, 6 mol dm^{-3} HNO_3, 6 mol dm^{-3} $HClO_4$, 3 mol dm^{-3} H_2SO_4 and 6 mol dm^{-3} HNO_3 during leaching at their boiling point temperatures under reflux for 4 h. In the 6 mol dm^{-3} HF and 6 mol dm^{-3} NaOH solution, only ~5% zircon is dissolved under similar conditions. The mechanical activation of zircon with NaOH at ambient temperature, by grinding in a ball mill for 300 h, is also ineffective with only 2% Zr(IV) dissolved. However, up to 86% zircon can be dissolved on leaching a sodium graphiteate baked mass with 6 mol dm^{-3} HCl under reflux for 1 h. The optimum conditions of banking were found to be 1273 K for 2.50 h with a Na_2CO_3: zircon wt. ratio of 0.60. Higher Na_2CO_3: zircon wt. ratios and longer baking times decreased the recovery percentage.

The investigation has found for the first time that zircon is completely and rapidly decomposed by fusion with 8 mol NaOH solutions to give a semi-crystalline fused mass. The rate of fusion was monitored by leaching Zr(IV) from the fused mass with 5 mol dm^{-3} HCl under reflux for 30 min. The optimized fusion conditions were 973 K for 15 min with a NaOH: zircon wt. ratio of 1.8, or mole ratio of 8:1, which gives the following reaction for fusion: $ZrSiO_4+8NaOH \rightarrow NaZrO_4+Na_4SiO_4+4H_2O$. The rate of dissolution of zircon in molten NaOH was found to follow the law: $1-(1-R)^{1/3}=(k/\rho r_0)$ $[NaOH/zircon]^a$ t. The calculated value of '*k*' was $10^{-4.00\pm0.004}$g $min^{-1}cm^{-2}$ (for ρ= 4.7 g cm^{-3}, r_o=26.5 μm) at 973 K and a=1.0. The calculated activation energy for fusion is 125 kJ mol^{-1} that indicat of a chemically controlled reaction with the slow step being the first reaction of NaOH with zircon.

Biswas *et al.*[318] reported a thorough investigation on the leaching and kinetics of extraction of Zr(IV) from a semi-crystalline zircon-NaOH fused material by

hydrochloric acid. The fused material was produced by mixing NaOH/zircon at a wt. ratio of 1.8 (mole ratio 9) at 973 K for 15 min. Conditioning was done by water washing, drying, grinding and sieving. The optimum conditions for dissolution of Zr(IV) were leaching by 4 mol dm^{-3}HCl under reflux for only 5 min with a solid to liquid ratio of 1.41:10 w(g)/v(mL). By applying staged leaching it was possible to obtain a solution containing up to 112 g dm^{-3} Zr(IV). The rate of leaching was found to be directly proportional to $[HCl]^2$ and very dependent on the temperature. The rate constant at 382 K with a particle diameter of 48.5±4.5 μm was determined to be $10^{-1.91}$ g dm^4 min^{-1} mol^{-2} and the activation, E_a, was 64.3 kJ mol^{-1} indicating chemical reaction control. Stirring had a little effect on the rate of dissolution due to the high porosity of the conditioned fused material. However, the rate was inversely proportional to the radius of the particles used. The novelty of the process is the fast rate of dissolution of the caustic fused materials to give a concentrated solution of Zr(IV).

2.3 The Literature Review on Lead Sulphate Processing

The following survey reports the various types of works related to the extraction, refining and processing of Pb from different sources by both pyro and hydrometallurgical methods. Literature survey also includes the chemistry and lead purification by hydrometallurgical process and other works related to the present investigation.

Lyakov and Nokolov[319] have reprocessed the scrap lead-battery paste by using diethylenetriamine. The lead from battery scrap pastes (containing 78-85% Pb, mainly as oxide, with smaller amount of metallic Pb and lead sulfide and sulfate was extracted nearly quantitatively on treating the paste for 20-25 min with an aqueous solution containing 150 mol dm^{-3} diethylenetriamine and 80 mol dm^{-3} H_2SO_4 at room temperature or 60° C with continuous stirring. The optimum liquid solid ratio was 7:1. Bubbling of CO_2 through the resulting solution at room temperature precipitated, the Pb as graphiteate.

Yamada *et al.*[320] has recovered lead as lead graphiteate of high purity from crude lead sulfate by leaching with an aqueous solution containing an alkylamine and either oxalic acid or an oxalate. The solution obtained by leaching was treated with CO_2 at >50° C to precipitate Pb graphiteate which was removed. The solution remaining was treated with sufficient dilute H_2SO_4 to decrease the CO_2 concentration in the

alkylamine to 2-4 mol dm^{-3} (pH 4.0-7.0) and then sufficient slaked lime was added to remove the SO_4^{2-} at >70° C. The concentration of alkylamine was increased by using an ion-exchanger and alkylamine was recycled to the leaching stage. The graphiteate obtained was treated further with an alkali metal graphiteate and an acetate or NaOH.

Takehara[321] reviewed the dissolution- precipitation reactions on the electrodes in the lead acid battery. At the discharge of β-PbO_2 in the positive electrode and Pb in the negative electrode, $PbSO_4$ deposited on both electrode surfaces through the large supersaturation of Pb^{2+} ion. Thus, the discharge reactions of the positive and the negative electrodes proceed smoothly, and the largest crystal size of $PbSO_4$ was obtained at 0.5-1.0 mol dm^{-3} H_2SO_4 with the largest Pb^{2+} ion concentration on the surface. The size of its $PbSO_4$ crystals became smaller at a higher current discharge through the formation of many of nuclei on the electrode surface. On the other hand, the charge reactions consisting of the anodic oxidation of $PbSO_4$ at the positive electrode and the cathodic reduction of $PbSO_4$ at the negative electrode, did not proceed in the same way as the discharge reactions, because $PbSO_4$ is a large ionic crystal without electronic or ionic conductivities and its solubility is very low in sulfuric acid solutions. The reaction site is considered to be the interface between β-PbO_2 of the positive active mineral, or Pb of the negative active material, and $PbSO_4$. At such an interface, Pb^{2+} ions can be adequately supplied from the $PbSO_4$ crystal, and a charge transfer reaction can occur on β-PbO_2 or Pb. The reaction rate depends on the electrochemical kinetics parameters, e.g., exchange charge-transfer rate, real areas of the interface between PbO_2 and Pb and $PbSO_4$, and the mass transfer in the narrow gap can be assumed to be like that of a thin layer cell. For the oxidation of $PbSO_4$ to β-PbO_2, and the charge-transfer process was the rate-determining step. For the reduction of $PbSO_4$ to Pb, the mass transfer process was the rate-determining step. For both processes, it was concluded that a large crystal size of $PbSO_4$ gives a smaller current because of the smaller reaction site area per unit volume.

Pashkov *et al.*[322] have reported the dissolution of the rotating disk electrode (RDE) of natural lead sulfide (galena) and the ground mineral in nitric acid solutions as a function of electrode potential, HNO_3 concentration and temperature. The rate of dissolution producing hydrogen sulfide slowly increases as the potential varies from +0.10 to -0.4 V (Ag/AgCl). The reaction order on nitric acid concentration has been

found to be 1.20±0.15 at 0.20 V and 0.90 at -04.0 (40° C), and the apparent activation energy is 35 kJ mol^{-1} in 1 mol dm^{-3} HNO_3 at 0 V, suggesting that the process is controlled by a chemical or electrochemical reaction. At higher biases the RDE of PbS dissolves for the most part anodically, showing the highest rate at ~0.70 V, whereas the rate as a function of acid concentration is maximal in 1 mol dm^{-3} HNO_3. The yield of sulfate increases with potential and is small for the leaching of both compact and ground galena, while its reaches 50% in the case of a flotation lead concentrate. Ferric ions catalyze the dissolution of compact and especially, ground galena, with the peak rate at the potential of immersed platinum electrode of 0.40-0.50 V. The Fe^{3+}/Fe^{2+} couple is concluded to act as an intermediator for the electron transfer between nitrate ions and the solid, indicating that the dissolution is electrochemical in nature.

A steady state potentiostatic experiments[323] on a galena rotating disc electrode in perchlorate solutions of varying pH values indicated that the primary reactions governing the anodic dissolution was $PbS \rightarrow Pb^{2+} + S + 2e$. A mechanism involving sulphur intermediate is proposed for this process. Cyclic voltametric studies with the use of rotating ring-disc electrodes in perchlorate and sulphate solutions revealed that the pH value at the electrode surface had a marked effect on the anodic dissolution. The morphology of the anodically produced sulphur had a bearing on the active-passive behaviour of galena. The species responsible for the passivation of the galena surface in sulphate and perchlorate solution were shown to be the basic lead sulphates.

The pyrometallurgic processing of the exhausted batteries has been reported by Smanitto *et al.*[324]. The recovery of metallic lead generates great amount of a by-product called slag. The slag is composed mainly of iron (≈60%) and lead (≈6%) and this residue cannot be disposed in conventional landfill due to the high lead content. This work presents a new methodology for the extraction of lead from slag, based on the complexing effect of EDTA, a chelating ligand that has the ability to solubilize several heavy metals. As the iron (Fe^{2+}/Fe^{3+}) have a formations constant with EDTA fluoride ion (F^-) was employed to mask the iron ions. The tests were carried out on a qualitative way confirming the lead extraction by the formation of a yellow precipitate of lead iodide.

In order to recover lead from the zinc leaching residues developed by Zheng *et al.*[325], a new technology involving selective reduction of lead sulfate to lead sulfide

with graphite, followed by flotation. The reduction thermodynamics of $PbSO_4$ was discussed and the effects of molar ratio of C to $PbSO_4$, reaction temperature and time were examined by thermogravimetry (TG) and XRD. Verification tests were further carried out to prove the conclusion of thermodynamic and TG analyses and the transformation extent could reach 86.45% under the optimal roasting conditions. The prepared galena was then subjected to micro-flotation tests, and the highest lead recovery could reach up to 75.32%.

2.3.1 The works published from the Metallurgical Research Laboratory of the Department of Applied Chemistry and Chemical Technology/ Engineering, Rajshahi University

Biswas *et al.*[326] used the infrared spectra to indicate the complexation of lead sulphate by ethanolamines through nitrogen during dissolution of battery scrap by ethanolamines. The IR. spectra have also used to indicate that the efficiency of reuse of mono- and di-ethanolamine greatly decreases due to the decomposition of amines during regeneration and also to the graphiteate absorption, whereas the slow decreasing efficiency of tri-ethanolamine is due to graphiteate absorption only. The UV-visible spectra indicate the formation of weak complexes between lead sulphate and tri-ethanolamine.

Biswas *et al.*[327] have worked on the recovery of Pb as $PbCO_3$ from waste battery scrap by leaching with an aqueous solution of mono-, di- and triethanolamines and subsequent stripping with Na_2CO_3 or $NaHCO_3$ solutions. Leaching in amines has been investigated with respect to contact time, amine concentration, and solid to liquid (S/L) ratio, particle size and temperature. Almost 100% Pb is dissolved within 90 min by 50% (v/v) triethanolamine (TEA) in water at 55° C provided that the S/L ratio is kept at 1/20 (kg dm^{-3}). Under similar experimental conditions, di-and monoethanolamines are not as effective as TEA. The percentage dissolution of Pb is considerably decreased with increasing S/L ratio, but the concentration of Pb in the leach solution is increased to a limiting value at 1/1 (kg dm^{-3}). Dissolution in stages at this limiting S/L ratio is recommended to obtain a leach solution containing 200 g Pb dm^{-3}. The dissolution rate is appreciably increased by reducing the average particle size of scrap powder. As stripping agent, 60 g $NaHCO_3$ dm^{-3} solution is as effective as 150 g Na_2CO_3 kg dm^{-3} solution. Equal volumes of leach and stripping solutions yield almost quantitative

precipitation of $PbCO_3$. Stripped solution may be regenerated and recycled with slight decrease in dissolution efficiency, particularly in the case of TEA.

Biswas *et al.*[328] have reported the rates of dissolution of lead sulphate from waste battery scrap in the form of flat pellets by aqueous triethanolamine (TEA) solution under various experimental conditions. Temperature dependence data indicate that the dissolution process is diffusion controlled (Ea = ~10 kJ dm^{-3}) above 45° C and below this temperature, the process appears partially chemically controlled (Ea= ~27 kJ dm^{-3}). In the lower temperature region under investigation, the chemical reaction which slows the dissolution is:

$$PbSO_{4(s)} + TEA_{(a.i)} \xrightarrow{slow} Pb(TEA)^{2+} SO_4^{2-}{}_{(a.i)}.$$

The rate constant, k, is 0.55 g s^{-1} m^{-2} $mol^{-0.75}$ at 20° C with agitation speed of 1600 min^{-1}. The rate is found to be 0.40th power dependent on stirring speed, which definitely indicates that the diffusion of TEA to and product species from the reaction site control the rate. The particle size of scrap powder used in making the pellets has little effect on the initial dissolution rate: 50 μm particles should be used to obtain uniform rates.

Biswas *et al.*[329] have also reported the rates of dissolution of lead sulphate from waste battery scrap in the form of powder (<500 μm) by aqueous triethanolamine (TEA) solution under different experimental conditions. At 30° C and at the phase mixing rate of 1400 rpm, the rate of dissolution may empirically be expressed as $-(dw/dt)=10^{-(2.39\pm0.05)}$. W_0. (S/L). [TEA] (1/t). Temperature dependence data indicate that the dissolution process is intermediate controlled (E_a= 13-40 kJ mol^{-1}) between 40 and 60°C, chemically controlled (E_a>40 kJ mol^{-1}) below 40° C and diffusion controlled (E_a<13 kJ mol^{-1}) above 60° C. At low temperature, the chemical reaction step which slows the dissolution is: $PbSO_{4(s)} + TEA_{(a)} \xrightarrow{slow} [Pb(TEA)]^{2+} SO_4^{2-}{}_{(a)}$. The rate is found to be independent of stirring speed (>800 rpm) at low temperature, whereas at higher temperature (50° C), the rate is ~0.33th power dependent of phase mixing speed.

CHAPTER 3
OBJECTIVE OF THE PRESENT INVESTIGATION

3 Objective of the Present Investigation

Bangladesh has vast agricultural fields but lacks mineral deposits. Virtually she does not possess any mineral mine. But the beach sands of Bangladesh (particularly in south eastern part), contain considerable amount of commercial minerals, like ilmenite, rutile, monazite, magnitite, zircon etc. Among these minerals ilmenite, zircon and monazite are very valuable.

Ilmenite is the most important ore mineral of titanium. It is the compound oxide of titanium and iron. Ilmenite can be used as source of pigment grade TiO_2 or Ti-bearing alloys for aero space shuttle. The production of titanium by hydrometallurgical process has appeared to be easier than pyrometallurgical process. Titanium is generally extracted as dioxide from ilmenite fraction by conventional sulphuric acid, hydrochloric acid leaching and precipitation route. However in the conventional process a large fraction of ilmenite is being rejected undissolsed and the co-dissolved associated transition elements such as Cr, Ni, V etc. may be co-precipitated with titanium which may seriously discolor the white pigment colour of titanium dioxide. The ilmenite found in Bangladesh contains the transition metals such as Cr, Ni, Mn etc., so the product obtained by the conventional method is colored. To improve the product quality, other ways are to be searched to utilize the ilmenite found in our country.

On the other hand, zircon can be used as the source of zirconia (ZrO_2) having wide application such as (i) nuclear reactors for cladding fuel rods, (ii) ceramic industry and (iii) medical field (bone marrow transplantation and surgical appliances). A long term research on the processing of ilmenite and zircons found in Bangladesh have been carried out in the Metallurgical Research Laboratory of DoACCE and the results have been published in a number of home and foreign journals[269-277, 310-318]. The processing of ilmenite and zircon faces difficulty due to their chemical inertness. Once these are solublized, the methods are available to get TiO_2 and ZrO_2 from the leach solution.

Furthermore, lead is one of the few metals which has to be recycled from all waste sources since the primary sources of lead e.g. the lead mines are almost exhausted. It is predicated that the primary source of lead may be exhausted within 10-15 years according to the world reserve of lead reported [330] (130 million metric ton). So the indigenous uses of lead and lead compounds will find it hard to obtain these

materials at a cheap rate in future. Already price of lead batteries and lead compounds have increased 5-10 times during the last 10 years.

Lead is main component of lead acid batteries. It has also wide applications in paint industry, machinery bearings, and protection materials of X-ray etc. A huge number of lead accumulators are used in motor vehicles of Bangladesh. Waste lead-accumulators create environmental pollution. In these waste accumulators, lead exists as sulphate. But the dissolution of lead sulphate is another chemical problem. It is insoluble in common acids and alkalies at ordinary temperature, as well as elevated temperature. It can be dissolved in expensive ethanolamine[326-329] and the leached solution can be easily treated to obtain Pb-oxide which in turn may be easily reduced to metallic lead but it is not applicable for large scale operations for its high price.

Bangladesh lacks mineral resources. In this context ilmenite and zircon available in the beach sand of our country may play a vital role in metallurgical sector. So it is essential to find out an easy technique, such as, electrochemical technique for ilmenite, zircon and lead sulphate with the highest possible dissolutions of titanium (with mineral acids), zircon (with mineral acids and bases), and lead (with mineral acids) and then for the recovery methods of titanium, zircon and lead as their oxides from the solution.

Therefore, the objective of the present investigation consists of the following:

i) Ilmenite, zircon and lead sulphate were to subject for grinding and sieving to collect <53 μm sized fraction.

ii) Analyses of ilmenite, zircon and lead sulphate by chemical and XRD pattern.

iii) Investigation the on effect of dissolution potential on the electrochemical dissolution of ilmenite, zircon and lead sulphate.

iv) Investigation on the effect of acid, base concentration on the electrochemical dissolution of ilmenite, zircon and lead sulphate.

v) Investigation the effect of temperature on the electrochemical dissolution of ilmenite, zircon and lead sulphate.

vi) Investigation on the effect of ilmenite/ zircon/ lead sulphate and graphite ratio on the electrochemical dissolutions of ilmenite, zircon and lead sulphate.

CHAPTER 4
MATERIALS AND METHODS

4.1 Chemicals Used, their Sources and Specifications

4.2 Specification of the Instruments used in this investigation

4.3 Preparation of Different Standard Solutions

4.4 Experimental Techniques

4.5 Electrochemical Measurement

4.6 Electrochemical Dissolution

4.7 Analytical Technique: Spectrophotometer

4.8 Spectrophotometric Estimation of Iron (III)

4.9 Spectrophotometric Estimation of Zirconium (IV)

4.10 Atomic Absorption Spectrophotometry

4 MATERIALS AND METHODS

4.1 Chemicals Used, their Sources and Specifications

All the chemicals used in this investigation excepting itmenite, zircon, lead sulphate and graphite powder were of analytical reagent grade. Doubly distilled water was used in the preparation of all solutions. Ilmenite and zircon sand (ilmenite and zircon fraction) used in this experiment were collected from the Bangladesh Atomic Energy Commissions Pilot Plant for separation of heavy minerals from beach sands at Kalatali, Cox's Bazar. Lead sulphate was collected from waste lead acid batteries and graphite was collected from dry cell. The supplied sand (ilmenite, zircon), lead sulphate and graphite were dry ground in a ball mill and seived to collect powder of different particle sizes. Specification of used other chemicals are given below:

SL. No	Name of the Chemical	Purity (%)	Source
1.	Titanium dioxide	99.0	E.Merck (Germany)
2.	Ferric ammonium sulphate	99.0	E.Merck (Germany)
3.	Sulphuric acid	98.5	E.Merck (Germany)
4.	Potassium bisulfate	99.0	E.Merck (Germany)
5.	Ammonium thiocyanate	98.0	Loba Chemical
6.	Orthophosphoric acid	85.0	BDH Chemicals Ltd.
7.	Hydrogen peroxide	30.0	E. Merck (Germany)
8.	Nitric acid	69-72	E. Merck (Germany)
9.	Standard Zirconyl chloride Solution	11 mmol dm^{-3}	BDH (England)
10.	Ethylenediaminetetraacetic acid disodium salt (EDTA)	>99.0%	BDH (England)
11.	Sodium graphiteate	99.8	FARCO (China)
12.	Pyrocatechol violet	Purified	Loba Chemical, Mumbay, India
13.	Sodium fluoride	>99.0%	E. Merck (Germany)
14.	Sodium hydroxide	>97.0%	Merck (India)
15.	Hydrochloric acid	36	BDH (England)
16.	Hydrofluoric acid	40	E. Merck (Germany)
17.	Perchloric acid	70	E. Merck (Germany)
18.	Acetic acid	100	E. Merck (Germany)
19.	Potassium permanganate	99.5	E. Merck (Germany)
20.	Sodium hydroxide	>97.0	Merck (India)

4.2 Specification of the Instruments used in this Investigation

Name of the instruments used in this investigation with their specifications are given below:

Instrument	Manufacturer
Ball Mill	Norton Chemical Process Products Division, SL. No. CV-75138, England.
Sieve Shaker	Karl Kolb (220V, 5Hz), Germany
Hydraulic Press	Apex Hydraulic Press, Apex Construction Ltd., London.
pH meter	Mettler- Toledo 320, England.
Shinko Balance	Shinko Denshi Co., Ltd (Model DJ-220A)
Spectrophotometer	WPAS, 104, made in UK.
Atomic Absorption Spectrophotometer with an auto sampler and a canon laser printer	Model AA-6800, Model ASC-6100, LBP-1210; Shimadzu Corporation, JAPAN.
Potentiostat/Galvanostat	Hokudo Denko HAB 151, Tokoyo, Japan.

4.3 Preparation of Different Standard Solutions

a) Different Acid Solutions

Acid solutions of different desired concentrations were prepared by proper dilution of the respective mother (concentrated) acid with doubly distilled water. 18 mol dm^{-3} sulphuric acid (sp.gr. 1.84), 12 mol dm^{-3} hydrochloric acid (sp.gr. 1.42), acetic acid (sp.gr. 1.09), hydrofluoric acid (sp.gr. 1.13), perchloric acid (sp.gr. 1.68), phosphoric acid (sp.gr. 1.75), acetic acid (sp.gr. 1.09) were used for dilution. 15% (v/v) sulphuric acid solution was prepared by diluting concentrated (98%) sulphuric acid.

b) Standard Titanium(IV) Solution

Accurately weighed 0.25 g commercially pure titanium dioxide and 5 g potassium bisulphate ($KHSO_4$) were taken in a platinum crucible and mixed throughly. The whole mass was then fused at fusion heat till the total oxide dissolved (the white mass turned to complete yellow liquid). The fused mass was then cooled at room temperature and dissolved in 15% sulphuric acid by gentle heating. The solution was washed carefully into a 500 cm^3 volumetric flask and made up to the with 15% sulphuric acid solution.

1 $cm^3 \equiv 0.001$ g of $TiO_2 \equiv 0.0006$ g of Ti

c) Standard Iron(III) Solution

Exactly 0.864 g Analytical Reagent Grade ferric ammonium sulphate [$NH_4Fe(SO_4)_2.12H_2O$] was weighed out in a 1000 cm^3 volumetric flask and dissolved in water. To the solution a few drops of concentrated hydrochloric acid and a few drops of 2% potassium permanganate solution were added. The solution was then made upto the mark with water. Then

1 $cm^3 \equiv 0.0001$ g of Fe

d) Ammonium Thiocyanate Solution

An aliquot of 152 g of A.R. grade ammonium thiocyanate was dissolved in water in 1 dm^3 volumetric flask, and the solution was made up to the mark with distilled water. The resulting solution was calculated as 2 mol dm^{-3}. This solution is used as colouring agent in iron estimation.

e) Pyrocatechol Violet Solution

Pyrocatechol violet is a dye soluble in distilled water. Generally, 40 mg of dye was dissolved in water in a 100 cm^3 volumetric flask and it was made up to the mark by adding distilled water. It was used to estimate zirconium(IV) in solutions.

f) Standard Zirconium(IV) Solution

Standard zirconyl chloride ($ZrOCl_2.8H_2O$) solution (supplied by BDH) was used as a source of standard zirconium(IV) solution required in the construction of calibration curbe for the spectrophotometric estimation of Zr(IV). 1 cm^3 of standard zirconyl chloride solution $\equiv$ 1mg of Zr $\equiv$ 0.001g of Zr

g) Ethylenediamine Tetraacetic Acid (EDTA) Solution:

The EDTA solution was prepared by taking 40 g of disodium ethylenediamine tetraacetic acid dissolved in water in a 1 dm^3 volumetric flask and water was added up to the mark and shaked well. EDTA solution was used for the estimation of zirconium in the aqueous phase.

4.4 Experimental Techniques

4.4.1 Preparation of ilmenite, zircon and lead sulphate sample

The samples i.e. ilmenite and zircon used in the investigation was collected in a single lot from Bangladesh Atomic Energy Commission's Pilot plant for separation of

heavy minerals from beach sands at Cox's Bazar. The lead sulphate was collected on dismantling locally available waste lead-acid batteries. Ilmenite, zircon and lead sulphate was dry ground to reduce the size and sieved to get different particle sizes. The experimental procedure in shown in Fig. 4.1

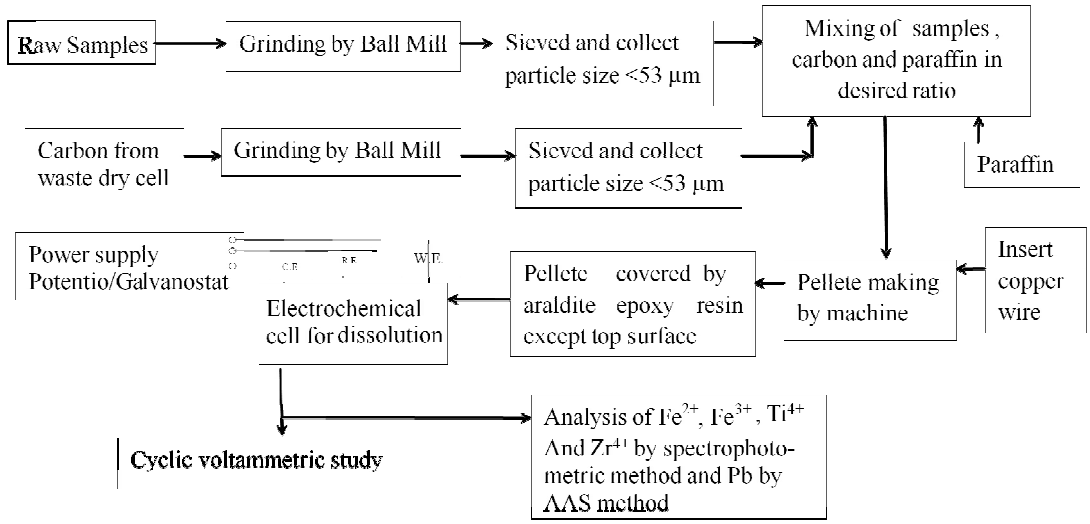

Figure 4.1: Experimental Procedure

Size reduction: ball mill

A Ball Mill (Norton, Chemical Process Products Division, SL No CV-75138) has been used for dry grinding of ilmenite, zircon and lead sulphate. It consists of two rolls and a porcelin bowl having an airtight lid. Samples and 40-50 porcelin balls of different sizes were taken in the bowl. The rolls were rotated slowly by means of an electric motor; as a result, the bowl placed on the rolls was rotated. The grinding action was achieved by the impact of balls in the bowl.

Size sorting: the sieve shaker

During the grinding operation, the particles of different sizes of the ground samples have been separated from time to time by a Kurl Kolb Sieve Shaker (220 V, 50 Hz) to avoid over-grinding. Three sizes, viz. 190 μm, 125 μm and 53 μm and over 53 μm sieves are charged to the Ball mill for regrinding; whereas the fraction is collected 53 μm sieve is stored in a dry bottle for use in the experiment. The sieving is affected by the simultaneous circular and vertical vibratory motions on the sieve.

Preparation of graphite powder

The graphite powder used in this investigation was the ground graphite rod in waste dry cell battery. The batteries were collected from local market. Graphite rods, collected from batteries, were scratched thoroughly with a knife to remove any adhered substance. Then boiled with detergent in water for 30 min and washed with water to remove the trace of any greasy matters. The dried rods were then crushed and ground in a glass mortar with a glass pestle. Finally the ground graphite was regroundin a ball mill and sieved.

Preparation of working electrode (Pellet)

To prepared the working electrode, the samples (ground ilmenite, zircon or lead sulphate power) was mixed with graphite powder in presence of liquid paraffin. For pellet of ilmenite, ilmenite: graphite: liquid paraffin ratio was either 2:1:0.1 or 4:3:0.1, for pellet of zircon, zircon: graphite: liquid paraffin was 1:1:0.1 and for pellet of lead sulphate, lead sulphate: graphite: liquid paraffin ratio was 3:1:0.1. Weight ratios were chosen. The desired samples, graphite and paraffin were mixed thoroughly and taken in a dice on inserting a copper wire within the mixture a presence of 2000 psi applied from a hydraulic pressure machine (Apex Construction Ltd. U.K.). The pellet is covered by araldite epoxy resin keeping top surface exposed. The diameter of the pellet (inner diameter of dice) was 1.4 cm and the surface areas of the pellets prepared werecalculated by the equation ($A= \pi r^2 = \pi d^2/4$) and the value exposed surface area was measured to be 1.5 cm^2. These were used as the working electrodes in this investigation. The electrode surface was polished with 2000 grade SiC paper and rinsed with deionized water before being used in an electrochemical measurement.

Temperature control unit

To investigate the effect of temperature on electrochemical dissolution at constant desired temperature, a Stuard Scientific Hotplate SH-1, U.K. was used. An accurate thermometer was used to check the actual temperature of the cell.

Balance

A SHINKO balance made by SHINKO DENSHI Co., Ltd. (model DJ-220A) has been used for all the weight measurements in this investigation. Its maximum capacity was 200 g with a sensitivity of 0.0001 g. The calibration of the balance was checked time to time by the standard weights supplied by the manufacturing company.

pH meter

pH was adjusted to 5.2 by a Mettler-Toledo 320 pH meter (England). The pH meter was furnished with a combined glass electrode having an ATC mode (automatic temperature compensation). Before taking reading the pH meter was standardized by standard buffer of pH 4 and pH 7.

After standardization of pH meter, the electrode was rinsed with sufficient distilled water; the residual water present on the surface of electrode was removed by a piece of filter paper. It was then placed within the test solution and kept in such a way for at least 5 min before taking the reading. The worm up time for the instrument was only fifteen min.

4.5 Basic Principles of Cyclic Voltammetry

4.5.1 Cyclic voltammetry

Cyclic voltammetry (CV) is a type of potentiodynamic electrochemical measurement. In a cyclic voltammetry experiment, the working electrode potential is ramped linearly versus time. Unlike in linear sweep voltammetry, after the set potential is reached in a CV experiment, the working electrode's potential is ramped in the opposite direction to return to the initial potential. These cycles of ramps in potential may be repeated as many times as needed. The current at the working electrode is plotted versus the applied voltage (that is, the working electrode's potential) to give the cyclic voltammogram trace. Cyclic voltammetry is generally used to study the electrochemical properties of an analyte in solution[331-333].

4.5.2 Experimental method

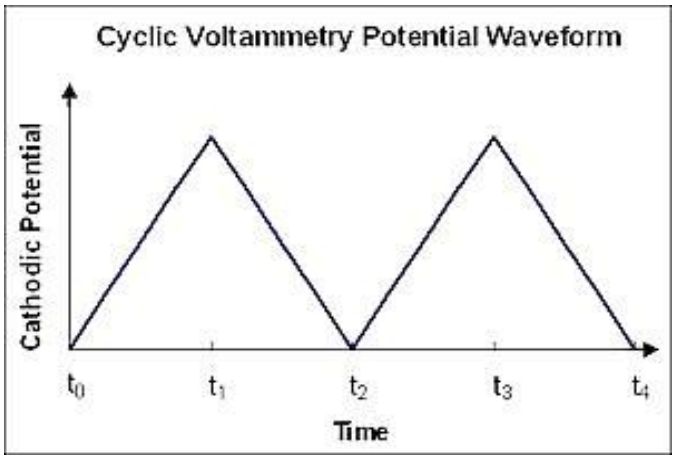

Figure 4.2 Cyclic Voltammetry Waveform

In cyclic voltammetry, the electrode potential ramps linearly versus time in cyclical phases (Fig. 4.2). The rate of voltage change over time during each of these phases is known as the experiment's scan rate (V s^{-1}). The potential is measured between the working electrode and the reference electrode, while the current is measured between the working electrode and the counter electrode. These data are plotted as current (*i*) versus applied potential (*E*, often referred to as just 'potential'). In Fig. 4.2, during the initial forward scan (from t_0 to t_1) an increasingly reducing potential is applied; thus the cathodic current will, at least initially, increase over this time period assuming that there are reducible analytes in the system. At some point after the reduction potential of the analyte is reached, the cathodic current will decrease as the concentration of reducible analyte is depleted. If the redox couple is reversible then during the reverse scan (from t_1 to t_2) the reduced analyte will start to be re-oxidized, giving rise to a current of reverse polarity (anodic current) to before. The more reversible the redox couple is, the more similar the oxidation peak will be in shape to the reduction peak. Hence, CV data can provide information about redox potentials and electrochemical reaction rates.

For instance, if the electron transfer at the working electrode surface is fast and the current is limited by the diffusion of analyte species to the electrode surface, then the peak current will be proportional to the square root of the scan rate. This relationship is described by the Cottrell equation. In this situation, the CV experiment only samples a small portion of the solution, i.e., the diffusion layer at the electrode surface.

4.5.3 Cyclic voltammetry of reversible couples

The utility of cyclic voltammetry is highly dependent on the analyte being studied. The analyte has to be redox active within the potential window to be scanned. Often the analyte displays a reversible CV wave (such as that depicted in Fig. 4.3), which is observed when all of the initial analyte can be recovered after a forward and reverse scan cycle. Although such reversible couples are simpler to analyze, they contain less information than more complex waveforms.

The waveform of even reversible couples is complex owing to the combined effects of polarization and diffusion. The difference between the two peak potentials (E_p), ΔE_p, is of particular interest.

$$\Delta E_p = |E_{pc} - E_{pa}|$$

This difference mainly results from the effects of analyte diffusion rates. In the ideal case of a reversible 1e- couple, ΔE_p is 59 mV. Typical values observed experimentally are greater, often approaching 70 or 80 mV. The waveform is also affected by the rate of electron transfer, usually discussed as the activation barrier for electron transfer. A theoretical description of polarization overpotential is in part described by the Butler-Volmer equation and Cottrell equation equations. In an ideal system the relationships reduces to

$E_{pa} - E_{pc} = \frac{56.5\ mV}{n}$ for an n electron process[332].

Focusing on current, reversible couples are characterized by $i_{pa}/i_{pc} = 1$.

When a reversible peak is observed, thermodynamic information in the form of a half cell potential $E^0_{1/2}$ can be determined. When waves are semi-reversible (i_{pa}/i_{pc} is close but not equal to 1), it may be possible to determine even more specific information.

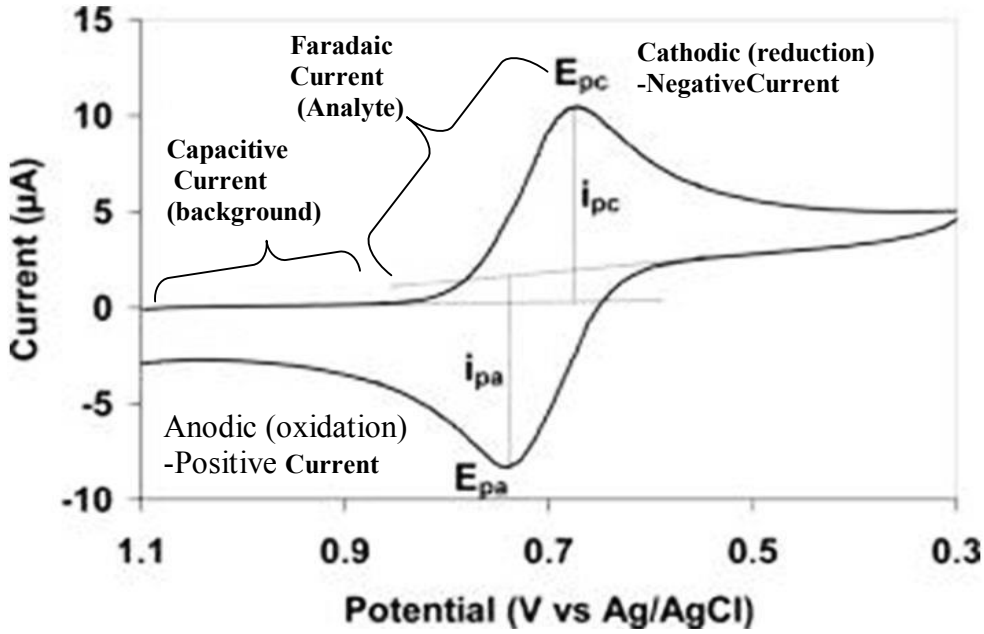

Figure 4.3 **Typical cyclic voltammogram where i_{pc} and i_{pa} show the peak cathodic and anodic current respectively for a reversible reaction. The y-axis shows the negative current.**

4.5.4 Applications

Cyclic voltammetry (CV) has become an important and widely used electroanalytical technique in many areas of chemistry. It is often used to study a variety of redox processes, to determine the stability of reaction products, the presence of intermediates in redox reactions, reaction[334]and electron transfer kinetics[335], and the reversibility of a reaction[336]. CV can also be used to determine the electron stoichiometry of a system, the diffusion coefficient of an analyte, and the formal reduction potential of an analyte, which can be used as an identification tool. In addition, because concentration is proportional to current in a reversible, Nernstian system, the concentration of an unknown solution can be determined by generating a calibration curve of current vs. concentration[337]. In cellular biology it is used to measure the concentrations in living ones[338]. In organometallic chemistry, it is used to evaluate redox mechanisms[339].

4.6 Electrochemical Measurement

Electrochemical investigations including potential step chronoamperometry, chronopotentiometry and cyclic voltammetry were carried out using a Hokudo Denko HAB-151 Potentiostat/Galvanostat, Tokyo, Japan, equipped with a potential sweeper.

Data were recorded in a computer through data acquisition system (USA) using WinDaq software. A three electrode system consisting of a pellet (ilmenite, zircon/lead sulphate graphite and paraffin mixture) of surface area as 1.54 cm^2 working electrode, a platinum (50 × 10 × 0.1 mm^3) counter electrode and a silver wire quasi-reference electrode were used in all electrochemical studies. The counter electrode was cleaned electrochemically in 1.5 mol dm^{-3} H_2SO_4–1.5 mol dm^{-3} H_3PO_4 mixtures, then rinsed with deionised water, and finally dried with acetone prior to use in all measurements. All voltammograms were obtained at temperature ranging from 30 to 85° C with various scan rates ranging from 5 to 100 mV s^{-1}. A sulphuric acidimmersed silver wire as quasi-reference electrode was used in all electrochemical experiments. All potentials in this work are quoted with respect to this Ag|AgCl reference electrode.

Cyclic voltammetry of the pellet has been studied in various H_2SO_4 solutions (for ilimenite), NaOH solutions (for zircon) and HNO_3 solutions (for lead sulphate). Cyclic voltammetry is a reversal technique and is the potential-scan equivalent of double potential step chronoamperometry. Cyclic voltammograms are reliable source to determine the dissolution potential of ilmenite, zircon and lead sulphate.

4.7 Electrochemical Dissolution

Electrochemical dissolution of ilmenite fraction of beach sand of Bangladesh was carried out in sulfuric acid solution (0.30 ~ 3.00 mol dm^{-3}) under constant potential methods in the ranging from -0.4 V to -1.2 V at temperatures ranging from 30 to 85° C. Following each dissolution experiment, the resulting solution was analysed for titanium and iron (ferrous and ferric) content. Titanium and iron content in the solutions were analysed colorimetrically using a visible Spectrophotometer (WPA S104, made in UK). In case of Ti(IV) estimation, a yellow colour was formed by addition H_2O_2 in H_2SO_4-H_3PO_4 mixture and estimated at 420 nm[339(a)]; whereas, Fe(III) was estimated by measuring the blood red colour (produced on addition of HNO_3-NH_4SCN) at 480 nm [339(b)]. The later analysis was carried out without and with HNO_3 oxidation for estimations of Fe(III) Fe(II) and Fe(III) contents.

Electrochemical dissolution of zircon fraction of beach sand of Bangladesh was carried out in NaOH solution (0.01 ~ 6.00 mol dm^{-3}) under constant potential methods ranging from -0.08 V to -0.83 V at temperatures ranging from 25 to 85° C. Following

each dissolution experiment, the resulting solution on formation of color with pyrocatechol violet was analysed colorimetrically at using a visible Spectrophotometer (WPA S104, made in UK).

Electrochemical dissolution of lead sulphate was carried out in HNO_3 solution (0.3 ~ 3.00 mol dm^{-3}) under constant potential methods in the ranging from 0.02 V to -0.52 V at temperatures ranging from 30 to 80° C. Following each dissolution experiment, the resulting solution was analyzed for Pb^{2+} ion by AAS.

4.8 Analytical Technique: Spectrophotometer

The spectrophotometer is used extensively for the determination of optical density or absorbance of the test colored solution which is proportional to concentration. The chief advantage of spectrophotometric analysis is it that it provides the simple, easier and prompt means of determining minute quantities of substances more accurately in comparison to the other methods as gravimetric, volumetric and so on methods.

The basic principle of most spectrophotometric measurement consists in comparing the color produced by the substance in unknown amount with the same color produced by a known amount of material being determined, both being measured in terms of optical density or absorbance under well-defined conditions. The quantitative comparison of these two solutions may in general, be carried out by one or more methods, one of which is based on the preparation of calibration curve by knowing the absorbance for the known concentrated solutions. The spectrophotometryis based on the Beer-Lambert law:

$$\log\frac{I_o}{I_t} = \varepsilon ct \qquad \ldots \quad \ldots \quad \ldots \quad \ldots \quad \ldots \quad (1)$$

where, I_o and I_t represent the intensity of incident and transmitted light and ε, c and t represent the molar extinction co-efficient, concentration in g-mole/L and the thickness of solution medium (cm), respectively. The term in the left hand side of Eq. (1) is called absorbance (A) or optical density (O.D.), whereas I_t/I_o is the transmittance (T).

The equation represents that the absorbance is proportional to the concentration, C. Hence by plotting 'A' (as ordinate) against concentration (as obscissa), a straight

line passing through the origin is usually obtained. Thus if the absorbances for a number of solution of known concentrations are determined with a spectrophotometer and a calibration curve is constructed, then the unknown concentration of the same substance can be read off from the calibration curve after measuring its absorbance.

Discrepancies in spectrophotometric analysis are usually observed when the colored solute ionizes, dissociates or associates in solution. Discrepancies may also occur when monochromatic light is not used. Throughout the whole investigation, concentration of Ti(IV), Fe(III) and Fe(II) have been determined on using a visible-Spectrophotometer (WPA S104, made in UK).

4.8.1 Spectrophotometric estimation of titanium(IV)

Hydrogen peroxide produces a yellow color [340(a)] with acidic titanium(IV) solution due to the formation of $TiO(SO_4)^{2-}$, or $Ti(H_2O_2)^{4+}$. Intensity of the colour produced is proportional to the amount of the element present in the solution (up to 0.5 g of TiO_2 per cm^3)

To prevent the hydrolysis of the ion to a basic sulphate and condensation to metatitanic acid, the final solution should be 1.50 to 3.00 mol dm^{-3} in sulphuric acid concentration. The colour intensity is influenced by temperature of the solution, so the temperature of the standard and test solutions should be the same.

4.8.1.1 Calibration curve for titanium(IV) estimation

In six different 100 cm^3 volumetric flasks, 1 cm^3, 2 cm^3, 3 cm^3, 4 cm^3, 5 cm^3 and 6 cm^3 standard solution of titanium (section 4.3.b) were taken. 1 cm^3 of 30% H_2O_2 solution and 1 cm^3 of syrupy phosphoric acid were added to each flask. Solutions turned yellow in color. All the flasks were then made up to the mark with 15% sulphuric acid and shaked well. A blank solution was prepared in the same way (without sample) and used to calibrate the spectrophotometer for '0' absorbance. The absorbance of the test solution was measured at 410 nm wavelength. By plotting the obtained absorbances against concentration a straight line was obtained. The calibration plot is shown in the Fig. 4.4.

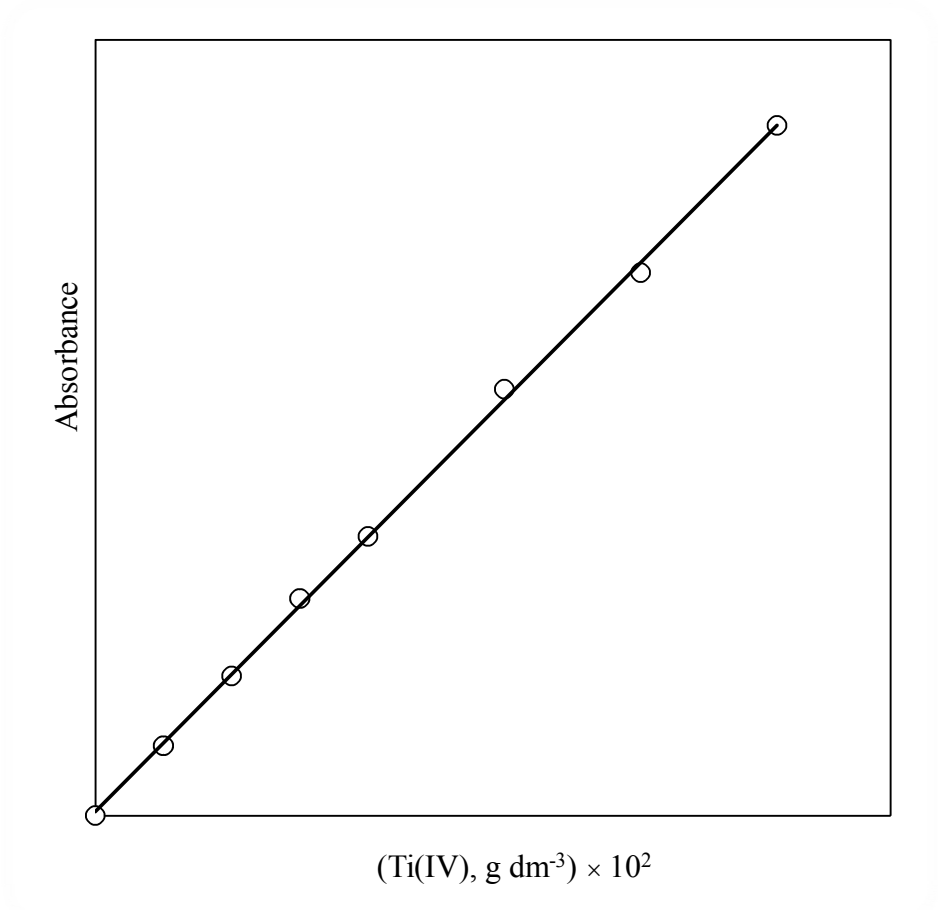

Figure 4.4 Calibration curve for colorimetric estimation of Ti(IV) at 410 nm.

4.8.1.2 Estimation of titanium(IV) content in the electrolysed solution

After electrolysis, concentration of titanium(IV) in the electrolysed solution was measured spectrophotometrically. At the end of the every successful electrolysis, an aliqout of the electrolysed solution was taken in a suitable volumetric flask after proper dilution with 15% sulphuric acid. To this 1 cm^3 of concentrated phosphoric acid was added to eliminate the effect of co-existing Fe^{3+}. 1 cm^3 of 30% H_2O_2 was then added to the solution to develop the yellow colour and made up to the mark with 15% sulphuric acid. By comparing the absorbance reading of the solution with the standards in the calibration curve, the concentration of Ti(IV) in the electrolysed solution was determined. From the electrolysed solution (for hydrochloric acid medium) the dissolved chlorine was eliminated properly by standard method.

4.8.1.3 Estimation of Ti(IV) content in the sample ilmenite

An aliquot of the stock solution prepared in section 4.3 b was taken in a suitable volumetric flask and diluted by 15% sulphuric acid solution. To the flask 1 cm^3 of 30% H_2O_2 was added followed by the addition of 1 cm^3 concentrated syrupy phosphoric acid. On diluting up to the mark by 15% H_2SO_4, the absorbance of the yellow color produced was measured spectrophotometrically and titanium content in the sample ilmenite was estimated with the help of the calibration curve given in Fig. 4.4.

4.9 Spectrophotometric Estimation of Iron(III)

Ferric ion (Fe^{3+}) reacts with thiocyanate to produce red coloured complexes. Depending upon the concentration of thiocyanate ion a series of complexes are obtained. These complexes can be formulated as $[Fe(SCN)n]^{3-n}$, where n=1,2,3.....6 [340(b)]. At low thiocyanate concentration the predominate coloured species is $[Fe(SCN)]^{2+}$, at 0.10 mol dm^{-3} thiocyanate concentration it is largely $[Fe(SCN)_2]^{+}$ and at very high concentration it is $[Fe(SCN)_6]^{3-}$. For the determination of Fe(III) spectrophotometrically, a large excess of thiocyanate should be used to increase the intensity and stability of the color via 100% formation of $[Fe(SCN)_6]^{3-}$. Strong acid such as hydrochloric/nitric acid of concentration 0.05-0.50 mol dm^{-3} should be present in the solution to suppress the hydrolysis of Fe(III). Sulphuric acid is not recommended, because sulphate ions have a tendency to form complexes with Fe(III).

4.9.1 Construction of calibration curve for Fe(III) determination

1 cm^3, 2 cm^3, 3 cm^3, 4 cm^3 and 6 cm^3 portions of the standard solution of iron (section 4.3.b) were taken in six different 100 cm^3 volumetric flasks. To each of the flask 5 cm^3 concentrated nitric acid (to oxidize the Fe^{2+} to Fe^{3+}) and 10 cm^3 20% ammonium thiocyanate solution were added, when a red color was developed. All of the flasks were then made up to the mark with distilled water. A blank solution was prepared to adjust the spectrophotometer to '0' absorbance, hence to calibrate the instrument. Absorbances of the solutions were measured at 480 nm. By plotting the absorbances against their respective concentrations, a straight line was obtained. The calibration curve is shown in the Fig. 4.5 as absorbance vs. Fe^{3+} concentration in g dm^{-3}.

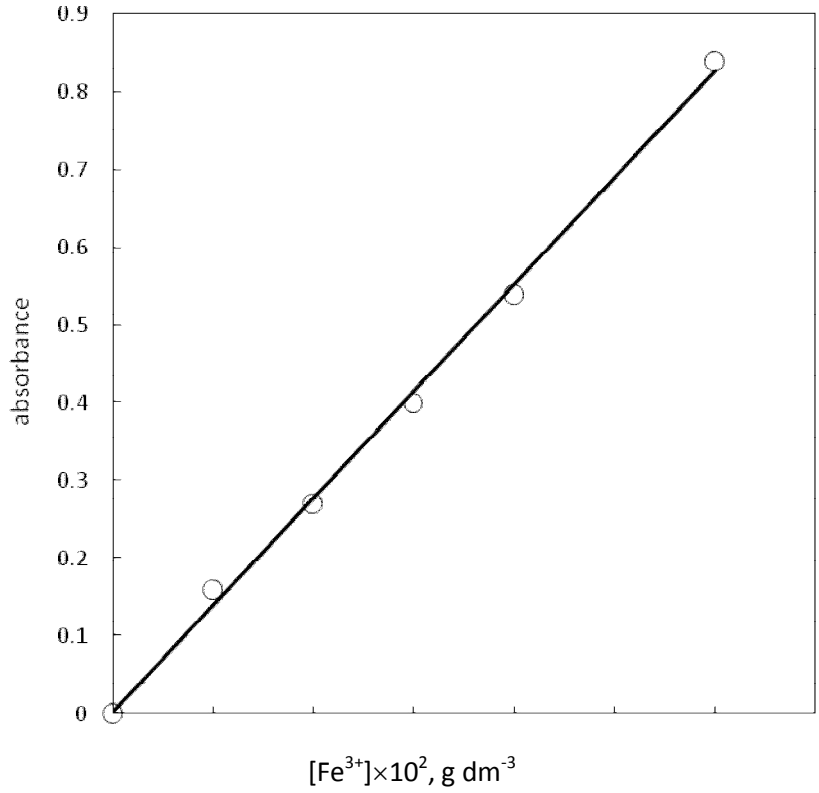

Figure 4.5 Calibration curve for colorimetric estimation of Fe(III) at 480 nm.

4.9.2 Estimation of iron(III) content in the electrolysed solution

Concentration of Fe(III) in electroysed solution was determined by spectrophotometric absorbance measurement. At the end of the every successful electrolysis, an aliquot of properly diluted electrolysed solution was oxidzed in a convenient volumetric flask by 5 cm^3 of 5 mol dm^{-3} nitric acid, 10 cm^3 20% ammonium thiocyanate solution was then added to produce red colour. The flsak was then made up to mark by distilled water. So, readings were taken after proper oxidation of the electrolysed solutions and at equal interval of time after addition of coloring agent.

4.9.3 Estimation of Fe(total) in the sample ilmenite and in electrolysed solution

The concentration of total iron content in the sample ilmeniteor inelectrolysed solution was measured by the determination of Fe(III) in the stock solution (section 4.3.b) or in electrolysed solution. An aliquot of the stock solution or electrolysed solution was taken in a volumetric flask and diluted to some extent. Content of the flask was oxidised carefully by 5 cm^3 5 mol dm^{-3} nitric acid and 3 drops of 2% potassium

permanganate solution on heating. To develop a red colour 10 cm^3 20% ammonium thiocyanate solution was added and the flask was made up to the mark with distilled water. Absorbance of the resulting solution was measured against a blank.

4.10 Spectrophotometric Estimation of Zirconium(IV)

Principle

Zirconium can be determined by several satisfactory methods. In the present investigation, more important pyrocatechol violet method has been used[341]. Zirconium(IV) reacts with pyrocatechol violet to producing a blue colouration. The pH should be 5.20. For the same concentration of reagent, the absorption maximum varies from 555 nm to 625 nm, according to the content of Zr(IV). The estimation has been performed at 590 nm using a WPA S-104 spectrophotometer (made in England). The method is not very accurate, but can be made very selective by working in the presence of EDTA.

Sensitivity: ε= 30,000- 40,000 at 590 nm.

Interfering ions

In the presence of EDTA, Sn(IV) interferes by precipitation; Th(IV) should be present in amounts less than 5 mg dm^{-3} (red colouration) and Ti(IV) in amounts less than 1 mg dm^{-3} , Cr(III) interferes at above 1 mg dm^{-3} (violet colouration with EDTA). Be(II) does not interfere but an excess of F^- should present, SO_4^{2-} does not interfere.

Regents

i) Disodium ethylenediamine tetracetate (EDTA), 40 g dm^{-3}.

ii) Sodium acetate (or sodium graphiteate), 2 mol, 272 g dm^{-3}.

iii) Pyrocatechol violet, 40 mg in 100 Cm^3 of water.

Operating procedure

The solution should preferably contain 50 dm^{-3} of Zr(IV). 3 mL of EDTA was added and pH was adjusted to 5.2 (monitored by a pH meter) by means of sodium graphiteate/sodium acetate. 2 Cm^3 of the dye was added and the volume was made up to 50 Cm^3. On dividing this solution in 200 to 300 mg of sodium fluoride was added to one part (used as reagent blank) and the mixtures were left for 30 min. Colorimetry was

performed at 590 nm in comparison with the solution containing the fluoride as a reference solution.

4.10.1 Construction of calibration curve for Zr(IV)

The standard zirconyl chloride solution was used as a standard solution for zirconium. 1 cm^3 of zirconyl chloride ≡ 1 mg of Zr ≡ 0.001 g of Zr. 1 cm^3 of the standard solution of zirconyl chloride was diluted to 100 cm^3 by water. Then 5 cm^3, 10 cm^3, 15 cm^3, 20 cm^3 and 25 cm^3, 30 cm^3 and 35 cm^3 portions of the diluted solution of zirconyl chloride were taken in seven different 100 cm^3 volumetric flasks. To each flask, 6 cm^3 of EDTA solution was added and then pH was adjusted to 5.20 (monitored by a pH meter) by means of sodium graphiteate crystal, and finally, 2 cm^3 of the dye (pyrocatechol violet) solution was added. As a result zirconium reacted with pyrocatechol violet to produce blue coloration; water was added to each flask to make up to the mark. To one part of the solution (about half) 200 to 300 mg of sodium fluoride was added and the solutions were left for 30 min. When a yellow colouration developed, in the fluoride added solution, it was used as the reference blank solution. It was used to make zero absorbance or 100% transmittance of the apparatus at 590 nm. Then the absorbance of the sample solution without fluoride addition was measured at 590 nm, in comparison to the solution containing the fluoride as a reference solution. By plotting these absorbance; against their respective concentration of the solution, a straight line up to Zr(IV) concentration of 0.0035 g dm^{-3} was obtained. The calibration curve is shown in Fig. 4.6.

4.10.2 Estimation of Zr content of the electrolysed solution

A suitable portion of the aqueous solution was taken in 100 cm^3 volumetric flask, to which 6 cm^3 EDTA (40 g dm^{-3}) was added and the pH was adjusted to 5.20 by adding anhydrous Na_2CO_3 and finally 2 cm^3 pyrocatechol violet solution was added to get a blue colouration and diluted with water up to the mark. On dividing this solution into two parts, to one part of the solution (about half) 200-300 mg of sodium fluoride was added and the solution was left for 30 min for developing a yellow coloration. The solution was used as the blank reagent. The zirconium(IV) content of the sample/solution should be very small so that absorbance should be read off between 0.03 to 0.3 and for this the sample might have to be diluted as required. The absorbance of the solution was then measured in comparison to the reference blank solution. For

this absorbance of the aqueous solution the concentration of Zr(IV) was determined from the calibration curve after multiplying by dilution time.

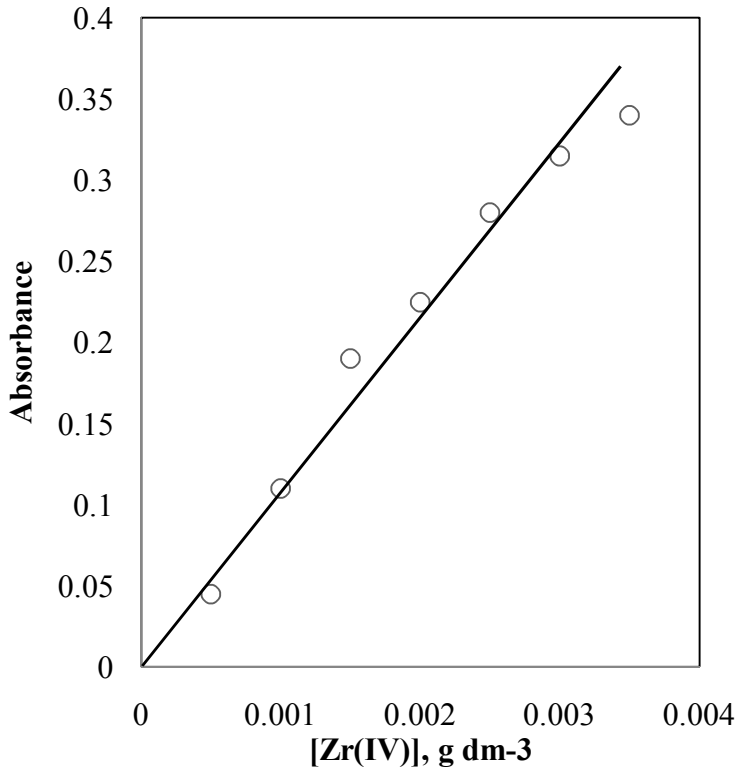

Figure 4.6 Colorimetric estimation of Zr(IV) by pyrocatechol violet method at 590 nm.

4.11 Atomic Absorption Spectrophotometry

4.11.1 General discussion

Atomic absorption is a process involving the absorption by free atoms of an element of light at a wavelength specific to that element, i.e. it is a means by which the concentration of metals can be measured. In Atomic Spectrometry, emission, absorption and fluorescence, energy is put into the atom population by thermal, electromagnetic, chemical and electrical forms of energy and converted to light energy by various atomic and electronic processes before measurement. Atomic Absorption Spectrometry is useful not only for the identification but also for the quantitative determination of many elements present in samples. The technique is specific, in that individual elements in each sample can be reliably identified and it is sensitive, enabling small amounts of an element to be detected down to around 1ppm level. Central Science Laboratory (CSL) of Rajshahi University has an Atomic Absorption Spectrophotometer (ModelNo.AA-6800) coupled with an auto sampler (Model

No.ASC-6100) and a canon laser printer (LBP-1210) from Shimadzu Corporation JAPAN. The AAS is providing facilities to carry out experiments with flame, granite furnace and hydride vapor generator.

Figure 4.7 Atomic Absorption Spectrophotometer (Model No. AA-6800) coupled with an auto sampler (Model No.ASC-6100) used in present investigation.

4.11.2 Principle of AAS

Atomic absorption (AA) spectroscopy uses the absorption of light to measure the concentration of gas-phase atoms. Since samples are usually liquids or solids, the metal atoms or ions must be vaporized in a flame or graphite furnace. The atoms absorb ultraviolet or visible light and make transitions to higher electronic energy levels. The metal concentration is determined from the amount of absorption. Applying the Beer-Lambert law directly in AA spectroscopy is difficult due to variations in the atomization efficiency from the sample matrix. Concentration measurements are usually determined from a working curve after calibrating the instrument with standards of known concentration.

4.11.3 Theory

4.11.3.1 Absorption

The absorption of energy by atoms provides a basis for quantitative analytical chemistry. The radiant energy or photons, absorbed by atoms are generally in the form of very narrow lines of characteristic wavelength originating from the visible or

ultraviolet spectrum. During the absorption process the outer valence electrons of the atoms are promoted to a higher orbital and the atom is electronically excited. There is a relationship and equilibrium between the populations of excited and unexcited atoms involving photons, and between atomic absorption and atomic emission spectroscopy.

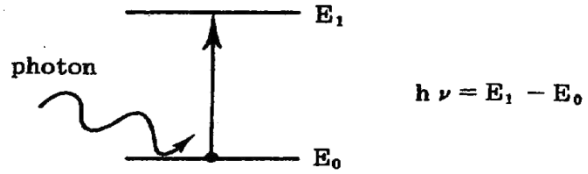

Figure 4.8 Light absorption process of atoms

A photon behaves in a similar manner to an alternating electric field and interacts with the negatively charged electrons in an atom. Under certain conditions a photon can be absorbed by an atom. The energy levels in an atom are quantized, that is they have certain well defined energies. As a consequence of this, the photon energy, hυ, must be exactly equal to the energy gap between a filled energy level E_0 the ground state, and an unoccupied energy level E_1 the first excited state.

4.11.3.2 Emission

The process of emission is the reversal of absorption. The atom in an excited energy level can revert to the ground state by emitting energy as a photon as represented below:

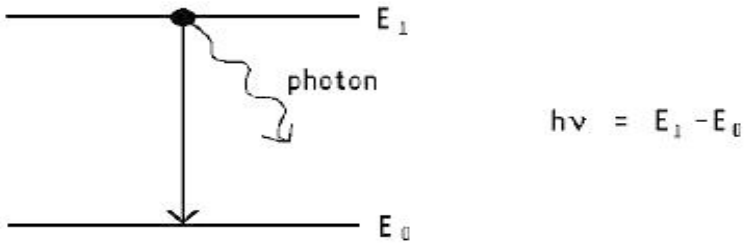

Figure 4.9 Light emission process of atoms

The photon of energy hυ is equal to the energy gap (E_1-E_0). The emission of a photon when the electron moves to the unexcited state from the excited state forms the basis of emission spectroscopy. In this technique the light generated in the emission process is measured at a specific wavelength. In any atom there are numerous permitted energy levels and numerous transitions permitted between different excited energy levels and the ground state.

4.11.3.3 Production of free atoms

The ability to produce uncombined and un-ionized atoms in an atomic vapour determines the success of an atomic absorption or fluorescence analytical procedure. In a flame at a temperature of 2000-3000 K the fine droplets of a solution contain molecules in solution previously aspirated. The solvent evaporates leaving behind small solid particles.

These particles melt and vaporize and the vapor consists of mixtures of compounds that decompose into free atoms which though transitory under these conditions, enable atomic spectra to be observed. The individual metal atoms which have been atomized absorb energy by collision and become either excited or ionized as shown in the simplified example for sodium chloride below.

Atomization $NaCl \leftrightharpoons Na+Cl$

Excitation $Na + h\upsilon \leftrightharpoons Na^*$

Ionization $Na \leftrightharpoons Na^+ + e^-$

4.11.4 The Beer-Lambert Law

The absorption that takes place in an atomic absorption system follows Beer's law, which is

$I = I_0 e^{-abc}$

$A = abc$

A = Absorbance = $-\ln T$

Where,

I = intensity of light leaving solution after absorption

I_0 = intensity of light falling on a solution before absorption

a = a proportionality constant

b = path length through sample

c = concentration of the solution

$T = \frac{1}{10}$ (T = Transmitance)

The Beer-Lambert Law is the fundamental law which relates absorption in a

solution to concentration of individual components in a solution. Although the basic principles of the Beer-Lambert Law apply to AAS it is not possible to use this relationship in the same way. This is because solutions (molecular concentrations) are homogeneous throughout the sample absorption path and the free atoms in the flame are not constant throughout the light path.

Hence the Beer-Lambert Law cannot be used directly to determine the concentration of an atom generated from a solution. It is necessary instead to use this equation:

Total absorption = constant × Nf

Where, the total absorption is equal to a constant times the number of free atoms in the light path (Nf), which is independent of temperature and energy of transition and relates the amount of absorption with the number of atoms in the light path.

4.11.5 Apparatus and operation

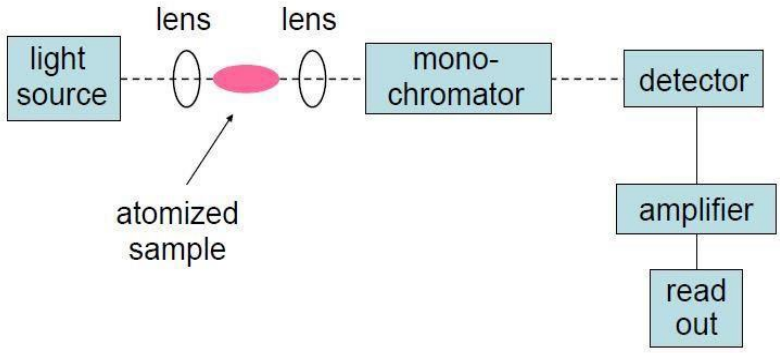

Figure 4.10 Schematic diagram of an atomic absorption spectrophotometer

4.11.5.1 Light Sources

The light source is usually a hollow cathode lamp of the element that is being measured. The hollow cathode lamp is stable, reliable, has a long operating life and is the standard source in Atomic Absorption Spectrometry. Lamps may be expected to run in excess of 5000 mA hours without failure and many have been known to run twice as long. The hollow cathode discharge lamp is known as a fine line source capable of producing spectra where fine structure could be studied.

4.11.5.2 Atomizers

A combustion flame provides the most convenient, stable and economic source of atomic vapours. For the production of free atoms and chemical effects of radicals and other substances present in the flame, the flame temperature is important. Arrange of temperatures from 2000 to 3000 K can be produced from fuel and oxidant mixtures which are safe to handle. Combustion gas mixtures vary and at the same or different temperatures may not have the same analytical properties. Propane, hydrogen and acetylene can be used as fuel gases and air or nitrous oxide used as the oxidant.

4.11.5.3 Monochromators

The function of the monochromator is to isolate light emitted from the primary radiation source and to isolate the most intense resonance line from non-absorbing lines close to it. A monochromator should be capable of separating two lines 0.1 nm apart or less when operating at minimum slit width. Prisms or Gratings are the two different devices used for dispersion of the wavelengths.

4.11.5.4 Detectors

The function of a detector is to measure the intensity of the light radiation falling on it and the most common type of detector is the photomultiplier. The detector must be able to cover the spectral range from 190-860 nm which poses some problems for sensitivity, particularly at the longer wavelengths. Photomultiplier sensitivity is determined by how photo-sensitive the coating material is on the cathode. The photomultiplier is a series of electrodes (ordynodes) each with an emissive surface and a positive potential relative to the previous electrode. When a photon hits the emissive surface an electron is ejected is accelerated and strikes the next dynode ejecting more electrons, until a shower of electrons reach the anode. In this way a single photon striking the emissive surface generates a whole shower of electrons and produces a significant electrical signal. The sensitivity of the system is dependent on the voltage between the dynodes. The higher the voltage the higher the amplification will be. Shot noise is the actual statistical variations in output caused by electron showers generated between dynodes as the dynode voltage increases. It is proportional to the square root of the intensity of radiation falling on the photocathode.

4.12 Detection of Pb Metal Concentration by AAS

4.12.1 Calibration curve for lead by AAS

Reference standard material was used to calibrate the Atomic Absorption Spectrophotometer. Lead standard solution (Pb 1000 ppm), manufactured by Kanto Chemical Co., Inc. Soka factory, Japan, and was used as reference standard material for the calibration. The initial concentration of the solution was 1000 ppm. From this solution 2.5 ppm, 5 ppm and 10 ppm solutions were prepared by quantitative way. Double distilled water was used as blank solution.

The meter readings (absorbance) were taken at 283.3 nm by Atomic Absorption Spectrophotometer. The calibration curve was prepared by plotting these meter readings against the irrespective concentrations of the solutions on the graph paper. The meter reading and calibration curve are shown in Fig. 4.11.

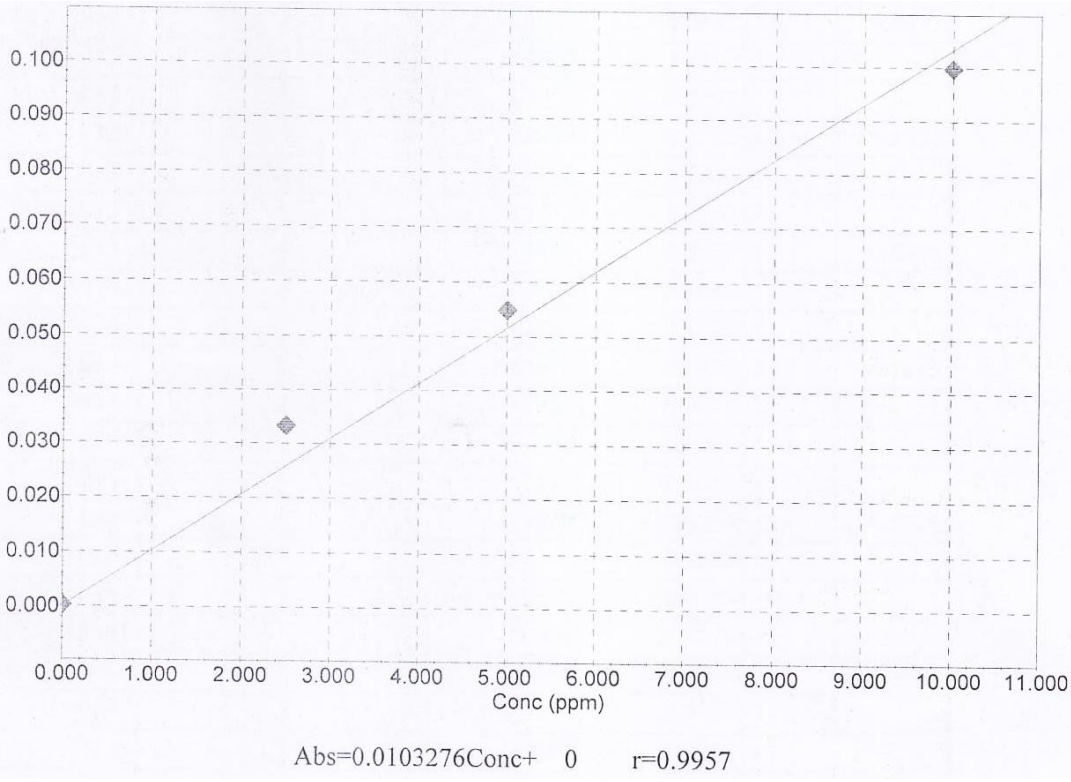

Figure 4.11 Calibration curve for lead estimation by AAS

CHAPTER 5
RESULTS AND DISCUSSION

5.1 A Study on the Electrochemical Dissolution of Ilmenite Fraction of Beach Sand of Bangladesh in Sulphuric Acid Solution

5.2 A Study on the Electrochemical Dissolution of Zircon Fraction of Beach Sand of Bangladesh in Sodium Hydroxide Solution

5.3 A Study on the Electrochemical Dissolution of Waste Product of Storage Battery ($PbSO_4$) in Nitric Acid Solution

5.1 A Study on the Electrochemical Dissolution of Ilmenite Fraction of Beach Sand in Sulphuric Acid Solution

5.1.1 Characterization of ilmenite fraction by XRD and EDAX

The collected ilmenite fraction was dry ground to less than 53 μm size and used for powder X-ray diffraction and X-ray energy dispersive spectroscopic (EDAX) analyses.

X-ray diffraction analysis has been carried out with a Philips PW 1716 diffractometer using CuK_α radiation (40 kV, 30 mA, scan speed: 0.01 °/s) to identify the compounds/phases existing in the ilmenite fraction. The acquired diffraction pattern for the powder specimen of the ilmenite fraction is shown in Fig. 5.1.1. The diffraction peaks at 2θ = 20.87° is for SiO_2 (Refn. Code. No. 01-083-2465); 23.91°, 32.65°, 35.33°, 40.33°, 53.13°, 70.35°, 74.59°and 78.91° are for $FeTiO_3$ (Refn. Code. No. 01-075-1204); 35.71° is for Fe_2O_3 (Refn. Code. No. 01-085-0987); 54.09°, 70.35°, 72.25° and 78.91° are for TiO_2 (Refn. Code. No. 01-072-0100); 32.65° & 40.33° are for (Fe, Mg)Ti_2O_5 (Refn. Code. No. 00-005-0425); 32.65°, 48.79°, 54.09°and 56.39° are for Fe_2TiO_5 (Refn. Code. No. 00-003-0374) and 53.13°, 56.39°, 61.77° and 63.47° are for $FeCr_2O_4$ (Refn. Code.No. 00-024-0511), respectively:

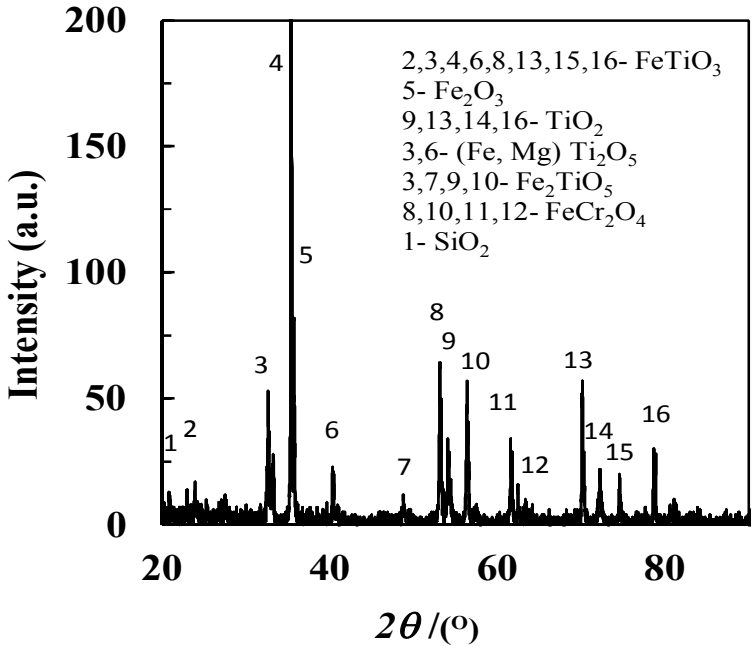

Figure 5.1.1 X-ray diffraction pattern of the ilmenite fraction of beach sand of Bangladesh.

X-ray energy dispersive spectroscopic (EDAX) analysis of the powder specimen of the ilmenite fraction has been carried out with (Skyray Instrument Inc., EDX 3600B, UK). Fig. 5.1.2 shows the EDAX profile of the ilmenite fraction. EDAX profile shows that Fe, Ti, Cr, Mn, Si and Zr are present in the ilmenite fraction of the beach sand of Bangladesh and among them Fe content is of the highest amount. EDAX analyses indicate the presence of iron beside its presence in ilmenite. XRD and chemical analyses data indicate that ilmenite fraction of the beach sand of Bangladesh contains about 62.8% $FeTiO_3$, 16.35% Fe_2TiO_5 and 14.72% Fe_2O_3 (as free and also as $FeCr_2O_4$ and (Fe, Mg)Ti_2O_5).

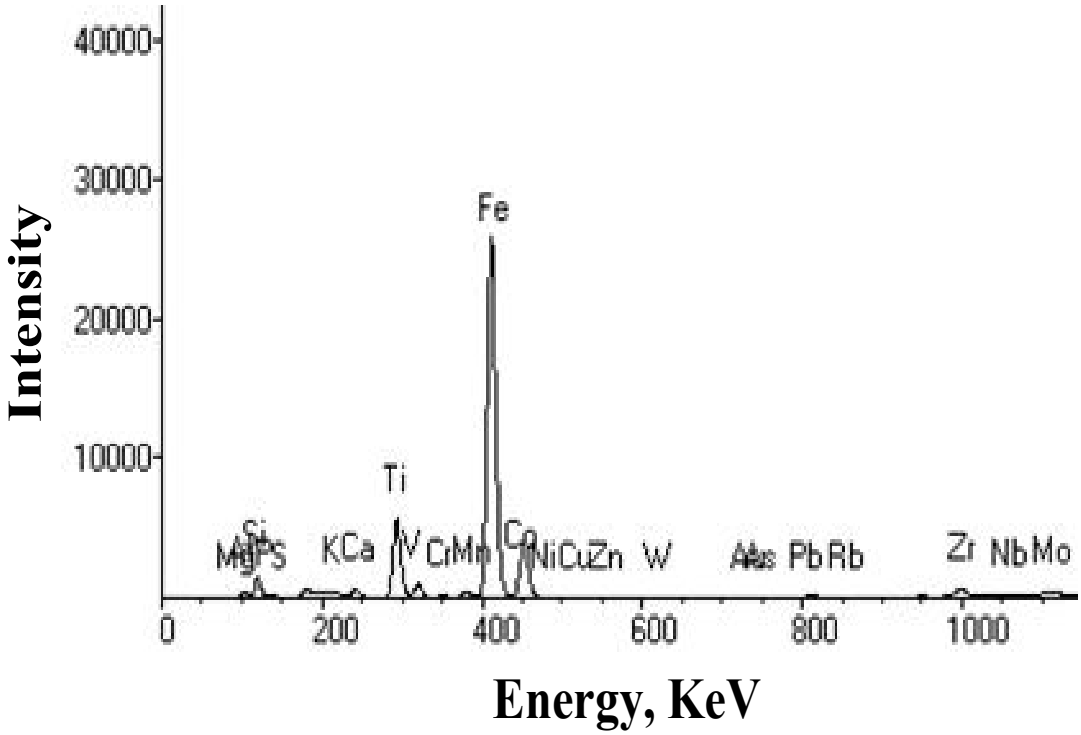

Figure 5.1.2 EDAX profile of the ilmenite fraction

5.1.2 Cyclic voltammetry of ilmenite-graphite-paraffin mixed pellet in H_2SO_4

5.1.2.1 Effect of mineral acid solutions on cyclic voltammogram

The cyclic voltammograms recorded on a pellet of 2:1:0.1 wt. ratio of ilmenite, graphite and paraffin mixed electrode in solutions of various mineral acids (H_3PO_4, HF, HCl, $HClO_4$, HNO_3, H_2SO_4) at 30^o C with a scan rate of 10 mV s^{-1} are shown in Fig. 5.1.3. The rest potential are 0.70 V, 0.72 V, 0.87 V, 0.60 V, 0.68 V and 0.62 V vs.Ag|AgCl reference electrodes for H_3PO_4, HF, HCl, $HClO_4$, HNO_3 and H_2SO_4, respectively. The scan towards negative direction consists of first and second reduction

waves C_1 and C_2 with the current starting to increase between 0.44 V to 0.63 V and -0.16 V to -0.42 V, respectively, in different acid solutions. An additional reduction wave C_3 is observed with the current again starting to increase between -0.61 V to -0.78 V in different acid solutions. The reverse scan consists of oxidation peaks P_a between 0.42 V to 0.70 V in different acid solutions. This figure shows the magnitude of the reduction and oxidation peaks current densitiesof ilmenite, graphite and paraffin mixed electrodein H_2SO_4 solution is higher than in other mineral acids indicating that H_2SO_4 acid solution is suitable to obtain higher dissolution rate of ilmenite fraction.

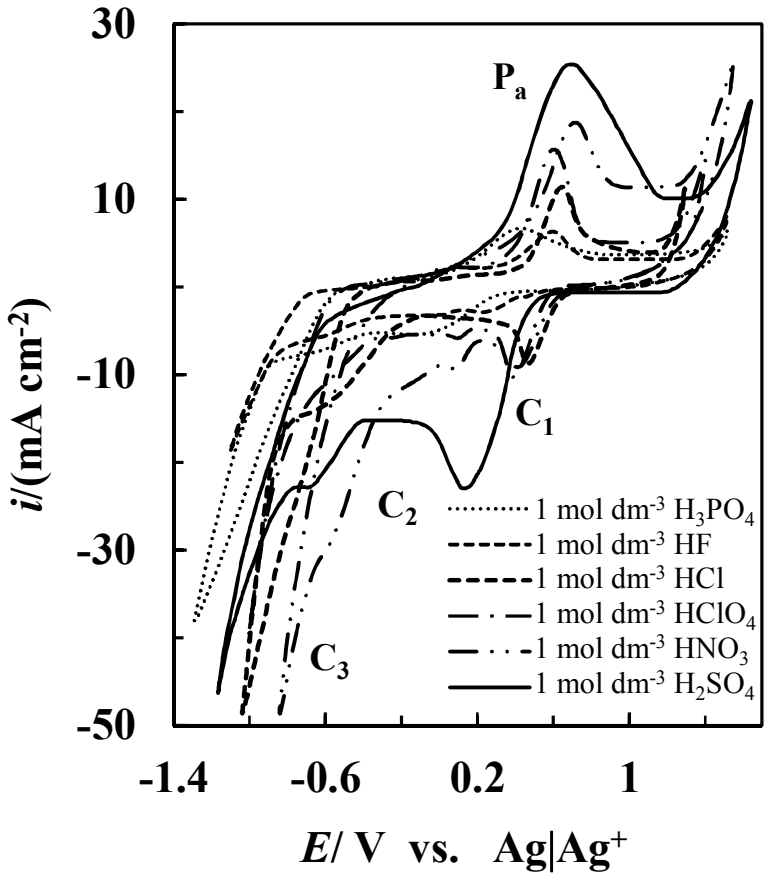

Figure 5.1.3 Cyclic voltammograms recorded on a pellet of ilmenite, graphite and paraffin mixed electrode in various acid solutions at 30° C with a scan rate of 10 mV s^{-1}.

5.1.2.2 Cyclic voltammetry of ilmenite-graphite-paraffin mixed pellet in H_2SO_4

The cyclic voltammogram recorded on a pellet of ilmenite, graphite and paraffin mixed electrode in 1 mol dm^{-3} H_2SO_4 solution at 30° C with a scan rate of 10 mV s^{-1} is

shown in Fig. 5.1.4. The rest potential is 0.12 V vs.Ag|AgCl reference electrodes. The scan towards negative direction (in the second cycle) consists of first and second reduction waves C_1 and C_2 with the current starting to increase at 0.52 V and -0.40 V, respectively. An additional reduction wave C_3 is observed with the current again starting to increase at -0.75 V. The reverse scan consists of first and second oxidation peaks P_{a1} and P_{a2} at -0.001 V and 0.70 V, respectively. Additional oxidation wave is observed with the current again starting toincrease at 1.37 V. The first reduction wave C_1 is absent in the forward scan of the first cycle. However in the first cycle, the magnitude of the current density in the second reduction wave C_2 is same as compared with the second cycle. On the other hand, the magnitudes of the first and second oxidation peak current densities (P_{a1} and P_{a2}) are increased in the second cycle as compared with the first cycle.

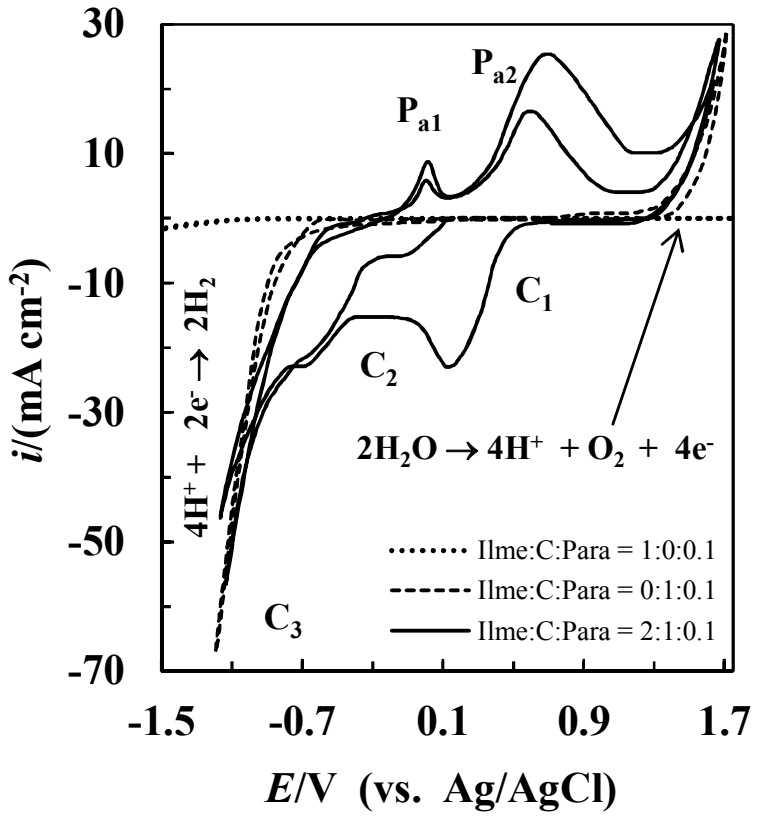

Figure 5.1.4 Cyclic voltammograms recorded on a pellet of ilmenite, graphite and paraffin mixed electrode in 1 mol dm^{-3} H_2SO_4 at 30° C with a scan rate of 10 mV s^{-1}.

Compared with the voltammogramobtained in the absence ofilmenite(dashed curve in Fig. 5.1.4),the reduction wave appearsat -0.70 V corresponds to the reduction

of hydrogen ion (H^+) in H_2SO_4 acid solution,while the oxidation wave appeared at 1.35 V corresponds to the evolution of molecular/gaseous oxygen according to the following reactions.

$$2H^+ + 2e^- \rightarrow H_2\uparrow \qquad \text{(at -0.70 V)} \qquad (5.1.1)$$

$$2H_2O \rightarrow 4H^+ + O_2\uparrow + 4e^- \qquad \text{(at 1.35 V)} \qquad (5.1.2)$$

The voltammogram in absence of graphite (dotted curve in Fig. 5.1.4) does not have any reduction and oxidation waves. This indicates that reduction of ilmenite is not possible in absence of graphite due to very low conductivity of ilmenite. The conductivity of ilmenite increases on addition of graphite in pellet. The solid curve in Fig. 5.1.4 indicates that first and second reduction waves are responsible for the reduction of ilmenite; whereas, the first and second oxidation peaks are attributed to the oxidation of the reduced species of ilmenite in this solution.

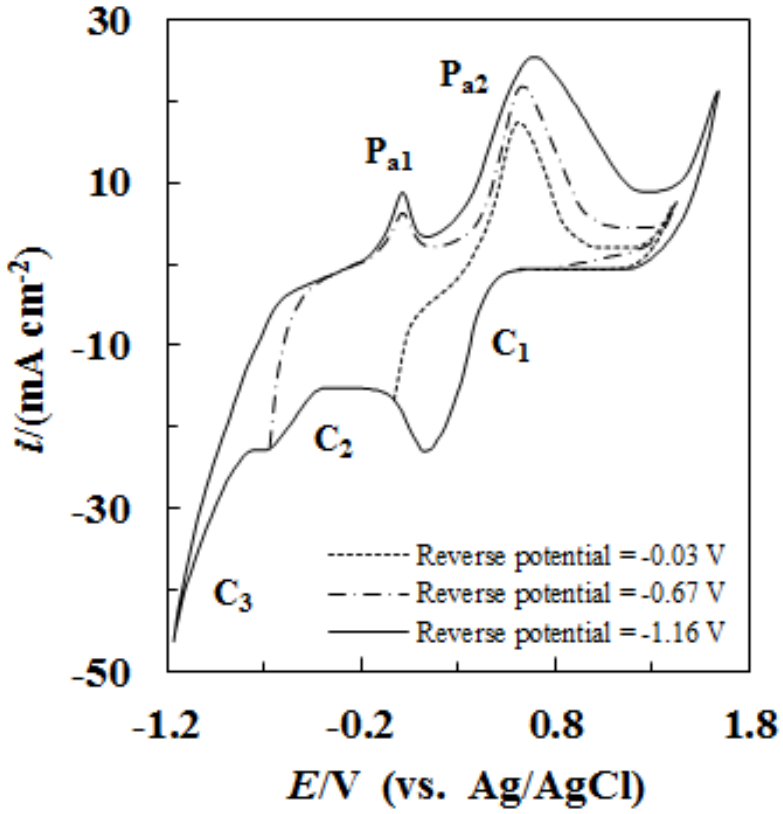

Figure 5.1.5 Effect of sweeping potential on the cyclic voltammograms recorded on a pellet of ilmenite, graphite and paraffin mixed electrode in 1 mol dm^{-3} H_2SO_4 at 30° C with a scan rate of 10 mV s^{-1}.

5.1.2.3 Effect of sweeping potential on the cyclic voltammogram

Fig. 5.1.5 shows the effect of cathodic sweeping potentials on the cyclic voltammogram recorded on a pellet of 2:1:0.1 wt. ratios of ilmenite, graphite and paraffin mixed electrode in 1 mol dm^{-3} H_2SO_4 solution at 30° C with a scan rate of 10 mV s^{-1}. It is readily seen that first reduction wave C_1 corresponds to the second oxidation peak P_{a2}. The second reduction wave C_2 corresponds to both first and second oxidation peaks P_{a1} and P_{a2}. The first cathodic peak at about 0.13 V probably involves the reduction of Fe^{3+} to Fe^{2+} either in solution or in solid phase. The second reduction wave is possibly associated with the reduction of $FeTiO_3$ and Fe_2O_3 fractions to Ti^{3+} and Fe^{2+}; and the first and second oxidation peaks are attributed to the oxidation of Ti^{3+} to Ti^{4+} and Fe^{2+} to Fe^{3+}, respectively, in solution:

$$Fe^{3+} + e^- \rightarrow Fe^{2+} \quad (\text{at } C_1) \quad (5.1.3)$$

$$FeTiO_3 + 3H^+ + e^- \rightarrow Fe^{2+} + Ti^{3+} + 3OH^- \quad (\text{at } C_2) \quad (5.1.4)$$

$$Fe_2O_3 + 3H^+ + 2e^- \rightarrow 2Fe^{2+} + 3OH^- \quad (\text{at } C_2) \quad (5.1.5)$$

$$Ti^{3+} \rightarrow Ti^{4+} + e^- \quad (\text{at } P_{a1}) \quad (5.1.6)$$

$$Fe^{2+} \rightarrow Fe^{3+} + e^- \quad (\text{at } P_{a2}) \quad (5.1.7)$$

Similar results have been reported by Zhang and Nicol[265] for the electrochemical reduction and dissolution of ilmenite in H_2SO_4 solution. The dissolved solution obtained at a constant potential dissolution method (-0.80 V) contains Fe^{2+}, Fe^{3+} and Ti^{4+} ions.This is also evident that several species appear during electrochemical dissolution of the ilmenite fraction of beach sand of Bangladesh.

5.1.2.4 Effect of ilmenite and graphite ratio on the cyclic voltammogram

The effect of ratio of ilmenite, graphite and paraffin in pellet (electrode) on the cyclic voltammograms (2^{nd} cycle) recorded in 1 mol dm^{-3} H_2SO_4 acid solution at 30° C with a scan rate of 10 mV $s^{-1}$is shown in Fig. 5.1.6. It is readily seen from the voltammograms that the magnitude of the first and second reduction peak and also the oxidation peak current densities are increased with the increase of ilmenite content in the pellet. It indicates that 2:1:0.1 wt. ratio of ilmenite-graphite-paraffin mixture ratio

of pellet will give higher dissolution rate of ilmenite fraction by constant potential and constant current methods.

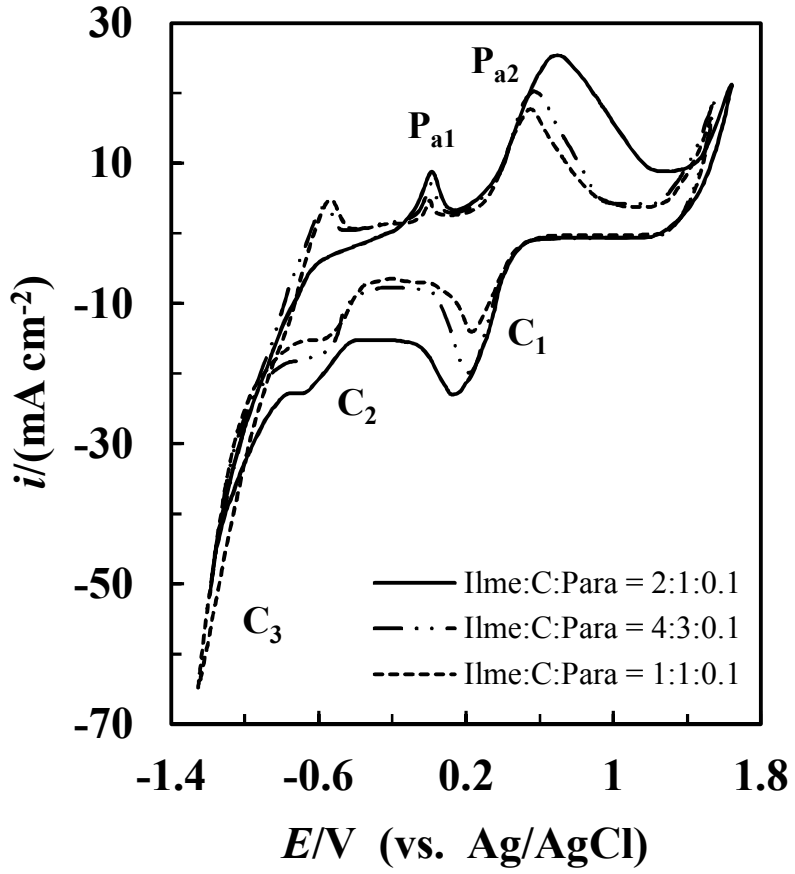

Figure 5.1.6 Effect of ilmenite to graphite ratio on the cyclic voltammograms (2nd cycle) recorded on a pellet of ilmenite, graphite and paraffin mixed electrode in 1 mol dm^{-3} H_2SO_4 at 30° C with a scan rate of 10 mV s^{-1}.

5.1.2.5 Effect of H_2SO_4 concentration on the cyclic voltammogram

Fig. 5.1.7 shows the effect of sulphuric acid concentration on the cyclic voltammograms (2nd cycle) recorded on a 2:1:0.1 (wt. ratio) ilmenite-graphite-paraffin mixed electrode at 30° C with a scan rate of 10 mV·s^{-1}. The magnitude of the reduction and oxidation peaks current densities in 1 mol dm^{-3} H_2SO_4 is high than in lower (0.3 mol dm^{-3}) and also higher (3 mol dm^{-3}) H_2SO_4 concentration, which indicates that 1 mol dm^{-3} H_2SO_4 acid solution is suitable to obtain higher dissolution rate of ilmenite fraction by electrochemical dissolution method.

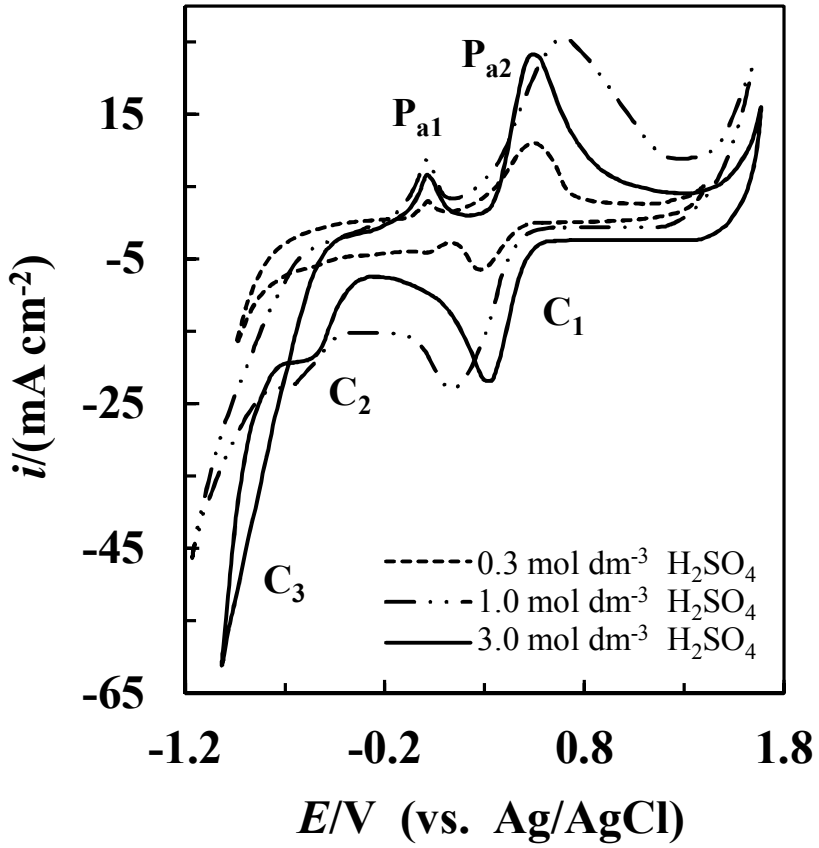

Figure 5.1.7 Effect of H_2SO_4 concentration on the cyclic voltammograms (2^{nd} cycle) recorded on a pellet of 2:1:0.1 ratio of ilmenite: graphite: paraffin mixed electrode at 30° C with a scan rate of 10 mV s^{-1}.

5.1.2.6 Effect of temperature on the cyclic voltammogram

The effect of temperature on the cyclic voltammograms (2^{nd} cycle) recorded on a 2:1:0.1 (wt. ratio) ilmenite-graphite-paraffin mixed electrode in 1mol dm^{-3} H_2SO_4 with a scan rate of 10 mV s^{-1} is shown in Fig. 5.1.8. Magnitudes of the reduction and oxidation peaks' current densities are increased with the rise of temperature. It is therefore concluded that higher dissolution rate of ilmenite fraction of beach sand of Bangladesh can be obtained from 2:1:0.1 (wt. ratio) ilmenite-graphite-paraffin mixed electrode in 1 mol dm^{-3} H_2SO_4 acid solution at 80° C.

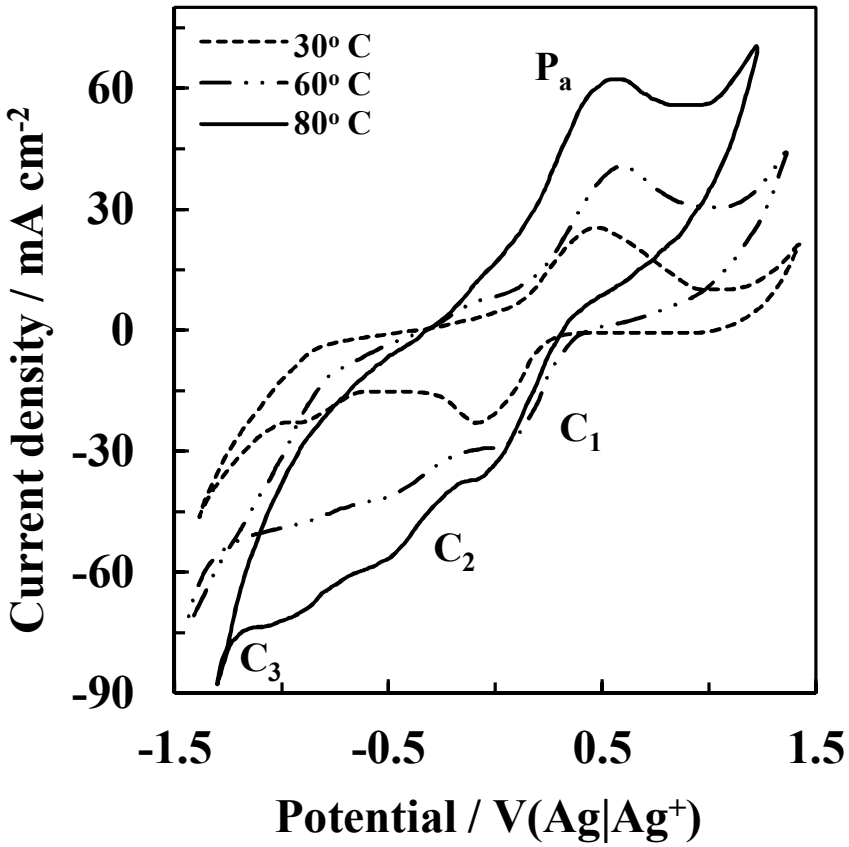

Figure 5.1.8 Effect of temperature on the cyclic voltammograms (2nd cycle) recorded on a pellet of 2:1:0.1 ratio of lilmenite: graphite: paraffin mixed electrode in 1 mol dm^{-3} H_2SO_4 with a scan rate of 10 mV s^{-1}.

5.1.3 Electrochemical dissolution study of ilmenite

5.1.3.1 Effect of time on the dissolution rate of iron and titanium from ilmenite

Variations of dissolution rate of ilmenite with time in 1 mol dm^{-3} H_2SO_4 at 80° C from 2:1:0.1 (wt. ratio) ilmenite- graphite- paraffin mixed pellet under constant potential method are shown in Fig. 5.1.9. The dissolution potentials are -0.80 V and -0.60 V vs. Ag|AgCl reference electrode. Initially, the dissolution rate of ilmenite fraction is sharply decreased with the increase of time up to 1 h and then the decreasing rate is significantly slow. The dissolution rate of iron is about 5 times to that of titanium at both the applied dissolution potentials for a fixed time. Therefore, dissolution time of 1 h has been selected in subsequent electrochemical studies.

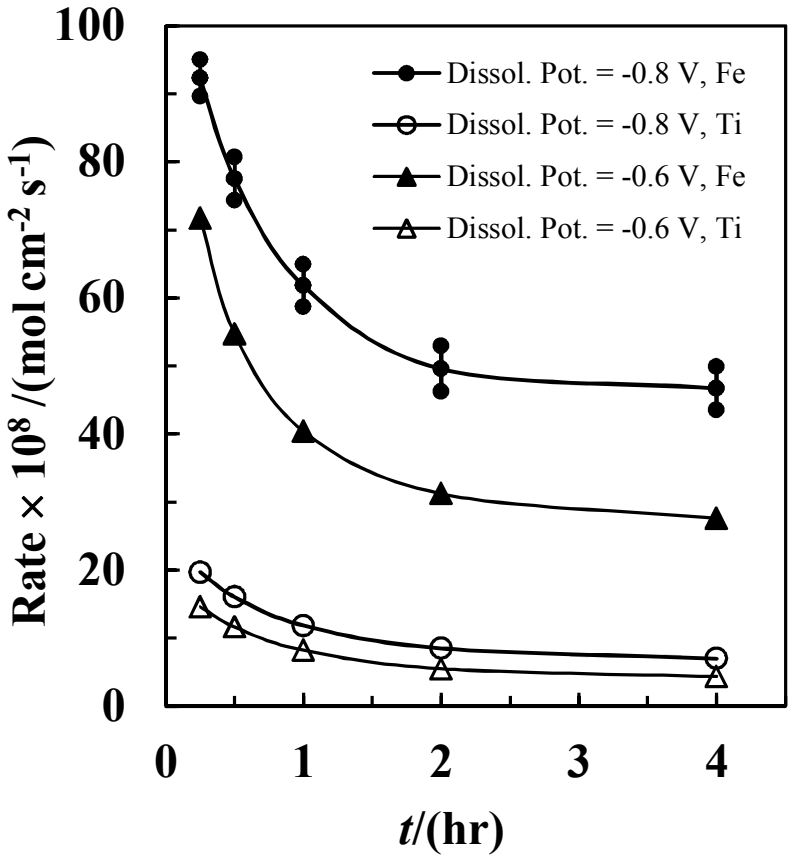

Figure 5.1.9 Effect of time on the dissolution rate of iron and titanium from 2:1:0.1 wt. ratio of ilmenite, graphite and paraffin mixed pellet in 1 mol dm^{-3} H_2SO_4 at 30° C. Applied dissolution potential:-0.6 V and-0.8 V.

5.1.3.2 Effect of temperature on the dissolution rate of iron and titanium from ilmenite

Fig. 5.1.10 shows the effect of temperature on the dissolution rate of ilmenite in 1 mol dm^{-3} H_2SO_4 from 2:1:0.1 wt. ratio ilmenite-graphite-paraffin mixed pellet at different applied potential method. Dissolutions of ilmenite have been carried out in the potential range of -0.20 V to -1.0 V and the temperature range of 30° C to 80° C. At constant potential, the dissolution rate is increased with the increase of temperature. The increasing rate is slow up to 60° C and then sharply increased with the rise of temperature. The ratio of the rate of iron dissolution to that of titanium at all applied dissolution potentials and temperature is about 5.00.

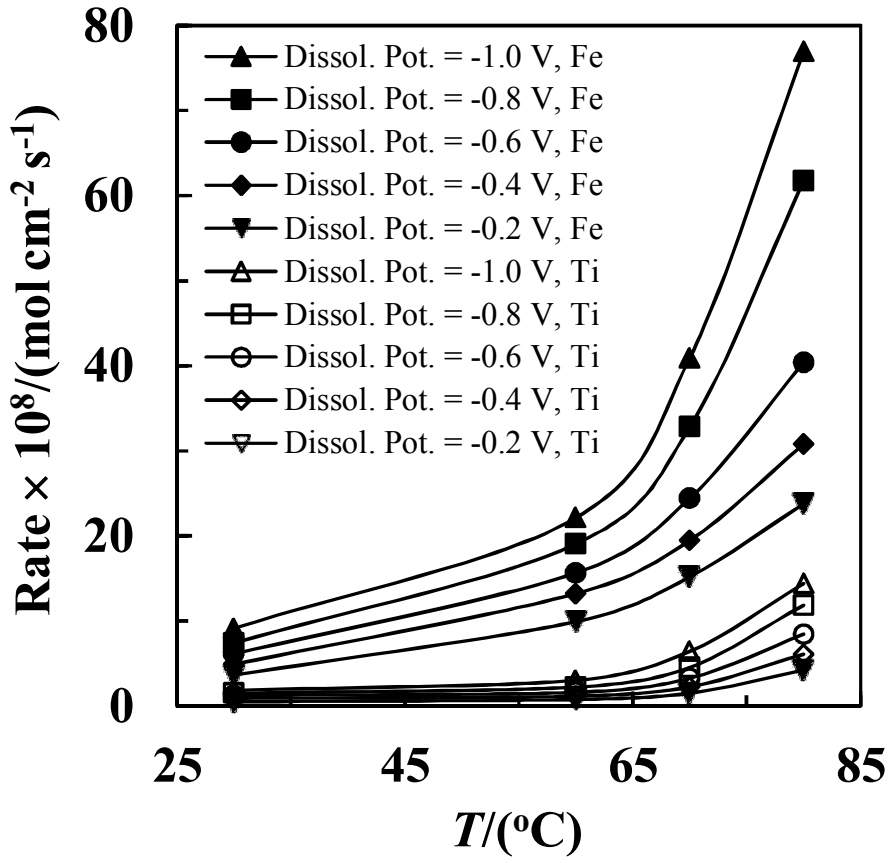

Figure 5.1.10 Effect of temperature on the dissolution rate of iron and titanium from 2:1:0.1 wt. ratio of ilmenite, graphite and paraffin mixed pellet in 1 mol dm^{-3} H_2SO_4 at different applied dissolution potential.

5.1.3.3 Effect of H_2SO_4 concentration on the dissolution rate of iron and titanium from ilmenite

The effect of H_2SO_4 concentration on the dissolution rate of ilmenite fraction at 80° C from 2:1:0.1 ilmenite-graphite-paraffin mixed pellets under constant potential method are shown in Fig. 5.1.11. At low applied reduction potentials (-0.20 V ~ -0.40 V), the dissolution rate is first increased up to 1 mol dm^{-3} H_2SO_4 solution and then the increasing rate is very slow. However at a more negative applied reduction potentials (>-0.40 V), the dissolution rate is first sharply increased up to 1 mol dm^{-3} H_2SO_4 solution and then it is decreased appreciably with the rise of acid concentration. At higher H_2SO_4 acid concentration (>1.00 mol dm^{-3}) and more negative applied reduction potentials (<-0.60 V), the dissolution rate of ilmenite fraction is decreased due to the starting of H_2 gas evolution which eventually decreases the active surface area of ilmenite pellet by adsorption.

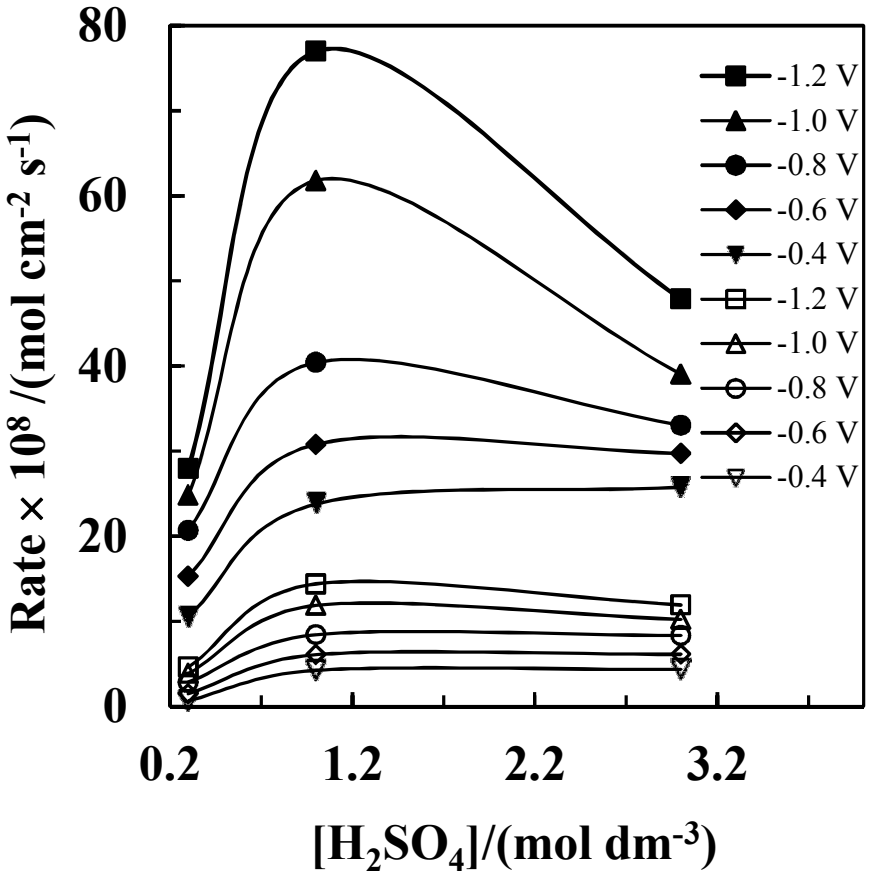

Figure 5.1.11 Effect of H_2SO_4 concentration on the dissolution rate of iron and titanium from 2:1:0.1 wt. ratio of ilmenite, graphite and paraffin mixed pellet at 80° C.

5.1.3.4 Arrhenius plot for the dissolution rate of ilmenite fraction

The Arrhenius plot for the dissolution rate of ilmenite fraction (log ν vs. $1/T$) at various dissolution potentials are shown in Fig. 5.1.12. The experimental data for a set of experimental parameter do not fall on a straight line; rather curve is obtained. The slopes of the tangential lines at higher temperature region give activation energy (E_a) of 50±10 kJ mol^{-1} and those at lower temperature region give E_a of ~15±5 kJ mol^{-1}. The values of E_a suggest the existence of a diffusion film which is destroyed at higher temperature. At lower temperature region, the process is diffusion controlled and with the rise of temperature, the process becomes chemically controlled.

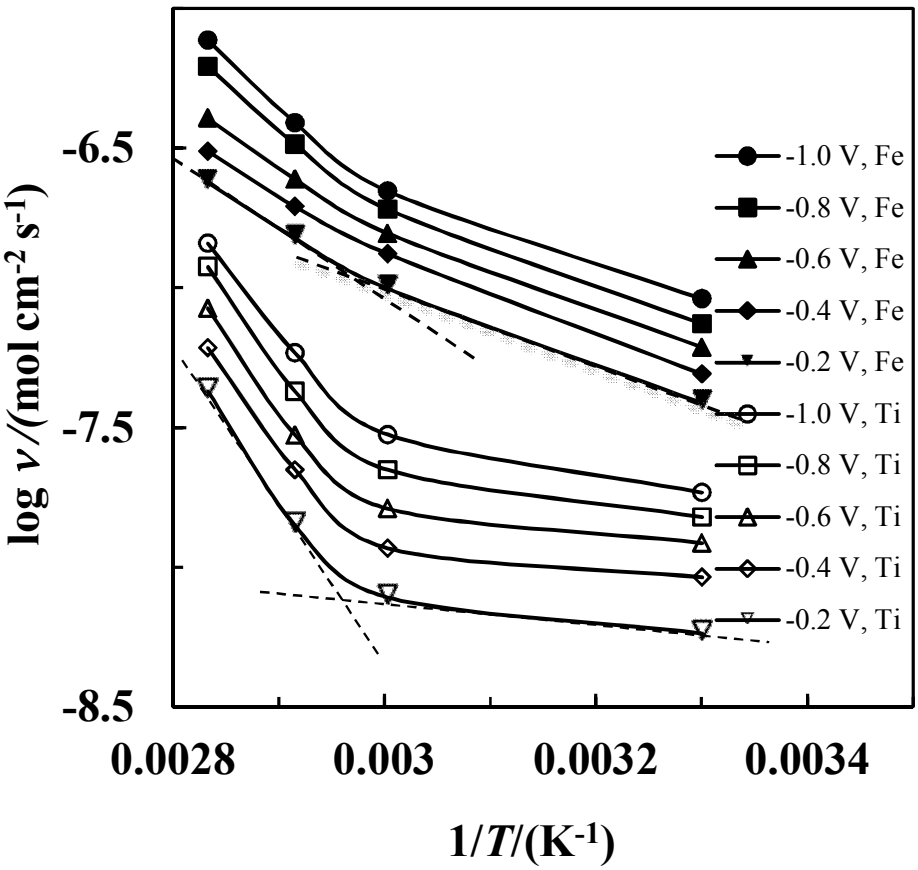

Figure 5.1.12 Arrhenius plot: log ν vs. inverse of absolute temperature (1/T) at various dissolution potentials.Ilmenite: graphite: paraffin = 2:1:0.1 and [H_2SO_4] = 1 mol dm^{-3}.

5.1.4 Conclusions

The dissolution of ilmenite fraction could not be obtained in H_2SO_4 acid solution without the addition of graphite in ilmenite fraction due to low conductivity of ilmenite fraction. The dissolution rate of ilmenite ($FeTiO_3$) and hematite (Fe_2O_3) is low at low applied reduction potentials (<-0.40 V) and temperatures (<60° C). At more negative potentials and higher temperatures, the dissolution rate of ilmenite is increased through increasing rate of the reduction of ilmenite to Fe^{2+} and Ti^{3+}. The dissolution rate is also increased on increasing acid concentration up to 1 mol dm^{-3}; and at higher acid concentration and higher reduction potentials, it is decreased due to the starting of H_2 gas evolution which eventually decreases the active surface area of ilmenite pellet by adsorption. The hematite phase in the mineral has a higher dissolution rate under reductive conditions than the ilmenite. The values of E_a in the higher and lower temperature regions are 50±10 kJ mol^{-1} and 15±5 kJ mol^{-1}, respectively. The values of

E_a suggest the existence of a diffusion film at lower temperature which is destroyed at higher temperature. At lower temperature region, the process is diffusion controlled and with the rise of temperature the process becomes chemically controlled.

5.2 A Study on the Electrochemical Dissolution of Zircon Fraction of Beach Sand in Sodium Hydroxide Solution

5.2.1 Characterization of zircon fraction by XRD and EDAX

The collected zircon fraction was dry ground to less than 53 μm size and used for powder X-ray diffraction and X-ray energy dispersive spectroscopic (EDAX) analyses.

X-ray diffraction analysis has been carried out with a Philips PW 1716 diffractometer using CuK_α radiation (40 kV, 30 mA, scan speed: 0.01 ^{o}/s) to identify the compounds/phases existing in the zircon fraction. The acquired diffraction pattern for the powder specimen of the zircon fraction is shown in Fig. 5.2.1. The diffraction peaks at 2θ = 19.873^o, 26.696^o, 33.667^o, 35.41^o, 35.908^o, 38.34^o, 40.548^o, 43.64^o, 45.079^o, 47.464^o, 52.031^o, 53.305^o, 53.388^o, 55.457^o, 59.626^o, 62.756^o, 67.698^o, 68.681^o, 69.55^o, 73.232^o, 75.228^o, 80.672^o, 82.369^o, 87.923^o, 88.616^o, 92.14^o, 93.175^{o}and 94.157^o are for zircon fraction ($ZrSiO_4$) (Refn. Code.No. 01-081-0589) of different phase:

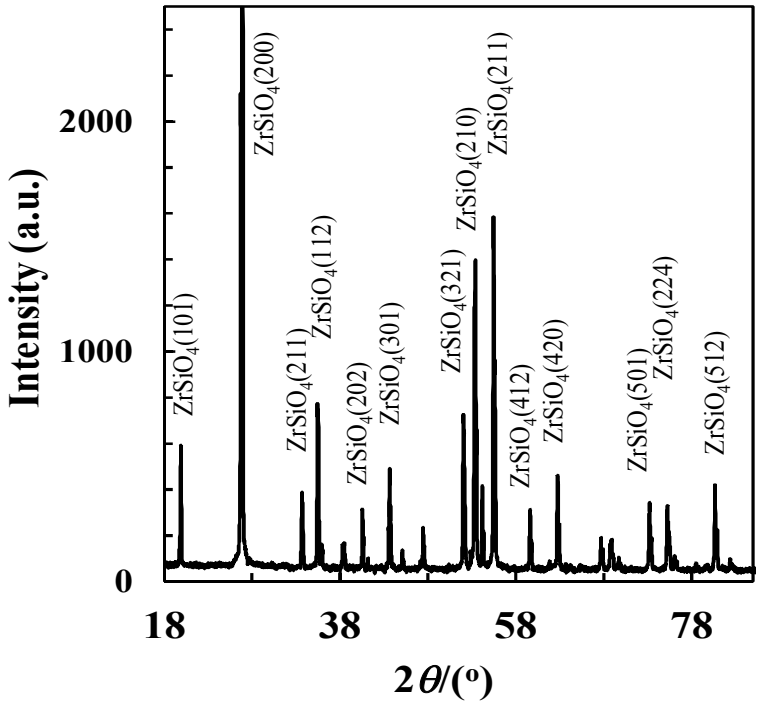

Figure 5.2.13 X-ray diffraction pattern of the zircon fraction of beach sand of Bangladesh. (International Centre for Diffraction Data Number: 01-081-0589).

X-ray energy dispersive spectroscope (EDAX) analysis of the powder specimen of the zircon fraction has been carried out with (Skyray Instrument Inc., EDX 3600B, UK). Fig. 5.2.2 shows the EDAX profile of the zircon fraction. EDAX profile shows that Zr, P, Si, Ca, K, Fe, Cu, Zn, Fe etc. are present in the zircon fraction of the beach sand of Bangladesh and among them Zr content is of the highest amount. XRD and chemical analysis data indicate that zircon fraction of the beach sand of Bangladesh contains about 97.17% $ZrSiO_4$.

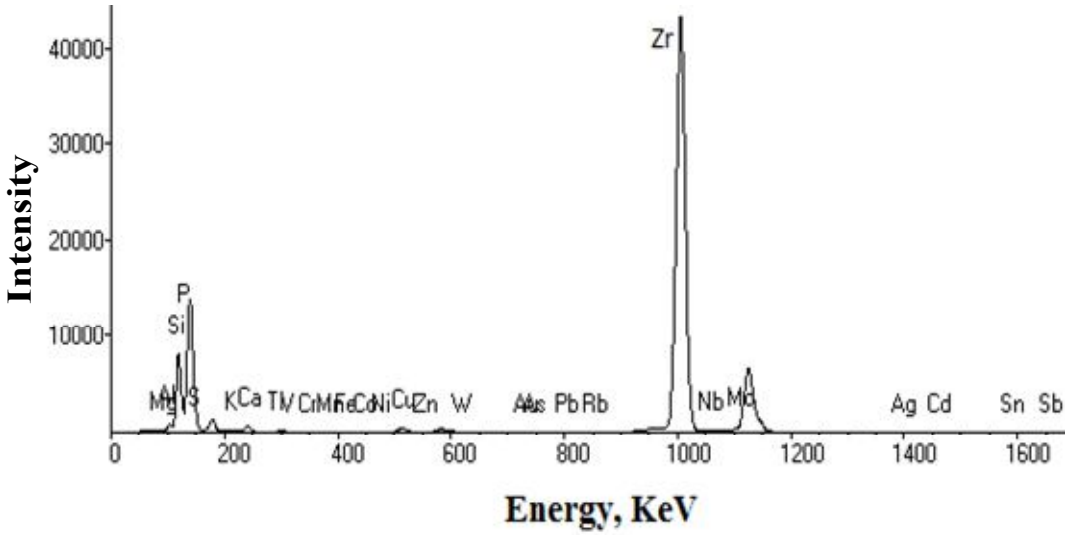

Figure 5.14 EDAX profile of the zircon fraction.

5.2.2 Cyclic voltammetry of zircon-graphite-paraffin mixed pellet

5.2.2.1 Cyclic voltammograms of zircon-graphite-paraffin mixed pellet in H_2SO_4 and NaOH solution

The cyclic voltammograms recorded on a pellet of 1:1:0.1 wt. ratio of zircon, graphite and paraffin mixed electrode in 1 mol dm^{-3} H_2SO_4 (solid curve) and NaOH (dashed curve) solutions at 30° C with a scan rate of 10 mV s^{-1} are shown in Fig. 5.2.3. The rest potentials are 0.078 V and 0.064 V vs. Ag|AgCl reference electrode forH_2SO_4 and NaOH solution, respectively. The scan towards negative direction (solid curve) consists first and second reduction waves C''_1 and C''_2 with the current starting to increase at -0.023 V and -0.35 V, respectively. Additional reduction wave (C''_3) is observed with the current again starting to increase at -0.65 V. The reverse scan consists one oxidation peak $P_a''_2$ at 0.33 V. Additional oxidation waveis observed with

the current starting to increase at 0.91 V. Compared with the voltammogram obtained in NaOH solution (dashed curve), the forward scan consists of two reduction waves (C''_1 at-0.027 V and C''_2 at -0.590 V), and the reverse scan consists two oxidation peaks ($P_a''_1$ at -0.18 V and $P_a''_2$ at 0.23 V) and an additional oxidation wave with the current starting to increase at 0.57V. The magnitude of the reduction and oxidation current densities in H_2SO_4 solution is higher than in NaOH solution. So the electrochemical dissolution rate of zirconium from zircon fraction will be high in H_2SO_4 as compared with NaOH solution. However, the pellet of zircon fraction has been destroyed during cathodic polarization at different applied dissolution potential and which is not observed in NaOH solution. Therefore, NaOH solution has been selected for the electrochemical dissolution study of zircon fraction.

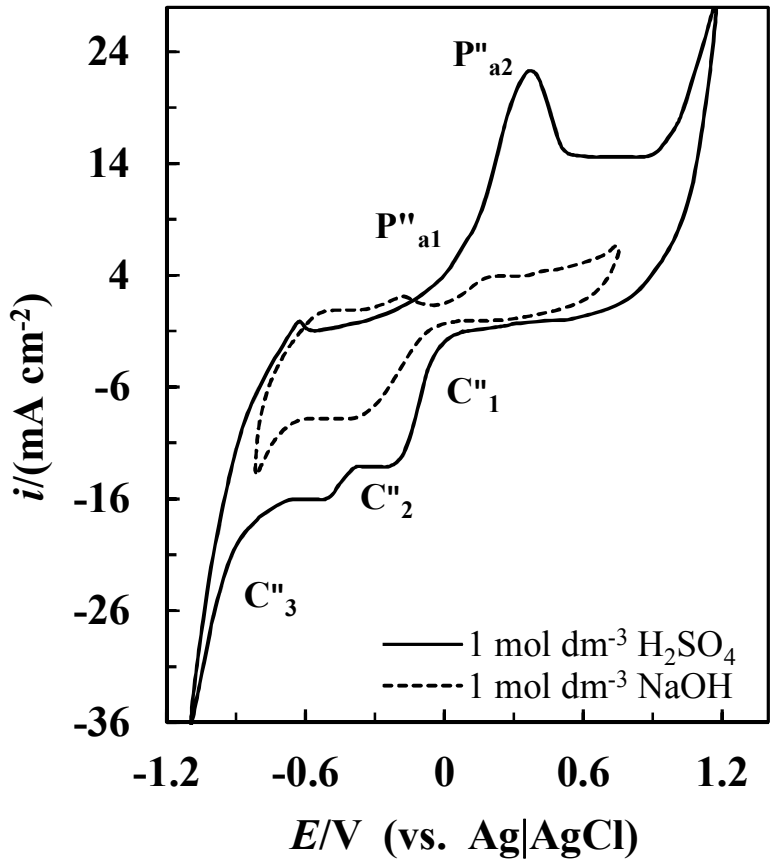

Figure 5.15 Cyclic voltammograms recorded on a pellet of zircon, graphite and paraffin mixed (1:1:0.1) electrode in 1 mol dm^{-3} H_2SO_4 and NaOH solutions at 30° C with a scan rate of 10 mV s^{-1}.

5.2.2.2 Cyclic voltammetry of zircon-graphite-paraffin mixed pellet in NaOH

The cyclic voltammograms recorded on a pellet of zircon, graphite and paraffin mixed electrode in 1 mol dm^{-3} NaOH solution at 30° C with a scan rate of 10 mV s^{-1} are shown in Fig. 5.2.4. The rest potential is 0.064 V vs.Ag|AgCl reference electrodes. The scan towards negative direction (in the second cycle) consists of first and second reduction waves C''_1 and C''_2 with the current starting to increase at -0.027 V and -0.590 V, respectively. The reverse scan consists of first and second oxidation peaks P''_{a1} and P''_{a2} at -0.18 V and 0.23 V, respectively. Additional oxidation wave is observed with the current again starting to increase at 0.57 V. However in the first cycle, the magnitudes of the current densities in the firstand second reduction waves are higher as compared with the second cycle. On the other hand, the magnitudes of the first and second oxidation peaks current densities (P''_{a1} and P''_{a2}) are increased in the second cycle as compared with the first cycle.

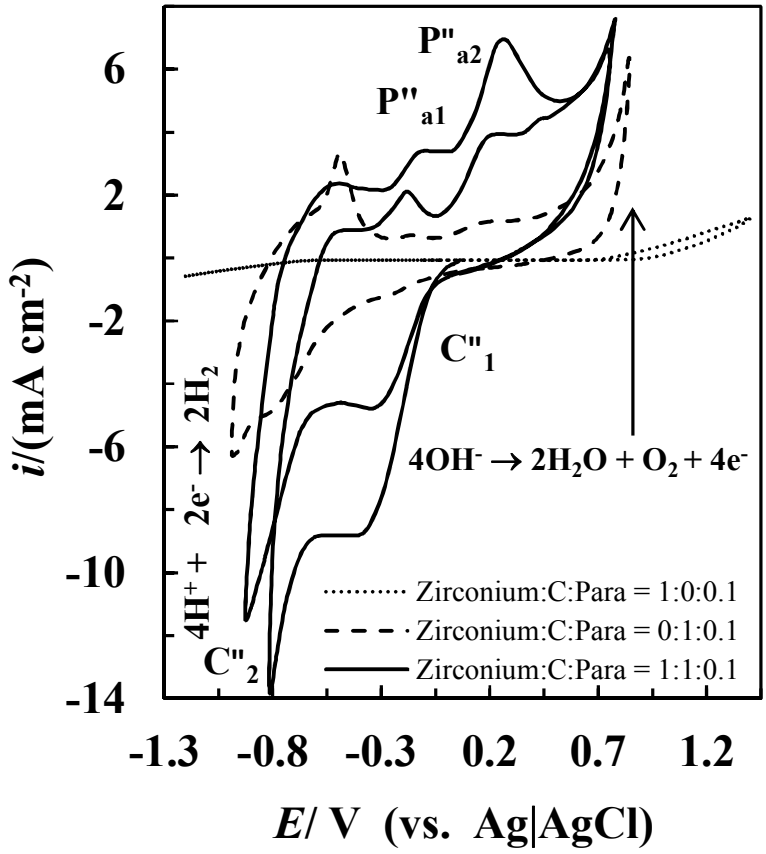

Figure 5.16 Cyclic voltammograms recorded on a pellet of zircon, graphite and paraffin mixed electrode in 1 mol dm^{-3} NaOH solution at 30° C with a scan rate of 10 mV s^{-1}.

Compared with the voltammogramobtained in the absence of zircon (the dashed curve in Fig. 5.2.4),the reduction wave appearingat -0.85 V corresponds to the reduction of hydrogen ion (H^+) in NaOH solution,while the oxidation wave appearingat 0.57 V corresponds to the evolution of molecular/gaseous oxygen according to the following reactions:

$$2H^+ + 2e^- \rightarrow H_2\uparrow \qquad \text{(at -0.85 V)} \qquad (5.2.1)$$

$$4OH^- \rightarrow 2H_2O + O_2\uparrow + 4e^- \qquad \text{(at 0.57 V)} \qquad (5.2.2)$$

The voltammogram in absence of graphite (dotted curve in Fig.5.2.4) does not have any reduction and oxidation wave. This indicates that reduction of zircon is not possible in absence of graphite due to very low conductivity of the electrode (zircon pellet). The conductivity of zircon increases on the addition of graphite in pellet. The solid curve in Fig. 5.2.4 indicates that the first reduction wave is responsible for the reduction of zircon; whereas the first and second oxidation peaks correspond to the oxidation of the reduced species of zircon in this solution.

5.2.2.3 Effect of sweeping potential on the cyclic voltammogram

Fig. 5.2.5 shows the effect of cathodic sweeping potentials on the cyclic voltammograms recorded on a pellet of 1:1:0.1 wt. ratios of zircon, graphite and paraffin mixed electrode in 1 mol dm^{-3} NaOH solution at 30° C with a scan rate of 10 mV s^{-1}. It is readily seen from the voltammograms that first reductionwave $C''_1$is correspond tothe second oxidation peak P''_{a2}. The second reduction wave (C''_2) corresponds to the first oxidation peak P''_{a1}. The first cathodic peak at about 0.297 V is probably involving the reduction of tetravalent zirconium to trivalent zirconium ion either in solution or in solid phase. The second reductive wave is possibly associated with the reduction of tetravalent silicon to trivalent silicon ion along with the reduction of hydrogen ion (H^+) to H_2 gas; and the first and second oxidation peaks are attributed to the oxidation of trivalent silicon to tetravalent silicon ion and trivalent zirconium to tetravalent zirconium ion respectively in solution according to the following reactions:

$$ZrSiO_4 + 3H_2O + e^- \rightarrow Zr^{3+} + H_3SiO_4^- + 3OH^- \qquad \text{(at } C''_1\text{)} \qquad (5.2.3)$$

$$H_3SiO_4^- + e^- \rightarrow SiO^+ + 3OH^- \qquad \text{(at } C''_2\text{)} \qquad (5.2.4)$$

$2H^+ + 2e^- \rightarrow H_2\uparrow$ (at C''_2) (5.2.1)

$SiO^+ \rightarrow SiO^{2+} + e^-$ (at P''_{a1}) (5.2.5)

$Zr^{3+} \rightarrow Zr^{4+} + e^-$ $\rightarrow$ (at P''_{a2}) (5.2.6)

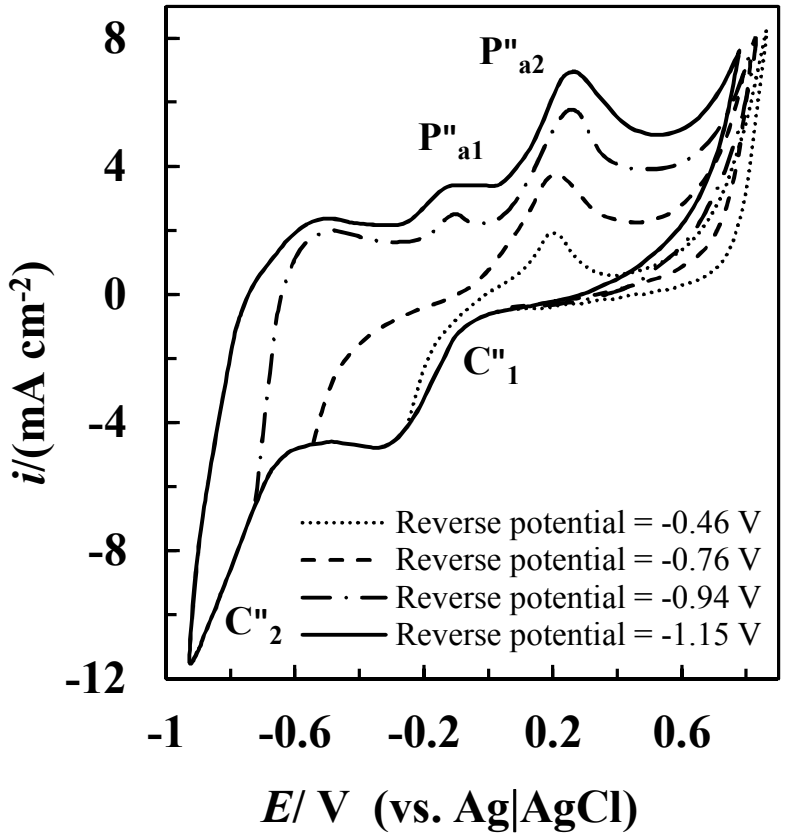

Figure 5.17 Effect of sweeping potential on the cyclic voltammograms recorded on a pellet of 1:1:0.1 ratio of zircon: graphite: paraffin mixed electrode in 1 mol dm^{-3} NaOH at 30° C with a scan rate of 10 mV s^{-1}.

5.2.2.4 Effect of zircon, graphite and paraffin ratio on the cyclic voltammogram

The effects of zircon, graphite and paraffin mixture ratio of pellet (electrode) on the cyclic voltammograms recorded in 1 mol dm^{-3} NaOH solution at 30° C with a scan rate of 10 mV s^{-1} are shown in Fig. 5.2.6. It is readily seen from the voltammograms that the magnitude of the first reduction peak (C''_1) and also the oxidation peaks (P''_{a1} and P''_{a2}) current densities are high at 1:1:0.1 wt. ratio of zircon-graphite-paraffin mixture ratio of pellet. It indicates that 1:1:0.1 wt. ratio of zircon-graphite-paraffin mixture ratio of pellet will give higher dissolution rate of zirconiumfrom zircon fraction by constant potential and constant current methods.

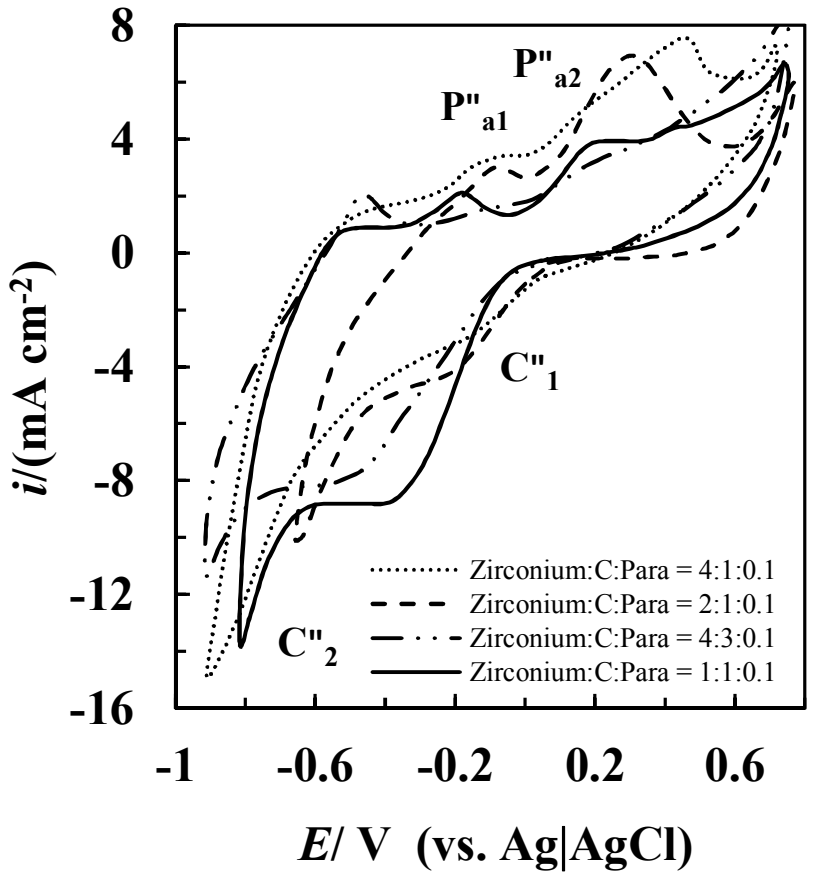

Figure 5.18 Effect of zircon, graphite and paraffin ratio on the cyclic voltammograms recorded on a pellet of zircon, graphite and paraffin mixed electrode in 1 mol dm^{-3} NaOH at 30° C with a scan rate of 10 mV s^{-1}.

5.2.2.5 Effect of NaOH concentration on the cyclic voltammogram

Fig. 5.2.7 shows the effect of NaOH concentration on the cyclic voltammograms recorded on a 1:1:0.1 (wt. ratio) zircon-graphite-paraffin mixed electrodes at 30° C with a scan rate of 10 mV s^{-1}. It is readily seen that the magnitude of the reduction and oxidation peaks current densities in 3 mol dm^{-3} NaOH is high as compared with lower (<0.01mol dm^{-3}) and also higher (>6 mol dm^{-3}) NaOH concentrations in the solution, which indicates that 3 mol dm^{-3} NaOH solution is suitable to obtain higher dissolution rate of zirconium by electrochemical dissolution of zircon fraction.

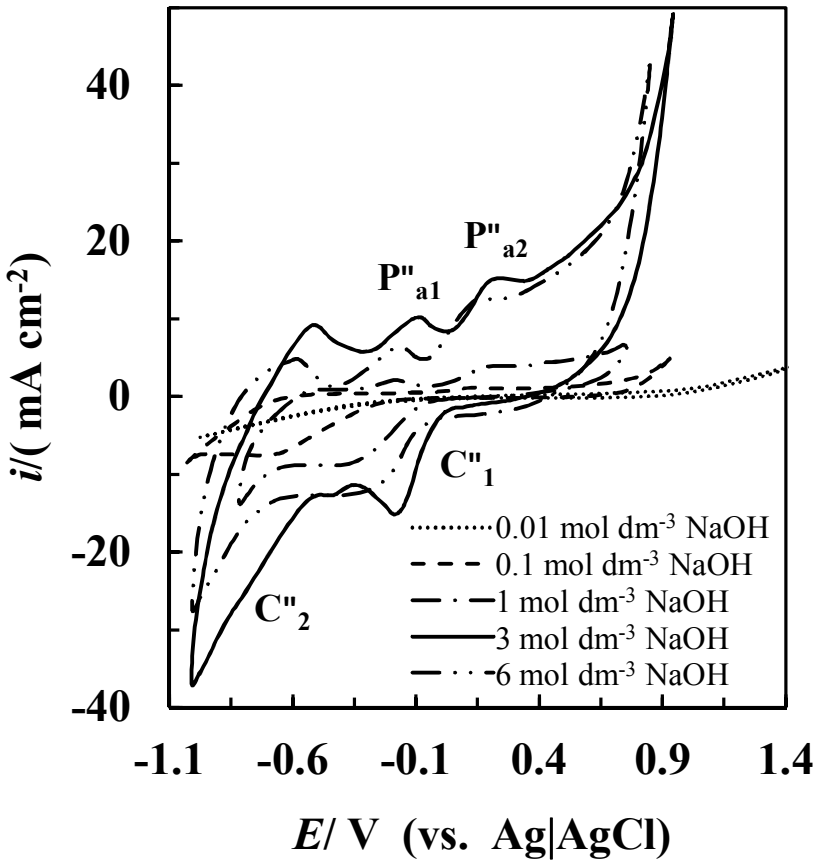

Figure 5.19 Effects of NaOH concentration on the cyclic voltammograms recorded on a pellet of 1:1:0.1 ratio of zircon: graphite: paraffin mixed electrode at 30° C with a scan rate of 10 mV s^{-1}.

5.2.2.6 Effect of temperature on the cyclic voltammogram

The effects of temperature on the cyclic voltammograms (2^{nd} cycle) recorded on a 1:1:0.1 (wt. ratio) zircon-graphite-paraffin mixed electrode in 3 mol dm^{-3} NaOH with a scan rate of 10 mV s^{-1} are shown in Fig. 5.2.8. The magnitude of the reduction and oxidation peaks current densities are increased with the rise of temperature. It is therefore concluded that higher dissolution rate of zirconium can be obtained by electrochemical dissolution method of the zircon fraction of beach sand of Bangladesh from 1:1:0.1 (wt. ratio) zircon-graphite-paraffin mixed electrodes in 3 mol dm^{-3} NaOH solution at 85° C .

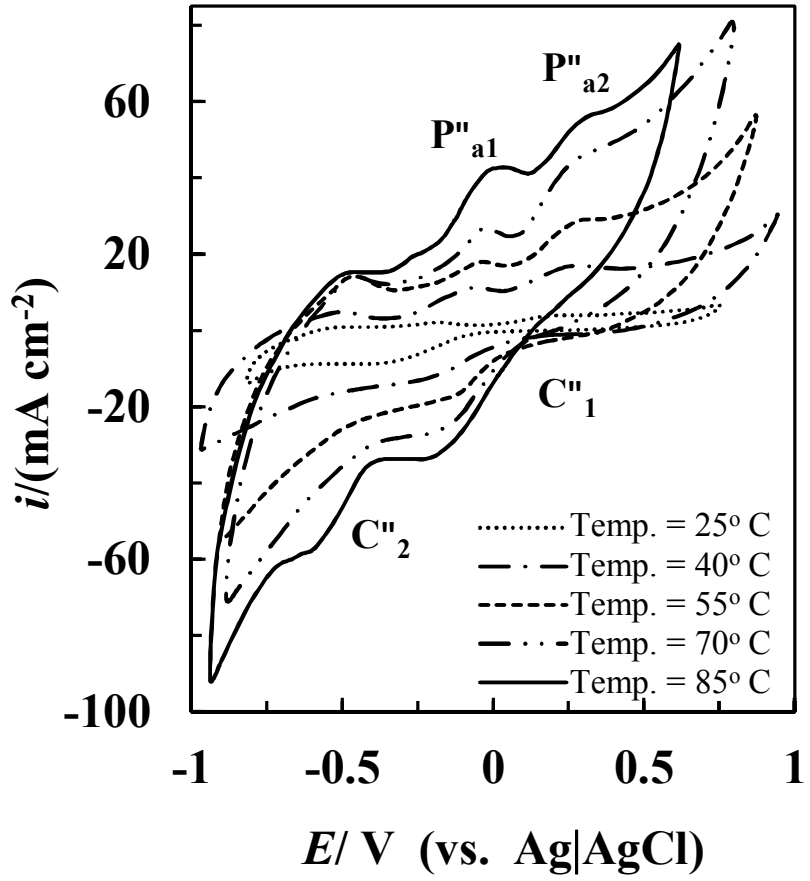

Figure 5.20 Effect of temperature on the cyclic voltammograms recorded on a pellet of 1:1:0.1 ratio of zircon: graphite: paraffin mixed electrode in 3.0 mol dm^{-3} NaOH with a scan rate of 10 mV s^{-1}.

5.2.3 Electrochemical dissolution study of zircon fraction

5.2.3.1 Effect of time on the dissolution rate of zirconium

Variations of dissolution rate of zirconium from zircon fraction with time in 3mol dm^{-3} NaOH solution at 30° C from 1:1:0.1 (wt. ratio) zircon-graphite-paraffin mixedpellet under constant potential method are shown in Fig. 5.2.9. The dissolution potentials are -0.68 V and -0.83 V vs. $Ag|Ag^{+}$ reference electrode. Initially, the dissolution rate of zirconium from zircon fraction is sharply decreased with the increase of time up to 1 h and then the decreasing rate is significantly slow. Therefore dissolution time of 1 h has been selected in all electrochemical studies.

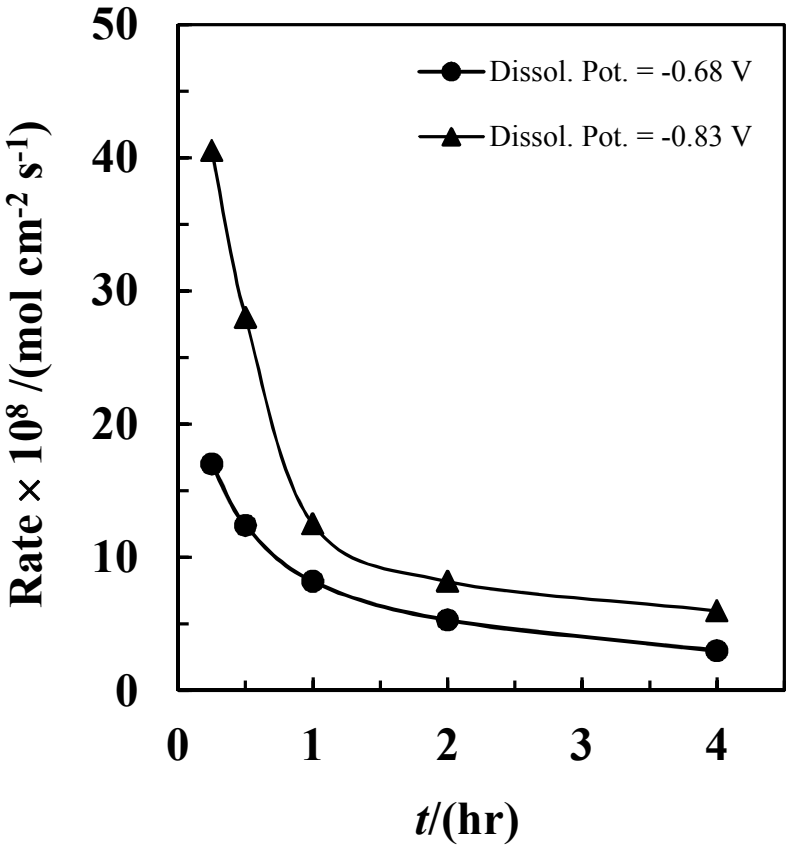

Figure 5.21 Effect of time on the dissolution rate of zirconiumfrom 1:1:0.1 wt. ratio of zircon, graphite and paraffin mixed electrode in 3.0 mol dm^{-3} NaOH at 30° C. Applied dissolution potential: -0.68 V and -0.83 V.

5.2.3.2 Effect of temperature on the dissolution rate of zirconium

Fig. 5.2.10 shows the effect of temperature on the dissolution rate of zirconium in 3 mol dm^{-3} NaOH solutions from 1:1:0.1 zircon-graphite-paraffin mixed pellets at different applied potential method. The dissolution of zircon fraction has been carried out in the potential ranging from -0.08 V to -0.83 V and the temperature ranging from 30° C to 85° C. At constant potential, the dissolution rate is increased with the increase of temperature. The increasing rate is significantly slow up to 55° C and then sharply increased with the rise of temperature.

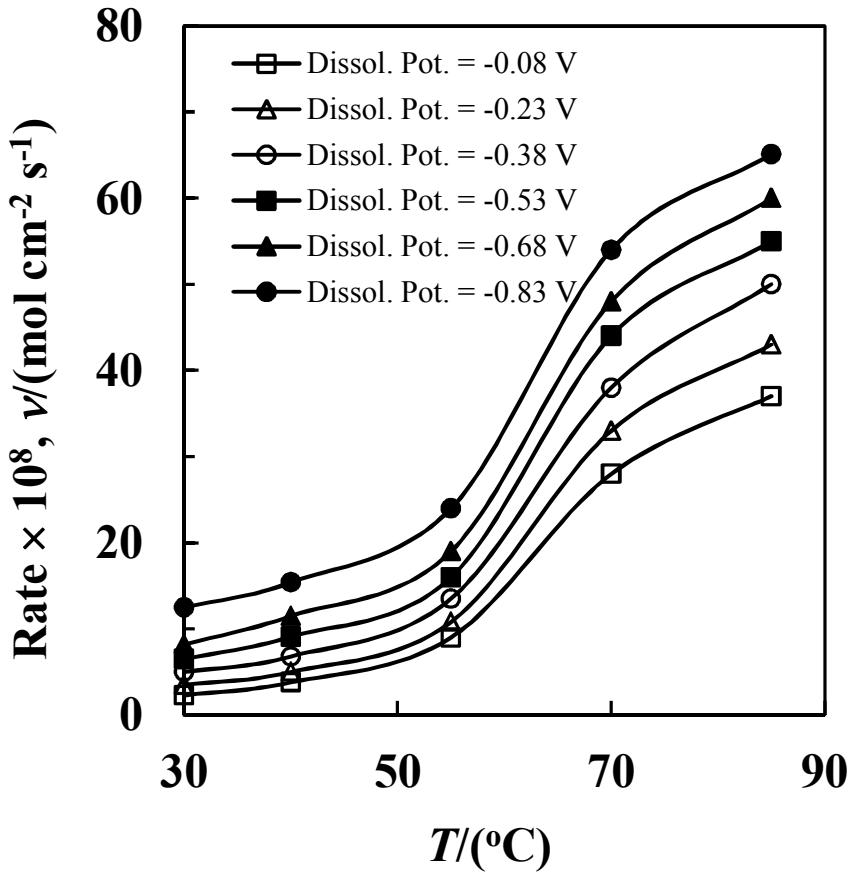

Figure 5.22 Effect of temperature on the dissolution rate of zirconium from 1:1:0.1 wt. ratio of zircon, graphite and paraffin mixed electrode in 3.0 mol dm^{-3} NaOH at different applied dissolution potential.

5.2.3.3 Effect of NaOH concentration on the dissolution rate of zirconium

The effects of NaOH concentration on the dissolution rate of zirconium at 85° C from 1:1:0.1 zircon-graphite-paraffin mixed pellets under constant potential method are shown in Fig. 5.2.11. The dissolution rate is first sharply increased up to 3 mol dm^{-3} NaOH solution and then it is decreased with the rise of NaOH concentration. At higher NaOH concentration (>3 mol dm^{-3}), the rate is decreased due to the lowering of the available reducible species on the surface of the pellets.

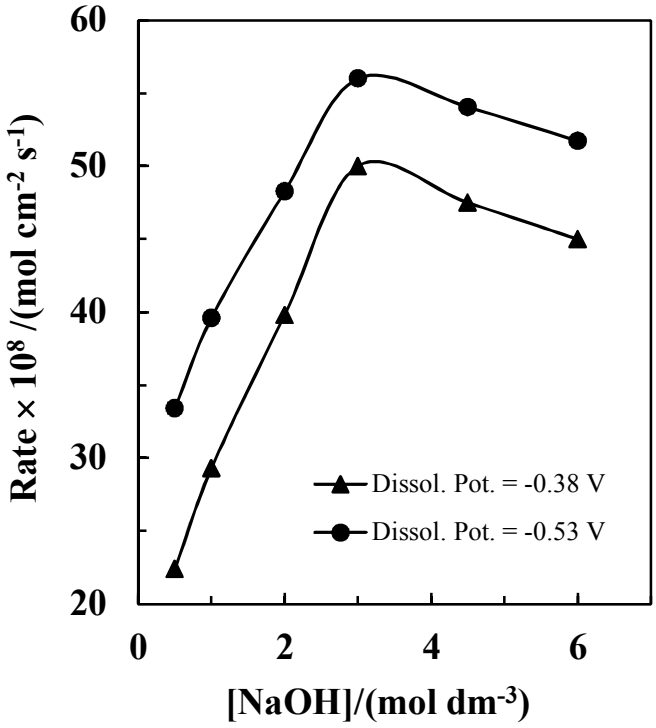

Figure 5.23 **Effect of NaOH concentration on the dissolution rate of zirconium from 1:1:0.1 wt. ratio of zircon, graphite and paraffin mixed electrode at 85° C.**

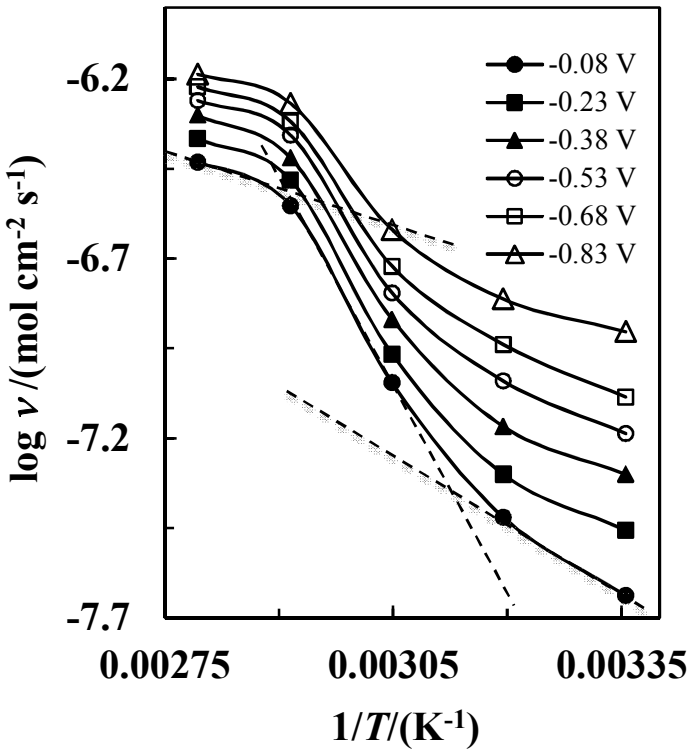

Figure 5.24 **Arrhenius plot: log v vs. inverse of absolute temperature (1/T) at various dissolution potentials. Zircon: graphite: paraffin = 1:1:0.1 and [NaOH] = 3 mol dm^{-3}.**

5.2.3.4 Arrhenius plot for the dissolution rate of zirconium from zircon fraction

The Arrhenius plot for the dissolution rate of zirconium from zircon fraction (log v) against inverse of temperature ($1/T$) at various dissolution potentials is shown in Fig. 5.2.12. The experimental data for a set of experimental parameter do not fall on a straight line; rather curve is obtained. The slopes of the tangential lines at intermediate temperature region (~70° C) give high values of activation energy (E_a) of 45±10 kJ mol^{-1} and those at lower temperature region (<30° C) give E_a of 20±5 kJ mol^{-1}. At higher temperature region (>70° C) the value of activation energy is again low as 23±1 kJ mol^{-1}. The values of E_a suggest the existence of a diffusion film which is destroyed at intermediate temperature region. At low temperature region, the process is diffusion controlled and with the rise of temperature, the diffusion layer/film is anyhow destroyed, so the process becomes chemically controlled at ~70° C. The low value of activation energy at higher temperature region is indicating the involvement of two parallel reactions.

5.2.4 Conclusions

The dissolution of zircon fraction could not be obtained in NaOH solution without the addition of graphite in zircon fraction due to low conductivity of zircon fraction. The dissolution rate of zircon ($ZrSiO_4$) is low at low applied dissolution potentials (<-0.30 V) and temperatures (<55° C). At more negative potentials and higher temperatures, the dissolution rate of zirconium is increased through increasing rate of the reduction of $ZrSiO_4$. The dissolution rate is also increased on increasing alkali concentration up to 3 mol dm^{-3}; and at higher alkali concentration, it is decreased due to lowering of the available reducible species on the surface of the pellets. The values of E_a in the higher (>70° C), intermediate (~70° C) and lower (<30° C) temperature regions are 23±1 kJ mol^{-1}, 45±10 kJ mol^{-1} and 20±5 kJ mol^{-1}respectively. The values of E_a suggest at low temperature region, the process is diffusion controlled and with the rise of temperature, the diffusion layer/film is anyhow destroyed, so the process becomes chemically controlled at ~70° C. The low value of activation energy at higher temperature region is as indicative to the involvement of two parallel reactions.

5.3 A Study on the Electrochemical Dissolution of Waste Product of Storage Battery ($PbSO_4$) in Nitric Acid Solution

5.3.1 Characterization of waste product of storage battery ($PbSO_4$) by XRD and EDAX

The collected waste product of storage battery ($PbSO_4$) was dry ground to less than 53 μm size and used for powder X-ray diffraction and X-ray energy dispersive spectroscopic (EDAX) analyses.

X-ray diffraction analysis has been carried out with a Philips PW 1716 diffractometer using CuK_α radiation (40 kV, 30 mA, scan speed: 0.01 ^{o}/s) to identify the compounds/phases existing in thewaste product of storage battery ($PbSO_4$). The acquired diffraction pattern for the powder specimen of the sample is shown in Fig. 5.3.1. The diffraction peaks at 2θ =23.28^o, 31.96^o, 36.16^o, 49.06^o, 52.14^o, 58.84^{o}and60.68^o are for PbO_2 (Refn. Code. No. 01-076-0564); 31.22^o, 36.16^o and 62.04^o are for Pb (Refn. Code. No. 00-004-0686) and the rest are $PbSO_4$ (Refn. Code. No. 01-082-1854), respectively:

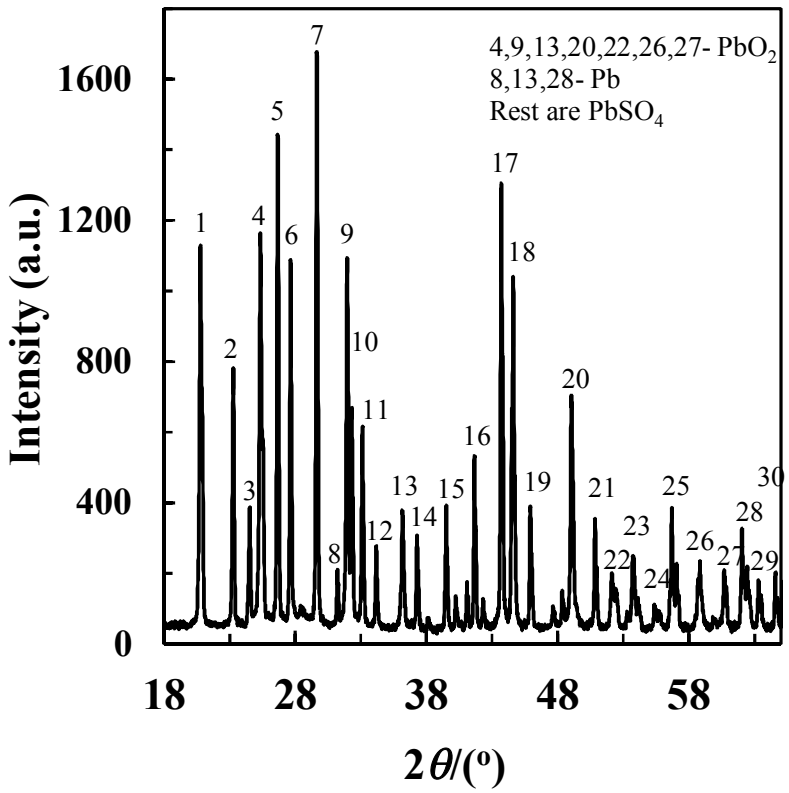

Figure 5.25 X-ray diffraction patterns of waste product of storage battery ($PbSO_4$).

X-ray energy dispersive spectroscopic (EDAX) analysis of the powder specimen of the waste product of storage battery ($PbSO_4$) has been carried out with (Skyray Instrument Inc., EDX 3600B, UK). Fig. 5.3.2 shows the EDAX profile of the waste product of storage battery ($PbSO_4$). EDAX profile shows that Pb, Fe, Al, Zn, Ni, Cu and Sn are present in the waste product of storage battery ($PbSO_4$) and among them Pb content is of the highest amount.

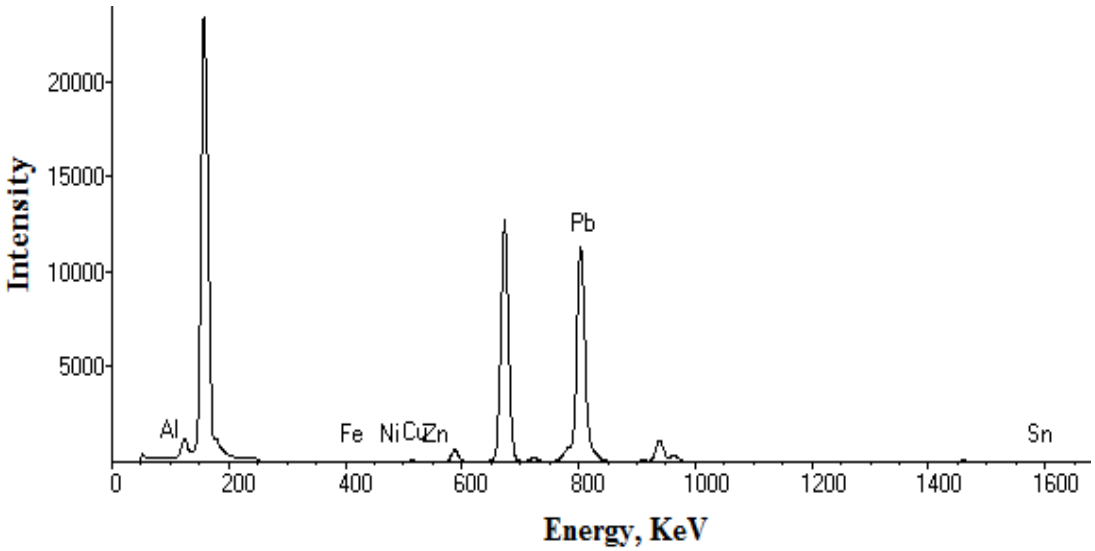

Figure 5.3.26 EDAX profile of the waste product of storage battery ($PbSO_4$).

5.3.2 Cyclic voltammetry of waste product of storage battery ($PbSO_4$)

5.3.2.1 Cyclic voltammetry of battery waste-graphite-paraffin mixed pellet in HNO_3

The cyclic voltammogram recorded on a pellet of battery waste, graphite and paraffin mixed electrode in 1 mol dm^{-3} HNO_3 solution at 30° C with a scan rate of 10 mV s^{-1} is shown in Fig. 5.3.3. The rest potential is 1.01 V vs.Ag|AgCl reference electrodes. The scan towards negative direction consists of first and second reduction waves C'_1 and C'_2 with the current starting to increase at 0.46 V and 0.12 V, respectively. An additional reduction wave C'_3 is observed with the current again starting to increase at -0.49 V. The reverse scan consists of first and second oxidation peaks $P'_{a1}$and P'_{a2} at 0.52 V and 1.32 V respectively. Additional oxidation wave is observed with the current again starting to increase at 1.40 V.

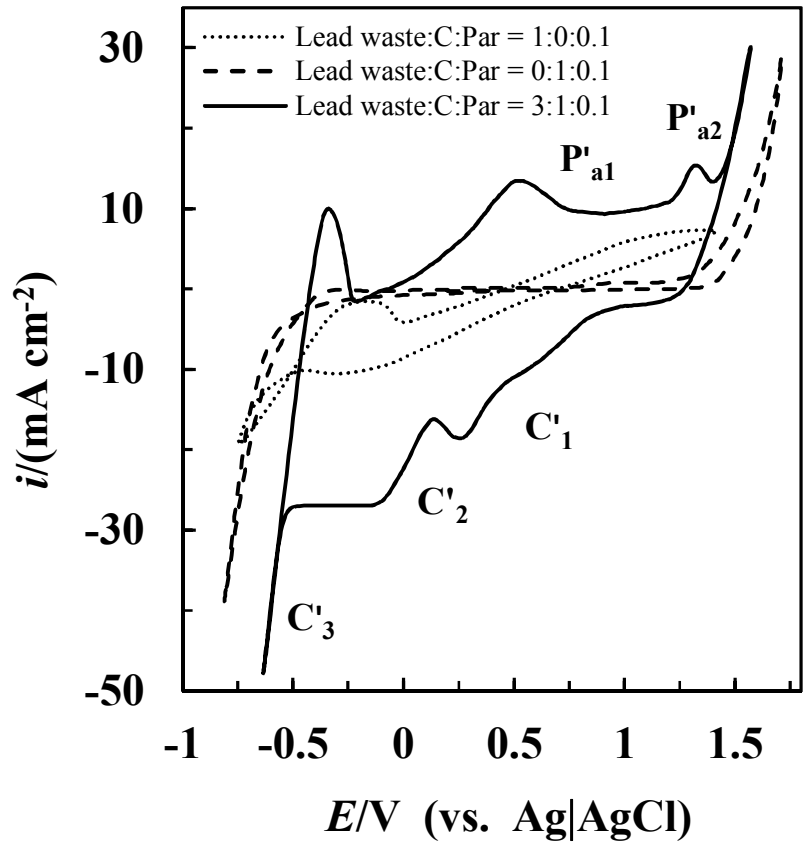

Figure 5.27 Cyclic voltammogrms recorded on a pellet of waste lead, graphite and paraffin mixed electrode in 1 mol dm^{-3} HNO_3 at 30° C with a scan rate of 10 mV s^{-1}.

Compared with the voltammogramobtained in the absence of battery waste (dashed curve in Fig. 5.3.3), the reduction wave appeared at -0.53 V corresponds to the reduction of hydrogen ion (H^+) in HNO_3 acid solution,while the oxidation wave appeared at 1.28 V corresponds to the evolution of molecular/gaseous oxygen according to the following reactions.

$$2H^+ + 2e^- \rightarrow H_2\uparrow \qquad \text{(at -0.53 V)} \qquad (5.3.1)$$

$$2H_2O \rightarrow 4H^+ + O_2\uparrow + 4e^- \qquad \text{(at 1.28 V)} \qquad (5.3.2)$$

The voltammogram in absence of graphite (dotted curve in Fig.5.3.3) consists of first small reduction wave at 0.16 V and second reduction wave at -0.46 V similar to solid curve in the forward scan. The reverse scan consist a small oxidation peak at 1.12 V which is also similar to solid curve. This indicates that reduction of battery waste is not possible in absence of graphite due to low conductivity of the electrode (battery

waste pellet). The conductivity of battery waste increases on the addition of graphite in pellet. The solid curve in Fig. 5.3.3 indicates that the first and second reduction waves are responsible for the reduction of battery waste; whereas the first and second oxidation peaks are attributed to the oxidation of the reduced species of battery waste in this solution.

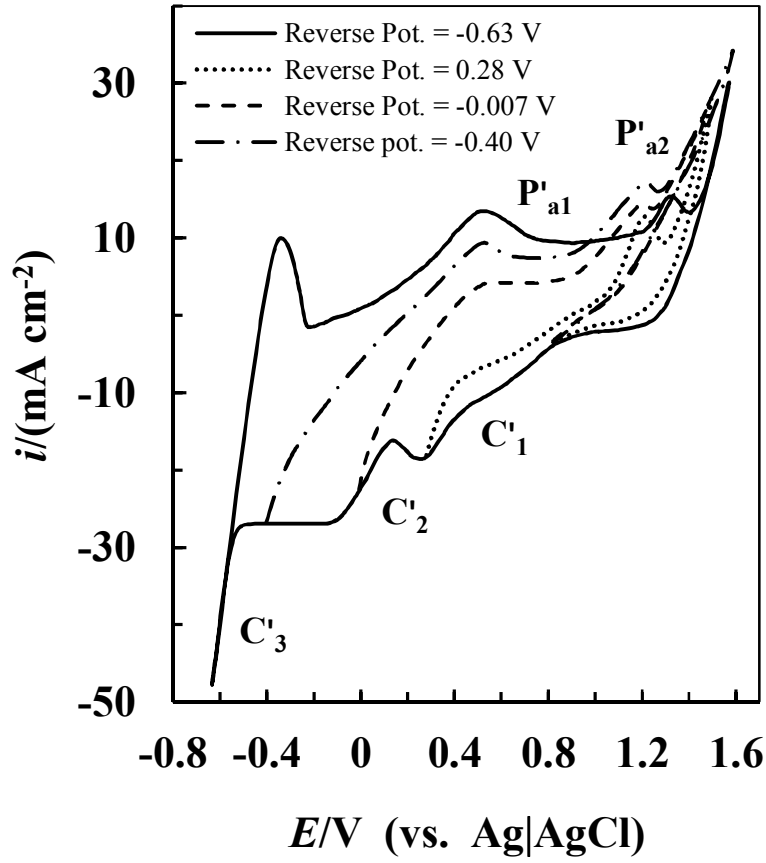

Figure 5.28 Effect of sweeping potential on the cyclic voltammograms recorded on a pellet of waste lead, graphite and paraffin mixture electrode in 1 mol dm^{-3} HNO_3 at 30° C with a scan rate of 10 mV s^{-1}.

5.3.2.2 Effect of sweeping potential on the cyclic voltammogram

Fig. 5.3.4 shows the effect of cathodic sweeping potentials on the cyclic voltammograms recorded on a pellet of 3:1:0.1 wt. ratios of battery waste, graphite and paraffin mixed electrode in 1 mol dm^{-3} HNO_3 solution at 30° C with a scan rate of 10 mV s^{-1}. It is readily seen from the voltammogram that first reduction wave C'_1 corresponds to the second oxidation peak P'_{a2}. The second reduction wave (C'_2) corresponds to the first oxidation peak P'_{a1}.

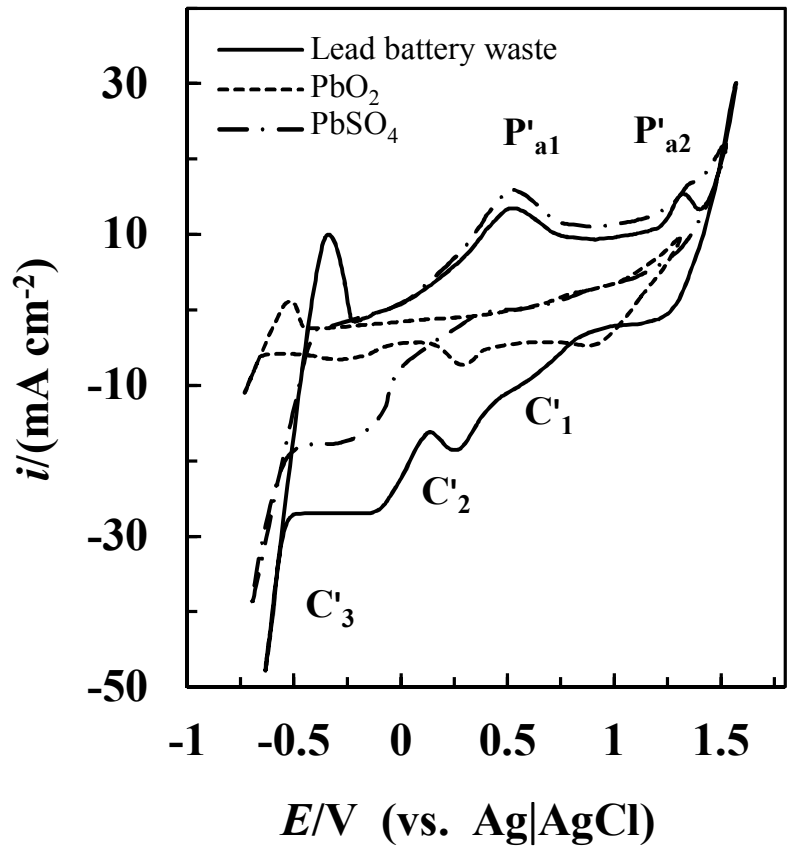

Figure 5.29 Effect of PbO_2, $PbSO_4$, and battery waste: graphite: paraffin mixture ratio on the cyclic voltammograms recorded on a pellet of battery waste, graphite and paraffin mixed electrode in 1 mol dm^{-3} HNO_3 at 30° C with a scan rate of 10 mVs^{-1}.

5.3.2.3 Cyclic voltammetry of PbO_2/$PbSO_4$/battery waste-graphite-paraffin mixed electrode in 1 mol dm^{-3} HNO_3

Cyclic voltammetryof PbO_2-graphite-paraffin and $PbSO_4$-graphite-paraffin mixed electrodes have been recorded in 1 mol dm^{-3} HNO_3 solution to identify the reactions involved in the reduction waves C'_1, C'_2 and oxidation peaks P'_{a1}, P'_{a2}. Fig. 5.3.5 shows the cyclic voltammograms of 3:1:0.1 wt. ratio of PbO_2/$PbSO_4$/battery waste: graphite: paraffin mixed electrode in 1 mol dm^{-3} HNO_3 solution at 30° C with a scan rate of 10 mV s^{-1}. In the forward scan, the voltammogram for $PbSO_4$-graphite-paraffin mixed electrode (dashed curve in Fig. 5.3.5) shows one reduction wave (correspond to C'_2 in solid curve) with the current starting to increase at 0.11 V. However, the reverse scan consists of first and second oxidation peaks at 0.52 V and 1.33 V similar to the solid curve (correspond to $P'_{a1}$and P'_{a2}) in Fig. 5.3.4. The reduction wave (C'_2) in dash dotted

curve involves the reaction of $PbSO_4/Pb^{2+}$ to Pb(0) and the oxidation peaks ($P'_{a1}$and P'_{a2}) correspond to the oxidation of Pb(0) to Pb(II) and Pb(II) to Pb(IV) respectively.

In case of PbO_2-graphite-paraffin mixed electrode, the forward scan consists of two reduction waves at 0.46 V and 0.12 V correspond to C'_1 and C'_2 in solid curve respectively. The reverse scan consists of a small oxidation peak at 1.31 V corresponds to P'_{a2} in solid curve. The reduction waves (C'_1 and C'_2) in dashed curve involve the reaction of PbO_2 to Pb(II) andPb(II) to Pb(0), respectively; and the small oxidation peak P'_{a2} correspond to the oxidation of Pb(II) to Pb(IV) similar to the solid curve in Fig. 5.3.5.

From the above information, it is concluded from Fig 5.3.4 (or solid curve in Fig 5.3.5) that the first cathodic peak at 0.46 V involves the reduction of PbO_2 to Pb(II) ion either in solution or solid phase. The second reduction wave is associated with the reduction of Pb(II) to Pb(0) and the first and second oxidation peaks are attributed to the oxidation of Pb(0) to Pb(II) and Pb(II) to Pb(IV) ion in solution according to the following reactions:

$$PbO_2 + 4H^+ + 2e^- \rightarrow Pb^{2+} + 2H_2O \quad \text{(at } C'_1\text{)} \quad (5.3.3)$$

$$Pb^{2+} + 2e^- \rightarrow Pb \quad \text{(at } C'_2\text{)} \quad (5.3.4)$$

$$Pb \rightarrow Pb^{2+} + 2e^- \quad \text{(at } P'_{a1}\text{)} \quad (5.3.5)$$

$$Pb^{2+} \rightarrow Pb^{4+} + 2e^- \quad \text{(at } P'_{a2}\text{)} \quad (5.3.6)$$

5.3.2.4 Effect of battery waste, graphite and paraffin ratio on the cyclic voltammogram

The effect of battery waste, graphite and paraffin ratio in mixture of pellet (electrode) on the cyclic voltammogram recorded in 1 $mol \cdot dm^{-3}$ HNO_3 acid solution at 30° C with a scan rate of 10 mV s^{-1} is shown in Fig.5.3.6. It is readily seen from the voltammograms that the magnitude of the first and second reduction (C'_1 and C'_2) and oxidation (P'_{a1} and P'_{a2}) peaks current densities are increased with the increase of storage battery waste content in the pellet. It indicates that 3:1:0.1 wt. ratio of battery waste-graphite-paraffin mixture in pellet will give higher dissolution rate of battery waste by constant potential and constant current methods.

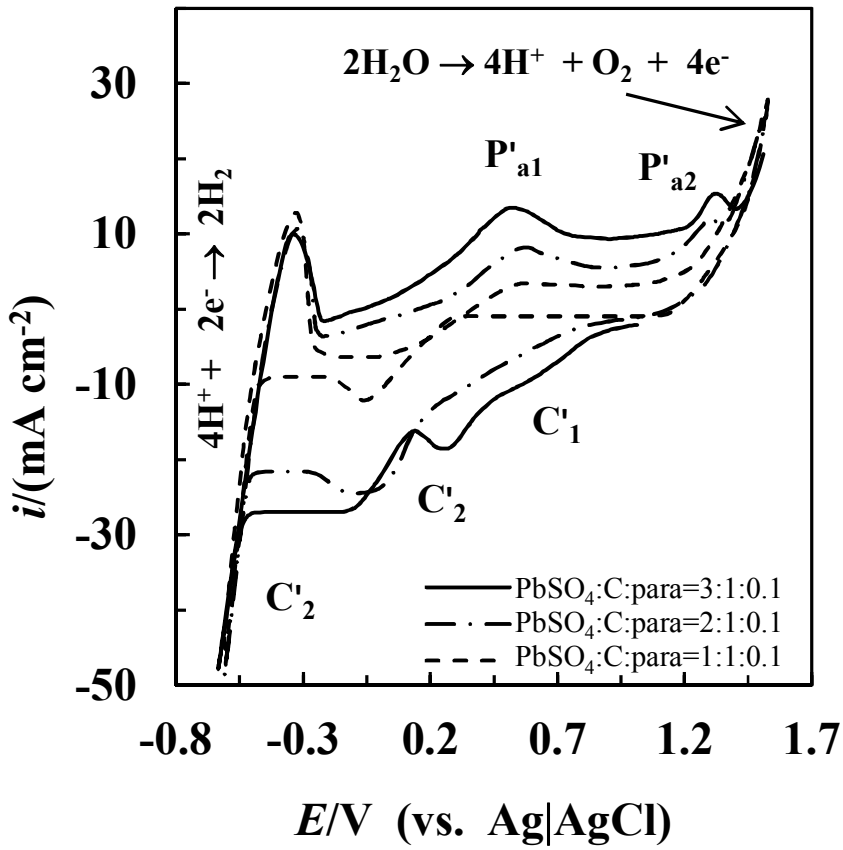

Figure 5.30 Effect of battery waste, graphite and paraffin ratio on the cyclic voltammograms recorded on a pellet of battery waste, graphite and paraffin mixed electrode in 1 mol dm^{-3} HNO_3 at 30° C with a scan rate of 10 mV s^{-1}.

5.3.2.5 Effect of HNO_3 concentration on the cyclic voltammogram

Fig. 5.3.7 shows the effect of nitric acid concentration on the cyclic voltammogram recorded on a 3:1:0.1 (wt. ratio) battery waste-graphite-paraffin mixed electrode at 30° C with a scan rate of 10 mV s^{-1}. The magnitude of the reduction and oxidation peaks current densities increases with the increase of HNO_3 concentration in the electrolyte and the high value is obtained in 3 mol dm^{-3} HNO_3 solutions. It indicates that 3 mol dm^{-3} HNO_3 solutionis suitable to obtain higher dissolution rate in electrochemical dissolution of battery waste. However, during electrochemical study pellet used in higher concentrated acid (2, 3 mol dm^{-3}) is destroyed. So 1 mol dm^{-3} HNO_3 solution have been selected for the electrochemical dissolution of storage battery waste.

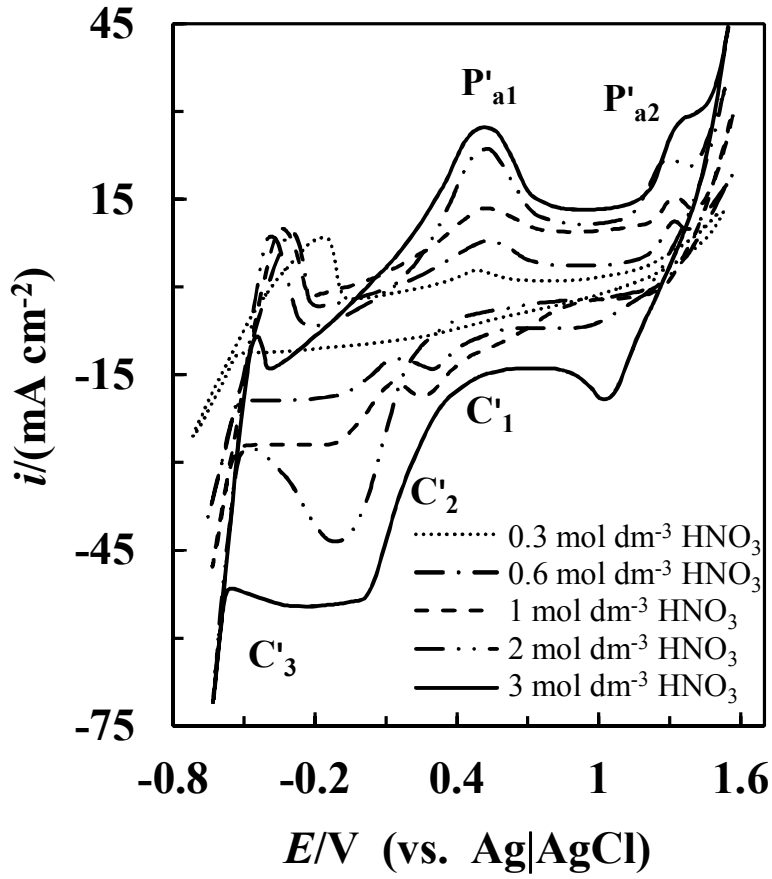

Figure 5.31 Effect of HNO_3 concentration on the cyclic voltammograms recorded on a pellet of 3:1:0.1 wt. ratio of battery waste: graphite: paraffin mixed electrode at 30° C with a scan rate of 10 mV s^{-1}.

5.3.2.6 Effect of temperature on the cyclic voltammogram

The effect of temperature on the cyclic voltammogram recorded on a 3:1:0.1 (wt. ratio) battery waste-graphite-paraffin mixed electrode in 1 mol dm^{-3} HNO_3 with a scan rate of 10 $mV \cdot s^{-1}$ are shown in Fig.5.3.8. The magnitude of the reduction and oxidation peaks current densities are increased with the rise of temperature. It is therefore concluded that higher dissolution rate of lead can be obtained from 3:1:0.1 (wt. ratio) battery waste-graphite-paraffin mixed electrode in 1 mol dm^{-3} HNO_3 acid solution at 80° C. However, the pellet is destroyed during electrochemical study at 80^{o} C. Therefore, the electrochemical dissolution study of storage battery waste has been carried between the temperatures ranging from 30° C to 75° C.

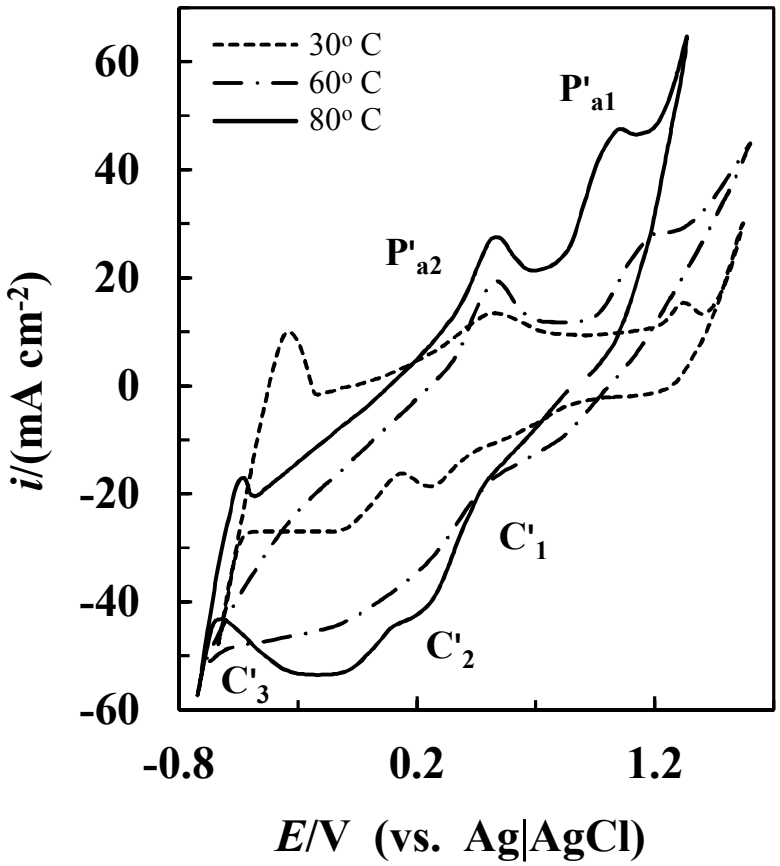

Figure 5.32 Effect of temperature on the cyclic voltammogram recorded on a pellet of 3:1:0.1 wt. ratio of battery waste: graphite: paraffin mixed electrode in 1 mol dm^{-3} HNO_3 with a scan rate of 10 mV s^{-1}.

5.3.3 Electrochemical dissolution study of waste product of storage battery ($PbSO_4$)

5.3.3.1 Effect of time on the dissolution of storage battery waste

Variations of dissolution rate of lead from storage battery waste with time in 1 mol dm^{-3} HNO_3 at 30° C from 3:1:0.1 (wt. ratio) storage battery waste-graphite-paraffin mixed pellets under constant potential method are shown in Fig.5.3.9. The dissolution potentials are 0.02 V, -0.22 V, and -0.32 V vs. $Ag|Ag^+$ reference electrode. Initially, the dissolution rate of lead from storage battery waste is sharply decreased with the increase of time up to 1 h and then the decreasing rate is significantly low. The value of dissolution rate of lead from storage battery waste in 1 mol dm^{-3} HNO_3 acid at different applied dissolution potential is almost similar. Therefore 1 h dissolution time has been selected in all electrochemical dissolution studies of storage battery waste.

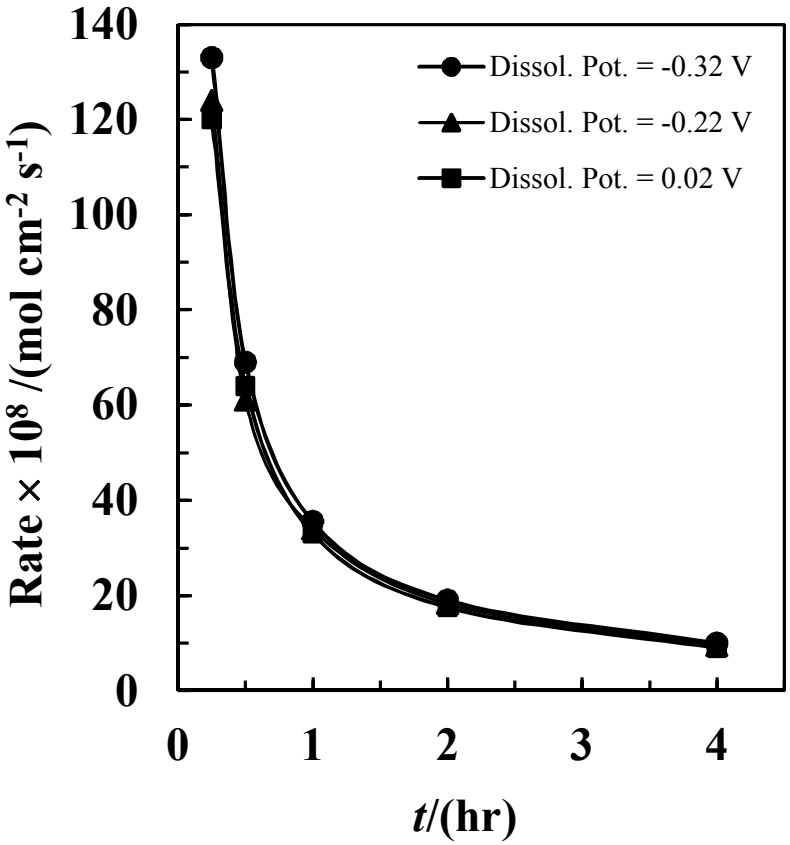

Figure 5.33 Effect of time on the dissolution rate of lead from 3:1:0.1 wt. ratio of battery waste: graphite: paraffin mixed electrode in 1 mol dm^{-3} HNO_3 at 30° C.

5.3.3.2 Effect of temperature on the dissolution rate of lead storage battery waste

Fig. 5.3.10 shows the effect of temperature on the dissolution rate of lead in 1 mol dm^{-3} HNO_3 from 3:1:0.1 battery waste-graphite-paraffin mixed pellet at different applied potential method. Dissolution of storage battery waste have been carried out in the potential ranging from 0.02 V to -.52 V and the temperature ranging from 30° C to 75° C. At constant potential, the dissolution rate oflead is increased with the increase of temperature. The increasing rate is slow up to 60° C and then sharply increased with the rise of temperature.

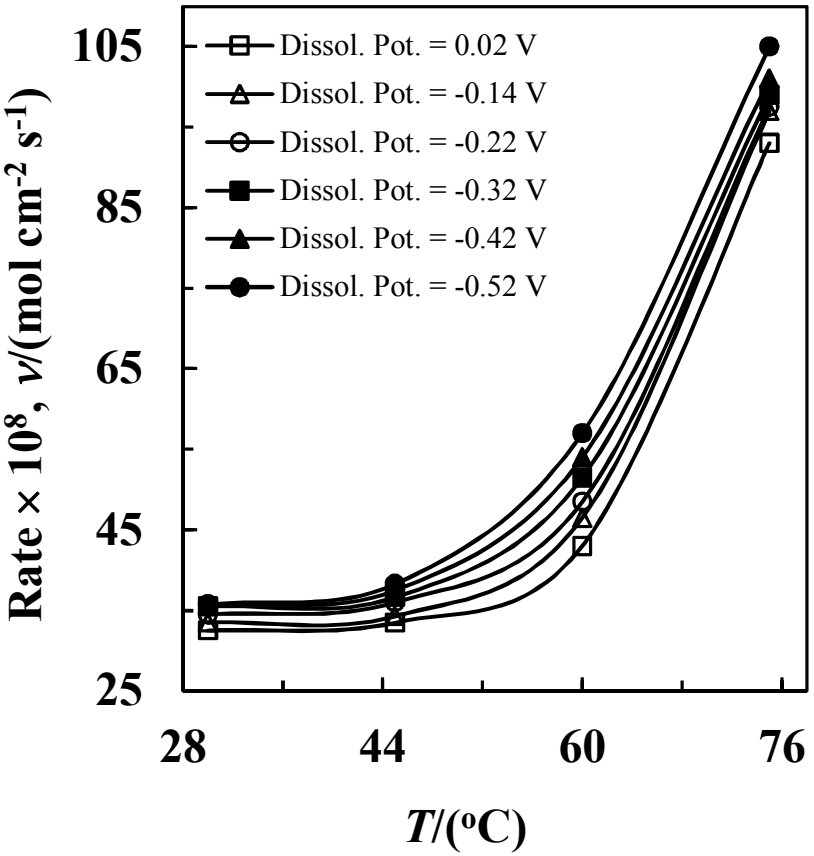

Figure 5.34 Effect of temperature on the dissolution rate of lead from 3:1:0.1 wt. ratio of battery waste: graphite: paraffin mixed electrode in 1 mol dm^{-3} HNO_3 at different applied dissolution potential.

5.3.3.3 Effect of HNO_3 concentration on the dissolution rate of lead storage battery waste

The effects of HNO_3concentration on the dissolution rate oflead at 30° C from 3:1:0.1 storage battery waste-graphite-paraffin mixedpellet under constant potential method are shown in Fig. 5.3.11. The dissolution rate of lead is first increased up to 1mol dm^{-3} HNO_3 solution and then the increasing rate is significantly slow. At higher HNO_3 concentration (>1.0 mol dm^{-3}), the slow increasing rate of the dissolution of storage battery waste is due to the starting of H_2 gas evolution which eventually decreases the active surface area of battery waste pellet by adsorption.

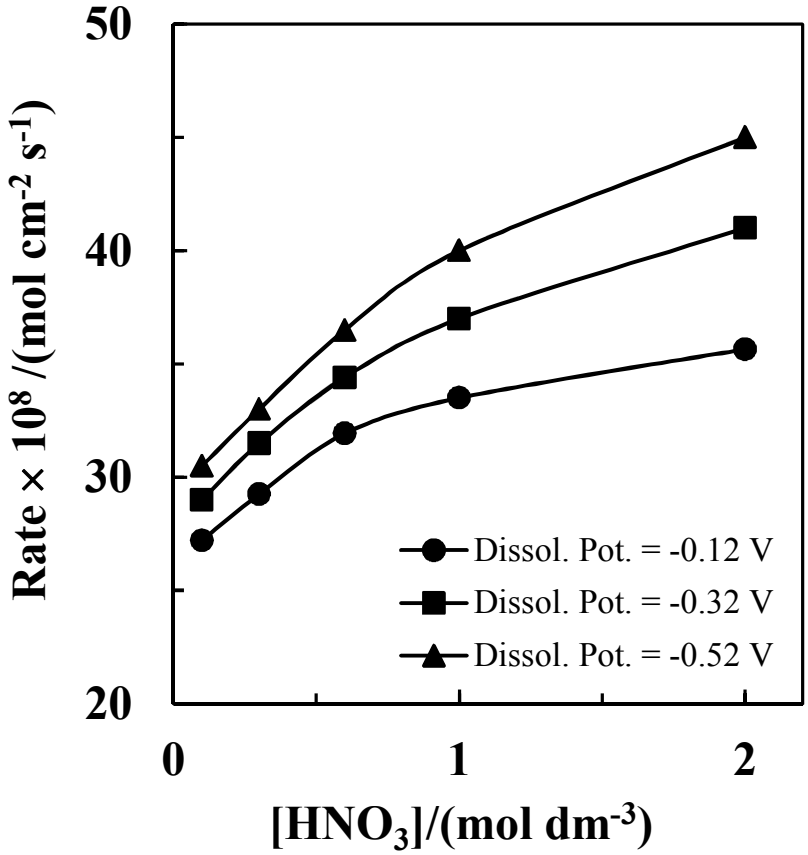

Figure 5.35 Effect of HNO_3 concentration on the dissolution rate of lead from 3:1:0.1 wt. ratio of battery waste, graphite and paraffin mixture at 30° C.

5.3.3.4 Arrhenius plot for the dissolution rate of lead from storage battery waste

The Arrhenius plot for the dissolution rate of lead from battery waste (log ν) against inverse of temperature ($1/T$) at various dissolution potentials is shown in Fig. 5.3.12. The experimental data for a set of experimental parameter do not fall on a straight line; rather curve is obtained. The slopes of the tangential lines at higher temperature region give activation energy (E_a) of 45±5 kJ mol^{-1} and those at lower temperature region give E_a of 2±1 kJ mol^{-1}. The values of E_a suggest the existence of a diffusion film which is destroyed at higher temperature. At lower temperature region, the process is diffusion controlled and with the rise of temperature, the process becomes chemically controlled.

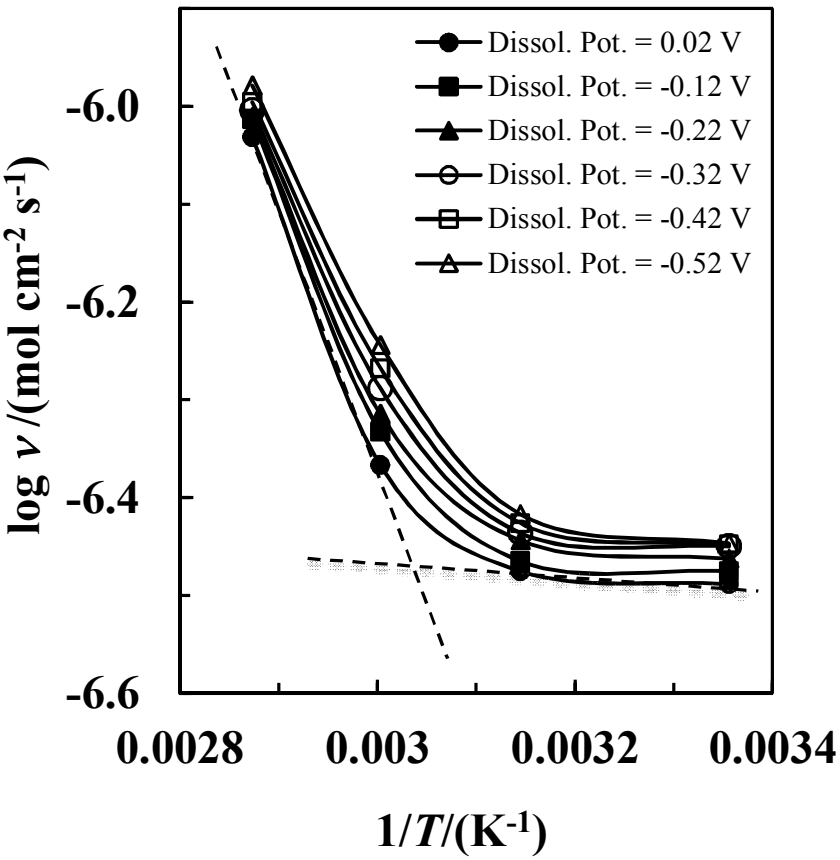

Figure 5.36 Arrhenius plot: log ν vs. inverse of absolute temperature (1/*T*) at various dissolution potentials. Battery waste: graphite: paraffin = 3:1:0.1 and [HNO_3] = 1 mol dm^{-3}.

5.3.4 Conclusions

The dissolution of storage battery waste product ($PbSO_4$) could not be obtained in HNO_3 solution without the addition of graphite in battery waste due to low conductivity ofbattery waste product ($PbSO_4$). The dissolution rate of lead from storage battery waste product ($PbSO_4$) is low at applied reduction potentials up to -0.52 V and temperatures below 60° C. At higher temperatures, the dissolution rate oflead from battery waste product ($PbSO_4$) is increased through increasing rate of the reduction of PbO_2 and $PbSO_4$. The dissolution rate of lead is also increased on increasing HNO_3 acid concentration up to 1 mol dm^{-3}, and at higher HNO_3 concentration (>1.0 mol dm^{-3}), the slow increasing rate of the dissolution of lead from storage battery waste is due to the starting of H_2 gas evolution which eventually decreases the active surface area of storage battery waste pellet by adsorption. The values of E_a in the higher (>60° C) and

lower temperature regions (<60° C) are 45±5 kJ mol^{-1} and 2±1 kJ mol^{-1}, respectively. The values of E_a suggest the existence of a diffusion film at lower temperature which is destroyed at higher temperature. At lower temperature region, the process is diffusion controlled and with the rise of temperature, the process becomes chemically controlling.

SUMMARY

The works done in the present investigation can be summarized under the following headings:

(A) Collection and characterization of ilmenite, zircon and lead sulphate

(B) Preparation of ilmenite, zircon and lead sulphate pellet

(C) Cyclic voltammetry of ilmenite/ zircon/ lead sulphate -graphite-paraffin mixed pellet

(D) Electrochemical dissolution study

(A)

The longest sea beach in the world, which belongs to the South-Eastern Coastal area of Bangladesh, is saturated with a huge reserve of heavy minerals like ilmenite, zircon, magnetite, rutile and garnet etc. The Beach Sand Exploitation Centre of BAEC at Kalatali (Cox's Bazar) separates ilmenite and zircon from the beach sand on the pilot plant scale; and the samples were collected from the above pilot plant in single lots. The lead sulphate was collected on dismantling of locally available waste lead-acid batteries. These three samples were analyzed by XRD and EDAX.

The composition of the received ilmenite sample was 38.50% TiO_2, 25.62% Fe_2O_3, 29.75% FeO, 1.20% SiO_2, 0.03% P_2O_5, 1.20% MnO_2 and 1.08% Cr_2O_3. The X-ray power diffraction pattern of ilmenite indicated the presence of $FeTiO_3$ (Refn. Code. No. 01-075-1204), Fe_2O_3 (Refn. Code. No. 01-085-0987), TiO_2 (Refn. Code. No. 01-072-0100), $(Fe,Mg)Ti_2O_5$ (Refn. Code. No. 00-005-0425), Fe_2TiO_5(Refn. Code. No. 00-003-0374), $FeCr_2O_4$ (Refn. Code. No. 00-024-0511), SiO_2 (Refn. Code. No. 01-083-2465) phases. EDAX analysis indicated the presence of iron beside its presence in ilmenite. XRD and chemical analyses data indicated that it contained about 62.80% $FeTiO_3$, 16.35% Fe_2TiO_5 and 14.72% Fe_2O_3 (as free and also as $FeCr_2O_4$ and $(Fe, Mg)Ti_2O_5$).

The acquired diffraction pattern for the powder specimen of the zircon fraction was mainly for zircon (ZrSiO4) as per Refn. Code. No. 01-081-0589). EDAX profile

indicated the presence of Zr, P, Si, Ca, K, Fe, Cu, Zn, Fe etc. in the zircon fraction of the beach sand of Bangladesh and among them Zr content is of the highest amount. XRD and chemical analyses data indicated that zircon fraction of the beach sand of Bangladesh contained about 97.17% $ZrSiO_4$.

The X-ray power diffraction pattern of the waste product of storage battery ($PbSO_4$) indicated the presence of $PbSO_4$ (Refn. Code. No. 01-082-1854), PbO_2 (Refn. Code. No. 01-076-0564), Pb (Refn. Code. No. 00-004-0686) phases. EDAX profile indicated that Pb, Fe, Al, Zn, Ni, Cu and Sn were present in the collected waste product of storage battery and among them Pb content was of the highest amount.

(B)

The pellets for electrochemical investigation were prepared by homonizing on mixing of powders of ilmenite/ zircon/ lead sulphate and graphite with small quantity of (as binder) liquid paraffin in definite ratios by mass. The mixture was placed in a steel holder of 3.30 cm depth and 1.40 cm diameter. A copper wire (10 cm long) was placed inside the mass of the holder. The holder was then placed in a pellet making machine (hydraulic press) to form a pellet on applying ~40 ton/sq. m. pressure. The pellet was covered by Araldite epoxy resin exposing the working surface of area 1.54 cm^2. The electrode surface was polished with 2000 grade SiC paper and rinsed with deionized water before each electrochemical measurement.

(C)

Cyclic voltammetry was considered as a reliable source to determine the dissolution potentials of ilmenite, zircon and lead sulphate. It was seen from the cyclic voltammetric studies that the dissolution of ilmenite was very difficult without the addition of graphite powder in ilmenite. The effects of ilmenite-graphite ratio, acid concentration and temperature on cyclic voltammograms were investigated to understand the dissolution process of ilmenite. The dissolution process of ilmenite could be presented by the following equations:

$$Fe^{3+} + e^- \rightarrow Fe^{2+}$$

$$FeTiO_3 + 3H^+ + e^- \rightarrow Fe^{2+} + Ti^{3+} + 3OH^-$$

$$Fe_2O_3 + 3H^+ + 2e^- \rightarrow 2Fe^{2+} + 3OH^-$$

$$Ti^{3+} \rightarrow Ti^{4+} + e^-$$

$$Fe^{2+} \rightarrow Fe^{3+} + e^-$$

The cyclic voltammograms indicated that the magnitude of the first and second reduction peaks' current densities and also the oxidation peak current density were increased with the increase of ilmenite content in the pellet. It indicated that higher dissolution rate of ilmenite fraction will be found from 2:1:0.1 wt. ratio of ilmenite-graphite-paraffin mixed electrode. The magnitudes of the reduction and oxidation peak current densities were higher in 1 mol dm^{-3} H_2SO_4 than in lower (0.30 mol dm^{-3}) and higher (3 mol dm^{-3}) H_2SO_4 acid concentration indicating that the higher dissolution rate of ilmenite would be found in 1 mol dm^{-3} H_2SO_4 acid solution. The magnitude of current densities corresponding to the reduction and oxidation peaks was increased with increasing of temperature. It was concluded that higher dissolution rate of ilmenite would be found from 2:1:0.1 (wt. ratio) ilmenite-graphite-paraffin mixed electrode in 1 mol dm^{-3} H_2SO_4 acid solution at 80° C.

The effect of time on the dissolution rate of iron and titanium in 1 mol dm^{-3} H_2SO_4 at 80° C from 2:1:0.1 ilmenite-graphite-paraffin mixed pellets under constant potential method was investigated. The dissolution potentials chosen were -1.00 V and -0.80 V vs. $Ag|Ag^+$ reference electrode. Initially, the dissolution rate of ilmenite was sharply decreased with the increasing time up to 1 hour and then the rate of decreased is very slow. So one hour electrochemical dissolution time was selected for the investigated system.

The dissolution of zircon fraction could not be obtained in NaOH solution without the addition of graphite in zircon fraction due to low conductivity of zircon fraction. The dissolution process of zircon could be presented by the following equations:

$$ZrSiO_4 + 3H_2O + e \rightarrow Zr^{3+} + H_3SiO^{4-} + 3OH^-$$

$$H_3SiO_4^- + e \rightarrow SiO^+ + 3OH^-$$

$$SiO^+ \rightarrow SiO^{2+} + e$$

$$Zr^{3+} \rightarrow Zr^{4+} + e$$

The cyclic voltammograms indicated that the magnitude of current densities corresponding to the first and second reduction peaks and also the current density of the oxidation peak was highest in 1:1:0.1 wt. ratios of zircon-graphite-paraffin mixed electrode. It indicated that higher dissolution rate of zircon fraction would be obtained from 1:1:0.1 wt. ratio of zircon-graphite-paraffin mixed electrode. The magnitudes of the reduction and oxidation peaks' current densities in 3 mol dm^{-3} NaOH is high than in lower (1 mol dm^{-3}) and higher (6 mol dm^{-3}) NaOH concentrations indicating that higher dissolution rate of zircon would be obtained in 3 mol dm^{-3} NaOH solution.

The magnitude of the reduction and oxidation peaks' current densities were increased with the increase of temperature. It was therefore concluded that higher dissolution rate of zircon would be found from 1:1:0.1 wt. ratio of zircon-graphite-paraffin mixed electrode in 3 mol dm^{-3} NaOH solution at 85° C.

The effect of time on the dissolution rate of zircon in 3 mol dm^{-3} NaOH solutions at 25° C from 1:1:0.1 wt. ratio of zircon-graphite-paraffin mixed pellet was investigated under constant potential method. The dissolution potentials chosen were -0.68 V and -0.83 V vs. $Ag|Ag^{+}$ reference electrode. Initially the dissolution rate of zircon was sharply decreased with the increase of time up to 1 hour and then the decreasing rate was found to be very slow. So one hour electrochemical dissolution time was recommended for the investigated system.

The dissolution of storage battery waste product ($PbSO_4$) could not be obtained in HNO_3 solution without the addition of graphite carbon in battery waste due to low conductivity of battery waste product (particularly $PbSO_4$). The dissolution process of storage battery waste product ($PbSO_4$) could be presented by equations given below:

$$PbO_2 + 4\,H^{+} + 2e \rightarrow Pb^{2+} + 2H_2O$$

$$Pb^{2+} + 2e \rightarrow Pb$$

$$Pb \rightarrow Pb^{2+} + 2e$$

$$Pb^{2+} \rightarrow Pb^{4+} + 2e$$

The cyclic voltammograms indicated that the magnitudes of the first and second reduction and oxidation peaks' current densities were increased with the increase of

storage battery waste content in the pellet. It indicated that 3:1:0.1 wt. ratio of battery waste-graphite-paraffin mixture ratio in pellet would give higher dissolution rate of battery waste by constant potential and constant current methods.

The magnitudes of the reduction and oxidation peaks' current densities were increased with the increase of HNO_3 concentration in the electrolyte and the high value was obtained in 3 mol dm^{-3} HNO_3 concentrations. It indicated that 3 mol dm^{-3} HNO_3 solutions were suitable to obtain higher dissolution rate in electrochemical dissolution of battery waste. However, storage battery waste in higher acid concentration (mol dm^{-3}), the pellet was destroyed during electrochemical study, and so 1 mol dm^{-3} HNO_3 solution was chosen selected for the electrochemical dissolution study of storage battery waste.

The magnitudes of the reduction and oxidation peaks' current densities were increased with the rise of temperature. It was concluded that higher dissolution rate of lead can be obtained from 3:1:0.1 (wt. ratio) of battery waste-graphite-paraffin mixed electrode in 1mol L^{-1} HNO_3 acid solution at 80° C. However, the pellet was destroyed during electrochemical study at 80° C. Therefore, the electrochemical dissolution study of storage battery waste was carried between the temperatures ranging from 30° C to 75° C.

The effect of time on dissolution rate of lead from storage battery waste was investigated and found that the rate was sharply decreased with the increase of time up to 1 h and then the decreasing rate was significantly slow. The value of dissolution rates of lead from storage battery waste in 1 mol dm^{-3} HNO_3 acid at different applied dissolution potential were almost similar. Therefore 1 h dissolution time was selected in all electrochemical dissolution studies of storage battery waste.

(D)

The dissolution rates of ilmenite ($FeTiO_3$) and hematite (Fe_2O_3) were low at low applied reduction potentials (<-0.40 V) and temperatures (<60° C). At more negative potentials and higher temperatures, the dissolution rate of ilmenite was increased through increasing rate of the reduction of ilmenite to Fe^{2+} and Ti^{3+}. The dissolution rate was also increased on increasing acid concentration up to 1 mol dm^{-3}; and at higher acid concentration and higher reduction potentials, it was decreased due to the starting of H_2 gas evolution which eventually decreased the active surface area of ilmenite pellet by adsorption. The hematite phase in the mineral had a higher dissolution rate

under reductive conditions than the ilmenite. The values of E_a in the higher and lower temperature regions were estimated as 50±10 kJ mol^{-1} and ~15±5 kJ mol^{-1}, respectively. The values of E_a suggest the existence of a diffusion film at lower temperature which was destroyed at higher temperature. At lower temperature region, the process was assigned as diffusion controlled and with the rise of temperature the process became chemically controlled.

The dissolution rate of zircon ($ZrSiO_4$) was low at low applied dissolution potentials (<-0.30 V) and temperatures (<55° C). At more negative potentials and higher temperatures, the dissolution rate of zirconium was increased through increasing rate of the reduction of $ZrSiO_4$. The dissolution rate was also increased on increasing alkali concentration up to 3 mol dm^{-3}; and at higher alkali concentration, it is decreased due to lowering of the available reducible species on the surface of the pellets. The values of E_a in the higher (>70° C), intermediate (~70° C) and lower (<30° C) temperature regions were found to be 23±1 kJ mol^{-1}, 45±10 kJ mol^{-1} and 20±5 kJ mol^{-1}, respectively. The value of E_a at low temperature region, suggested that the process was diffusion controlled. With the rise of temperature, the diffusion layer/film was anyhow destroyed to convert the process to be chemically controlled at ~70° C. The low value of activation energy at higher temperature region was an indicative to the involvement of two parallel reactions.

The dissolution rate of lead from storage battery waste product was low at applied reduction potentials up to -0.52 V and temperatures below 60° C. At higher temperatures, the dissolution rate of lead from battery waste product was increased through increasing rate of the reduction of PbO_2 and $PbSO_4$. The dissolution rate of lead was also increased on increasing HNO_3 acid concentration up to 1 mol dm^{-3}; and at more higher HNO_3 concentration (>1.0 mol dm^{-3}), the slow increasing rate of the dissolution of lead from storage battery waste was due to the starting of H_2 gas evolution which eventually decreased the active surface area of storage battery waste pellet by adsorption. The values of E_a in the higher (>60° C)) and lower temperature regions (<60° C) were calculated to be 45±5 kJ mol^{-1} and 2±1 kJ mol^{-1}, respectively. The values of E_a suggested the existence of a diffusion film at lower temperature which was destroyed at higher temperature. At lower temperature region, the process is diffusion controlled and with the rise of temperature, the process became chemical controlling.

REFERENCES

1. H. Sibum, G. Volker, O. Roidl, F. Habashi, H. U. Wolf, "Titanium, Titanium Alloys, and Titanium Compounds" in Ullmann's Encyclopedia of Industrial Chemistry 2005, Wiley-VCH, Weinheim. doi: 10.1002/14356007.a27095.
2. M. A. Hunter and A. Jones, Trans. Electrochem. Soc., **66** (1934) 22.
3. G. F. Comstock, Metal Progress, **27** (1935) 36.
4. C. G. Bieber and M. P. Back, U.S. Patent No. 2, 117, 284, May 17 (1938).
5. A. Zhukova and A. Sovalova, Lakokrasochruyu Ind. 2a, 2, (1934) 11.
6. A. German patent, No. 666, 750, 07 Oct (1938); *Chem. Abs*. **33**, 210 (1939).
7. I. I. Afanasev, Solovev, Sovet. Met., 6 (1934) 299; *Chem. Abs*. **29**, 4528 (1935).
8. F. L. Hess and T. L. Gillson, Op. Cit., 893.
9. Mineral Resources of the United State, U. S. Geo. Surv. Part I 41b (1927).
10. E. P. Youngman, U. S. Bur. Mines Inform. Circ. 6386 (1930).
11. S. African Mining Eng. J. 54, (1943) 137; *Chem. Abs*. **38**, 3388 (1944).
12. M. Legraye. Ann. Soc. Geol. Belg. Bull. 63 (1939-1940) 167; *Chem. Abs*. **34**, 210 (1940).
13. J. L. Gillson, Econ, Geol., 27 (1932) 554; *Chem. Abs*. **26**, 5517 (1932).
14. P. Evrand, Ann. Soc. Geol. Belg., Bull., 110 (1943) 67B; *Chem. Abs*. **40**, 5363 (1946).
15. A. Stella. Attiaccad. Lincei, 15 (1932) 336; *Chem. Abs*. **26**, 5517 (1932).
16. V. S. Swaminathan, Proc. 15th Indian Sci. Congr., 287 (1928); *Chem. Abs*. **25**, 2946 (1931).
17. U. S. Bur. Mines Minerals Yearbook, 782 (1937).
18. U. S. Bur. Mines Foreign Minerals Quarterly, 2 (1939), No. 3, 10.
19. A.V. Moss, Medd. Gronland, 103 (1938) 76; *Chem. Abs*. **34**, 1946 (1940).
20. E. P. Youngman, Op. Cit., 23.

21. T. L. Watson and S. Taber, Op. Cit., 31.

22. L. L. Shilin, Trudy Inst. Geol. Nauk SSSR, No. 10 (1940); *Chem. Abs.* **35**, 1958 (1941).

23. N. H. Fisher, Australian Mineral Resources. Survey Sum. Rept. No. 1 (1945); *Chem. Abs.* **41**. 3019(1947).

24. W. O. Johnston, Jr., Rev. Quim. Ind., 13 (1944) 19; *Chem. Abs.* **39**, 3096 (1945).

25. G. Gutzeit and P. Kovaliv, Arch. Sci. Phys. nat. 21(1939) 260; *Chem. Abs.* **34**, 3139 (1940).

26. T. Nakano; Kwagaku Kogyo Siryo. 14(1941) 30; *Chem. Abs*. 35, 7662 (1941).

27. C. O. Hutton, Newzealand J. Sci. Technol. 21B (1940) 190; *Chem. Abs*. **41**, 1959 (1947).

28. D. N. Wadia, Rec. Dept. Mineral Ceylon. Profess. Paper No. **1** (1943); *Chem. Abs*. **39**, 1372 (1945).

29. P. Legoux and P. Faucheux, Congr. Intern. Mines Met. Geol, appl., 7e Session. Paris, Oct (1935), Geol. **1**,187; *Chem. Abs*. **30**, 8093 (1936).

30. U. S. Bur. Mines Rept. Invest. No. **4208** (1948).

31. D. F. Holbrook, Arkansas Resources and Development Commission, Div. Geol. Bull. No. **13** (1948) 16; *Chem. Abs*. **42**, 8724 (1948).

32. P. Legoux and P. Foucheux, Congr. Intern. Mines Met. Geol. appl., 7e Session. Paris, Oct (1935), Geol. **1**, 187; *Chem. Abs*. **30**, 8093 (1936).

33. J. Barksdale, Titanium, its Occurrence, Chemistry and Technology, The Ronald Press, New York, p. **33** (1949).

34. E. Farnworth, S. L. Jones and I. McAlpine, The Production, Properties and Uses of Zirconium Chemicals (1980); Ed. R. Thompson, in Speciality Inorganic Chemistry, Royal Society of Chemistry, London, Special Publication No. **40**. 248 (1980).

35. K. Pearson, *Ind. Miner.* **380**, 25 (1999).

36. R. Taylor, *Ind. Mine.* **409**, 69 (2001).

37. R. Nielsen and T. W. Chan, in Ulman's Encyclopidia of Industrial Chemistry, VCH publishers, Weinheim. Germany, A 28, 543 (1996).

38. W. B. Blumenthal, Zirconium and Zirconium Compounds, In Krik- Othmer Encyclopedia of Chemical Technology, 4th Ed.; Ed. M. Howe-Grant, John Wiley, New York. **25**, 853 (1998).

39. R. Burt, *Miner.* Eng., **11(12)**, 1291 (1999).

40. B. G. Hyde and S. Anderson, Inorganic Crystal Structures, A Wiley Interscience Publication, New York (1989).

41. J. J. Molapisi, The Removal of Radioactive Compounds from Fluorozirconic Acid Solutions, M.Sc. Thesis, Pretoria University, Pretoria (1998).

42. W. B. Blumenthal, The Chemical Behaviour of Zirconium, Van Nostrand Company Inc., New York (1958).

43. A. K. Mukherji, Analytical Chemistry of Zirconium and Hafnium, Pergamon Press (1970).

44. E. Balan, D. R. Neuville, P. Trocellier, E. Fritsch. J. P. Muller and G. Calas, *Am. Miner.,* **86**, 1025 (2001).

45. S. Rois, E. K. H. Salje, M. Zhang and R. C. Ewing, *J. Phys.; Condens. Matter,* **12**, 2401 (2000).

46. M. Zhang, E. K. H. Salje, I. Farnam, A. Graeme Barber, P. Daniel, R. C. Ewing, A. M. Clark and H. Leroux *J. Phys.: Condens. Matter,* **12**, *1915* (2000).

47. T. Murakam, B. C. Chakoumakos, R. C. Ewing, G. R. Lumpkin and W. J. Weber, *Am. Miner*, **76**, *1510* (1991).

48. E. K. H. Salje, J. Chrosch and R. C. Ewing, *Am. Miner.,* **84**, *1107* (1999).

49. T. Geisler, R. T. Pidgeon, R. Kurtz, W. V. Bronswizk and H. Schleicher, *Am. Miner.,* **88**, *1496* (2003).

50. S. Ellsworth, A. Navnotsky and R. C. Ewing, *Phys. Chem. Minerals,* **21**, *140* (1994).

51. W. J. Weber, R. C. Ewing and L. M. Wang, *J. Mater. Res*., **9**, *688* (1994).

52. E. Farnworth, S. L. Jones and I. McAlpine, The Production, Properties and Uses of Zirconium Chemicals, Magnesium Elektron Ltd., Twickenham, U.K. (1980).

53. S. Mirdha and M. S. Islam, Report presented at the 10th Annual Convention of Bangladesh Association for the Advancement of Science, Dhaka, March 22-27 (1985).

54. M. A. B. Biswas, *Nucl. Sci. & Appl.*, **11**(1978): 43 and 75.

55. M. A. B. Biswas, *Nucl. Sci. & Appl.*, **1(1)** (1989): 22-26.

56. M. A. B. Biswas, *Nucl. Sci. & Appl.*, **14 & 15** (B) (1983): 88-95.

57. M. A. B. Biswas, *Nucl. Sci. & Appl.*, **16 & 17**(B) (1985): 69.

58. M. A. B. Biswas, *Nucl. Sci. & Appl.*, **12 & 13** (B) (1981): 74-83

59. Ibid, p. 77.

60. Ibid, p. 79.

61. A letter to Prof. M. F. Islam from Dr. M. A. B. Biswas of beach sand exploitation center of Bangladesh Atomic Energy Commission at Cox's Bazar, Letter No. Administration -11(2)/87, date.25 Oct. (1987).

62. M. A. Awwal; S. A. Tarafdar and A. M. Huq, Nucl. Sci. & Appl. **9(B)** (1976): 43.

63. C. Kim, Y. Lee and S. K. Ong. Factor effecting EDTA extraction of lead-contaminated soils, *Chemosphere* **51** (2003) 845-853.

64. S. Amrate, D. E. Akretche, *Chemosphere* **60** (2005) 1376-1383.

65. M. A. Kreusech, M. J. J. S. Ponte, N. M. S. Kaminari, C. E. B. Marino and V. Mymrin, *Resour Conserv. Recycl.* **52** (2007) 368-380.

66. I. Thornton, R. Rautiu, S. Brush, Lead. The Facts, Allan Printing, London, 2001.

67. R. Jolly, C. Rhin, *Resour. Conserv. Recycl.* **10** (1994) 124-137.

68. S. Ahmed, Role of applied research in the development and promotion of industrial technology in a developing country (Bangladesh). A paper presented at a seminar on transfer of technology, sponsored by the Bangladesh Council of Scientific and Industrial Research, Dacca, January (1976).

69. Monthly Statistical Bulletin of Bangladesh, Bangladesh Bureau of Statistics, statistics division, Ministry of Planning, Government of the People's Republic of Bangladesh, (July-Dec/Dec.) (1985-1986); May (1986).

70. R. T. Towner, Outlook for Australia's Titanium minerals industry. In: Proe. OUTLOOK 94. Australian Bureau of Agricultural and Resource Economics, Canberra, 1-3 February, **173**, (1994).

71. T. Ullman, Encyklopadie der Technischen Chemie, Band **18**. Weinheim (1989).

72. R. Stevens, Zirconia and Zirconia Ceramics, Magnesium Elektron Ltd. Twickenham, UK (1986).

73. F. Farnoworth, S. L. Jones and 1. McAlpine, The production, properties and uses of zirconium chemicals, Magnesium Electron Ltd., Twickenham, UK (1986).

74. R. Nielsen and T. W. Chang, Ulmans Encyclopedia of Industrial Chemistry, **A (28),** *543* (1996).

75. A. J. Phillips, *J. Am. Ceram. Soc.,* **1**, *791* (1918).

76. E. G. Pugh, *US Pat., 1376161* (1920).

77. A. C. Bidaye, S. Venkatachalam and C. K. Gupta, *Min. Metal. Trans.,* **30(B),** *205* (1999).

78. P. R. Menon, J. M. Juneja and T. S. Krisnan, *Bull. Am. Ceram. Soc.,* **59b**, *635* (1980).

79. D. E. Melliss, *Bull. Soc. Chim.,* **14**, 204 (1870).

80. G. H. Bailey, *J. Chem. Soc.,* **49**, 481 (1886); *Chem. News.,* **60**, 17&32 (1889).

81. E. C. Rossiter and P. H. Sanders, *J. Soc. Chem. Ind.*, **40**, 70 (1921).

82. M. R. Houchin, B. E. Jenkins and H. N. Sinha, Mineral, Materials and Industry, 14th Congress of the Council of Mining and Metallurgy Institute (1990).

83. A. Manhique, Z. Kwela and W. W. Foeke, *Ind. Eng. Chem. Res.*, **42**, *777* (2003).

84. W. W. Focke and W. J. DeWet, *S. A. I. Chern. Eng. J.,* **11**, *29*(1999).

85. N.A. Mohammed and A. M. Daher, *Hydrometallurgy,* **65**, *103* (2002).

86. L. Troos, *Compt. Rend.*, **61**, *109* (1865); **116**, *1227 & 1428* (1893).

87. L. Burgess, Trans. *Am. Electro-Chem. Soc.*, **47**, *173* (1925).

88. H. Moissan and F. Lengfeld, *Compt. Rend.*, **122**, *651* (1896).

89. O. Hutchins, *US Pat.*, 1427816 (1922).

90. C. J. Kinzie, *US Pat.*, 1494426 (1924).

91. H. Herzfeld, *German Pat.*, 200878 (1914).

92. P. Jost and P. Plocker, *German Pat.*, 285981 (1914).

93. T. R. Huglund, *Brit. Pat.*, 232549 (1924).

94. F. Dubois and A. A. De Silveria, *Ann. Chim. Phys.*, **14**, 110 (1820).

95. J. J. Berzelius, *Ibid,* **29(2)**, 337(1825).

96. F. Stoiba, *Listy's Chem.*, **13**, 119 (1889).

97. P. Bertheir, *Ann. Chim. Phys.*, **(2) 50**, 362 (1832) & **59**, 192 (1843); **(3) 7**, 74 (1843).

98. J. Gordon. *German Pat.*, D. R. P. 1340888 (1920).

99. N. J. Berlin, *J. Prokt. Chim.* **58**, 147 (1853).

100. L. E. Barton and C. J. Kinjie, *US Pat.*, 1451004(1923).

101. J. C. G. De Marignae, Compt. Rend., **50**, 952 (1860); Ann. Chim. Phys. **(3), 60,** 257 (1860).

102. S. Z. Haider, Introduction to Modern Inorganic Chemistry; p. 484.

103. A. Smaniotto, A. Antunes, I. do N. Filho, L. D. Venquiaruto, D. de Oliveira, A. Mossi, M. Di Luceio, H. Treichel and R. Dallago; *Journal of Hazardous Materials*, **172** (2009) 1677-1680.

104. D. C. Harris, *Quantitative Chemical Analysis*, 5th ed., W. H. Freeman & Co., 1999.

105. Y.-X. Zheng, W. Liu, W.-Q. Qin, J.-W. Han, K. Yang and H.-Luo; *Probl. Miner. Process.* **51(2)**, 2015, 535-546.

106. J. O. Nriagu, *Lead & Lead Poisoning in Antiquity; Environmental Science and Technology*, A Wiley-Interscience Publication, Canada, John Wiley & Sons, Inc.,1983,p. 205.

107. S.C.Gilfillan, 1965. *J. Occup. Med.* 7: 53-60.

108. L. G. Berry; B. Mason and R. V. Dietrich, Mineralogy (2nd Edition), Concepts. *Description. Determination. CBS,* CBS Publishers & Distributors (India) p. 158.

109. A. Betekhtin A Course of Mineralogy, Translated from the Russian by V. AGOL, Translation Editor A. Gurevich. Moscow Peace Publishers,(a) p 180, (b) p204, (c) p 230, (d) p 184, (e) p 200, (f) p 232, (g) p 208, (h) p 212, (i) p229, (j)p 186,(k)p 190,(l)p l9l,(m)p 196, (n)p221.

110. R. N. Adams., Carbon Paste Electrodes. *Anal. Chem.*, **30**(1958): 1576.

111. W. Joseph; D. K. Balashaheb and B. Mojtabaloep Chem., New Maxicow Electronal. *Chem. Interfacial Electrochem*, 1985. **194 (2)**; *Chem. Abs*. **103**, 185757 (1985).

112. P. Udehert and G. Bidan, (Dep. Rech. Fondam, Cent. Etud. Nucl. 38041 Grenoble, Fr.). *Sysnth. Met.* 1986, **14(1-2)**; *Chem. Abs.*104. 232754 (1986).

113. J. R. B. Rodriguez, A. C. Garica and P. T. Blanco, (*Dep. Phys. Anal, Chem., Univ. Ovcido, Oviedo Spain* 33071). *Electrochem. Acta*, (1989), **34(7)**; *Chem. Abs.* **111**, 86127 (1985).

114. M. T. Mouhandess, F. Chassagneux; B. Durand; Z. Z. Sharara; and O. Vittori, (*Lab. Chim. Miner. 111, Univ. Claude Bernard Lyon I*, 69622 *Villeurbanne, Fr.*). *J. Mater. Sci* (1985), **20(9)**; *Chem. Abs.* **103**, 185698 (1985).

115. L. Myriam and A. Albertine, (*Lab. Chim. Anal., Univ. Pierce et Marie Curie*, 75005 Paris, Fr.). *Electrochim. Acta*, (1986), **31(1)**; *Chem. Abs.* **104**, 158044 (1986).

116. N. G. Kemeleva; V. A. Zakh Zadharov; A. S. Niyhzbekova; and M. G. Bedzhanova, (USSR). *Electrochim. Protsessyna Tverd. Electrodakh, Alma. Ata*, (1985). 43, (Russ), From Ref. Zh. Khim. (1986); *Chem. Abs.* **106**, 23B333 (1987).

117. F. Chassagneux, B. Durand and O. Vittori, (Lab. Chim. Miner. 111, Univ. Claude Bernard -Lyon **I**. 69622 Villeurbanne, Fr.). Mater. Sci. Monogr. (1987), 38 B (High. Tech. Comm., Pt. B); *Chem. Abs*. **107**, 85950 (1987).

118. F. Mebsout; J. M. Kauffmann, G. J. Patriarchi; J. Vereecken and G. D. Cristian, (Pharm. Inst., U.L.B., Brussels, Belg.). Electroanalysis (N. Y.) (1989), **1(3)**; *Chem. Abs*. **111**. 30195 (1988).

119. D. Bauer and M. Ph. Gaillochet. *Electrochim. Acta.* **19** (1974): 597.

120. M. Lamache, *Electrochim. Acta*, **24** (1979): 79.

121. Kh. Z. Branina; V. V. Asphur and R. P. Lesunova, Communication 2. Various electrode-polarisation conditions. Zh. Anal. Khim. **29** (1974): 1788.

122. J. Wanh, and B. A. Freiha, Talanta, **30** (1983): 317.

123. M. E. Rice, Z. Galus and R. N. Adams, *Electronal. Chem.*, **143** (1983): 89.

124. M. C. Brage; M. Lamache and D. Bauer, *Electrochim. Acta*, **24** (1979): 25.

125. P. Vitorge and M. Lamache *Electrochem. Acta*, **24** (1979): 811.

126. T. Kuwana and W. French, *Anal. Chem.*, **36** (1964): 241.

127. W. K. Choi; E. A. Torma; R. W. Ohline and E. Ghali, *Hydrometallurgy*, **33** (1993): 137.

128. Kh. Z.Branina and R. P. Lesunova, Communication 1. Zh. Anal. Khim. 29 (1972): 1302.

129. M. Lamache and Bauer, D. *J. Electronal. Chem.*, **79** (1977): 359.

130. M. Ya Yampol'sskaya; Tsvetn. Met., **6**, 89 (1977); *Chem. Abs*: **87**, 120883 (1977).

131. A. R. Grover and S. D. Kulpati; Plant Maint, Impert Substitution, **11(1)**, 14 (1978), *Chem. Abs*: **90**, 41747 (1979).

132. S. Nair, A. V. Francis and S. S. lyer; Plant Maint, Impert Substitution, **11(1)**, 24 (1978); *Chem. Abs.* **90**, 74831 (1979).

133. S. H. Hwan, J. H. Oh. and C. Yongn; Pogochawon Kaepal Yonguso, **8**, 237 (1980); *Chem. Abs*. **93**, 243346 (1980).

134. G. M. Martinez, J. M. Gomes and M. M. Wong; Rep. Invest. U.S., *Bur. Mines*., R 18563 (1981) 17 P ; *Chem. Abs*, **96**, 21933 (1982).

135. A. Luszezkiewicz; Pr. Nauh, Inst. Chem. Nieorg. Metal Pierwiastkow Rzadkich Politech, Wroclow, **50** (1984); *Chem. Abs*. **102**, 135538 (1985).

136. A. Luszczkiewicz and W. Glapa; Fizykochem, Probl. Mineralargii, **17**, 205 (1985); *Chem. Abs.* **104**, 54014 (1986).

137. A. Luszczkiewicz and M. Kurzyca; Fizykochem. Probl. Mineralargii, **18**, 19 (1986); *Chem. Abs.* **106**, 70768 (1987).

138. A. Luszczkiewicz, M. Kurzyca, T. Steinhoft and K. Swurkot; Anna., Przegl. Gorz, **44**, 12 (1988); *Chem. Abs*. **110**, 216660 (1989).

139. V. A. Skripko, M. F. Anikin, A. V. Yashin and V. I. Kotvitzkaya; Tsveln, Met., **12**, 74 (1985); *Chem. Abs*. **104**, 72218 (1986).

140. H. Ayranci; Marmara Univ. Fen. Bilimri Derg., **4**, 614 (1987); *Chem. Abs*. **109**, 40242 (1988).

141. H. Ayranci; Marmara Univ. Fen. Bilimri Derg., **4**, 53 (1987); *Chem. Abs*. **109**, 41202 (1988).

142. M. Jamil, A. Abidi and D. Danish, Nucleus, **24**, 1722 (1987); *Chem. Abs*. **109**, 112864 (1988).

143. G. Weintraub; US Patent No. **1**, 014, 793, 16 Jan (1912); *Chem. Abs*. **6**, 671 (1912).

144. P. Farup; US Patent No. **1**, 087, 575, 17 Feb (1914); *Chem. Abs*. **8**, 1354 (1914).

145. P. Farup; US Patent No. **1**, 156, 22, 12 Oct (1915); *Chem. Abs*: **9**, 3215 (1915).

146. G. Jebsen; US Patent No. **1**, 333, 819, 16 May (1920); *Chem. Abs*: **14**, 1416 (1920).

147. J. Blumenfeld, US Patent No. **1**, 504, 669, 12 Aug (1924); *Chem. Abs*. **18**, 3257 (1924).

148. W. F. Wasburn; US Patent No. **1**, 889, 027, 29 Nov. (1933); *Chem. Abs*. **27**, 1457 (1933).

149. E. N. Kramer, US Patent No. **2**, 180, 961, 21 Nov. (1930); *Chem. Abs*. **34**, 1826 (1940).

150. C. L. Schonidt; US Patent No. **2**, 130, 565, 30 Sept. (1938); *Chem. Abs*: **38**, 9414 (1938).

151. E. A. Sancedo and J. J. Bruraster; *Chem. Abs*: **89**, 63038 (1978).

152. A. Kulling, W. Nespitab and H. Steinhansen; Ger. Offen. **2**, 729, 755 (Cl. C 01 G 23/04), 11 Jan (1979), *Chem. Abs*: **90**, 206677 (1979).

153. K. Yoshio, Y. Katssumi and Kurayasuo; Ger, Offen-2, 842, 090 (Cl. Col G 23/06), 13 Dec. (1979); *Chem. Abs*. **92**, 149343 (1980).

154. R. B. Davis and J. A. Radm, (NL. Industries, Inc.) Ger Offen. 3, 030, 177 (Cl. Col G23/053), 26 Feb (1981); *Chem. Abs*. **94**, 194395 (1981).

155. L. J. Waldman; K. Edgar; K. Achim and J.A. Rahm; (NL Industries, Inc.), US 4275041 (Cl. 423-82; Col G23/053), 23 Jun. (1981); *Chem. Abs*. 95, 83147 (1981).

156. R. B. Davis (NL Industries, Inc.), Belg. 886, 430 (Cl. C22 Bol), 01 a pr (1981); *Chem. Abs*. **95**, 171934 (1981).

157. D. L. Motov, G. K. Maksimora; O. S. Afanaseva and L. A. Ilyushkina (Institute of Chemistry and Technology of Rare Elements and Mineral Raw Materials Apatity) USSR, 842, 026 (Cl. C0l G23/053), 30 June (1981); *Chem. Abs*. : **95**, 206237 (1981).

158. G. Lailach, G. R. W. Gerhand, G. Walter and M. W. Director; (Bayer A.G.) Ger. Offen. DE 3, 343, 257 (Cl. C0l G23/053), 05 June (1985); *Chem. Abs.* : **103**, 39316 (1985).

159. K. N. Han; T. Rubcumintara and M. C. Fucrstenau (Dep. Metall. Eng., South Dakota Sch. Mines Technet., Rapid City, SD 57701 USA). Metall. Trans. 18B (2) (1987); *Chem. Abs.* : **107**, 26467 (1987).

160. T. Sugawara, Y. Tanno and G. Suzuki (Min. Coll. Akita, Univ., Japan 010). Sozai Busseigaku Zasshi, 3 (1), 78 (1990) (Japan); Chem. Abs. : 114, 232370 (1991).

161. S. Daisuke, Y. Sakai, T. Suzuki, K. Muraoka and S. Tanaka (Mitsubishi Materials Cor. ; Tahkem Product Corp.) Jpn. Kokai Tokkyo Koho JP 05 09, 029 (93, 09, 029) (Cl. C0lG 23/053), 19 Jan (1993); *Chem. Abs.* : **118**, 194648 (1993).

162. F. E. Bachman, US Patent No. **1**, 489, 417, 04 Apr (1924).

163. I. Katim, Laporan-Lenbaga Metal. Nas. (Indonesia), 14, LMN/76 (1976) 16P; *Chem. Abs.* : **91**, 160934 (1979).

164. P. Farup, US Palent No. 1, 831, 852, 17 Nov. (1932); *Chem. Abs* : **26**, 638 (1932).

165. B. R. Davis and J. A. Rahm. (NL Industries, Inc.) US 4, 288, 416 (Cl. 423-82; Col G23/053), 08 Sep. (1981); *Chem. Abs.* : **95**, 189466 (1981).

166. E. P. Belyakova; Ya. G. Goroshchenko and A. A. Dvernyakova, Ukr. Kin. Zh., **34**, 1184 (1968); *Chem. Abs* : **70**, 49539 (1969).

167. A. R. Hall and V. G. Giaum. (International Nickel Co., Inc.) US-4, 247, 523 (Cl. 423-82; C0l G 23/00), 27 Jan. (1981); *Chem. Abs.* : **94**, 160468 (1981).

168. J. Maure (Sulzer-Escher Wyss A. -G) Ger. De 3, 744, 575 (Cl C0l G23/047), 08 June (1989); *Chem. Abs.* : **111**, 156942 (1989).

169. R. A. Oderinde, E. A. Olanipekun, and K. O. Esuoso, Bull. Chem. Soc. Ethiop. 6 (2) (1992); *Chem. Abs*: **119**, 31945 (1993).

170. A. I. Vorobeichik, T. A. Pryokina, V. V. Boldyrev, E. G. Avvakumar, H. V. Kosova and T. I. Samsonova, *Chem. Abs.* : **99**, 197328(1983).

171. A. I. Vorobeichik, T. A. Pryokina, V. V. Boldyrev, E. G. Avvakumar, H. V. Kosova and T. I. Samsonova, *Chem. Abs.* : **99**, 197329(1983).

172. T. A. Pryakhina, A. I. Vorobeichik, E. G. Avvakumaor and V. V. Boldyrev, Chem.Abs:103, 145239 (1985).

173. R. V. Kuprina, S. A. Fuilatova, Ya. G. Goroshchenko, Yu. S. Pashuta, and V. N. Yankovich, Kim, Technol, (Kiev) 2, 19, (1981) (Russ); *Chem. Abs.*: **95**, 27191 (1981).

174. R. A. Pochekovskii, L. M. Lenev, N. S. Dyachenko, I. S. Sutyagin, V. V. Kurushin and A. F. Kuznetsov; USSR, 808, 368 (Cl. Col G23/04), 28 Feb (1981); *Chem. Abs.*: **95**, 171934 (1981).

175. H. Rick, G. Watter, W. Peter and P. Peter; Ger offen. 2.951,746 (Cl.CO1 G23/00), 02 (1981); *Chem. Abs*: **95**, 171950 (1981).

176. J. A. Rahm and D. G. Cole, (NL industries, Inc.) U. S. 4, 288, 415 (Cl. 42382; Co1/G23/053), 08 Sep (1981); *Chem. Abs.*: **95**, 189465 (1981).

177. J. A. Rahm and D. G. Cole, (NL industries, Inc.) Fr. Demande FR2, 463, 100 (Cl. Co1/G23/053), 20 Feb (1981); *Chem. Abs.*: **96**, 8844 (1982).

178. K. U. Konotopchik, A. I. Vorrbeichik, F. P. Sheinkman, I. P. Drbrovolskii and A. I. Kravchenko; USSR, SU1, 002, 246 (C1. C01 G23/00), 07 Mar (1983); *Chem. Abs.*: **99**, 25006 (1983).

179. G. G. Samoilova, K. U. Konotopchik, V. F. Ryazanov, Yu. I. Kamyshan and A. N. Borrolstov, USSR, SU1, 125, 194 (C1. CO1 G23/00), 23 Nov (1984); *Chem. Abs.*: **102**, 97749 (1985).

180. V. I. Andreeva, D. S. Domenko, V. A. Golovin, A. M. Gareev and L. V. Ivanova; USSR, SU1, 134, 545 (C1 CO123/053), 15 Jan (1985); *Chem. Abs.*: **102**, 169156 (1985).

181. I. P. Dobrovol Skilie, A. I. Kravchenko, V. A. Tyustin, V. G. Solokhin, R. M. Sadykov, L. I. Travnikov, I. N. Zabrodin, V. P. Marchenko, N. S. Lobko and A. N. Kii; USSR, SU 1, 130, 529 (C1. CO1 G23/00), 23 Dec (1984); *Chem, Abs.*: **102**, 169193 (1985).

182. R. Gerken, W. Gerhard, G. Lilack, G. Waler, M. W. Diecter, Ger, often. DE 3, 343, 256 (C1.COl G 23/053), 05 Jun (1985); *Chem. Abs.*: **103**, 39315 (1985).

183. E. Klein, Ger Offten, DE 3, 439, 217 (C1. CO1 G23/053), 30 Apr (1986); *Chem. Abs.*: **104**, 209477 (1986).

184. H. J. Roehrborn, Ger, Offten. DE3, 418, 269 (C1 CO1G23/047), 21 Nov (1985); *Chem. Abs.*: **104**, 112229 (1986).

185. G. Lailach, R. Gerken, V. D. Klaus and V. Gorg., Ger Offten. DE 3, 513, 121 (C1CO1 G23/053), 23 Oct (1986); *Chem: Abs.*: **105**, 229290 (1980).

186. G. Denecker, V. Werner, L. Joel and S. Domain, Ger Offten DE 3, 524,053 (Cl COl G 23/053), 08 Jan (1987); Chem. Abs: 106, 87154 (1987).

187. A. P. Koverda, J. V. Luzgina, I. I. Kalinichenko, A. B. Lundin, R. M. Sadykov and Yu. Pervashin; *Chem. Abs.*: **110**, 60520 (1989).

188. Yu. A. Gruzdev. N. I. Lobko, L. P. Dolya, V. A. Tyustin, R. M. Sadykov and V. Yu. Pervashinum; SU 1, 421, 697 (C1 COl G23/053), 07 Sep (1988); *Chem. Abs.*: **110**, 60521 (1989).

189. M. Yokota and M. Naka, *Chem. Abs.*: **119**, 206436 (1993).

190. N. N. Stremilova, N. F. Ryabehikova, V. A. DrozdenKo, Yu. A. Snetkov, D. V. Zaviriskii, I. A. Galeta, N. I. Lobko and L. I. Travnikov; USSR, SU1, 292, 835 (Cl. CO9 C1/36), 07 May (1988); *Chem. Abs.*: **109**. 192247 (1986).

191. N. N. Stremilova. V. M. Khomyakov, V. A. Aleinikov, V. K. Prokudina and V. I. Khakonov; USSR, SU1, 444, 340 (C1 CO9 C1/36), 15 Dec (1988); *Chem. Abs.*: **110**, 214822 (1989).

192. J. R. Hans; Ger. Offten. DE 3, 418, 269 (C1 CO1 G23/ 047) 19 Nov (1985); *Chem. Abs.*: **104**, 1122298 (1988).

193. H. H. Buckman; British Patent No. 206, 284, 29 Aug (1922); *Chem. Abs.*: **18**, 1209 (1924).

194. H. J. Ahonen; Finn. F1 62, 519 (C1. COl G23/047) 30 Sep (1982); *Chem. Abs.*: **98**, 201982 (1983).

195. E. Gock, Ger. Offten. DE 3, 635, 010 (ClCOl G23/053) 14 April (1986); *Chem. Abs.*: **108**, 207172 (1988).

196. V. P. Koryukova, E. V. Sabanov and L. I. K. Chuk; *Chem. Abs.*: **94**. 49 634 (1981).

197. E. V. Sabanor, V. P. Koryukova, L. I. K. Chuk; *Chem. Abs.*: **95**, 139218 (1981).

198. I. G. Farbenid, French Patent No. 35, 377, 25 May (1928); *Chem. Abs.*: **24**, 3865 (1930).

199. I. Tung, C. Chang and Y. Hsu; Japan Kokai, 7741, 197 (C1 COl G 23/06) 30 Mar (1977); *Chem. Abs.*: **88**, 107473 (1978).

200. V. S. Nayar, *Chem. Age. India*, **28**(1), 33 (1977).

201. G. K. Maksimova, D. L. Motov and A. G. Artemenkov; Izv. Sib. Otd. Akad. Nauk. SSSR, Ser, Khim Nank 3, 48 (1981); *Chem. Abs.*: **95**, 84160 (198)

202. K. Achin, *Chem. Abs.*: **102**, 97658 (1985).

203. H. Stuetgens, B. Holle, J. Rademachers, H. Heinricha and H. G. Zander; Ger. Offen. 2, 726, 418 (Cl CO1 G23/ 00) 13 Sep (1979); Chem. Abs.: 92, 149363 (1980).

204. Yu. S. Pashuta and A. F. Kuznetsov., USSR, 812, 724, (C1. COl G23/053), 15 May (1978); *Chem. Abs.*: **95**, 135155 (1981).

205. V. I. Pogorelov, N. A. Baitenevo and N. D. Khyashchilsiaya, USSR Patent No. 560,830 (Cl COl G23/04) Jun 05 (1977); *Chem. Abs*. **87**, 87145 (1977).

206. V. I. Pogorelov, N. A. baitenero, B. M. Burilibaev, N. D. Khyasheilskaya, M. D. Kozhnazarova, R. S. Islamov and A. F. Chikodanov; *Chem. Abs*.: **86**.: 123792 (1977).

207. D. Negovi, C. Panait and I. Bobirnav, Chin., 30, 546 (1979); *Chem. Abs.*: **91**, 19880 (1979).

208. E. Livadaru, S. Curcaneeau, A. Trula and I. M. Sava, *Chem. Abs.*: **105**, 81710 (1986).

209. C. L. LO and S. T. McKay, Ger. Offen 1, 300, 535 (Cl. COlG), 07 Aug (1969); *Chem. Abs.*: **72**, 5359 (1970).

210. B. T. Judd; *Chem. Abs.*: **105**, 9993 (1986).

211. A. P. Vander Meer and G. Vander Lee; Eur. Pat. Appl. EP 390, 293 (Cl C22B7/02), 03 Oct (1990); *Chem. Abs.*: **114**, 27669 (1991).

212. R. J. Orth and K. C. Liddell; *Chem. Abs*.: **107**, 100188 (1987).

213. J. Burastero; Rev. Ing. 22, 37 (1977); *Chem. Abs.*: **88**, 75962 (1978).

214. H. N. Sinha; *Chem. Abs.*: **102**, 135596 (1985).

215. J. J. Burastero; *Chem. Abs.*: **89**, 26786 (1987).

216. W. K. Tolley, S. Africa Patent No. 7802, 641 (ClC22 B 34/00) may 27 (1979); *Chem. Abs.* **91**, 94849 (1979).

217. M. S. Jakkiwar, R. H. Tupkary and V. M. Kokras; Trans. Indian Inst. Met. 3,33 (1980); *Chem. Abs.*: **94**, 18835 (1981).

218. W. K. Tolley; UK Pat. Apple, 2,040,270 (Cl.CO1G23/04), 28 Aug (1980); *Chem. Abs.*: **94**, 210973 (1981).

219. W. K. Tolley; Ger. Often, 2,944,239 (C1. CO1. G23/04), 14 May (1981); *Chem. Abs.*: **95**, 99980 (1981).

220. K. Browice; *Chem. Abs.*: **95**, 154465 (1981).

221. M. Zaharescu, A. Wohl, M. S. Mihaiu, E. Livadaru, A. Truta and A. Leahu; *Chem. Abs.*: **99**, 7632 (1983).

222. M. G. M. U. Islamil, J. Amrasekera and J. S. N. Kumara Shinghe; *Chem. Abs.*: **99**, 142398 (1983).

223. M. I. Levin, A. M. Leonov and A. A. Titov; *Chem. Abs.*: **99**, 1620000 (1983).

224. C.T. Lee, H.S. Choi, Y. H. Ryoo and Y. Saeki; *Chem. Abs.*: 198531 (1983).

225. J. Kurihara, K. Koike and H. Watanebe; *Chem. Abs*.: **102**, 98886 (1984)

226. M. C. L. Patterson and J. Cameron, Trans. Indst. Min. Metall., Sut. C, 94, C219-C223 (1985); *Chem. Abs.*: **104**, 92770 (1986).

227. H. Yoshikoshi and K. Nakahara, Jpn. Koai Tokkyo Koho JP 6256, 323 (8758, 323) (Cl. CO1 G23/00), 12 Mar (1987); *Chem. Abs.*: **106**, 198684 (1987).

228. H. H. Buckman, British Patent No. 206, 284, Aug 29 (1922); *Chem. Abs.*: **18**, 1209 (1928).

229. A. S. Garica and N. G. D. Santos; *Chem. Abs.*: **112**, 40122 (1990).

230. M. K. Hussen, G. A. Kolta and S. Z. El-Tauril, Egypt J. Chem. 19(1), 143 (1978); *Chem. Abs.*: **91**, 126585 (1979).

231. H. Yoshikoshi, S. Yamashita and K. Nakahara, Jpn. Kokai Tokkyo Koho JP 61, 135, 920 [86, 136. 920] (C1. CO1 G23/047) 24 Jun (1986); *Chem. Abs.*: **105**, 136450 (1986).

232. R. A. Hard and M. A. Pcieto; US 4, 390, 365 (Cl. 75-84, 4; COl- G23/047), 28 Jun (1983); *Chem. Abs.* **99**, 74610 (1983).

233. E. Narita, T. Hitoshi, I. Hitoshi, O. Tokas and O. Taijiro; *Chem. Abs.*: **99**, 40546 (1983).

234. O. Taijiro; Jpn. Kokai Tokkyo Koho Jp 5815, 031 [8315,031] [C1. COl G23/053], 28 Jan (1983); *Chem. Abs*.: **99**, 77382 (1983).

235. R. A. Baldarin, W. C. Laughlin, K. P. Patel and S. J. Patricin; U.S. Patent No. 476552 (C1. 75-1T; C22B1/06) 09 Aug (1988); *Chem. Abs.*: **109**, 153637 (1988).

236. R. B. Smith, A. Tetlow and G. L. Thompson; *Chem. Abs.*: **110**, 11495 (1989).

237. L. Turker, I. Girgin and D. Goodall; *Chem. Abs.*: **110**, 42441 (1989).

238. Y. Wang, Z. Faming and G. Shenging; Shuomingshu CN 87, 100993 (Cl. COlG23/07), 30 Nov (1988); *Chem. Abs*.: **110**, 215770 (1989).

239. K. W. Tolley and W. C. Laughlin; US 4, 2698, 09 (Cl. 432-70; COl G32/053), 26 May (1981); *Chem. Abs.*: **95**, 101054 (1981).

240. K. C. Liddell; *Chem. Abs.*: **110**, 42486 (1989).

241. P. Farup; U.S. patent No. 1, 831, 852, 17 Nov (1932); *Chem. Abs.*: **26**, 638 (1932).

242. R. C. Behera and A. K. Mohanty; Trans. Indian Inst. Met., 37, 215 (1984); *Chem. Abs.* **102**, 82192 (1985).

243. Sumitomo Metal Industry Ltd.; Myochu Kogyo K. K. JPN. Koai Tokkyo Koho JP 59, 208, 052 [84, 208, 052] (Cl. C22 C33/10) 26 Nov (1984; *Chem. Abs.*: **102**, 98947 (1985).

244. Sumitomo Metal Industry Ltd.; Myochu Kogyo K.K. JPN. Koai Tokkyo Koho JP 59,208,050 [84,208,050] (C1.C22 C 33/08)26 Nov (1984); *Chem. Abs.*: **102**, 984487 (1985).

245. L. Pellereau, M. Jacmart and G. Lcbnis; Franch patent No. 690, 348, 21 Feb (1930); *Chem. Abs.* **25**, 1108 (1931).

246. G. Blaskeariez and K. Boreurice; *Chem. Abs.*: **93**, 97694 (1980).

247. J. A. Easteal and T. Anthony; *Chem. Abs*.: **94**, 159047 (1982).

248. W. Zhang, Z. Zhu and Y. Chen; *Hydrometallurgy*, **108,** 177 (2011).

249. T. Laxmi, S. S. Srikant, D. S. Rao and R. B. Rao; *International Journal of Mining Science and Technology*, **23**, 725 (2013).

250. A. A. Baba, S. Swaroopa, M. K. Ghosh and F. A. Adekola; *Transactions of Nonferrous Metals Society of China*, **23**, 2743 (2013).

251. M. Mozammel and A. Mohammadzadeh, *Measurement*, **66**, 184 (2015).

252. L. Jia, B. Liang, L. Lu, S. Yuan, L. Zheng, X. Wang and C. Li; *Hydrometallutgy*, **150**, 92 (2014).

253. V. S. Gieesh, V. P. Vinod, S. K. Nair and G. Ninan, *International Journal of Mining Ptocessing*, **134**, 36 (2015).

254. F. Wu, X. Li, Z. Wang, C. Xu, H. He, A. Qi, X. Yin and H. Gua, *Hydrometallurgy*, **140**, 82 (2013).

255. B. N. Akhgar, M. Pazouki, M. Ranjbar and A. Hosseinnia, *International Journal of Mining Processing*, **124**, 138 (2013).

256. T. Tao, Q. Chen, H. Hu, Z. Yin and Y. Chen, *Transactions of Nonferrous Metals Society of China*, **22**, 1232 (2012).

257. A. Janssen and A. Putnis, *Hydrometallurgy*, **109**, 194, (2011).

258. X. Xiong, Z. Wang, F. Wu, X. Li and H. Guo, *Advance Powder Technology*, **24**, 60 (2013).

259. L. Zhang, H. Hu, Z. Liao, Q. Chen and J. Tan, *Hydrometallurgy*, **107**, 40 (2011).

260. C. Sasikumar, D. S. Rao, S. Srikanth, N. K. Mukhopadhyay and S. P. Mehrotra, *Hydrometallurgy*, **88**, 154 (2007).

261. N. El-Hazek, T. A. Lasheen, R. EI-Sheikh and S. A. Zaki, *Hydrometallurgy*, **87**, 45 (2007).

262. C. Li, B. Liang and L.Suo, *Hydrometallurgy*, **89**, 1 (2007).

263. S. Zhang and M. J. Nicol, *Hydrometallurgy*, **97**, 146 (2009).

264. L. Zhang, H. Hu, L. Wei, Q. Chen and J. Tan, *Separation and Purification Technology*, **73**, 173 (2010).

265. S. Zhang and M. J. Nicol, *Hydrometallurgy*, **103**, 196 (2010).

266. E. Jaya Kumari, S. Berckman, Y. Yegnaraman and P. N. Mohandas, *Hydrometallurgy*, **65**, 2-3, September 2002, 217-225.

267. A. F White, M. L. Peterson and M. F. Hochella Jr, *Geochimica of Cosmochimica Acta*, **58**, 8, April (1994), 1859-1875.

268. S. Jayasekera, Y. Marinovich, J. Avraamides and S. I. Bailey, *Hydrometallurgy*, **39**, 1-3, October 1995, 183-199.

269. R. K. Biswas and M. G. K. Mondal, *Hydrometallurgy*, **17**, 385 (1987).

270. R. K. Biswas, M. A. Habib and N. C. Dafader, *Hydrometallurgy*, **28**, 119 (1992).

271. R. K. Biswas, M. F. Islam, M. A. Habib, *Hydrometallurgy*, **42**, 367 (1996).

272. R. K. Biswas, M. F. Islam and M. A. Habib, *Indian Journal of Engineering and Materials Sciences,* **1**, 267 (1994).

273. R. K. Biswas, M. F. Islam and M. A. Habib, *Bangladesh J. Sci. Ind. Res.,* **33**, 426 (1998).

274. R. K. Biswas, M. F. Islam and M. A. Habib, *Bangladesh J. Sci. Ind. Res.,* **32**, 103 (1997).

275. R. K. Biswas, M. F. Islam and M. A. Habib, *Bangladesh J. Sci. Ind. Res.*, **34**, 13 (1999).

276. M. A.Habib, R. K. Biswas, P. K. Sarkar and M. Ahmed, *Bangladesh J. Sci. Ind. Res.*, **38**, 1 (2003).

277. R. K. Biswas and A. K. Chakraborty, *Indian Journal of Engineering and Materials Sciences,* **3**, 48 (1996).

278. R. Stevens, Zirconia and Zirconia Ceramics, *Magnesium Electron Ltd. Twickenham,* UK (1986).

279. M. Weibull, Lunds, Univ, Arsskrift, **2**, 18 (1882).

280. H. S. Cooper, *US Pat.*, 1527470 (1925).

281. M. R. Houchin, D. H. Jenkins and H. N, Sinha, *Ceram. Bull,* **69**, 1706 (1990).

282. M. R. Houchin, D. H. Jenkins and H. N. Sinha, *US Pat.*, 4746497.

283. P. V. Anathapadmanabhan, K. P. Sree Kumar, K. V. Iyer and N. Venkatramani, J. Alloys Comps. **196**, 251 (1993).

284. F. Farnoworth, S. L., Jones and I. McAlpine, The Production, Properties and Uses of Zirconium Chemicals, *Magnesium Electron Ltd., Twickenham,* UK (1986).

285. R. Nielsen and T. W. Chang, *Ulmans Encyclopedia of Industrial Chemistry*, A (**28**), 543 (1996).

286. H. Rose, Pogg. Ann., **48**, 575 (1840); 108, 20 (1859).

287. J. Korner, *US Pat.*, 1467275 (1923).

288. J. D. Hancock, Min, *Sci. Eng.*, **1** (9), 25 (1977).

289. A. Manhique, Z. Kwela and W. W. Foeke, Ind. Eng., *Chem. Res.*, **42**, 777 (2003).

290. N. A. Mohammed and A. M. Daher, *Hydrometallurgy*, **65**, 103 (2002).

291. H. S. Choi and H. Cross. Canad. Min. *Metall. Bull.*, **57**, 966 (1964).

292. H. S. Choi., Canad. Min. *Metall. Bull.*, **58**, 193 (1965).

293. A. M. Abdel-Rehim, *I.J. Min. Proce.,* **76**, 234 (2005).

294. A. M. Amer, Physiol. *Prob. Min. Proce.,* **40**, 61 (2006).

295. T. Puclin, W. A. Kaczmarek and B.W. Ninham, Mater. *Chem. Phys.*, **40**, 73 (1995).

296. N. J. Welham, J.Am. *Ceram. Soc.*, **55** (9), 2217 (2002).

297. N. J. Welham, Metal. *Meter. Trans.* B, **29**, 603 (1998).

298. A. Kaiser, M. Lobert and R. Telle; *Journal of European Ceramic Society*; Vol-**28**, 11, 2008, p. 2199-2211.

299. E. M. Larsen, Advances in Inorganic Chemistry and Radiochemistry, Vol-13, 1970, p. 1-133.

300. J. Nawrocki, I. M. Rigney, A. Mc Cormick and P.W. Carr, *Journal of Chromatography A*, Vol **657**, 2, 31 Dec. (1993), p. 229-282.

301. P. T. Mwakio, *Geochimica et Cosmochimica Acta*, Vol. **49**, 2, Feb. (1985), p. 453-458.

302. M. Mao, D. Fornasiero, J. Ralston, R. S. C. Smart and S. Sobicrag; *Colloids and Surfaces A: Physicochemical and Engineering Aspects*, Vol. **85**, 1, 6 June (1994), p. 37-49.

303. A. Domenecha, N. Montoyab and J. Alarconb; *Electrochimica Acta*; Vol. **56**, 20, 1 Aug. (2011), p. 7104-7111.

304. A. Domencha, F. J. Torres and J. Alarconb; *Electrochimica Acta*, Vol. **49**, 26, 15 Oct (2004), p. 4623-4632.

305. J.-L. Paquettea, B. Moineb and M. A. F. Rakotondrazafy; *Precambrian Research*, Vol-**121**, 1-2, 28 Feb (2003), p. 73-84.

306. J. J. Schwartza, B. E. John, M. J. Cheadle, J. L. Wooden, F. Mazdab, 1, S. Swapp and C. B. Grimes, *Chemical Geology*; Vol-**274**, 1-2, 15 June (2010). p. 68-81.

307. T. Puclin, W. A. Kaezmarek and B. W. Ninham, *Materials Chemistry and Physics*, Vol-**40**; 2, March (1995), p. 105-109.

308. L. Xua, Y. Xiaoc, A. van Sand Wijk, Q. Xu and Y. Yang; *Journal of Nuclear Materials*, Vol. **466**, Nov. (2015), p. 21-28.

309. H. H. Li H. Nersisyan, K.-T. Park, S.-B. Park, J.-G. Kim, J.-M. Lee and J.-H. Lee; *Journal of Nuclear Materials*; Vol-**413**, 2, June 15 (2011), p. 107-113.

310. R. K. Biswas and M. A. Hayat; *Nuclear Sciences and Applications*; Vol. **168**, 17, Series. B, October (1985),

311. R. K. Biswas and M. A. Habib; *Journal of the Bangladesh Chemical Society*, 1994, **7** (2), 158-166.

312. R. K. Biswas and M. A. Hayat; *Hydrometallurgy* **63** (2002) 149-158.

313. R. K. Biswas and M. A. Hayat, *Hydrometallurgy* **65** (2002), 205-216.

314. R. K. Biswas, M. A. Habib and M. A. Hayat; *Pak. J. Sci. Ind. Res* 2004 47 (5) 325-331.

315. R. K. Biswas and M. A. Hayat, *Hydrometallurgy* **75** (2004), 45-54.

316. R. K. Biswas, M. A. Habib, A. K. Karmakar and M. R. Islam; *Industrial & Engineering Chemistry Research; American Chemical Society*, 2012, 51, 13552-13561.

317. R. K. Biswas, M. A. Habib, A. K. Karmakar and M. R. Islam; *Hydrometallurgy* **103** (2010), 124-129.

318. R. K. Biswas, M. A. Habib, A. K. Karmakar, and M. R. Islam; *Hydrometallurgy* **103** (2010), 130-135.

319. N. Lyakov and T. Nokolov; *Metalurgiya (Sofia)*. **29** (10), 24-8 (Bulg) (1974).

320. M. Yamada, N. Wakamatsu and S. Nakauo, (Dowa Mining Co. Ltd.), Japan. 74, 44, 819 (Cl. C0lg), 30 Nov. (1974) Chem. Abs.: 82, 173167f.

321. Z. Takehara, *Power sources,* **85**, 1, Jan. 2000, 29-37.

322. G. L. Pashkov, E. V. Mikhlina, A. G. Kholmogorov and Y. L. Mikklin, *Hydrometallurgy*, **63**, 2. Feb. 2002; 171-179.

323. R. L. Paul, M. J. Nicol, J. W. Diggle and A. P. Saunders; *Electrochimica Acta* , **29**, 7, July 1978, 625-633.

324. A. Smaniotto, A. Antunes, I. D. N. Filho, L. D. Venquiaruto, D. de Oliveria, A. Mossi, M. Di Luccio, H. Treichel and R. Dallago; *Hazardous Materials*; **172** (2009) 1677-1680.

325. Y.-X. Zheng, W. Liu, W.-Q. Qin, J.-W. Han, K. Yang and H. Luo; *physiochem. Probl. Miner. Process.* **51(2)**, 2015, 535-546.

326. D. A. Begum, R. K. Biswas and M. F. Islam; *Bangladesh Chemical Society*, Vol **2**, No. 1, 39-45, 1989.

327. D. A. Begum, M. F. Islam and R. K. Biswas, *Hydrometallurgy*, **22** (1989), 259-266.

328. D. A. Begum, M. F. Islam and R. K. Biswas, *Hydrometallurgy*, **23** (1990, 397-403.

329. D. A. Begum, M. F. Islam and R. K. Biswas; *Bangladesh Chemical Society*, **3** (1), 35-43, 1990 (June).

330. T. R. A. Davey. CSIRO, DIV. of Chemical Engineering, G. M. Willis, University of Melbourne, Dept. of Metallurgy, 24-J. Metals, March (1977)

331. A. J. Bard, L. R. Faulkner (2000-12-18). Electrochemical Methods: Fundamentals and Applications (2ed.). Wiley. ISBN 0-471-04372-9.

332. R. S. Nicholson, S. Irving (1964-04-01).*Analytical Chemistry*. **36**(4): 706-723.

333. J. Heinze (1984). *Angewandte Chemie International Edition in the English*. **23**(11):831-847.

334. R. S. Nicholson (1965), *Anal. Chem*. **37**: 1351-1355.

335. D. Vall, S. D. Vall; McCreery, Richard (1999). *Anal. Chem*. **71**: 4594-4602.

336. A. M. Bond, Felberg, Stephen (1998). *J. Phys. Chem*. **102**: 9966-9974.

337. Carriedo, Gabino (1988), *J. Chem. Educ*. **65**: 1020.

338. R. M.Wightman (2006), *Science*. **311** (5767): 1570-1574.

339. W. E. Geiger, Organometallics 2011, volume 30, pp. 28-31.

340. J.Basset, R. C. Denney, G. H. Jeffery, J. Mendham. Vogel's textbook of quantitative inorganic analysis [B]. 4th Edition, ELBS, William Clowes & Sons Limited, Beccles and London, 1978, (a) p. 750, (b) p.741.

341. G. Charlot, Colorimetric determination of elements, Elsever, p.438 (1964).

PAPERS FOR THE PUBLICATION FROM THE WORK OF THIS THESIS

1. M. Rostom Ali*, R. K. Biswas, Md. Golam Zakaria "A study on the electrochemical dissolution of ilmenite fraction of beach sand in sulphuric acid solution" Journal of Electrochemistry, Accepted on June, 2016.

2. M. Rostom Ali*, R. K. Biswas, Md. Golam Zakaria "A study on the electrochemical dissolution of zircon fraction of beach sand in sodium hydroxide solution" Journal of Electrochemistry, communicated.

3. M. Rostom Ali*, R. K. Biswas, Md. Golam Zakaria "A study on the electrochemical dissolution of waste product of storage battery ($PbSO_4$) in nitric acid solution" Journal of Electrochemistry, communicated.